Computational Modelling of Hydrated Yttrium Containing Silicate Glasses for in situ Radiotherapy

A Thesis Submitted for the Degree of Doctor of Philosophy

Jahangir Malik

Department of Chemistry

University College London

March 2014

Dedication

I have always loved reading dedications in books, and I had never thought that one day it would be my turn to write one.

Dedicating a book to someone is a splendid act of love and a powerful sign of respect and admiration.

I love, admire and respect too many individuals to choose one to represent them all, so I dedicate this thesis to you, without knowing your name, as I am sure you recognised yourself in these words.

Thank you, my dearest friend.

Declaration

I, Jahangir Malik, confirm the work presented in this thesis is my own. Where information has been derived from other sources, I confirm that this has been indicated in the thesis.

Gordon Street, London, U.K, March 2014

Publications

- Hydration Effects on the Structural and Vibrational Properties of Yttrium Aluminosilicate Glasses for *in situ* Radiotherapy.

  Jahangir Malik and Antonio Tilocca.

  The Journal of Physical Chemistry B, 2013, 117, 14518 – 14528

- Bioactive Glasses as Potential Radioisotope Vectors for *in situ* Cancer Therapy: Investigating the Structural Effects of Yttrium.

  Jamieson K. Christie, Jahangir Malik and Antonio Tilocca.

  Physical Chemistry Chemical Physics, 2011, 13, 17749 – 17755

Abstract

The present work discusses various types of yttrium-containing silicate-based glasses that are proposed for use for *in situ* cancer radiotherapy. The work firstly deals with yttrium aluminosilicate (YAS) glasses and then follows on to yttrium-containing bioglasses both with and without the presence of phosphorus.

The application of yttrium-based glasses as radionuclide vectors for *in situ* radiotherapy relies on the durability of the glass in a physiological system: leaching of activated ^{90}Y ions from the glass matrix into the bloodstream should be minimised as much as possible immediately after injection and before their radioactive decay. In order to understand the relationship between glass composition, structure and durability at an atomistic level, we have carried out classical molecular dynamics (MD) simulations on different yttrium-containing silicate-based glass compositions, specifically three yttrium aluminosilicate glasses: YAS17, 24 and 30, where 17, 24 and 30 denote the molar % of yttrium, as well as yttrium-containing bioglass (YBG) with and without the presence of phosphorus. Each of the glass compositions listed were hydrated at three levels of included water content. The present simulations primarily aim at understanding how different water content influences the bulk structural features critical for the glass durability, such as the network connectivity and nanosegregation. The dry yttrium glasses were thus hydrated with increasing water amounts, and the analysis of the structures has highlighted marked hydration effects on network-former and network-modifier coordination, as well as on the preferential aggregation of yttrium ions, regulated by surrounding OH groups. Hydration of YAS (with increasing yttria content) and YBG (with and without phosphorus) is shown to increase glass durability through strengthening of the silicate network, which is important for the durability of such glasses in radiotherapy applications. The overall coordination of oxygen to network formers and modifiers of yttrium glasses are increased due to the association of hydroxyl groups. Hydroxyl groups have also been found to have a preference to coordinate more towards network modifiers than network formers, which is common to both YAS (with increasing yttria content) and YBG (with and without phosphorus). Other results are also discussed, mainly in the context of the physico-chemical characteristics which make yttrium glasses suitable for *in situ* radiotherapy.

Contents

List of Figures

List of Tables

List of Equations

Acknowledgments

I would like to take the opportunity to thank the extraordinary people who have helped and supported me through my Ph. D. experience. I would firstly like to thank my primary supervisor Dr. Antonio Tilocca and secondary supervisor Prof. Jonathan Knowles (UCL Eastman Dental Institute), who have both provided me with guidance, support and advice. I would also like to thank my colleagues, who have made the past four years a more enjoyable experience, in particular Isaac Sugden, Alan Lobo, Richard Ainsworth, Nuruzzaman Noor, Nicolas Constantino and Will Travis.

I would like to thank a few of my lecturers from my undergraduate university, Queen Mary University of London; Dr. Isaac Abrahams, Prof. Alice Sullivan and Dr. Peter Wyatt.

Thank you to everybody who continued to interact with me during the past months, despite the fact that I have, undoubtedly, talked of little else but my thesis; Saira Tabbassum Malik, Mohsin Mahmood Malik, Mahvish Malik and Bilal Akbar Malik.

I would like to thank the M3S Industrial Doctoral Centre; Prof. Nora De Leeuw and Dr. Zhimei Du. I would like to thank the Engineering and Physical Sciences Research Council (EPSRC) and the UCL Eastman Dental Institute

Finally, and most significantly Dr. Jamieson Christie where at the beginning of my life at UCL was a friend, colleague, collaborator and later a supervisor. I am very grateful for his support, guidance and wisdom. I wish him the very best in his future life and career in Computational Chemistry.

1 Introduction

Amorphous materials have short-range order but no long-range order. Short-range order is order seen on the length scales of single atoms and their immediate neighbours. Long-range order refers to periodic structural order extending throughout the material. Fully crystalline structures have both short and long range order i.e. one can identify one atom and its neighbours (short range order), as well as identifying repeating structural units within the same structure, due to periodicity within crystal structures which does not dominate within amorphous structures. Amorphous materials have a significant amount of topological and chemical order. This refers to local environment e.g. coordination, nearest neighbours, bond lengths, bond angles etc, which are often relatively similar, although not identical as in the case of an ideal crystal. Unlike the case for a crystal, the order decreases rapidly with respect to distance, where the distances to second neighbours are more uncertain than for the first neighbours, for example. The decrease of spatial correlation is experimentally examined using diffraction experiments and is important for a model to demonstrate [1]. Glasses are a general type within the broader group of amorphous materials. Glasses are formed by rapid cooling of a high-temperature liquid, which results in the structure freezing in position instantaneously. The amorphous glass that has formed in this way is metastable to the crystalline form. The frozen amorphous glass is thermodynamically higher in energy compared to the same substance which is cooled slowly into a crystalline form. The rapidly cooled solidified amorphous glass, maintains a great amount of structural disorder relative to the crystalline state [1-3].

Amorphous materials, particularly glass, have been used as biomaterials. The discovery by Larry Hench *et al*. found a range of compositions for modified phospho-silicate glasses which have the ability to create a chemical bond between the glass and organic tissue [4]. This created and developed a new frontier within biomedicine. Indeed, from that time the idea was enhanced and improved to develop materials that could be successfully incorporated into the human body for clinical applications (in the ligaments, bone, muscle etc. [5, 6]). Amorphous glasses can repair, replace and substitute tissues and/or organs within the body. When a material is synthesized for actual usage, a trial and error method is often used to determine the worthiness of such a material, to develop it further for specific applications. More recently, powerful computational tools have opened a new dimension to the science concerned behind the chemical and

physical structure of glasses and moreover, bioactivity. Computer simulations require bespoke software programmes that achieve similar results to alternative experimental techniques. Using computers and other resources enables the atomistic study of the nature and chemistry behind the bioactivity of glasses, which allows certain gaps to be filled concerning the fundamental knowledge regarding glass and such bioactivity.

Radiotherapy is a way to treat cancer [7-14]. A technique of radiotherapy named brachytherapy incorporates the radioactive source directly into the human body either permanently or temporarily. A promising technique of brachytherapy [15] is the use of glass microspheres to carry the radioactive source. The spherical shape and the chemical resistance of the glass particles make them a suitable material in the treatment of cancer in such places as the liver. No sharp edges of glass would remain and this would reduce damage to healthy tissues [16]. Some specific types of cancer are more difficult to treat than others e.g. liver cancer. Liver cancer is often a terminal illness, after diagnosis of the disease the patient typically has a life expectancy of approximately three months. Surgery of the liver is not very often used, mainly because of the high probability of causing metastases [15]. Chemotherapy can be used after elimination of malign cells, which could worsen the clinical condition of the patient if not removed. Chemotherapy generally causes only temporary relief [15]. Radiotherapy treatments that utilize an external radiation source can ultimately harm surrounding neighbouring tissues. The dose of radiation applied is carried out in multiple parts or steps which tend to minimize the side effects related to irradiation. This process is still not enough to minimise damage to surrounding tissues, essentially irradiation specific to cancer cells is desired, as these are the only cells one would like irradiated. From external radiotherapy, usually this type of treatment requires an average of ten irradiations over a period of 30 days with doses of approximately 2500 rads [16]. However, if the radiation source is localised such as in brachytherapy, doses of up to 15,000 rads can be used in a single step, which is enough to kill cancer cells, and the localised dose prevents significant harm to healthy surrounding tissues. Glass microspheres with diameter sizes of 20 – 40 micrometers (17 Y_2O_3 – 19 Al_2O_3 – 64 SiO_2 (mol %)) have been used in brachytherapy cancer treatments [16-18]. The isotope ^{89}Y is transmuted to ^{90}Y via neutron activation resulting in a beta emitter with a half life of 64.1 hours. [19] Other parts of the glass structure i.e. ^{30}Si and ^{27}Al are also activated which are also beta emitters of radiation. The half-life of Si and Al are a lot lower i.e. 2.25 minutes for Al and 2.62 hours for Si [19] and so these are less important. Such microspheres are durable to body fluids and are non-cytotoxic [20]. After

neutron activation of the microspheres, they are injected directly to the cancer site resulting in a high dose of radiation localised only in the tumour. Such glasses have been submitted to clinical tests for the treatment of liver and kidney cancers [20-28].

The yttrium aluminosilicate glasses we propose for study are to be of a sol-gel form. Bioactive glasses were prepared for the first time using the sol-gel process in the 1990s [29]. Porous bioglasses can be prepared from the hydrolysis and polymerization of metal hydroxides, alkoxides and/or inorganic salts. A wide bibliography, including excellent reviews, has dealt with this synthesis method and application [30]. During the sol-gel process, the gelling stage occurs around room temperature. Gels, aerogels, glasses, dense oxides, etc., can be made by sol-gel processing, thus facilitating the incorporation of organic and biological molecules within the network [31], or even cells within silica matrices [32]. Moreover, sol-gel processes can be combined with chemistry of surfactants, resulting in a new generation of highly ordered mesoporous materials for biomedical applications. Contrary to melt-quench derived bioglasses, sol-gel glasses are not prepared at high processing temperatures, which allows for the incorporation of thermally unstable molecules. In addition, and due to the high surface area and porosity derived from the sol-gel process, the range of bioactive compositions is wider, also exhibiting higher bonding rates together with excellent degradation / solubility and resorption properties [33, 34]. The actual structure of a sol-gel glass, especially containing yttrium, can affect properties such as those mentioned earlier. Since the structure is so important to the chemical and physical characteristics of the glass, it is clearly important to understand what structure is best for biological and radio-therapeutic applications. The difference between glasses prepared via the sol-gel process and those quenched from the melt, is mainly in the surface structure of the glass, which is hydrated. Hydration of certain glass types enhances bioactivity compared to that of melt-quench derived bioglasses [35, 36]. Obtaining models of sol-gel glasses of yttrium aluminosilicate glass requires adapting the interatomic potential and the computational method.

A limited amount of information is available regarding sol-gel bioactive glasses and those containing yttrium, from computer simulations [37], NMR [38], IR spectroscopy [39], and neutron and X-ray diffraction [40]. Although the studies listed have very little to do with the compositions we may be interested in, some general characteristics and features are of importance. YAS glass is a disordered system with a network consisting of mainly four-coordinated silicon and aluminium atoms, where yttrium acts as a network modifier that has a higher coordination number and greater bond distance to its

neighbouring oxygen atoms. Silicon and aluminium in an yttrium aluminosilicate are known to be network formers, by the Zachariasen's definition [41], for cations, which according to his rules, in association with oxygen form the random network of glasses. The term *network former* is generally adopted for oxides capable of glass formation. Oxygen ions which act as bridges between the polyhedral structural units are called *bridging oxygens (BO)*. In addition to the network former, oxides which do not participate in forming the network structure are called *network modifiers* i.e. yttrium. The YAS system is difficult to describe or probe using standard experimental techniques, especially when resolving contributions from different atomic environments within the amorphous structure [42]. Computer simulations [43-59] can therefore provide insight where standard experimental techniques cannot. Modelling glasses using computational techniques [43-59] will allow for the optimisation of the glass structure required for the biomedical application.

1.1 *Hydrated Yttrium Aluminosilicate Glasses for in situ Cancer Radiotherapy*

The procedure used to create a variety of glasses via the melt quench technique is carried out using conventional glass technology. Bioactive glasses have been produced using this conventional method for some time [60]. This conventional technique requires the glass to be created using grains of oxides or carbonates, which are mixed, melted and homogenized to high temperatures e.g. 1250 – 1500 degrees Celsius [60]. This temperature does of course vary according to the glass being synthesized, some glass components e.g. yttria grains melted into aluminosilicates require even higher melting temperatures which provide an inefficient synthetic route and in turn become expensive to run. The molten glass is then poured into a steel or graphite mould to form bulk glasses. The glass can be, if necessary, ground and polished to make the glass better for its application.

There are disadvantages found from the conventional glass technology used to synthesize bioactive glasses i.e.

1 High purity is difficult to maintain and achieve when creating an optimally functioning bioactive glass. Of course, if the glass is not of high purity the glass will not work to the best of its ability. This is primarily linked to the high

temperatures and homogenisation techniques required for the molten glass system. Depending on the composition of the glass, components of the glass system can be very chemically reactive and can dissolve platinum crucibles. The amount of platinum dissolved is not very high but does cause for concern as even a few platinum ions will incorporate themselves into the molten glass disturbing or destroying the glass network and resulting in an impure glass which will have decreased bioactivity.

2 Processing steps such as grinding, polishing, fritting, sieving etc. all expose the glass to potential contaminants and negative effects on bioactivity such as discussed in 1.

3 There is a compositional limitation imposed upon bioactive glasses and glass ceramics synthesized using conventional high-temperature processes. This is primarily due to the high temperatures required to equilibrate silica (SiO_2) in the molten form at temperatures of 1713 degrees Celsius. Even at such high temperatures, the silica melt is highly viscous and can become more viscous when incorporating other components e.g. alumina (Al_2O_3) or yttria (Y_2O_3).

4 High processing temperatures in platinum crucibles and multiple handling steps increase the production costs significantly. The costs do not only come from the use of energy but also items such as lab equipment, labour, maintenance, quality control etc. However lowering energy costs are a real benefit to the manufacturer.

Sol-gel [61-74] processing is an alternative to conventional glass technology which can be carried out at lower temperatures. In the last decade the sol-gel process has become widely spread and increasingly popular among inorganic materials chemists [60]. The work in this thesis is based on hydrated yttrium silicate glasses which examines the effect of water on the bulk internal structure of the glass. Although hydrated glasses are not sol-gel, the properties of a sol-gel may share many characteristics to that of the same glass composition which is hydrated instead. The bulk internal structure of a sol-gel is hydrated, similarly to that of yttrium silicate glasses in this work. Surfaces, surface hydration, pores, voids and their chemical/physical structures present on sol-gel glasses are not present on yttrium glasses that have been investigated in this work, which is the main difference between the two types of glasses i.e. sol-gel and hydrated. Nevertheless,

this is an important first step investigating many of the essential features that should be present in actual sol-gel glasses.

Yttrium aluminosilicate (YAS) glasses play an important role in technology. It has been used in a wide number of applications [60]; one example is that of optics and additives for the promotion of sintering of ceramics [60]. It has also been applied to the field of cancer radiotherapy. Conventional external radiotherapy ejects radiation to a tumour from a radiation source. The power and dose of this radiation is limited in order to prevent damage to surrounding healthy living tissue in the patient. *In situ* cancer radiotherapy using YAS involves injecting micro particles of the glass containing active radionuclides (^{90}Y) in the blood flow supplying a tumour: the latter is then directly reached by a high and localised dose of radiation, without the damage to healthy surrounding tissues produced by conventional external radiotherapy. YAS glass microspheres act as a vector carrying radioisotopes of yttrium that require excitation to the radioactive state. Here the YAS glass will be injected into the blood vessels around the locality of the tumour or into the tumour itself where the YAS glass remains throughout treatment. The YAS glass composition should have high chemical durability, which is of crucial importance for the safety of the patient. The glass should release as little yttrium as possible into the bloodstream while still being radioactive, where the half life of yttrium is approximately 2.7 days. An understanding of how yttrium is incorporated into the glass as well as other properties of the vector carrying the radioisotopes are critical for the success of the therapy: for instance, the vector should be a biocompatible material, stable in the physiological environment long enough to avoid releasing the radioisotopes before their decay. A detailed understanding of the structural and dynamical factors which control properties crucial for the radiotherapeutic use of YAS is currently unavailable.

Computer simulations are an effective way of examining amorphous or glassy systems at the atomistic level. Such examination can deepen the understanding of specific properties e.g. durability and its relation to composition [75]. For the purpose of this work we have carried out classical molecular dynamics (MD) simulations to investigate thoroughly YAS and YBG glasses. The purpose for using classical MD simulations is due to relative ease of study of large systems, which results from the use of an empirical interatomic potential used [76]. On the contrary Car-Parinello molecular dynamics (CPMD) [77] simulations are limited to only a few hundred atoms. The size of simulation of CPMD is adequate for the study of short range and vibrational features [78-

[82] but would hinder the investigation of medium range structural properties e.g. clustering behaviour [41, 83], with enough statistical resolution. The distribution of cations on the medium-range length scale is important for the glass durability in solution. Clustering and aggregation on these length scales has been suggested [84, 85] as an inhibitor of bioactivity in bioactive glasses, where it is also known that clustering of modifiers affect ionic transport [86]. Classical MD uses predefined force fields which can be used to simulate various types of systems, biological or inorganic, that contain up to millions of atoms [87-99]. The time length for a simulation of this size can be up to the microsecond scale, where the accuracy and reliability of the model is completely and exclusively determined by the force field implemented for that particular system. On the contrary, *ab initio* MD can be used instead for a system that is intrinsically difficult if not impossible to model via classical MD. In classical MD, the predefined potential (the classical interatomic potential) does not have the capacity to model chemical reactions, or breaking or formation of bonds. Here, *ab initio* methods [100-109] are used instead.

1.2 *Hydrated Yttrium Bioglasses for Cancer Radiotherapy*

Conventional radiotherapy is used to treat patients who have cancer by irradiating their tumours from an external source using an x-ray beam. Using an x-ray beam of high energy will damage surrounding healthy living tissue where the tumour is present. The maximum dose is therefore limited so safety is ensured to the patient. The capacity to produce the desired effect of using an external x-ray source for tumours that are found deep in the body e.g. liver or kidney, are reduced. Internal or *in situ* radiotherapy [18, 27] is a method by which radioactive isotopes such as ^{90}Y are implanted either into the tumour or into the blood vessels localized around the tumour. This method enables a high and localized dose of radiation to be delivered to the tumour. This reduces the affect of damaging healthy living tissue around the tumour. This method of treatment has proven more effective than that of conventional radiotherapy [110, 111].

Yttrium ions which supply the high and localised dose of radiation to the tumour are embedded into aluminosilicate glass microspheres. The biocompatibility of such glass microspheres is affected largely by the composition of the glass i.e. what ingredients are used to form the glass, which is especially synthesized for this application. The physical size, shape, density, porosity and more importantly intrinsic or physical hydration can also increase or decrease the level of biocompatibility. These factors are also important in relation to glass durability and absorption. Once a glass

system has been synthesized for its specific application, these factors will aid transport of hydrated or dry microspheres, which vary in shape, through and into blood vessels surrounding tumours [110]. As the activated microspheres are injected into the blood stream, the durable glass network will prevent the yttrium ions from leaching out into the body. It is for this reason especially that a high level of importance is placed upon the chemical durability of the YAS glass system [18]. ^{90}Y has a half-life of 2.7 days and therefore for radiotherapy requires a glass design which enables durability for a few weeks.

Once the yttrium radioactivity decays, the targeted organ will later contain impurities derived from YAS glass. This is a problem which is concerned with the long term effects of YAS glass. Due to the high five-year survival rate of patients treated using *in situ* radiotherapy (46% [111], compared to <7% via conventional radiotherapy) the impurities gathered from YAS can remain within the organ for many years after implantation. The effect of these impurities on the organ in which treatment was given remains unknown. An attractive alternative to YAS glasses involves the use of radionuclide carriers that have a proven long-term biocompatibility and higher biodegradation in a physiological environment. If this is achievable, then the use of such glasses can be applied to a wider expanse of tumours found in various regions in the body which are far too fragile to operate on using conventional radiotherapy. Brachytherapy of cervical, brain and other tumours using glasses which have higher biocompatibility or biodegradability properties will enable a reduction in post-treatment surgery. Post-treatment surgery often requires the removal of capsules, metallic wires etc that were initially placed in the organ that carried the radiation and carries risk to the patient [112].

An intriguing possibility in this direction is the involvement of bioactive silicate glasses (BG's) [6]. Currently the applications of such BG's are to mend bone, facial and periodontal problems. BG's are very useful as they have a combination of beautiful characteristics i.e. 1) high biocompatibility 2) the ability to develop chemical bonds and integrate with existing tissue (bioactivity) 3) the potential to stimulate regeneration of new tissues [113, 114]. Due to these properties, BG's cause several transformations during the initial stages after implantation where the surface of the BG's makes contact with the physiological environment. When this occurs a number of soluble ionic species are formed as the slow degradation of the glass network takes place. By taking BG's for their properties and blending yttrium into the network (YBG's) of such a glass the

biocompatibility of the radionuclide vector can be enhanced [113]. The ability of BG's to make bonds that can take place with hard and soft tissue can further improve the efficacy of treatment. This would massively benefit from the natural ability of the carrier to repair and stimulate growth of new healthy tissue, replacing the cancerous cells destroyed by the treatment with yttrium radioisotopes.

A fragile balance exists for YBG's: a composition suitable for radiotherapy applications should be stable enough to avoid releasing any radioactive yttrium into the bloodstream during the initial stage of treatment, but at the same time, retaining the unique feature of surface reactivity and ability to interact with the biological host tissue. The high sensitivity of the bioactive glass durability to the composition depends on the relative amounts of ingredients used, these are: SiO_2, CaO, Na_2O and P_2O_5. By finely tuning the composition, the production of a glass which has properties, physical and chemical characteristics specific for its application can be enabled. Often scientific techniques are used to probe and adjust the suitability of new compositions targeted for certain applications, but care and attention is required over the interpretation of results achieved for BG's. Trends of data and results must be analysed and rationalized correctly as the nature of BG's is very complex.

In order to establish an optimised bioactive glass carrier for yttrium radioisotopes, a task must be carried out beforehand. This task involves determining whether and to what extent yttrium incorporation affects the durability of the yttrium-free bioactive glass composition. The balance mentioned earlier is due to two separate yet intertwined factors: high levels of bioactivity are linked with quick dissolution rates of all ions, including yttrium in the physiological environment. As a result, the amount of yttrium leached from a highly bioactive composition might also exceed a threshold considered safe for radiotherapy applications.

1.3 ***Structure of a Hydrated Yttrium Silicate Glass***

In situ cancer radiotherapy of yttrium aluminosilicate glasses (YAS) involves injecting microparticles of a vector containing active radionuclides (yttrium or others) in the blood flow supplying a tumour: the latter is then directly reached by a high and localised dose of radiation, without the damage to healthy surrounding tissues produced by conventional external radiotherapy. The properties of the vector carrying the radioisotopes are critical for the success of the therapy: for instance, the vector should be a biocompatible material, stable in the physiological environment long enough to

avoid releasing the radioisotopes before their decay. As a detailed understanding of the structural and dynamical factors which control properties crucial for the radiotherapeutic use of these materials is currently unavailable.

Yttrium aluminosilicate glasses have been modelled via classical and *ab initio* molecular dynamics techniques by Tilocca and Christie [42, 115]. It is clear from the evidence given from their papers what the features and structures of a standard bulk yttrium aluminosilicate are at the atomistic level. They have reported the coordination numbers, Q^n connectivity distributions, radial distribution functions and bond angles of relevant species within their glass system. These types of information directly allow the structure of a glass to be determined at an atomic level. These types of information are also relevant to that of the hydrated glasses we have investigated. If we know what the structure is for example within a dry (unhydrated) yttrium aluminosilicate system, it will be a good starting point to discuss, compare and contrast existing data of bulk yttrium aluminosilicate systems to that of hydrated yttrium aluminosilicates. Although, a hydrated yttrium aluminosilicate glass is not strictly a sol-gel, it is a good starting point in studying a glass in an actual sol-gel form.

Having an amorphous glass system comprising of yttrium, aluminium, silicon and oxygen atoms creates a bulk yttrium aluminosilicate. If the same elements are used but with the addition of hydrogen atoms, this will cause changes to the structure of the standard bulk yttrium aluminosilicate glass system. What these changes are exactly is a question that is of great importance. It is known that changing a single structural feature of a glass, can in turn chemically enhance or destroy its chemical and physical properties when used as a biomaterial.

Since amorphous solids do not have long-range order, the important features are therefore the short-range and medium-range structure. The short-range structure involves bond lengths, bond angles, coordination etc. Medium-range structure involves connectivity or more importantly Q^n distributions for certain network formers. Radial distribution functions (RDF) (pair correlation functions) of certain species within the glass can be calculated. This would give information on the periodicity of the structure. Since glasses are amorphous one would assume not to see sharp peaks that resemble periodicity found in crystal structures. Instead what is seen are fewer peaks which gradually decrease in intensity, where the peaks tend to be broader than those found in an RDF of a crystal. As well as demonstrating the glass being amorphous, other data can be achieved. Bond lengths can be determined e.g. Si-O RDF will show a bond length of

1.6 Å, seen from the first maximum of the RDF pattern giving rise to the average interatomic distance between silicon and oxygen atoms.

Information from those listed above will give a direct insight into what the structure of a glass actually looks like at an atomistic level. From this we can deduce the chemical or physical characteristics of the glass that would allow it to become suitable for its purpose. The compositions of the glass would then be tailored in order to achieve the optimal structure suitable for a bioactive glass required for cancer radiotherapy.

Hydrating YAS possibly affects and impacts various parts of the YAS structure. Firstly the hydrogen atoms will have a tendency to create covalent bonds with available oxygen atoms. This will create hydroxyl (OH) groups that will either remain by themselves in the YAS structure or be bonded to silicon and/or aluminium. If the hydroxyl groups coordinate to silicon and aluminium, this will cause the number of bridging oxygens to decrease, causing silicons and/or aluminiums to become Q^0, Q^1 or Q^2 species (see section 3.3.2). Since hydrogen can have a maximum of one bond (which is already connected to an oxygen) this would mean that the oxygen atoms will no longer link to adjacent network former cations i.e. Si or Al. For example, if a bond of O – Si – O – Al exists in YAS, then by hydrating YAS the bonds may break in the structure into O – Si – OH and OH – Al etc. This would impact the Q^n distributions for silicon and aluminium. The Q^n distributions are more likely to be therefore $Q^0 \rightarrow Q^3$ for both Si and Al. Some silicon and aluminium atoms may have more than one hydroxyl group coordinated to them also decreasing the Q^n distribution of network former cations (see section 3.3.2). It has already been seen for unhydrated YAS17 that the Si and Al Q^n distributions are mainly Q^3 and Q^4 [42].

Hydrogen atoms or hydroxyl groups (hydrogen already attached to oxygen) may have a preference to attach to silicon atoms than aluminium. For example, if there were ten free hydroxyl groups potentially attaching to a network former cation (Si or Al), five hydroxyl groups may preferentially attach to silicon, whereas three may attach to Al and the remaining two may want to exist as free entities within the YAS glass structure.

It is important to mention that not all hydroxyl groups may be attached to network formers (Si or Al). Some hydroxyl groups may be present in the YAS system as free entities that may not find an appropriate coordinate bond to Si or Al. This will in turn cause the environment of YAS to become basic, at the same time as maintaining charge neutrality. Some hydroxyl groups, similarly to how oxygen coordinates to yttrium modifier cations in unhydrated bulk YAS and YBG glass systems, may

coordinate to yttrium modifier cations in the glass network.

It has also been demonstrated by the work of Tilocca and Christie for YAS17 [42] that yttrium clustering takes place in certain regions of the YAS17 glass structure. It will be very interesting to see if by hydrating YAS can either promote or destroy yttrium clustering that takes place in YAS17 [42, 115]. The distribution of cations on the medium-range length scale is important for the glass durability in solution. Clustering and aggregation on these length scales has been suggested [84, 85] as an inhibitor of bioactivity in bioactive glasses, where it is also known that clustering of modifiers affect ionic transport [86]. The connections between structure and bioactivity are well understood by simulations by Tilocca *et al.* [42, 116-118]. Specifically the network connectivity (Q^n distributions) and clustering relate to the structure of a glass, which is very strongly connected to bioactivity of a glass is concerned.

The medium-range structure of the network can be defined by studying the Q^n distributions. For example, the YAS glass system contains only silicon and aluminium as network formers, whereas yttrium is considered a network modifier. The total Q^n for a specific atom x is the number n of bridging oxygens bound to x, where a bridging oxygen is an oxygen bound to x. The network connectivity (NC) of species A is calculated as the weighted average of the total Q^n over all A atoms, and represents the average number of BO in the coordination shell of A [83]. The network connectivity is a good way to describe the durability of a glass in an aqueous physiological medium: a low (~2) silicon network connectivity characterizes more soluble, thus more bioactive, glass compositions. On the contrary, network connectivities (NC) greater than 3 relate to non-bioactive glass compositions [149].

2 Methodology

2.1 *Molecular Dynamics*

Probing the structure of a material used for biological purposes (a biomaterial) at a microscopic level is a difficult task. The structure of a biomaterial is highly complex with physico-chemical properties and interactions which control its purpose or activity. A typical example is the use of bioactive implants used for treating patients who require bone repair or replacement. These bioactive implants are usually inorganic materials such as glasses, ceramics or a combination of the two. These materials developed for such a purpose are able to interact and become a part of a patient's physiological environment [113, 119, 120]. Many interactions take place simultaneously and dynamically, causing an interface to form between the biomaterial and the surrounding external medium. After time these interactions will allow for the biomaterial slowly to become a part of the external medium e.g. a biomaterial for bone repair will anchor itself firmly via chemical and physical bonds onto the natural bone of a patient requiring care. The same can be applied to drug delivery systems, antibacterial agents etc. where they completely dissolve instead of becoming a part of the body once their purpose or task has been fulfilled [113]. During the first stages of the bioactive fixation process, interactions between ionic inorganic species dominate for bioglasses, these interactions increase in number and are also supplemented and later replaced by further interactions between the inorganic surfaces and biomolecules e.g. collagen or tissue growth factors. This leads to a bond forming between the artificial implanted material and the natural tissue located within a patient's body.

Analysis can be carried out on the surface of a material experimentally e.g. NMR [38], IR spectroscopy [39], and neutron and X-ray diffraction [40]. These techniques show microscopic effects and processes occurring at the junction between an implant and the biological medium it is in contact with, with good space and time resolution [121]. In order to gain a deeper insight into how biomaterials function, these processes must be seen at an atomic scale. The atomic scale is where interatomic separations are as small as 0.1 nm with a time resolution of ~ 10^{-6} s or less. It is therefore computer simulations which play a key role to provide a direct route to explore structural and physical properties of materials. Computer simulation techniques are a powerful and invaluable tool when probing the properties of a biomaterial at a level beyond the reach of experimental techniques.

Computers continue to grow faster and more powerful as the years go by. Availability of supercomputers and parallel simulation codes optimized for bespoke systems and scenarios are available and can be used to maximize computing resources [122, 123]. The molecular dynamics method is at the moment a common technique to model relatively large systems and scenarios e.g. periodic solids, liquids, biomolecules etc [124, 125]. Molecular dynamics provides snapshots of a system at different times, where a series of snapshots come together to form a trajectory where a system will evolve over time [124]. These trajectories will form under certain operating conditions e.g. room temperature and pressure [124].

Molecular dynamics simulations carried out in this work are of the classical form which uses predefined force fields [123] which can be used to probe biological systems and materials that contain up to millions of atoms [123, 126] of time length of up to microseconds. The accuracy of this method depends strongly on the force field used during the simulation.

2.1.1 Molecular Dynamics Method

Molecular dynamics involve the numerical integration of classical equations of motion on atoms using Newtonian physics.

$$\vec{F}_i = m_i \vec{a}_i ; \vec{F}_i = - \partial V / \partial \vec{R}_i \ (i = 1, \dots , N) \qquad \text{Eq. 2.1}$$

where $\vec{R}_i$ and $\vec{a}_i$ are the positions and accelerations of atom i, m_i is the mass of the atom i, $\vec{F}_i$ is the total force acting on atom i, and $V = V(\vec{R}_1, \dots , \vec{R}_N)$ is the potential function. The potential function is a key ingredient of an MD simulation. Once the potential V is defined, the above equation allows for the propagation of an initial configuration $\Gamma(0) = \{R(t = 0); P(t = 0)\}$, where $R = \{R_1, \dots , R_N\}$ and $P = \{p_1, \dots , p_N\}$ are the individual positions R_i and momenta p_i, respectively, along discrete subsequent time points, separated by the timestep Δt. The appropriate timestep (Δt) for a MD process depends on the fastest motions that characterize the system. For example, high-frequency vibrations would require the timestep (Δt) to be short enough to limit the errors in the integration of such fast motions, while avoiding an unnecessarily short Δt, which will not waste computational time and power. Depending on the mass of the

lightest atoms in the system, typical values for classical MD simulations range between 0.1 and 10 fs. The positions $\vec{R}(0)$ of atoms at the start of a simulation are defined by placing them in a cubic box where initial velocities to each of the atoms are set to zero. A classical molecular dynamics program, e.g. DL_POLY [37], would by default, apply forces and velocities to the atoms that give rise to the evolution of the total system.

2.1.2 Verlet Algorithm

A simple time progression algorithm is called the Verlet algorithm [124]. This works by including the forward and backwards steps into the progression. The basic idea is to write two third-order Taylor expansions for the positions *r(t)*, one forward and one backward in time. Calling *v* the velocities, *a* the accelerations, and *b* the third derivatives of *r* with respect to *t*, that is:

$$\mathbf{r}(t+\Delta t) = \mathbf{r}(t) + \mathbf{v}(t)\Delta t + (1/2)\mathbf{a}(t)\Delta t^2 + (1/6)\mathbf{b}(t)\Delta t^3 + O(\Delta t^4)$$

Eq. 2.2

$$\mathbf{r}(t-\Delta t) = \mathbf{r}(t) - \mathbf{v}(t)\Delta t + (1/2)\mathbf{a}(t)\Delta t^2 - (1/6)\mathbf{b}(t)\Delta t^3 + O(\Delta t^4)$$

Combining the two equations above produces a final progression giving the following:

$$\mathbf{r}(t+\Delta t) = 2\mathbf{r}(t) - \mathbf{r}(t-\Delta t) + \mathbf{a}(t)\Delta t^2 + O(\Delta t^4) \qquad \text{Eq. 2.3}$$

This is the basic form of the Verlet algorithm. Since we are integrating Newton's equations, *a(t)* is just the force divided by the mass, and the force is in turn only a function of the positions *r(t)*. The velocities can be computed by:

$$\mathbf{v}(t) = \frac{\mathbf{r}(t+\Delta t) - \mathbf{r}(t-\Delta t)}{2\Delta t}. \qquad \text{Eq. 2.4}$$

2.1.3 Microstates and Ensembles

A single configuration (microstate) [124] Γ of a system that contains *N* atoms is shown by six components for each atom i.e. {R} and {P} which are position and momentum vectors. Phase space is defined as all the possible Γ = {R;P} microstates. A molecular dynamics simulation of N_{run} timesteps will form a trajectory {Γ (0), Γ (Δt), Γ

$(2\Delta t),..., \Gamma\ (N_{run}\ \Delta t)\}$ in phase space, which is the order of N_{run} successive instantaneous configurations made by the system throughout its dynamical evolution. The quantity for total energy *E* is conserved during MD, which favours a trajectory in a segment of phase space, where all microstates share the same total energy *E*. The individual configurations of an MD trajectory are all unique and different from one another but they are a part of a common constant energy segment of the phase space. A collection of microstates that share the same total energy or some other different macroscopic quantity form a statistical ensemble [124]. The NVE ensemble is where all microstates have the same number of particles, volume and total energy. NVE ensembles are a natural form to simulate a system via MD. Different ensembles can be generated, e.g. by using an external thermostat or barostat, to give the NVT (canonical) or NPT (isothermal-isobaric) ensemble. Choosing an appropriate ensemble for a simulation depends on the situation requiring investigation. For example the NPT ensemble is an appropriate choice over any other ensemble when wanting to simulate processes in a laboratory, which are carried out at constant temperature and pressure rather than constant volume.

2.1.4 Periodic Boundary Conditions

The numbers of atoms in a real material or system are far too great to be simulated via molecular dynamics techniques, which is due to the computational power employable today. Regardless of how many atoms *N* are simulated for a system computationally, it will always be a fraction compared to the number of atoms found in a real macroscopic sample, of the order of Avogadro's number i.e. ~ 6 x 10^{23}. As a result the ratio between the numbers of atoms found at a boundary and that found in the bulk of the system, would be much higher in a simulated system than in a real system, where almost all atoms would be treated as bulk. An answer to solving this problem is to employ periodic boundary conditions [124] in systems carrying out molecular dynamics simulations. Periodic boundary conditions are applied to a central box of atoms which form the system. This box of atoms is reproduced infinitely along each axis x, y and z and -x, -y and -z. This allows for an atom to leave the central box, which would be mirrored by the image of the same atom in the adjacent box, entering the central box from the opposite side. Using periodic boundary conditions removes boundaries so that every atom in the central box is embedded in a bulk-like environment. The application

of PBC to crystalline solids is always employed as the central box has the symmetry of the periodic unit cell. Periodic boundary conditions are also effective for liquids and disordered solids. For systems that contain disorder, the artificial periodicity created by PBC is a small drawback compared to the advantages in removing fictitious surface effects. Periodic boundary conditions are employed for systems that do not require simulation of surface processes e.g. gas adsorption or reactivity at a solid surface or evaporation of a liquid sample. If quantities listed in the latter wanted to be simulated, one would have to reintroduce an exposed surface via slab geometry. This is where PBC are removed or changed along one direction and only act in two directions [127].

2.2 *Introduction to Potentials*

Amorphous substances create a certain challenge to any predicted potential; this is due to disorder implying a wide range of binding environments [3]. To fit the potential in the first place, there is a "memory" of the structures used to develop any empirical potential. This means that the predicted potential will likely be adequate for structures topologically similar to what was used and included in fitting the database, but on the other hand, could easily be unreliable for different topologies [3]. The desirable ability of a potential to describe a large range of local bonding environments properly, is called *transferability* [3].

2.2.1 Interatomic Potentials

Calculating energies and geometries are also key areas of interest in addition to calculating electronic properties of a structure. In order to investigate and determine such properties, simple classical models can be implemented to illustrate accurately the interatomic interactions. Classical simulations that use interatomic potentials are inexpensive in comparison to quantum-mechanical (QM) methods which take up more time. Classical simulations are founded upon predictions, which when in combination, leads to a system named the Born model of solids [42, 124].

Forces between atoms in space depend solely on their positions, and they can be combined to create a potential energy function. The two key components that relate to the energy of the system is shown in Eq. 2.5

$$E = \frac{1}{2}\sum_{\mathbf{T}}{}'\sum_{A}\sum_{B}\frac{q_A q_B}{|\mathbf{R}_{AB}-\mathbf{T}|} + U^{short-range}(\mathbf{R}_1,...,\mathbf{R}_M). \qquad \text{Eq. 2.5}$$

The long-range-electrostatic interaction between charged species is that found as the first term on the right hand side of the equation. Here q_a and q_b are the charges of atoms A and B. $\mathbf{R_{AB}}$ is the distance between atoms A and B and finally **T** is the translational vector for a system that has lattice. For an amorphous system, the translational vector **T**, is omitted. When or if T = 0, the term with A = B should be absent. A short-range potential is also seen in Eq. 2.5, here it represents other phenomena such as Pauli repulsion, dispersive forces etc. $R_{1, ..., }$ R_m are the locations of M ions present within the system.

2.2.2 Electrostatic energies

When assessing the electrostatic energies of a system, a problem is often stumbled upon regarding the electrostatic sum given as the first term of Eq. 2.5, where it converges only conditionally. This means it is not feasible to calculate the electrostatic energies of the lattice by merely totalling interactions taking place within a sphere, which is relatively large in radius, and to disregard interactions of atoms found outside. If the radius of the sphere is made larger, it is still not possible. An alternative process had therefore been introduced by Ewald (1921) that is generally used instead [42]. This alternative procedure requires separating the conditionally convergent sum into two convergent sections. The first part relates to real space, whereas the second part relates to reciprocal space, and each of the two converge quickly. The first of the two parts can be seen as point charges associated with a Gaussian charge distribution of identical magnitude and opposite sign, which is centred on the point charge, as seen in Fig. 2.1a. The Gaussian charge distributions are seen to partition each of the point charges that each of them are surrounding. This causes the interaction between them to decrease. Equation 2.6 explains this. From Equation 2.6 q_a refers to the charge on atom A and α is a user defined value.

$$\rho_A(\mathbf{r}) = \frac{q_A \alpha^3}{\pi^{3/2}} \exp(-\alpha^2 \mid \mathbf{r} - \mathbf{R}_A \mid^2) \qquad \text{Eq. 2.6}$$

The summation of electrostatic energy of each the point charges with addition to partitioning of Gaussian densities will lead to Equation 2.7:

$$U_{real}^{Coulomb} = \frac{1}{2}\sum_{A,B} q_A q_B \sum_{\mathbf{T}}{}' \frac{\mathrm{erfc}(\alpha |\mathbf{R}_{AB}+\mathbf{T}|)}{|\mathbf{R}_{AB}+\mathbf{T}|} \qquad \text{Eq. 2.7}$$

Here, the error function erfc (x) is given by Equation 2.8:

$$erfc\ (\mathrm{x}) = \frac{2}{\pi^{1/2}} \int_{x}^{\infty} \exp(-t^2)dt \qquad \text{Eq. 2.8}$$

This is a sequence that converges, which can be approximated and condensed in real space.

Fig. 2.1a Fig. 2.1b

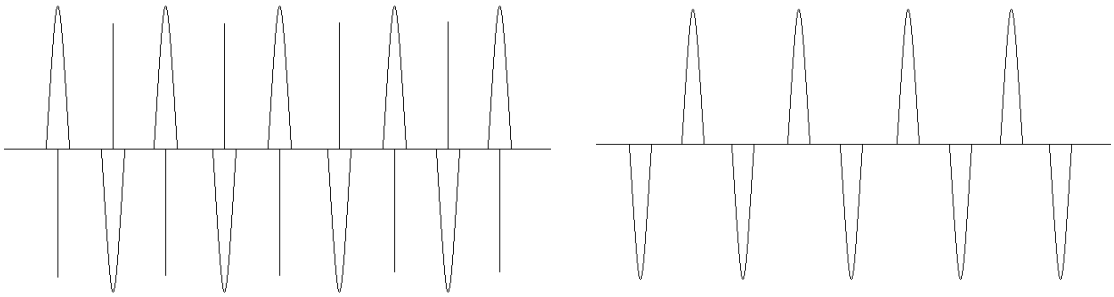

FIGURE 2.1: Ewald sum charge distribution.
a) Energy of distributions in real space.
b) Energy of distributions in reciprocal space.

In addition, another Gaussian charge distribution can be added to maintain charge neutrality. This can be represented in Fig. 2.1b. The second distribution provides an electrostatic energy that is relatively easy to calculate in reciprocal space. This is shown in Equation 2.9.

$$U_{reciprocal}^{Coulomb} = \frac{1}{2}\sum_{\mathbf{G}\neq\mathbf{0}}\sum_{A,B} \frac{q_A q_B}{\pi V_{cell}} \frac{4\pi^2}{G^2} \exp(-G^2/4\alpha^2)\cos(\mathbf{G}\cdot\mathbf{R}_{AB}) \qquad \text{Eq. 2.9}$$

G represents reciprocal space vectors and V_{cell} is volume of the unit cell. Finally, the unauthentic interactions of each of the Gaussian densities with itself, which are included in real space is shown in Eq. 2.10.

$$U_{self-energy}^{Coulomb} = \frac{\alpha}{\pi^{1/2}} \sum_{A} q_A^2 \qquad \text{Eq. 2.10}$$

These must be removed to give the true electrostatic energy:

$$U^{Coulomb} = U_{real}^{Coulomb} + U_{reciprocal}^{Coulomb} - U_{self-energy}^{Coulomb} \qquad \text{Eq. 2.11}$$

2.2.3 Short–range Interatomic potentials

The total short-range energy is expressed in Eq. 2.12. U_{AB} refers to two-body interactions and U_{ABC} refers to three-body interactions. Higher-body interactions require additional terms [118].

$$U^{short-range}(\mathbf{R}_1,...,\mathbf{R}_M) = \sum_{A,B} U_{AB}(\mathbf{R}_A,\mathbf{R}_B) + \sum_{A,B,C} U_{ABC}(\mathbf{R}_A,\mathbf{R}_B,\mathbf{R}_C) + ... \quad \text{Eq. 2.12}$$

One of the most important contributions to short-range forces that are found within two-body interactions that incorporate two diverse effects are 1) the Pauli repulsion interaction between ions due to electronic clouds being in close proximity and 2) the attractive dispersion force usually referred to as London forces or van der Waals attraction, which comes about due to the relationship of electronic motions prevalent in various atoms. Often when simulating semi-ionic or fully ionic systems, the most well-used functional form of short-range two-body potentials is the well-known and established Buckingham potential used for un-bonded species (Equation 2.13) [117, 118]

$$U_{AB}^{Buck}(R_{AB}) = A\exp\left(-R_{AB}/\rho\right) - \frac{C}{R_{AB}^6} \quad \text{Eq. 2.13}$$

Here, symbols A, ρ and C denote adjustable parameters and are constants highly specific towards the structures. The first term in the Buckingham form describes the repulsive interactions which come about due to Pauli forces. The second term represents the attractive interactions due to van der Waals forces. At short distances the repulsive forces dominate over the attractive ones, and therefore are very repulsive between the two bodies.

The Morse potential is a convenient model for the potential energy of a bonded diatomic molecule. The functional form of the potential is:

$$U_{AB}^{\text{Morse}}(R_{AB}) = E_0[\{1-\exp(-k(r-r_0))\}^2 - 1] \quad \text{Eq. 2.14}$$

Here R_{AB} is the distance between the atoms A and B, r_o is the equilibrium bond distance, E_o is the well depth (defined relative to the dissociated atoms), and k controls the 'width' of the potential (the smaller k the broader the well).

2.2.4 Three-body Harmonic Potential

The second of the main contributions to short-range energy is the three-body energy, which is adequate to describe covalent and semi-covalent bonding. This is due to the directional relationships of such interactions. This is expressed as the harmonic potential: (Equation 2.15a)

$$U(\theta_{jil}) = \frac{k}{2}(\theta_{jil} - \theta_0)^2 \qquad \text{Eq. 2.15a}$$

Here θ_0 is the equilibrium angle between three atoms (*j*, *i* and *l*) and *k* is a fitted constant (see Figure 2.2). A modified alternative version of harmonic potential is the truncated three-body harmonic potential, which has the following form.

$$U(\theta_{jil}) = \frac{k}{2}(\theta_{jil} - \theta_0)^2 \exp[-(r_{ij}^8 + r_{il}^8)/\rho^8] \qquad \text{Eq. 2.15b}$$

A diagram i.e. Figure 2.2 is given to describe further the individual terms in Eq 2.15a, 2.15b and 2.15c below:

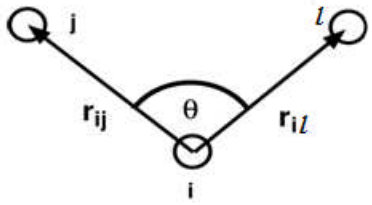

Fig. 2.2

The difference between Equation 2.15a and 2.15b is the additional exponential term. ρ is a constant, whereas r_{ij} are the bond distances between atoms i and j and r_{il} are the bond distances between atoms i and l.

A screened three-body harmonic potential is also expressed in the equation below (Eq 2.15c) Extra constants ρ_1 and ρ_2 terms are present.

$$U(\theta_{jil}) = \frac{k}{2}(\theta_{jil} - \theta_0)^2 \exp[-(r_{ij}/\rho_1 + r_{il}/\rho_2)] \qquad \text{Eq. 2.15c}$$

Four-body interactions show little contribution towards the total energy of ionic or semi-ionic systems, so they are in fact typically only used to model some polyanions. They are not used in this work.

Short-range interactions decrease to zero very quickly as interatomic distances increase. This means that we can assume, not all atoms interact with one another, but instead with only those atoms held within some distance R_c. This cut-off radius, R_c, must be great enough in order to include all atomic interactions and those outside of this region will be assumed to have insignificant effect [117, 118], and be set to zero.

2.2.5 The shell model

The rigid-ion model (RI) models point charges [124], which carry no dipole moments. The shell model for atomic polarisability was proposed by Dick and Overhauser [128]. Here the ions are treated as a pair of charges, Figure 2.3, connected by an elastic spring.

Fig 2.3: Core-Shell model of an Ion.

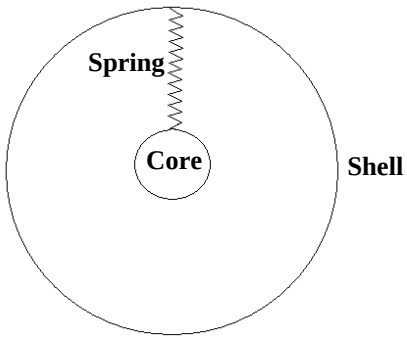

The core is where the majority of mass is located and has a positive charge, X, as opposed to the shell which surrounds the heavy core. The shell has very little mass relative to the core. Core and shell charges are of opposite *sign* but their absolute values are different. The charges X and Y are not interacting via Coulombic forces but instead using a harmonic spring force which attaches the two sites together. The harmonic spring has a constant k.

$$U_A^{core-shell} = \frac{1}{2} k \left| \mathbf{R}_A^{core} - \mathbf{R}_A^{shell} \right|^2 \quad \text{Eq. 2.16}$$

The coordinates of the core and shell of the polarisable ion are taken as R_A^{core} and R_A^{shell}. The sum of the charges of the core and the shell equals the charge of the whole ion.

As the short-range forces of interaction are solely due to the forces of attraction/repulsion of electron clouds, short-range forces will in turn act between individual shells. As the distance between the core and shell are increased, in a larger dipole moment of the ion will occur. It is exemplified in Equation 2.17, where the polarisability α of the ion in this model is given.

$$\alpha = \frac{Y^2}{k} \qquad \text{Eq. 2.17}$$

The shell model has been highly successful in a large range of condensed phase systems. It has been used in ionic solids and liquids as well as their interfaces to aqueous solutions [129-134]. The shell model has been extended to model silicate glasses by the work of A. Tilocca *et al* [81-83, 116]. Simulations carried out using the shell model give a better representation of medium-range order, needed for network connectivity and clustering, as shown by a comparison of shell-model and rigid ion potentials carried out by Tilocca [41].

2.2.6 Friction in core-shell term

When the oxygen core-shell velocities increase, the kinetic energy of the core-shell rises thus an unphysical increase in temperature of the core-shell is observed due to friction. The frequency of oscillation of the core shell increases. To remove this increase in kinetic energy between the core and shell through the spring, it is important to add a dampener to the spring so that if a rise in kinetic energy is observed for the core-shell, the dampener will rid the core-shell system i.e. the spring, of any excess kinetic energy, thus resulting in an overall decrease in kinetic energy for the core-shell system.

Modifications were introduced into FORTRAN modules found within DL_POLY 2.20 [37, 129] by Antonio Tilocca. The addition of 'friction' was unique in the sense that DL_POLY 2.20 did not originally contain this term. The 'friction' term was added to the program so that if a system being modelled contained oxygen core-shell entities, 'friction' would decrease the temperatures between the core-shell if high kinetic energies / temperatures are gained during simulation. This 'friction' term therefore served as buffer to high temperature gains between oxygen core-shells in the simulation. If the temperature of the core-shell became too high it would cause the spring between the core-shell to break and result in the light mass shell displacing itself far away from

its dense heavy massed core. This resulted in a system crash and thus was introduced in order to prevent simulations of hydrated glasses from crashing as they proved fragile to simulate compared to the unhydrated forms.

$$U_A^{core-shell} = \frac{1}{2} k \left| \mathbf{R}_A^{core} - \mathbf{R}_A^{shell} \right|^2 \qquad \text{Eq. 2.16}$$

$$m_s \frac{d^2x}{dt^2} + c\frac{dx}{dt} + k_{cs}x = 0 \qquad \text{Eq. 2.18}$$

Equation 2.18 shows the frictionally dampened equation of motion for oxygen shells O_s, which includes the force contributions from the core shell interaction. m_s is the mass of the shell at (0.2 a.u), x is the shell displacement of the core along the core-shell axis, c is the dampening coefficient and finally k_{cs} is the core shell spring constant (74.92038 eV $Å^{-2}$).

2.3 *Simulation Methods*

2.3.1 Creating "Random Supercell Structures"

Initial structures were created before molecular dynamics simulations could be carried out. The initial structures were created by placing only the necessary number of atoms for each element within a cubic box. These atoms were quasi-randomly distributed within the cubic box using a computer software program designed especially for such a task. For example, one would like to re-create the YAS17 [42] glass system. YAS17 has the following stoichiometry: 17.1 mol % Y_2O_3, 18.96 mol % Al_2O_3, and 63.94 mol % SiO_2. This corresponds to 92 Y_2O_3, 102 Al_2O_3 and 344 SiO_2 groups, or 184 atoms of yttrium, 204 atoms of aluminium, 344 atoms of silicon and lastly 1270 atoms of oxygen if we want ~2000 atoms. All of these atoms are placed into the cubic box quasi-randomly, where the dimension of the cubic box is adjusted to replicate the experimental density of 3.2 g/cm^3 in the YAS17 glass system. The cubic box for this glass would therefore have a box length of 29.97 Å. In order to prevent the atoms from starting unphysically close together, atoms were not initially placed closer than 80% - 90% of their typical interatomic distance. The same procedure is used when creating initial configurations for yttrium bioglasses, YBG, either with or without phosphorus.

The procedure used for creating initial random configurations for hydrated glasses does not differ much. Before atoms for each element are placed into the cubic box one by one, as previously discussed, we instead first insert the hydroxyl groups. The number of hydroxyl groups being inserted into the cubic box depends on the glass composition and level of hydration required. For example, if one would like to create a hydrated version of the bulk glass YAS17, one first would need to consider by how much one would like to hydrate the glass without harming or manipulating any of the stoichiometries previously stated for YAS17 (17.1 mol % Y_2O_3, 18.96 mol % Al_2O_3, and 63.94 mol % SiO_2). By taking the BULK glass we need to figure out the total number of oxygen atoms present in our system i.e. 1270. In order to hydrate the glass with 100 hydroxyls, we would take 50 oxygen atoms away from the bulk glass i.e. 1270 – 50 = 1220 oxygen atoms remain, and add 100 hydroxyl groups where each new oxygen is attached to a hydrogen atom with an interatomic distance of 1 angstrom. Charge neutrality is maintained. If we want to hydrate the glass with 200 hydroxyl groups we would again take the total number of oxygen atoms in the bulk glass of

YAS17 at 1270 and subtract by 100 this time, therefore giving 1170 remaining oxygen atoms, which will be replaced by 200 hydroxyl groups, and so on. This is an easy method carried out in order to maintain electro-neutrality and prevent instability in the glass system. Once all hydroxyl groups have been placed within the box, constraints are put in place so each of the hydroxyl groups are placed at least 5.0 angstroms away from one another to prevent unphysical interactions and energies from forming. Once this has been done, the cubic box containing hydroxyl groups will have the other atoms i.e. silicon, aluminium, yttrium and finally oxygen which remain unattached to hydrogen, silicon, aluminium and yttrium. The system containing all of these atoms is forced to recreate the correct physical density of the hydrated glass by reference to varying the cubic box length as previously discussed. Again, in order to prevent the atoms from starting unphysically close together, atoms were not initially placed closer than 80% - 90% of their typical interatomic distances. The same procedure is used for creating initial random configurations for hydrated yttrium bioglasses with and without phosphorus i.e. YBG. The densities chosen for YAS and YBG glasses are discussed in sections 4.0, 5.1 and 5.2 respectively.

2.3.2 Method for Simulating Non-hydrated Yttrium Silicate Glasses

Molecular dynamics simulations were carried out using the DL_POLY 2.20 program [37, 129]. The time step involved in such simulations is 0.2 fs. The long-range Coulombic interactions were calculated using the Ewald summation cut-off of 12 Å and the short-range interatomic potentials were truncated at 8Å.

$$U_{AB}^{Buck}(R_{AB}) = A\exp\left(-R_{AB}/\rho\right) - \frac{C}{R_{AB}^{6}} \qquad \text{Eq. 2.13}$$

Buckingham interatomic potentials (Eq 2.13) are known to exhibit a disadvantage. At small distances of R, the power term dominates the exponential term which creates a potential well. This forces atoms within the pair to approach each other at unphysically close distances.

Once the initial random structure has been generated, molecular dynamics simulations are then carried out upon it. The melt-quench method is used to prepare the model. The glass is computationally formed by rapid cooling of a high-temperature

liquid, which results in the structure freezing in position instantaneously.

The random initial structure is kept at 3500K for 200ps under an NVT trajectory, which is carried out to equilibrate the model above its melting temperature. The model is then cooled continuously to 300K at nominal cooling rate of 10K/ps. After this step the model would then undergo a further equilibration run at 300K for 300ps. The first 200ps of the 300K run is discarded. The last 100ps formed the production run from which a number of configurations are extracted that are uniformly spaced every 50 fs. This methodology has been used to simulate reliable models of types of glasses [41, 42, 75, 81-83, 113, 116] , which compare well to experiment.

The same procedure is used for simulating Yttrium bioglasses with and without phosphorus i.e. YBG.

2.3.3 Method for Simulating Hydrated Yttrium Silicate Glasses.

Once the initial random structure has been generated for hydrated glasses, molecular dynamics simulations are then carried out. The melt-quench method was used to prepare the model; however, very high melting temperatures were not used due to the weakness or sensitivity of hydrogen within the system causing instability. The glass is computationally formed by rapid cooling of a gently heated hydrated liquid, which results in the structure freezing in position instantaneously. The random initial structure would first undergo a 'four phase zero' stage (Figure 2.4) where the structure undergoes an energy minimisation at each of the four stages allowing for atoms to adjust within the structure so unphysical interactions and energies are eliminated. The first stage of the 'four phase zero' was carried out for 2ps i.e. over 10,000 0.2fs steps at zero kelvin where the hydroxyl groups are frozen in place. After this step, a second zero is carried out at a temperature of 300K, again the hydroxyl groups are still frozen in place but other atoms are allowed to remain mobile. Once the second phase has completed phase one and two are repeated in the exact same manner. After the fourth zero had been completed the configuration was then taken and allowed to reach a temperature of 300K for 300ps with a timestep of 0.2fs over 1,500,000 steps under an NVT trajectory, the hydroxyl groups from this stage forward were allowed to move freely and naturally under the interatomic forces. This step is carried out to equilibrate the model at room temperature. After completion of the previous step the model is heated to 600K for 300ps with a

timestep of 0.2fs over 1,500,000 steps. After heating at 600K had completed, the structure is further heated to 900K for 300ps with a timestep of 0.2fs over 1,500,000 steps. If the system crashed at 900K the system would undergo a 'single phase zero' (as carried out earlier during the four-phase zero procedure) to minimise any high energies, which were the likely cause of the crash in the first place. After the 'single phase zero' the system is then heated again at 900K for 300ps at a rate of 0.2fs over 1,500,000 steps. After successful equilibration at 900K, the configuration is cooled continuously to 300K at nominal cooling rate of 10K/ps. After this step the model would undergo a last equilibration run at 300K for 300ps. The last 100ps at 300K run formed the production run that can be analysed for the purpose of obtaining results.

The same methodology is used for simulating hydrated yttrium bioglasses (YBG). The 'four phase zero' is first carried out and heating for 300ps at each temperature stage: 300K, 600K, 900K and 1200K takes place. The only differences here are that each of the yttrium bioglass models were able to reach higher heating temperatures of 1200K instead of 900K for YAS glasses. The same cooling rate was used i.e. 10K/ps. After cooling a production run was carried out for 100ps at 300K, where positions of atoms, trajectories, are required for giving results.

Figure 2.4: Four-phase-zero / Heating and Cooling of Yttrium Containing Glasses

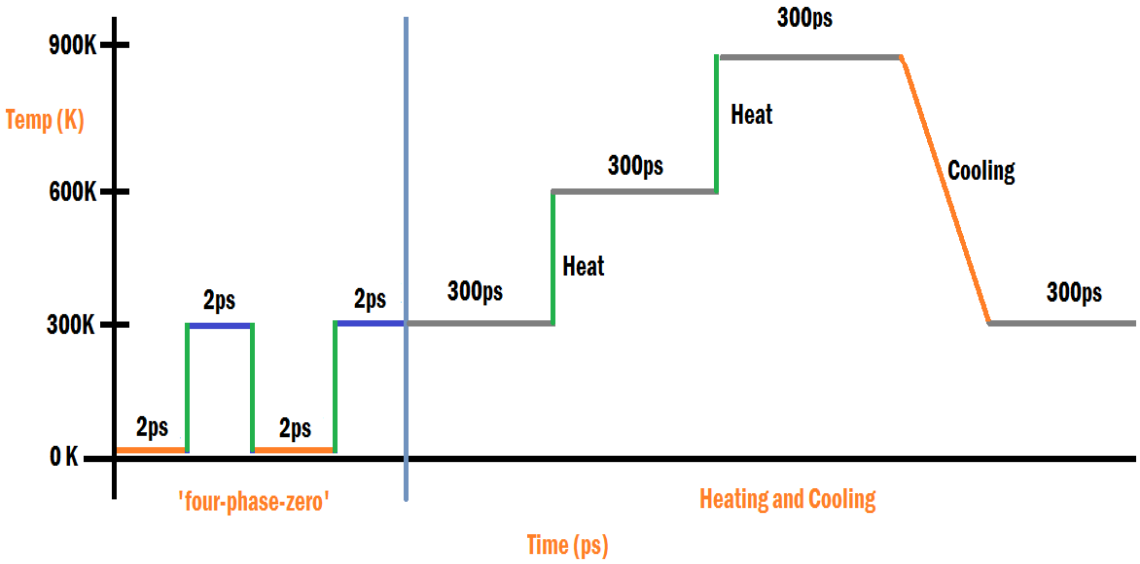

2.4 *Calculating Buckingham Potentials via GULP*

2.4.1 Standard Fitting

In order to produce results of a proposed system/simulation using interatomic potentials [131-134], it is important to derive and obtain a reliable set of potential parameters for the system in question. There is much data available, published within the literature, with reference to interatomic potentials that could be important for the system in question. However for more bespoke systems, potentials may need to be derived in order to carry out MD. There are two main methods by which interatomic potentials are fitted. GULP [135] facilitates fitting empirical interatomic potentials through reproducing experimental data as well as being derived from data achieved through calculations that may have been run from *ab initio* simulations. For the purpose of this project, fitting from experimental data was carried out rather than using *ab initio*. The key value to note when fitting interatomic potentials are the sum of squares (defined in Eq. 2.19) regardless of what type of fitting one considers taking. The sum of squares is essentially the quantity used to measure the quality of fit carried out by GULP. One should hope to have the sum of squares converge to zero at the end of fitting the interatomic potential of the system in question. Usually when a process like this is implemented only in a few cases the sum of squares can converge to zero and this is often found when interatomic potentials fully reproduce experimental data, this is found for example when fitting a Morse potential to a bond length, frequency or dissociation energy. The sum of squares is shown as F in the equation below:

$$F = \sum_{\text{all observables}} w(f_{\text{calc}} - f_{\text{obs}})^2 \qquad \text{Eq. 2.19}$$

Quantities f_{calc} and f_{obs} are the calculated and observed values of given observables, where w denotes the weighting factor. There are an infinite number of possible fits, depending upon weighting factors. The weighting factor for each observable depends on different things, for example, reliability of data (i.e. a crystal structure proves more reliable as compared to an elastic constant measurement) and relative number of the quantities. One varies interatomic potentials parameters in order to acquire the lowest

sum of squares value to fit the potential. In order to solve the least squares problem, GULP uses a Newton-Raphson [135] functional minimisation approach. Minimising the sum of squares is usually performed using numerical first derivatives. Properties that are derived using second derivatives are hard to employ for analytical derivatives. The gradient norm (Gnorm) is a value given from the output file of GULP after having completed a fitting procedure.

2.4.2 Relaxed Fitting

When fitting interatomic potentials, obtaining an improved sum of squares does not necessarily mean that the result (fit) will be considered to be of better quality. This is based on ones judgement upon fulfilling certain measures relating to the fitting process. A conventional way is to compare and contrast the optimised structural parameters using the fitted potential to the initial experimental structural parameters instead of looking directly at the forces calculated. It is worth noting that a relaxed fit can be started if a reasonable set of interatomic potential parameters are achieved within a certain range. Here energy minimisation will be easier to achieve. A conventional fit should usually be carried out first to obtain an approximate set of parameters. Once an approximate set of parameters are found then those parameters are put in place of ones previously used and are re-fitted again but also using keyword ‘relax’.

2.5 *Molecular Dynamics Simulation Details for Yttrium Containing Glasses*

2.5.1 Molecular Dynamics Simulation Details for YAS Glasses

Throughout we used the following interatomic potentials. Parameters given in Table 2.1 are Buckingham potentials (BP) developed by M. J. Sanders, M. Leslie and C. R. A. Catlow [134] for crystalline SiO_2 (i.e. Si_{core} — O_{shell} and O_{shell} — O_{shell}) and those by A. Tilocca, N. H. de Leeuw and A. N. Cormack [133]. Other potential parameters i.e. Al_{core} — O_{shell} and Y_{core} — O_{shell} [115] were developed using the shell model approach. The latter set of BP parameters were fit using the General Utility Lattice Program (GULP) [135] in previous research and are summarised in Table 2.3.

The short range interaction of aluminum cations with oxygen shells (Al_{core} — O_{shell}) were shown by an additional Buckingham function (Table 2.3). The parameters of the Buckingham potential were fitted to the crystal structures of three aluminosilicate structures (α, β, γ) — Al_2SiO_5, and two yttrium aluminate structures $Y_3Al_5O_{12}$, using GULP [135]. The short-range interaction of yttrium cations with oxygen (Y_{core} — O_{shell}) shells were also represented by an additional Buckingham function (Tab. 2.3). The parameters of the Buckingham potential were fitted to the crystal structures of four yttrium disilicate structures (α, β, γ, δ) — $Y_2Si_2O_7$, and two yttrium aluminate structures $Y_3Al_5O_{12}$, using GULP [135]. All of these potentials were incorporated into the FIELD files of DL_POLY.

The charges of the elements are summarised in Table 2.4.

Table 2.5 shows the oxygen core-shell harmonic spring potential. The spring constant used in the shell model is one which connects the core (X) and shell (Y) together.

Table 2.6 shows the truncated three-body O_{shell} — Si_{core} — O_{shell} harmonic potential and Table 2.7 shows the screened three-body O_{shell} — Al_{core} — O_{shell} harmonic potential.

Table 2.1: Buckingham Potential Parameters ($Si_{core} - O_{shell}$ / $O_{shell} - O_{shell}$)

Buckingham Potential Parameters [134]			
Species	**A (eV)**	**ρ (Å)**	**C (eV Å ^{6})**
$Si_{core} - O_{shell}$	1283.9100	0.3205	10.6616
$O_{shell} - O_{shell}$	22764.3000	0.1490	27.8800

Table 2.2: SM1 Buckingham Potential Parameters ($Al_{core} - O_{shell}$ / $Y_{core} - O_{shell}$)

SM1 Buckingham Potential Parameters			
Species	**A (eV)**	**ρ (Å)**	**C (eV Å ^{6})**
Al_{core} - O_{shell} [136]	1460.300	0.2991	0.0000
Y_{core} - O_{shell} [118]	1519.279	0.3291	0.0000

Table 2.3: SM2 Buckingham Potential Parameters ($Al_{core} - O_{shell}$ / $Y_{core} - O_{shell}$)

SM2 Buckingham Potential Parameters			
Species	**A (eV)**	**ρ (Å)**	**C (eV Å ^{6})**
Al_{core} - O_{shell}	1567.9521	0.2991	0.0556
Y_{core} - O_{shell}	1444.8360	0.3470	0.1000

Table 2.4: YAS Identity of Species, Core/Shell, Mass and Charges

Element	**Species**	**Charge**	**Mass (au)**
silicon	Core	+4	28.0388
aluminium	Core	+3	26.9820
yttrium	Core	+3	88.9060
oxygen	Core	+0.84819	15.8000
oxygen	Shell	–2.84819	0.2000

Table 2.5: The Core-Shell Harmonic Potential ($O_{core} - O_{shell}$)

Core – Shell Harmonic Potential [42, 71]	
Species	**k_{cs} (eV Å $^{-2}$)**
$O_{core} - O_{shell}$	74.92

Table 2.6a: Truncated three body harmonic potential (O_{shell} — Si_{core} — O_{shell})

Truncated Three-body Harmonic Potential [133]					
Interaction	**k (eV rad^{-2})**	**θ_0 (deg)**	**$Si_{core} - O_{shell}$ (Å)**	**ρ (Å)**	**$O_{shell} - O_{shell}$ (Å)**
O_{shell} — Si_{core} — O_{shell}	6.15	109.47	1.95	1.0	2.5

Table 2.6b: Screened three-body harmonic potential (O_{shell} — Al_{core} — O_{shell})

Screened Three-body Harmonic Potential						
Interaction	**k (eV rad^{-2})**	**θ_0 (deg)**	**ρ_1 (Å)**	**ρ_2 (Å)**	**$Si_{core} - O_{shell}$ (Å)**	**$O_{shell} - O_{shell}$ (Å)**
O_{shell} — Al_{core} — O_{shell}	100.00	109.47	1.00	1.00	1.95	2.2

Table 2.7: Friction term in modified DL_POLY 2.20 for oxygen shells O_s

Friction	
Friction (kg/s)	40.00

2.5.2 Molecular Dynamics Simulation Details for YBG glasses

The following potentials were used to simulate unhydrated and hydrated glasses.

Table 2.8: Yttrium Bioglass Buckingham Potential Parameters

Buckingham Potential Parameters			
Species	**A (eV)**	**ρ (Å)**	**C (eV Å ^{6})**
[134] $Si_{core} - O_{shell}$	1283.9100	0.32050	10.6616
[115, 137] $P_{core} - O_{shell}$	1120.09133	0.334772	0.00000
[115, 137] $Y_{core} - O_{shell}$	1444.8360	0.34700	0.10000
[115, 137] $Ca_{core} - O_{shell}$	2152.3566	0.309227	0.09944
[115, 137] $Na_{core} - O_{shell}$	56465.3453	0.193931	0.00000
[134] $O_{shell} - O_{shell}$	22764.3000	0.14900	27.8800
[131] $Si_{core} - OH_{shell}$	983.560	0.321	10.662
$P_{core} - OH_{shell}$	814.2000	0.334772	0.00000
$Ca_{core} - OH_{shell}$	1222.715	0.309227	0.09944
$Na_{core} - OH_{shell}$	47095.911	0.193931	0.00000
[138] $OH_{shell} - O_{shell}$	22764.300	0.149	13.940
[138] $OH_{shell} - OH_{shell}$	22764.300	0.149	6.970

Table 2.9: Morse Potential ($H - OH_{shell}$)

Morse Potential [138]			
Intra- molecular	**D/eV**	**(Å)**	**R_o**
$H - OH_{shell}$	7.0525	3.1749	0.9485

Table 2.10: Intra-molecular Columbic interaction (%) ($H - OH_{core}$)

Intra-molecular Columbic interaction (%)[138]	
$H - OH_{core}$	100

Table 2.11: Core-Shell Harmonic Potential ($O_{core} - O_{shell}$ / $OH_{core} - OH_{shell}$)

Core – Shell Harmonic Potential	
Species	**k_{cs} (eV Å $^{-2}$)**
[133] $O_{core} - O_{shell}$	74.92
[138] $OH_{core} - OH_{shell}$	74.92

Table 2.12: YBG Identity of Species, Core/Shell, Mass and Charges

Element	**Species**	**Charge**	**Mass (a.u)**
silicon	Core	+4	28.0388
phosphorus	Core	+5	30.974
yttrium	Core	+3	88.9060
sodium	Core	+1	22.990
calcium	Core	+2	40.078
oxygen	Core	+0.84819	15.8000
oxygen	Shell	–2.84819	0.2000
hydroxy-oxygen	Core	0.900	15.800
hydroxy-oxygen	Shell	-2.300	0.200
hydrogen	Core	0.400	1.008

Table 2.13: Screened three-body harmonic potential (O_{shell} — Si_{core} — O_{shell} / O_{shell} — P_{core} — O_{shell})

Screened Three-body Harmonic Potential [115, 137]						
Specie	**k (eV rad^{-2})**	**θ_0 (deg)**	**p_1 (Å)**	**p_2 (Å)**	**$Si_{core} - O_{shell}$ (Å)**	**$O_{shell} - O_{shell}$ (Å)**
O_{shell} — P_{core} — O_{shell}	50.000	109.47	1.00	1.00	1.95	2.2
O_{shell} — Si_{core} — O_{shell}	100.000	109.47	1.00	1.00	1.95	2.2

2.6 *Relevant Data*

2.6.1 Coordination

The coordination number of an atom in a molecule or crystal is the number of its nearest neighbours, determined by simply counting the other atoms to which it is bonded (by either single or multiple bonds). For example, [SiO_4] has Si as its central cation, and a coordination number of 4. Figure 2.5 demonstrates what [SiO_4] looks like in a typical tetrahedral arrangement. Fig 2.5 shows each oxygen satisfying one bond to the central Si.

Figure 2.5

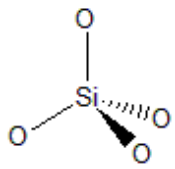

The cutoff distances used while calculating coordination for hydrated and unhydrated YAS, YBG and YBG-P glasses are given below where O are normal oxygens and OH are hydroxyl oxygens:

YAS Cutoffs:	Si - O/OH: 2.00	Al- O/OH: 2.35	Y- O/OH: 3.00
YBG Cutoffs:	Si - O/OH: 2.00	P- O/OH: 2.00	Y- O/OH: 3.00
	Ca- O/OH: 3.20	Na- O/OH: 3.20	
YBG-P Cutoffs:	Si - O/OH: 2.00	P- O/OH: 2.00	Y- O/OH: 3.00
	Ca- O/OH: 3.20	Na- O/OH: 3.20	

2.6.2 Radial Distribution Function

The radial distribution function (or RDF) describes how, on average, the atoms in a system are packed around each other. This is an effective way of describing the average structure of a disordered molecular system such as amorphous solids. For liquids, where there is continual movement of the atoms and a single snapshot of the system shows only the instantaneous disorder, it is extremely useful to be able to deal with the average structure.

The RDF is plotted as a function of the distance between two atoms. A typical RDF plot shows a number of important features. Firstly, at short interatomic distances

the RDF is zero. This indicates the effective width of the atoms, since they cannot approach each other any more closely. Secondly, a number of obvious peaks appear which indicate that the atoms pack around each other in 'shells' of neighbours. The occurrence of peaks at long range indicates a high degree of ordering. Usually, at high temperature the peaks are broad, indicating thermal motion, while at low temperature they are sharper. They are particularly sharp in crystalline materials, where atoms are found at well-defined interatomic distances. At very long range amorphous RDF's tend to a value of 1, which happens because the RDF describes the average density at this range.

2.6.3 Connectivity (Q^n)

The number n of bridging oxygen (BO) atoms associated with the SiO_4 tetrahedron is an important index when describing the glass structure. The Q^n is defined as a species that has n bridging oxygens (BO) bonded to it. For example, a Q^3 species of silicon, is a silicon with three bridging oxygens (BO) from either O-Si or O-Al and one non-bridging oxygen (NBO) from O-Y in the SiO_4 tetrahedron. The Q^n distribution shows the percentage of tetrahedra with n BO. MD simulations allow the calculation of Q^n distributions by computational analysis and direct comparison to NMR. Figure 2.6a demonstrates how, for example, the silicon network connectivity varies due to an increase in the number of non-bridging oxygens (NBO's) found by O-Y species bridging to the central silicon.

Fig 2.6a:

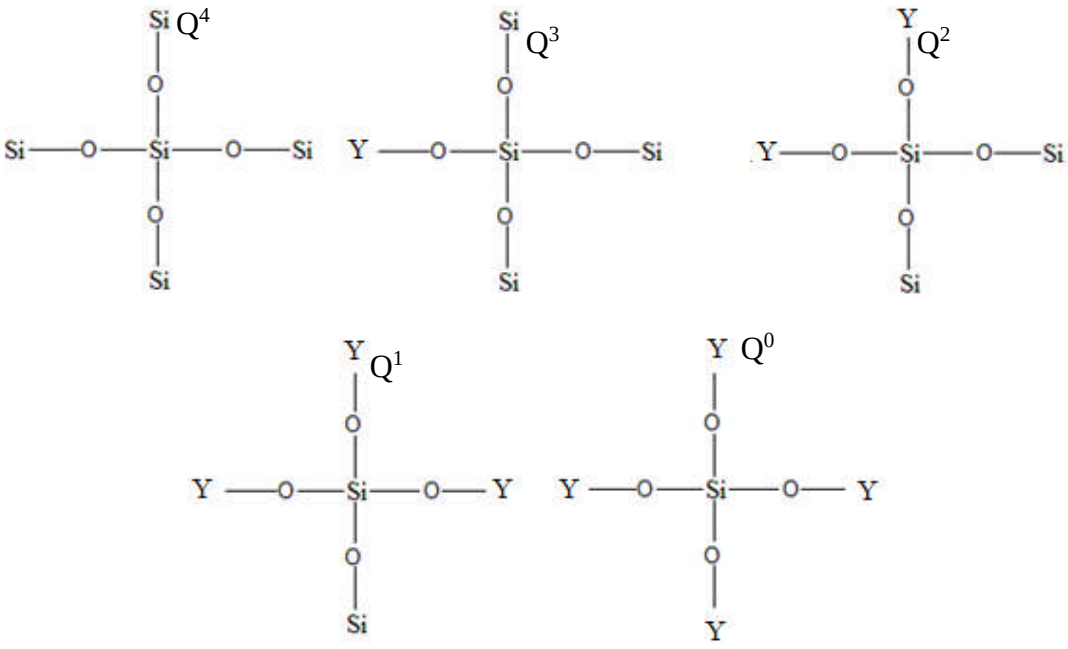

Al Q^n distributions are also accounted for. Here the central network former cation Si is replaced by Al and the surrounding bridging oxygens can be O-Al or O-Si. The non-bridging oxygen atoms are still O-Y. It is also worth noting that Al within glasses generally posses higher coordination numbers (between four and six) than silicon which typically has a well-defined coordination of four.

The above cases and figures are true for bulk glasses which do not contain any hydration. If the bulk glass were hydrated then another species i.e. – OH, would be one that can be incorporated into the Q^n speciation for both Si and Al. Figure 2.6b shows an example of how Q^n species of Si are affected by an increase in coordination of hydroxyl groups to the silicon atom. The same stands true for Al if aluminium possessed the central position in the below diagrams instead of silicon.

Fig 2.6b:

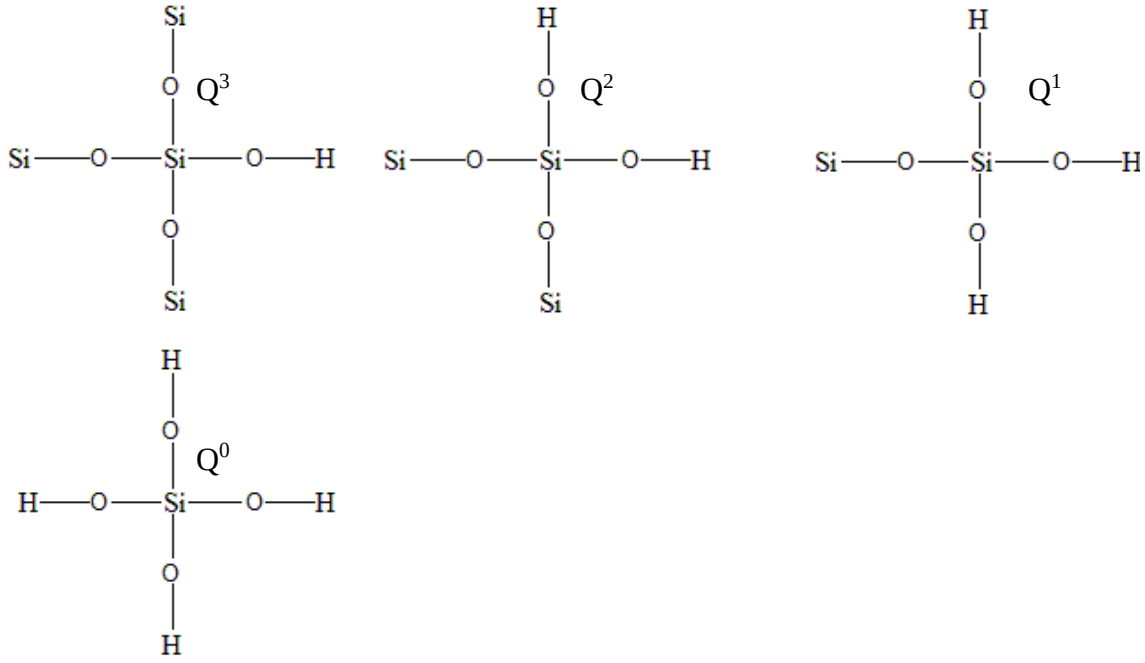

The partial A-B Q^n is defined as the number n of A-O-B linkages which start from the same atom of type A and lead to an atom of type B. Each A-O-B linkage is counted, even if two or more share the same central oxygen atom. If three- and higher-coordinated oxygen atoms exist, this definition of partial Q^n can exceed the A-O coordination number, and in that case the sum of the partial Q^n is not equal to the total Q^n.

2.6.4 Bond Angle

The position of each atom is determined by the nature of the chemical bonds by which it is connected to its neighbouring atoms. The molecular geometry can be described by the positions of these atoms in space, evoking bond lengths of two joined atoms and bond angles of three connected atoms. The bond length is defined to be the average distance between the centres of two atoms bonded together. A bond angle is the angle formed between three atoms across at least two bonds. Figure 2.7a shows between what species bond angles are measured.

Fig 2.7a.

From Figure 2.7a it is seen that bond angles are measured between a central atom and two oxygen anions. The same bond angle is measured for Yttrium i.e. O – Y – O.

Fig 2.7b.

In Figure 2.7b other bond angles are also measured. The central oxygen anion is surrounded by either Al or Si and hydrogen i.e. Si – O – H and Al – O – H . The same bond angle is measured for that of Y – O – H.

2.6.5 Clustering

The distribution of the cations on the medium-range length scale is important for the glass durability in solution. Clustering and aggregation on these length scales has been suggested [84, 85] as an inhibitor of bioactivity in bioactive glasses, where it is also known that clustering of modifiers affect ionic transport [86].

If one wanted to compare clustering between two differing glass compositions which contain different amounts of e.g. Si and Y ions, direct comparison of the raw radial-distribution functions of such cations proves difficult to expose the relative

differences. The observed coordination number (N_{MD}) is the integral of the radial distribution function up to its first minimum for a pair of atoms (A-B), can be compared to that expected if the same density of ions were positioned randomly and uniformly throughout the glass structure. If atoms of one type of species are homogeneously distributed throughout the glass model, and the nearest-neighbour distance cut-off were r_c, then the homogeneous coordination number N_{hom} would be (4/3) π r_c^3 p, where p is the number density of the specific type of atoms [139]. N_{MD} can be compared to this value, where the ration r= N_{MD} / N_{hom} can be used as a measure of clustering, with deviations from unity denoting clustering [140, 141]. CN_{A-B} is the coordination number between atoms A and B, where A is the central atom. N_A is the total number of atoms of species A and finally V_{box} is the total volume of the box.

$$R_{A-B} = \frac{N_{MD}}{N_{hom}} = \frac{CN_{A-B} + 1}{\frac{4}{3}\pi r_c^3 \frac{N_B}{V_{box}}} \qquad \text{Eq. 2.20}$$

In principle, this analysis can be used with respect to any distance, but for the purpose of this work we used the cutoff distance r_c which denotes the first coordination shell, as this is where the nanoscale aggregation we are interested in will be apparent.

2.6.6 Field Strength

Dietzel in 1942 examined direct Coulombic interactions [115] i.e.

$$U_{ab} = (z_a e)\,(z_b e) / (r_a + r_b)^2 \qquad \text{Eq. 2.21}$$

U_{ab} is the attractive force between two charged (z_a and z_b) ions a and b. Where r is the radius of the ion. Dietzel categorized cations using

$$F.S = z_a/r^2 \qquad \text{Eq. 2.22}$$

Where F. S is the field strength with respect to the charge of ion a and its atomic radius r.

3 Results & Discussion

3.1 *Bulk Yttrium Aluminosilicate Simulations*

The purpose of simulating YAS17 using SM1 and SM2 was to verify which set of potentials performs best at modelling YAS17 glass system. This is by looking at results such as bond distances, coordination, Q^n distributions etc. Whichever set of potentials (SM1 or SM2) performs best at modelling the YAS17 will be used to simulate other YAS glasses in future work.

A total of four MD simulations were completed on the same composition of glass. The glass composition used for this study was YAS17. YAS17 is a yttrium aluminosilicate with the composition of: 17.1 mol % Y_2O_3, 18.96 mol % Al_2O_3 and 63.94 mol % SiO_2 and a density of 3.2g/cm^3. YAS17 has been thoroughly investigated by the work of Christie and Tilocca [42]. Their work provided a foundation of what one could expect for the simulations in this work. Each of the four simulations was completed using the potentials from Tables 2.1 – 2.6 in section 2.4.4. Each of the four simulations required new starting random initial configurations (see section 2.4.1). The first two of the four simulations were carried out using the Al – O and Y – O potentials of Catlow and Bush (SM1) (section 2.4.4 (Table 2.2)). The remaining two simulations were carried out using the Al – O and Y – O potentials fitted by us using GULP (SM2) (section 2.4.4 (Table 2.3)). All four simulations followed the procedure in section 2.2.2. For the purpose of this work, the first two simulations that were carried out using the Al – O and Y – O potentials of Catlow and Bush [136] will be called **SM1** i.e. Shell-Model 1. The remaining two simulations carried out using the Al – O and Y – O potentials calculated by us will be called **SM2** i.e. Shell-Model 2.

The results for the two simulations carried out for each of the potentials were averaged. The purpose of this was to enhance further the statistical analysis of results and therefore increase reliability. Standard deviations were obtained by averaging the results over two models where applicable. A single set of data is therefore presented for each potential type used. The results of YAS17 modelled via SM1 were compared against YAS17 modelled via SM2 which were compared to YAS17 modelled via the Teter potential [42] which is a rigid-ion model, rather than shell-model.

3.1.1 Short-range structure

The coordination numbers for cation-oxygen atom pairs are shown below in Table 3.1. The comparisons have been made between models simulated using SM1 and SM2. Another comparison has been made to the work by Tilocca and Christie examining YAS17 bulk glasses modelled via the Teter potential [42]. The pair-distribution functions are given in Figures 3.1 – 3.4. The bond-angle distributions are seen in Figures 3.5 – 3.7.

Figure 3.1: YAS17 SM1 vs. SM2 Si – O Pair Distribution Function

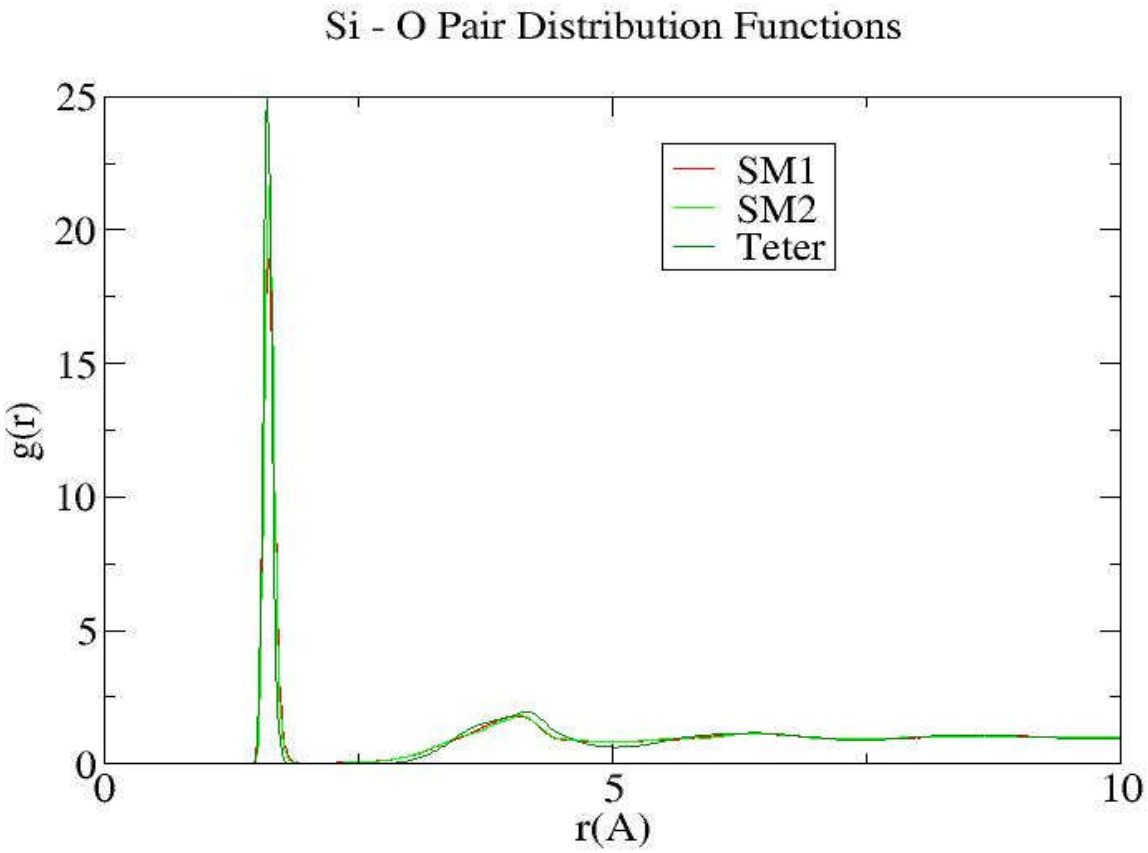

Figure 3.2: YAS17 SM1 vs. SM2 Al – O Pair Distribution Function

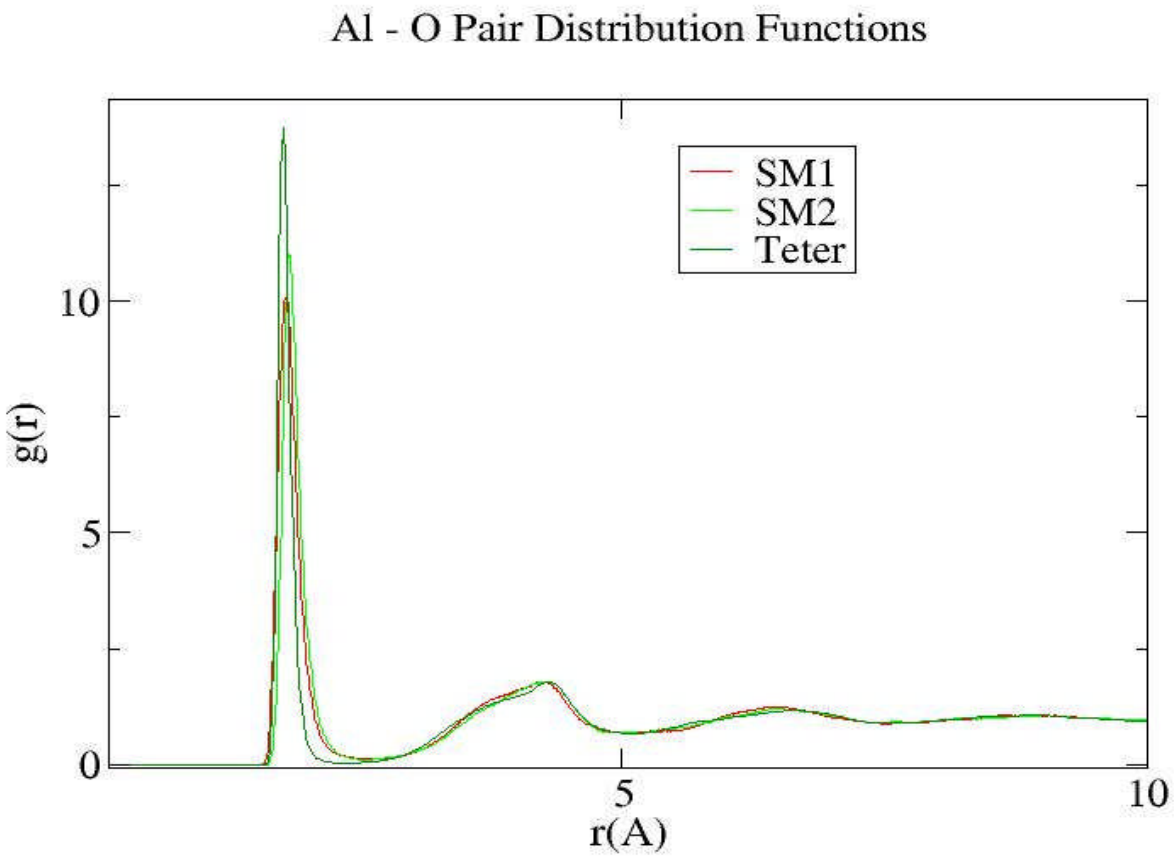

Figure 3.3: YAS17 SM1 vs. SM2 Y – O Pair Distribution Function

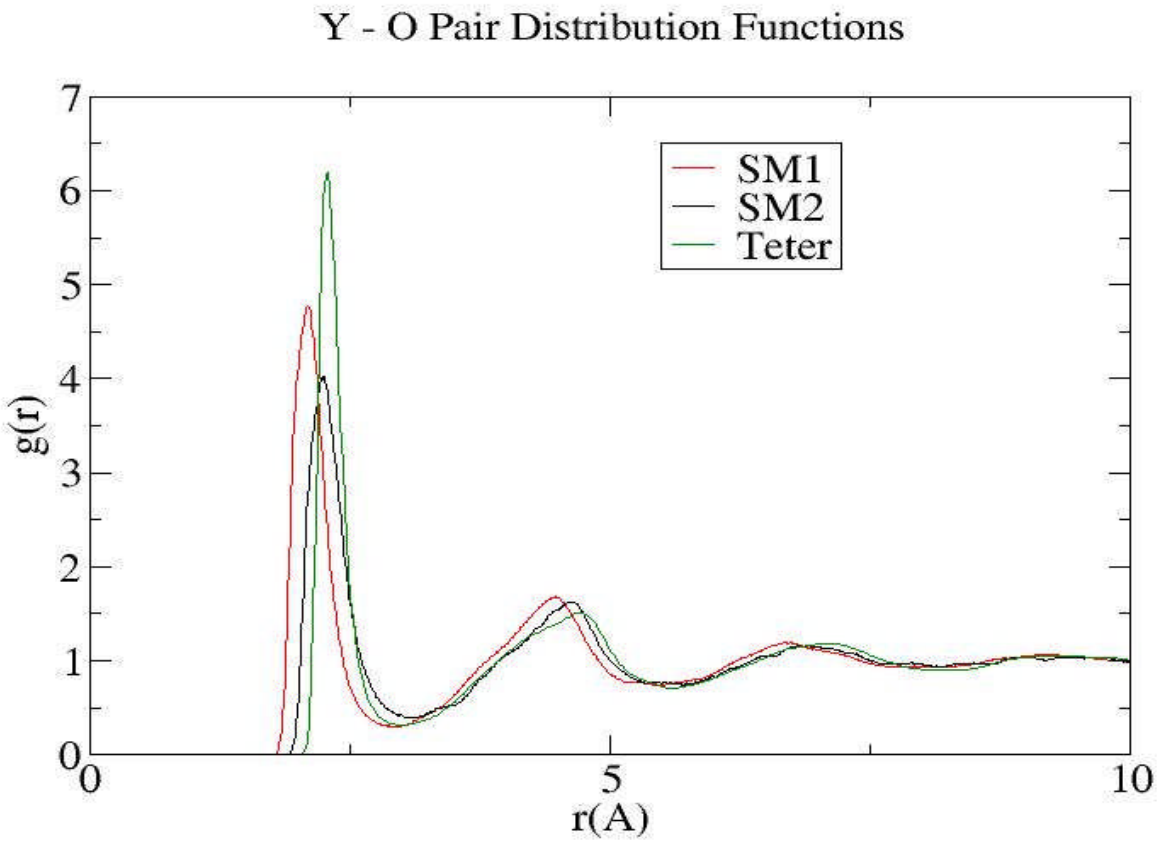

Figure 3.4: YAS17 SM1 vs. SM2 O – O Pair Distribution Function

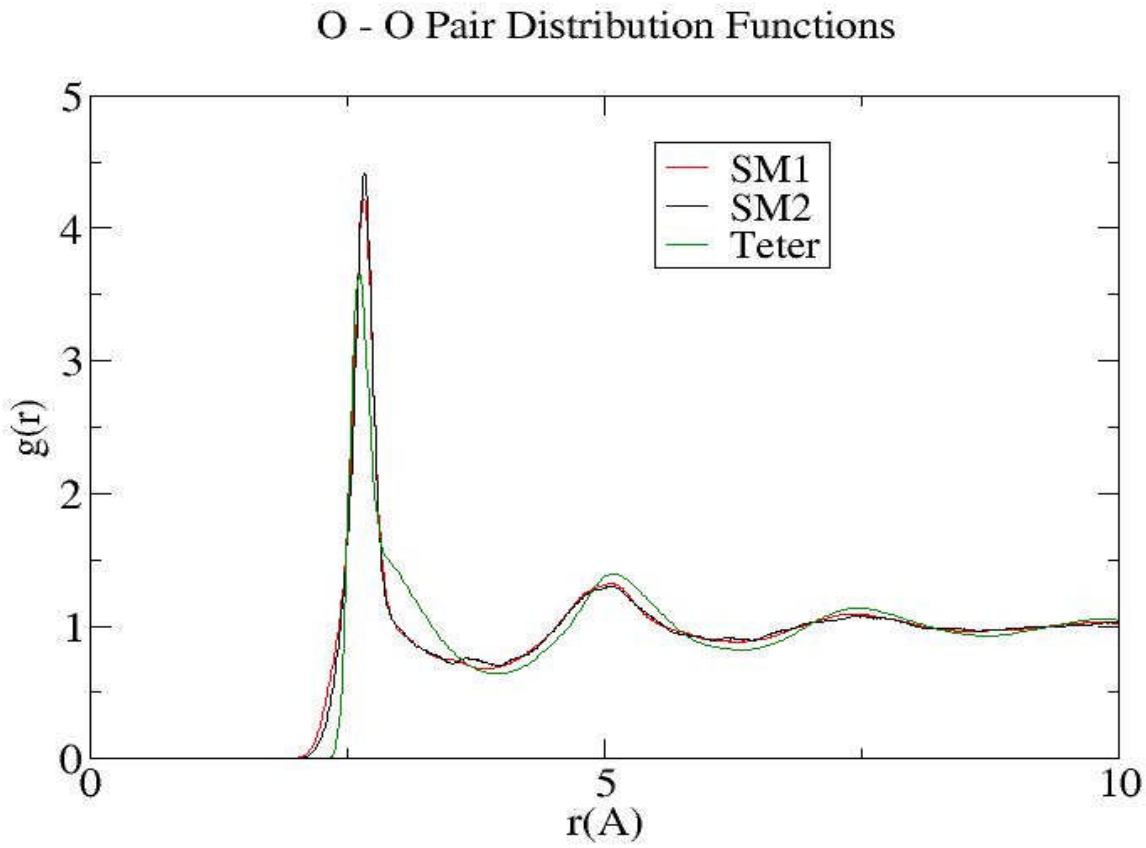

Table 3.1: Si – O, Al – O and Y – O coordination numbers for YAS17 modelled via SM1 and SM2.

	Si – O (%)		Al – O (%)		Y – O (%)	
Coordination	SM1	SM2	SM1	SM2	SM1	SM2
3	0.71	0.20	0.01	0.00	0.34	0.01
4	99.29	99.80	27.78	21.59	5.58	3.65
5	0.00	0.00	61.25	62.46	36.07	24.56
6	0.00	0.00	10.90	15.69	39.06	46.42
7	0.00	0.00	0.05	0.26	16.37	19.73
8	0.00	0.00	0.00	0.00	2.54	5.55
9	0.00	0.00	0.00	0.00	0.04	0.08
10	0.00	0.00	0.00	0.00	0.00	0.00
Average	3.99	4.00	4.83	4.95	5.73	5.99

A) Silicon

The Si – O bond length found in YAS17 using SM1 is 1.620 Å whereas the mean bond length for YAS17 modelled by SM2 is 1.625 Å and both are comparable to the work by Tilocca and Christie [42] where they found a bond length of 1.614 Å. Other MD and diffraction studies of YAS glasses have shown a bond length of 1.60 Å [142, 143]. Silicon is an atom that has a well-defined coordination of four. The YAS17 glass simulated using SM1 and SM2 showed nearly all silicon atoms to have a coordination of four (see Table 3.1). There are no silicon atoms with a coordination of five or higher, again which agrees with previous experimental and modelling data [142, 143] which showed coordination numbers of 3.9 – 4.0.

The average (O – Si – O) bond angle for YAS17 using SM1 is 109.27º whereas the average (O – Si – O) bond angle for YAS17 using SM2 is 109.19º (see Figure 3.5). One would expect a bond angle of this kind since virtually all silicon atoms in YAS17 modelled using SM1 and SM2 are four coordinated. The peaks of these O – Si – O bond angle distributions are close to the ideal tetrahedral bond angle of 109.47º.

B) Aluminium

The bond distance of Al – O is 1.80 Å and 1.83 Å for YAS17 using SM1 and SM2 respectively. The values obtained are in agreement with 1.79 Å and 1.82 Å obtained in previous structural studies of YAS using experimental and modelling techniques [142, 143].

NMR studies of YAS glasses have shown that aluminium can have a range of

coordination numbers i.e. from four to six in YAS [144, 145] and other related glass types [146]. A coordination of four is commonly seen for aluminium however.

The coordination numbers for YAS17 using SM1 is 4.83 and for SM2 is 4.95 (See Table 3.1). The coordination numbers are slightly higher than those found in the work by Tilocca and Christie [42], where they found a coordination of 4.05 for YAS17. However, it is worth noting that coordination numbers found for SM1 and SM2 respectively coincide with diffraction experiments which gave 4.5 +/- 0.5 for a glass with 11% yttria [143]. The shell-model [42] approach to simulating YAS glasses is likely to be more reliable than simulations carried out using the Teter potential i.e. rigid-ion model approach as the shell-model accounts for the polarisablity of all oxygen anions.

Since there is a broad range of coordination numbers of aluminium using either SM1 or SM2, one may expect the same for O – Al – O bond-angle distributions. For SM1, there are three peaks which are of importance from Figure 3.6. The bond-angle distribution shows the following peaks at 78^{o} and 96 ^{o} respectively which correspond to 4 and 5 coordinated aluminium atoms. From left to right the peaks show decreasing intensity. For YAS17 modelled by SM2, the O – Al – O bond-angle distributions shows two major peaks. The first is found at an angle of 89^{o} and the second peak which is very broad and low intensity has an angle of 152^{o}. The bond angle distributions of YAS17 modelled by both SM1 and SM2 are very broad; this is mainly due to there being a broad range of Al – O coordination numbers, which largely consists of four, five and six coordinated aluminium, as we see from Table 3.1.

C) Yttrium

The mean Y – O bond length of YAS17 using SM1 is 2.15 Å and for SM2 is 2.25 Å. The mean Y – O bond length has been reported at 2.39 Å by the work of Christie and Tilocca for YAS17 [42]. The actual Y – O distance has not been measured experimentally for YAS glasses, however the mean distance received from the simulations of YAS17 using SM1 and SM2 are close to the work of Tilocca and Christie [42] as well as 2.32 Å [147] and 2.28 Å [148] found experimentally for binary yttria-alumina glasses.

The Y – O coordination numbers for YAS17 modelled via SM1 is 5.73 and for SM2 is 5.99. Such coordination numbers compare reasonably well to those of binary yttria-alumina glasses experimentally observed, where coordination numbers of 6.9 +/- 0.4 [147] and 6.64 +/- 0.33 [148] were found. A wider range of bonding environments is

observed for yttrium than either silicon or aluminium. Here six- or seven-coordinated yttrium atoms are most commonly seen, while some yttrium atoms have been seen to have coordination numbers of as low as three and as high as ten.

The bond angle distribution of O – Y – O is seen (Figure 3.7) with two main peaks at 67.5^{o} and 90^{o} respectively for YAS17 modelled via SM1. YAS17 modelled by SM2 shows peaks at 58^{o}, 70^{o} and 91^{o}. Since a high number of Y coordination numbers are present, which range from three to ten, acute bond-angle O – Y – O distribution peaks are expected, and observed.

The exact effects of yttrium within the glass structure are not well understood. There are technical difficulties in carrying out ^{89}Y NMR [145]. Schaller and Stebbins [145] expect that yttrium and other rare-earth elements such as lanthanum change the glass network, by stabilising the formation of negatively charged species such as non-bridging oxygen atoms. This is investigated below.

Figure 3.5: SM1 vs. SM2 O – Si – O Bond angle distributions for YAS17

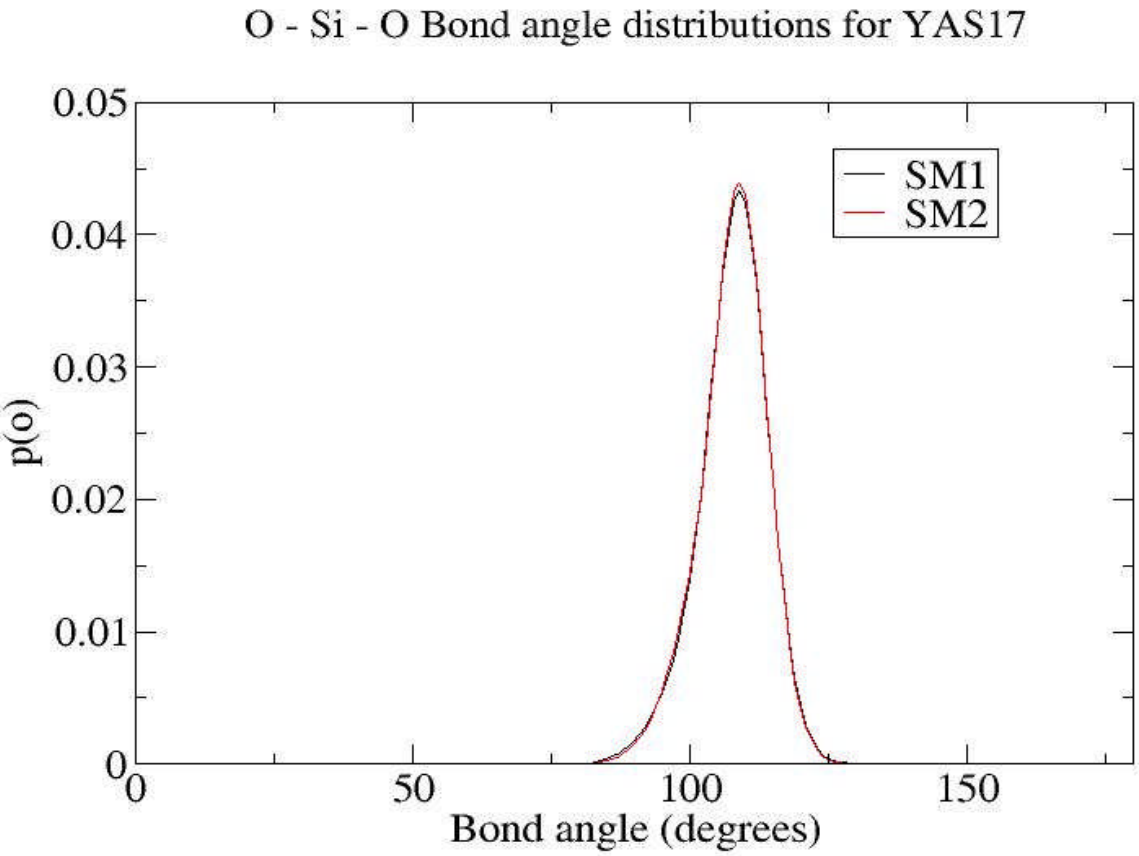

Figure 3.6: SM1 vs. SM2 O – Al – O Bond angle distributions for YAS17

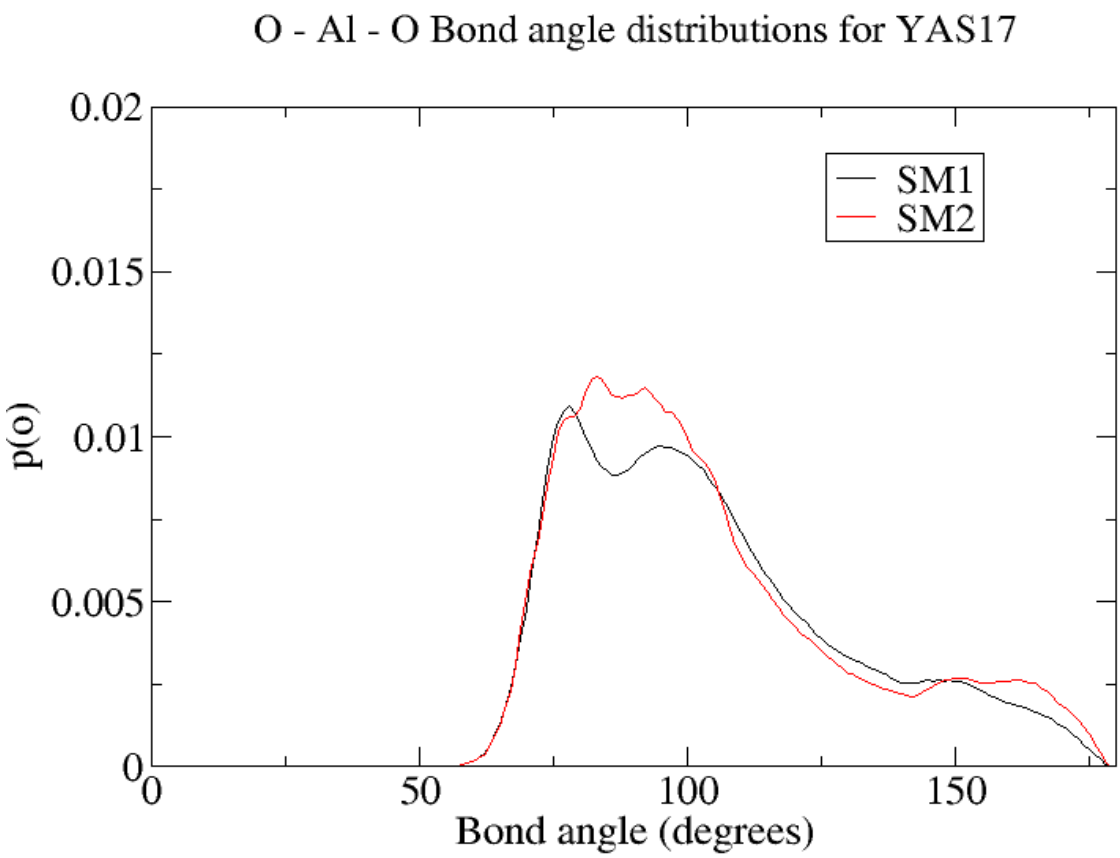

Figure 3.7: SM1 vs. SM2 O – Y – O Bond angle distributions for YAS17

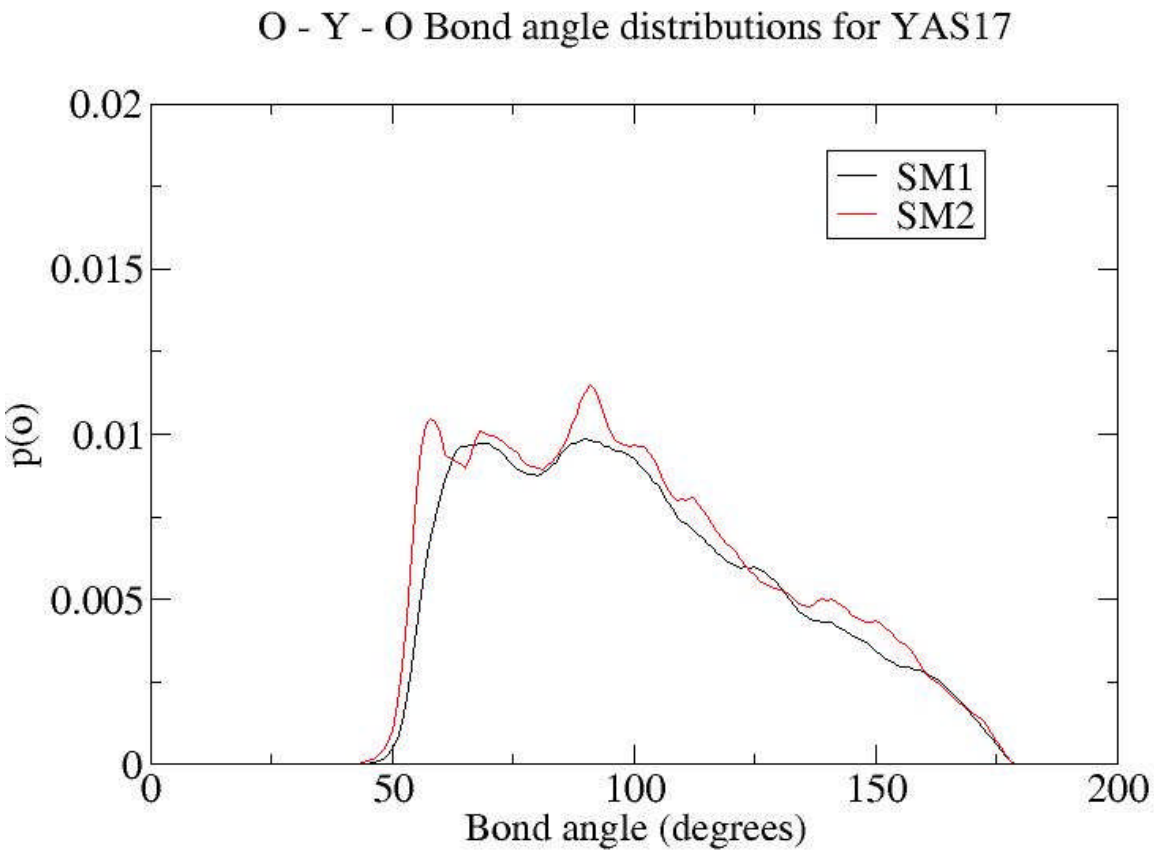

3.1.2 Medium-range Structure

The structure of pure silica glass has silicon atoms tetrahedrally bonded to four surrounding oxygen atoms. Each oxygen atom is attached to two silicon atoms, bridging two silicate tetrahedra. Silicon atoms have a network connectivity of four, denoting all silicon atoms in the pure silica glass have four bridging oxygen (BO) neighbours. Adding specific network modifiers and network intermediates to the pure SiO_2 glass structure will diminish the number of bridging oxygens (BO) for silicon (i.e. Si – O – Si), in turn lowering Q^n connectivity for silicon i.e. $Q^4 \rightarrow Q^3 \rightarrow Q^2 \rightarrow Q^1 \rightarrow Q^0$. This allows the formation of non-bridging oxygens (NBO) in the glass structure.

The structure of YAS glass is such that two network formers are present i.e. silicon and aluminium, where both network-forming cations present are interconnected via bridging oxygen atoms. A bridging oxygen is defined as any oxygen atom bonded to two or more silicon and aluminium cations. Other oxygen atoms, including free oxygen atoms, not bonded to any network former, are defined as non-bridging. Adding specific network intermediates and modifiers into the structure of a glass can greatly affect the medium-range structure, which in turn affects the durability of a glass in a physiological environment [41, 149]. The study of medium-range structure in YAS glass is an important feature, which may strongly rely upon the glass composition and/or the amount of yttrium.

A) Aluminium and Silicon Q^n

The medium-range structure of the network can be defined by studying the Q^n distributions. The YAS glass system contains only silicon and aluminium as network formers, whereas yttrium is considered a network modifier. The total Q^n for a specific atom x is the number n of bridging oxygens bound to x, where a bridging oxygen is an oxygen bound to x. The network connectivity (NC) of species A is calculated as the weighted average of the total Q^n over all A atoms, and represents the average number of BO in the coordination shell of A [83]. The network connectivity is a good way to describe the durability of a glass in an aqueous physiological medium: a low (~2) silicon network connectivity characterizes more soluble, thus more bioactive, glass compositions. On the contrary, network connectivities (NC) greater than 3 relate to non-bioactive glass compositions [149].

The total Q^n distribution and network connectivity show that YAS17 modelled via SM1 has approximately the same silicon interconnectivity as YAS17 modelled via SM2 (Table 3.2). The composition of the glass between YAS17 SM1 and YAS17 SM2 are the same so one would expect that the connectivities to remain the same. The same effect is found for aluminium interconnectivity.

Table 3.2: Total Q^n distributions and network connectivities (NC) for the Si and Al cations in YAS17 modelled via SM1 and SM2.

	Si Q^n (%)		Al Q^n (%)	
n	SM1	SM2	SM1	SM2
0	0.000	0.437	0.055	0.264
1	3.394	2.060	0.153	0.292
2	21.671	20.579	0.251	0.320
3	42.102	41.878	6.911	3.589
4	32.832	35.046	30.175	26.979
5	0.000	0.000	52.710	54.099
6	0.000	0.000	9.898	14.749
NC	3.04	3.09	4.65	4.78

Table 3.3: Total Q^n distributions and network connectivities (NC) for the Si and Al cations in YAS17 modelled via Teter potential. [42]

n	Si Q^n (%)	Al Q^n (%)
0	0.19	0.00
1	3.17	0.52
2	16.10	3.73
3	39.20	27.30
4	41.40	65.40
5	0.00	2.85
6	0.00	0.20
Average	3.19	3.67

3.1.3 Effect of Different Buckingham Terms (SM1 – SM2)

In this section, we compare the results for the two different potentials used.

The differences between YAS17 being modelled via SM1 and SM2 are discussed by comparing the silicon, aluminium and yttrium coordination numbers as well as the silicon and aluminium Q^n distributions. Firstly the comparisons are made regarding coordination numbers in Table 3.1.

Table 3.1: Si – O, Al – O and Y – O coordination numbers for YAS17 modelled via SM1 and SM2.

	Si – O (%)		Al – O (%)		Y – O (%)	
Coordination	SM1	SM2	SM1	SM2	SM1	SM2
3	0.71	0.20	0.01	0.00	0.34	0.01
4	99.29	99.80	27.78	21.59	5.58	3.65
5	0.00	0.00	61.25	62.46	36.07	24.56
6	0.00	0.00	10.90	15.69	39.06	46.42
7	0.00	0.00	0.05	0.26	16.37	19.73
8	0.00	0.00	0.00	0.00	2.54	5.55
9	0.00	0.00	0.00	0.00	0.04	0.08
10	0.00	0.00	0.00	0.00	0.00	0.00
Average	3.99	4.00	4.83	4.95	5.73	5.99

The coordination of silicon, whether being modelled via SM1 or SM2, remains unchanged. The coordination of silicon is well-defined at four where oxygen coordinates around silicon tetrahedrally. Aluminium however shows different coordination numbers of 4.83 and 4.95 via SM1 and SM2 respectively. Both SM1 and SM2 are shell-model potentials i.e. potentials which were calculated with the inclusion of the core-shell potential for polarisable oxygen. The difference between these aluminium coordination numbers are related to the potentials used during simulation which are responsible for the Al – O interaction, while the aluminium potential in SM1 and SM2 both have the Buckingham form, the values of the aluminium Buckingham potentials are different and are given in Tables 3.4 and 3.5.

Table 3.4: SM1 Buckingham Potential Parameters

SM1 Buckingham Potential Parameters			
Species	**A (eV)**	**ρ (Å)**	**C (eV Å ^{6})**
Al $_{core}$ - O $_{shell}$ [136]	1460.300	0.2991	0.0000
Y $_{core}$ - O $_{shell}$ [118]	1519.279	0.3291	0.0000

Table 3.5: SM2 Buckingham Potential Parameters

SM2 Buckingham Potential Parameters			
Species	**A (eV)**	**ρ (Å)**	**C (eV Å ^{6})**
Al $_{core}$ - O $_{shell}$	1567.9521	0.2991	0.0556
Y $_{core}$ - O $_{shell}$	1444.8360	0.3470	0.1000

YAS17 modelled by SM1 gives rise to a lower number of 5 and 6 coordinated Al – O species than compared to that modelled via SM2 which has a greater number of 5 and 6 coordinated Al – O species (Table 3.1).

The yttrium coordination found from modelling YAS17 via SM1 is 5.73 and 5.99 in SM2. Again, an increase is seen in coordination, like that found for aluminium, for SM2 over SM1. YAS17 modelled by SM1 gives rise to a lower number of six-, seven- and eight-coordinated species than compared to that modelled via SM2 which has a greater number of six-, seven- and eight-coordinated species (Table 3.1).

The network connectivities for silicon and aluminium are also affected by the different Buckingham potentials seen in Tables 3.3 and 3.4. The Q^n distributions and their network connectivities are given below in Table 3.2.

Table 3.2: Total Q^n distributions and network connectivities (NC) for the Si and Al cations in YAS17 modelled via SM1 and SM2.

	Si Qn (%)		Al Qn (%)	
n	SM1	SM2	SM1	SM2
0	0.000	0.437	0.055	0.264
1	3.394	2.060	0.153	0.292
2	21.671	20.579	0.251	0.320
3	42.102	41.878	6.911	3.589
4	32.832	35.046	30.175	26.979
5	0.000	0.000	52.710	54.099
6	0.000	0.000	9.898	14.749
NC	3.04	3.09	4.65	4.78

The silicon network connectivities are similar as we model YAS17 via SM1 and SM2. The Buckingham potential parameters responsible for modelling Si – O interactions are the same between SM1 and SM2 which is responsible for why the silicon network connectivities are so similar. The composition of the glass between YAS17 SM1 and YAS17 SM2 are the same so one would expect that the connectivities to remain the same. However, the different potentials could cause different network connectivities.

The aluminium network connectivities are slightly different however. YAS17 being modelled via SM1 showed that aluminium atoms were mostly Q^5, whereas YAS17 being modelled via SM2 showed a decrease in the number of Q^4 species and an increase in the number of Q^5 and Q^6 species thus giving rise to a higher network connectivity (Table 3.2). The SM2 potential makes aluminium more integrated into the network, strengthening the network because of the higher number of Q^5 and Q^6 species found in the YAS17 system. The SM1 potential makes aluminium in YAS17 less integrated into the network compared to YAS17 modelled via SM2. In the end the $Y_{core} - O_{shell}$ potential from SM2 was thought best suited for simulations of YAS glasses. The $Al_{core} - O_{shell}$ from SM1 was also thought to be a better suited potential for other simulations of YAS glasses and these were used throughout the remainder of this work.

3.2 *Y – OH $_{shell}$ Potential*

The Buckingham parameters for the Y – O(H) interactions were obtained by fitting to the yttrialite structure, using the Schroeder [136] approach to take into account the different O(H) charge. The reason for this was due to the unavailability of a suitable crystal structure which contained yttrium, silicon and hydroxyl-oxygen species to which the Y – O(H) $_{Shell}$ Buckingham parameters could be fit. The formal charges of oxygen, yttrium and silicon in the yttrialite structure were adapted (Table 3.6) using the Schroeder [136] approach and Buckingham Potentials already developed in section 2.5.1 and those listed below in Tables 3.7 - 3.9 were used to calculate Y – O(H) $_{Shell}$ Buckingham parameters.

Table 3.6: Auxiliary charges formed from using the Schroeder [136] method.

Specie	Type	Initial Charges	Final Charges
Y	core	3.000	2.510
Si	core	4.000	3.347
O	core	0.848	0.655
O	shell	-2.848	-2.328

Table 3.7: Buckingham potential parameters (Si $_{core}$ – OH $_{shell}$ / OH $_{shell}$ – OH $_{shell}$)

Buckingham Potential Parameters [138]			
	A (eV)	**ρ (Å)**	**C (eV Å ^{6})**
Si $_{core}$ – OH $_{shell}$	983.56	0.320520	10.661580
OH $_{shell}$ – OH $_{shell}$	22764.30	0.14900	6.97

Table 3.8: Core-Shell harmonic potential (OH $_{core}$ – OH $_{shell}$)

Core – Shell Harmonic Potential [138]	
	k_{cs} (eV Å $^{-2}$)
OH $_{core}$ – OH $_{shell}$	74.92

Table 3.9: Three body harmonic potential (OH $_{shell}$ — Si $_{core}$ — OH $_{shell}$)

Three-body Harmonic Potential [138]				
	k_{3b} (eV rad^{-2})	**θ_0 (deg)**	**Si $_{core}$ – OH $_{shell}$ (Å)**	**OH $_{shell}$ – OH $_{shell}$ (Å)**
OH $_{shell}$ — Si $_{core}$ — OH $_{shell}$	2.097	109.47	1.8	3.2

3.2.1 Fitting of Y – OH $_{shell}$ Buckingham Potential Parameters

The Y – OH_{shell} Buckingham potential parameters were fit according to the crystal structure $Y_2Si_2O_7$ (shown in Figure 3.8) found by Sadiki and Coutures [77]. Yttrium atoms are coloured in light blue, oxygen atoms are red and silicon atoms are light brown.

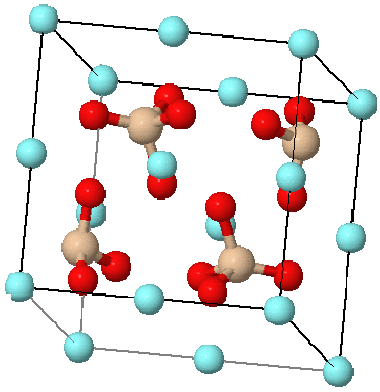

Figure 3.8

Table 3.10: Elements: Y Si O

Name: Diyttrium Disilicate (Gamma)

Formula: $Y_2Si_2O_7$ - Space Group: P121/M1 (11)

	Exp. / Initial	Final	Difference	Units	Percent
Volume	281.3623	283.536822	2.174537	Angs**3	0.7000
a	7.5000	7.361150	-0.138850	A	-1.8500
b	8.0600	7.85	-0.208901	A	-2.5900
c	5.0200	5.265239	0.245239	A	4.8900
alpha	90.0000	90.0000	0.0000	Degrees	0.0000
beta	112.0000	111.285357	-0.714643	Degrees	-0.6400
gamma	90.0000	90.0000	0.0000	Degrees	0.0000

Parameter No.	Parameter Original	Parameter Final	Parameter Type	Species
1	777.000	886.853242	Buckingham	A
2	0.347	0.347	Buckingham	ρ
3	0.100	0.100	Buckingham	C

Table 3.11: The newly calculated Y – OH $_{shell}$ Buckingham parameters

Buckingham Potential Parameters			
Species	**A (eV)**	**ρ (Å)**	**C (eV Å ^{6})**
Y $_{core}$ - OH $_{shell}$	886.853242	0.3470	0.1000

The fitted Y – OH $_{shell}$ potential caused very little deviance from the initial crystal structure. The overall change in volume was 0.7%. The cell parameters a, b and c did not change very much also as seen in Table 3.11. We can be confident in using this potential into the incorporation of hydrated YAS glasses.

The purpose for calculating the above Buckingham potential is for the incorporation into MD simulations of hydrated YAS glasses. Hydrated YAS glasses will have to incorporate other interatomic potentials that satisfy all interatomic contributions within the structure (Section 3.3).

3.3 *Test of the potentials: Hydrating an Yttrium aluminosilicate*

The following section of this research deals with the use and incorporation of the Y – OH_{shell} potential calculated in section 3.2 (Table 3.11). Other interatomic potentials required to satisfy all other new interatomic contributions present within hydrated YAS glasses are also necessary to model the other interatomic interactions. In order to test the interatomic potential calculated in section 3.2 and other potentials necessary for all interatomic contributions, it was necessary for the potentials to be involved into an actual MD simulation. This is so we could firstly check to see if the potential would model the hydrated YAS glass accurately and secondly to check the reliability of the potential(s) with respect to being used on simulations of hydrated YAS glasses differing in composition.

The test involved a stable structure of bulk YAS17 glass at 300K. The chosen structure and composition was of YAS17 (modelled using SM2). Here, three new hydrogen atoms were attached to oxygen atoms already bonded to silicon atoms inside of the stable 300K bulk YAS17 glass system. In order to give space to the three new hydrogen atoms, and to maintain charge neutrality, a yttrium atom was removed from nearby within the stable 300K bulk YAS17 glass structure. The three new hydrogen atoms were placed at a distance of 1.00 Å away from their adjacent oxygen atoms. Once this had been completed a simulation was carried out to check the potentials of all interatomic contributions taking place within YAS17 containing the three additional hydrogen atoms. The composition of this glass for this study is named YAS+(3H). The simulation was completed using DL_POLY 2.20. The structure was kept at a temperature of 300K and underwent a simulation for 50 ps continuously. The mean bond distance calculated for Si – OH_{shell} is 1.75 Å where literature has reported a value for Si – O to be 1.60 Å [142, 143]. We believe the bond distance is different between Si – OH and Si – O as hydrogen would cause the extension of the bond length i.e. the oxygen to be attracted towards hydrogen slightly more pulling it away from silicon.

The mean OH_{shell} – H bond distance calculated is 1.00 Å where literature has reported a value of 0.969 Å [150]. The mean bond angle measured for Si – OH_{shell} – H is 109.87^o where literature reported a value of 118^o for a hydrated silica system [150]. The bond angles are close but not the same but this may be due to the composition of the glasses being different. Bond angle distributions of Si – OH_{shell} – H are given below in Figure 3.9. The values reported for both the bond angle and bond distances are close to

the distances and bond angles found in literature and is a good sign that the potentials are working effectively. Figure 3.10 is a visual aid to emphasise the Si – O – H found in the test simulation of YAS+(3H). Oxygen is shown in red, hydrogen in blue, silicon in yellow and aluminium in green. Yttrium network modifier cations are white.

Figure 3.9: Si – O – H Bond angle distributions for YAS+(3H)

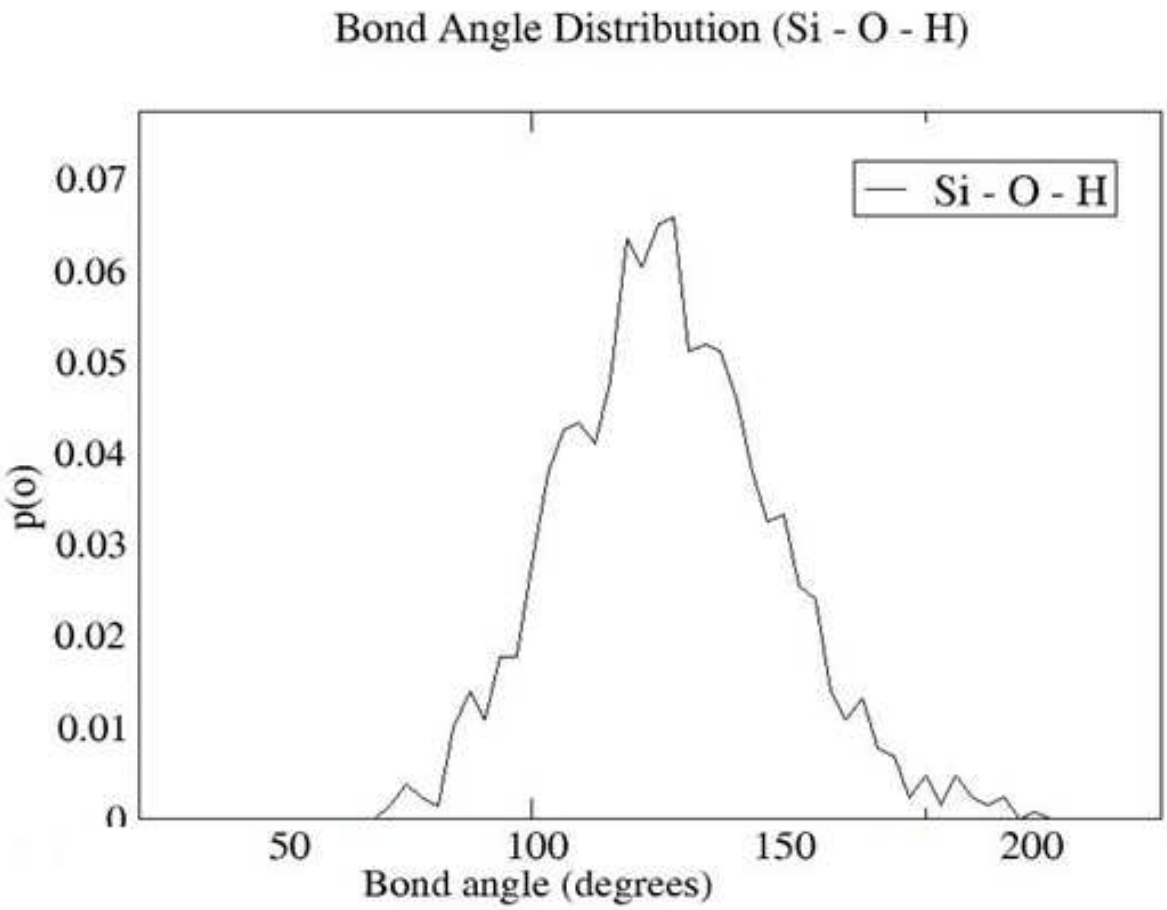

Figure 3.10: Picture from simulation of Si – O – H system found during the test.

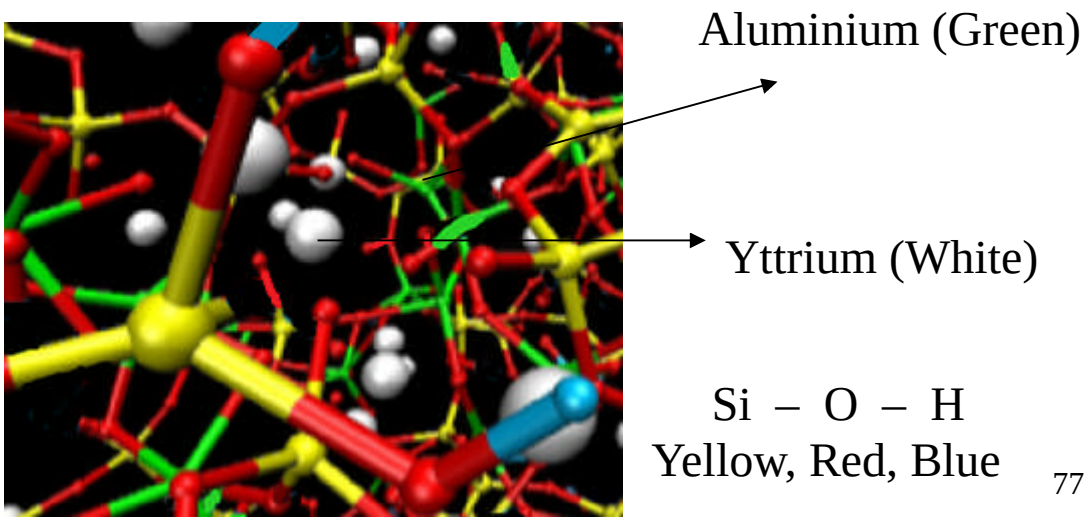

The first simulation was a small test where three hydrogen atoms were attached to a silicon atom by removal of a neighbouring yttrium atom. This part of the test relies on enlarging the sample of hydrogen in YAS17. For the purpose of this study a single simulation was completed on a composition of glass named YAS+H. YAS+H is a hydrated yttrium aluminosilicate glass based on YAS17 [42]. The YAS+H glass composition was given a density of 3.2g/cm^3. The hydrogen content was calculated at 5.4 x 10^{-3} mol/g. This amount of hydrogen content is comparable to the sol-gel bioglass of 70S30C (5.98+/-0.30)x10^{-3} mol/g experimentally prepared by Julian Jones *et al* [151]. The YAS+H is a yttrium aluminosilicate containing hydrogen with the composition of:

UNHYDRATED YAS+H: 17.10 mol % Y_2O_3, 18.96 mol % Al_2O_3, and 63.94 mol % SiO_2

Scaled: 92 Y_2O_3, 102 Al_2O_3 and 344 SiO_2

Hydrated YAS+H [92 Y_2O_3, 102 Al_2O_3, 344 SiO_2] – 60 O from (Y_2O_3), +120 OH

The simulation was completed using a new starting random initial configuration (section 2.3). The simulation was carried out using the potentials and other data listed in section 2.5 (Tables 2.1, 2.3 (SM2) – 2.6), section 3.2 (Table 3.11) and those listed below (Tables 3.12 – 3.16). The simulation was completed using DL_POLY 2.20. The structure was kept at a constant temperature of 300K and had undergone a simulation for 80 ps continuously. Since we have hydrated YAS we can expect a change in the glass structure relative to standard YAS17 modelled via SM1 or SM2.

Table 3.12: Buckingham Potential Parameters for the inclusion of OH

Buckingham Potential Parameters			
Species	**A (eV)**	**ρ (Å)**	**C (eV Å ^{6})**
[136] Al $_{core}$ - OH $_{shell}$	1142.678	0.299	0.000
[138] Si $_{core}$ – OH $_{shell}$	983.560	0.321	10.662
[138] OH $_{shell}$ – O $_{shell}$	22764.300	0.149	13.940
[138] OH $_{shell}$ – OH $_{shell}$	22764.300	0.149	6.970

Table 3.13: OH identity of Species, Core/Shell, Mass and Charges

Element	**Species**	**Charge**	**Mass**
hydroxy-oxygen	Core	0.900	15.800
hydroxy-oxygen	Shell	-2.300	0.200
hydrogen	Core	0.400	1.008

Table 3.14: Core-Shell Harmonic Potential ($OH_{core} - OH_{shell}$)

Core – Shell Harmonic Potential [138]	
Species	**k_{cs} (eV Å $^{-2}$)**
$OH_{core} - OH_{shell}$	74.92038

Table 3.15: Morse Potential ($H - OH_{shell}$)

Morse Potential [138]			
Intra- molecular	**D/eV**	**A/Å^{-1}**	**R_0/Å**
$H - OH_{shell}$	7.05	3.17	0.93

Modifications were made to some FORTRAN modules in DL_POLY 2.20. The changes made were to accommodate for the Coulombic interaction i.e. Table 3.16. When simulating YAS glasses for the first time during the testing phase, the bond distance observed for O – H was seen to have a value of approximately 0.8 angstroms. This distance was much less than the actual O – H bond distance of 1.0 angstroms. The reason for this discrepancy is because the Morse potential described in DL_POLY does not take into consideration the Coulombic interactions taking place between a hydrogen atom and oxygen core. It was therefore necessary to input the missing interaction (repulsion between like entities) between the positively charged hydrogen atom and positively charged oxygen core thus giving rise to a simulated hydrated YAS glass with a correctly modelled O – H bond distance of 1.0 angstroms.

Table 3.16: Intra-molecular Columbic interaction (%) ($H - OH_{core}$)

Intra-molecular Coulombic interaction (%) [138]	
$H - OH_{core}$	100

3.3.1 Short-range structure

The coordination numbers for relevant atom pairs in the YAS+H models are shown below in Table 3.17. Radial distribution function between anions and cations are given in Figures 3.11 – 3.14. The bond-angle distributions are given in Figures 3.15 and 3.16.

Table 3.17: Amounts of Si, Al and Y atoms with given Si – O, Al – O and Y – O coordination numbers for YAS+H model.

Coordination	Si – O (%)	Al – O (%)	Y – O (%)
1	0.00	0.00	0.00
2	0.00	0.00	0.00
3	1.20	0.03	0.00
4	98.79	24.34	1.15
5	0.01	58.05	15.45
6	0.00	17.09	41.79
7	0.00	0.23	31.90
8	0.00	0.00	8.83
9	0.00	0.00	0.80
10	0.00	0.00	0.07
Average	3.99	4.92	6.35

A) Silicon

The Si - O bond length found in YAS+H is 1.615 Å and is comparable to the work by Tilocca and Christie [42] where they found a bond length of 1.614 A. Other MD and diffraction studies of YAS glasses have shown a bond length of 1.60 Å [142, 143]. The mean Si – OH bond length is 1.625 Å. This peak can be found on the RDF plot for the Si – OH pair (Figure 3.11). The first peak is found at 1.625 Å. This peak is in agreement to the Si – O bond distance [142, 143]. Figure 3.16 shows the bond angles between Si – O – H, Al – O – H and Y – O – H.

Figure 3.11: Si – O / Si - OH Pair distributions functions for YAS+H

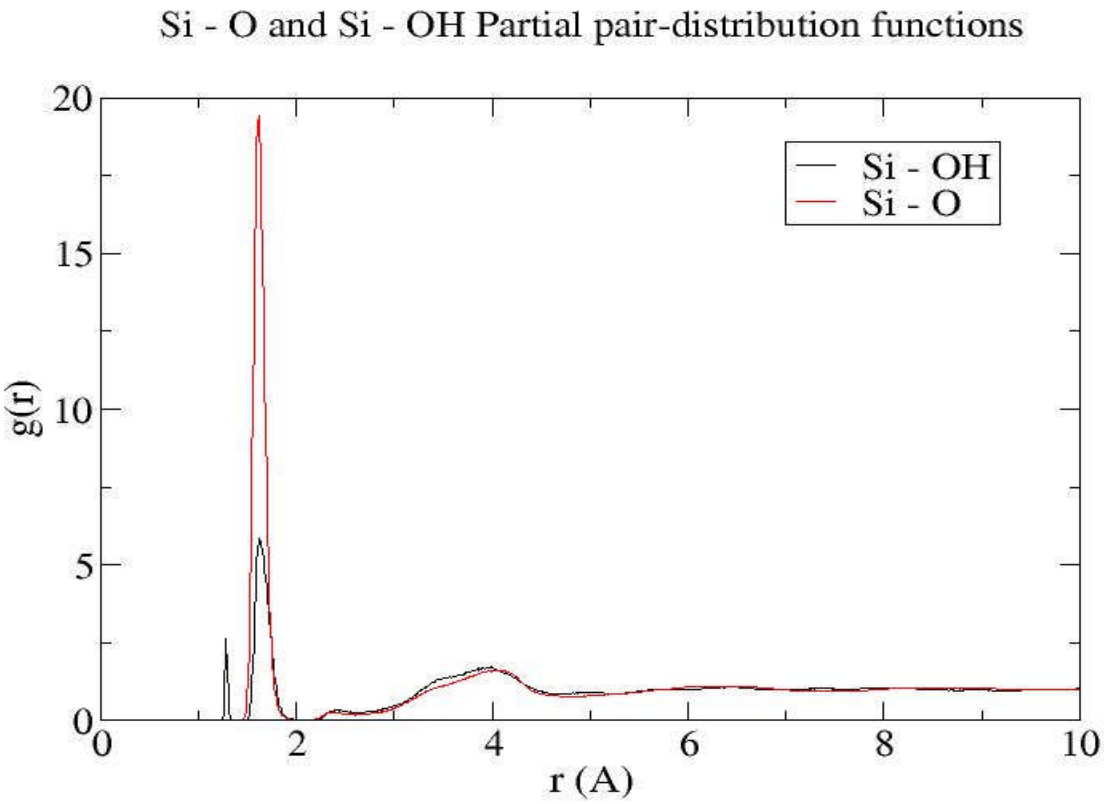

Silicon is an atom that generally has a well-defined coordination of four. YAS+H simulated showed nearly all silicon atoms to have a coordination of four (Table 3.17). There are virtually no silicon atoms with a coordination of five or higher, again which agrees with previous experimental and modelling data [142, 143] which showed coordination numbers of 3.9 – 4.0. The average O – Si – O bond angle for YAS+H is 109.85^{o} (Figure 3.15). One would expect a bond angle of this kind since virtually all silicon atoms in YAS+H are four-coordinated. The peaks of these O-Si-O bond angle distributions are close to the ideal tetrahedral bond angle of 109.47^{o}. The average Si – O – H bond angle for YAS+H is 112.00^{o} which is close to the value of 112.20 ^{o} found from the modelling work by Thaddeus and McCarthy [150].

B) Aluminium

The bond distance of Al – O is 1.775 Å. The value obtained is close to 1.79 Å and 1.82 Å obtained in previous structural studies of YAS [142, 143]. The mean bond length for Al – OH was calculated to be 1.875 Å which is comparable to the (Al – O) values found by modelling techniques i.e. 1.79 Å and 1.82 Å [142, 143]. We believe the bond distance is different between Al – OH and Al – O as hydrogen would cause the

extension of the bond length i.e. the oxygen to be attracted towards hydrogen slightly more pulling it away from aluminium.

Figure 3.12: Al – O / Al - OH Pair distribution functions for YAS+H

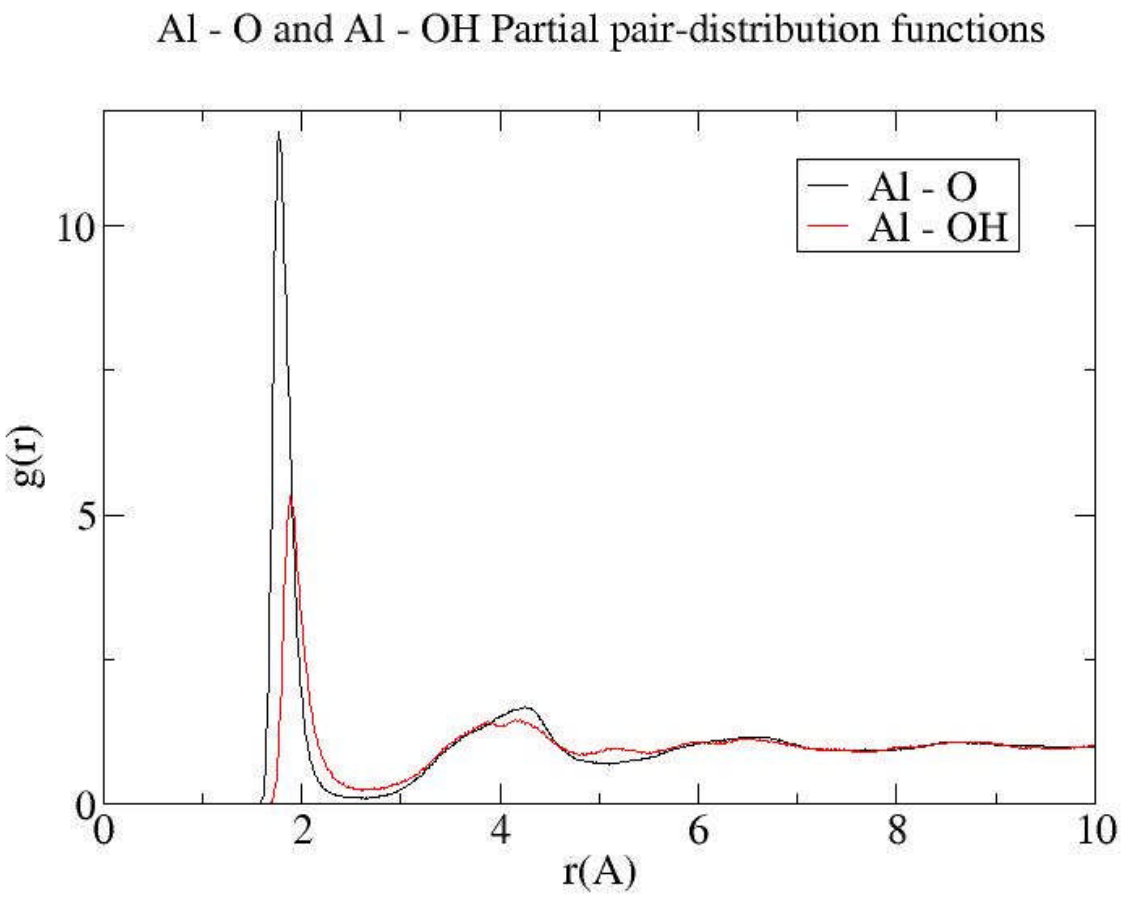

NMR studies of YAS glasses have shown that aluminium can have a range of coordination numbers i.e. from four to six in YAS [144, 145] and other related glass types [146]. A coordination of four is most commonly seen for aluminium however.

The aluminium coordination number in YAS+H is 4.92. This coordination is greater than that found in the work by Tilocca and Christie, where they found a coordination of 4.05 for YAS17 [42] However, it is worth noting that the coordination listed for YAS+H does coincide with diffraction experiments which gave 4.5 +/- 0.5 for glass with 11% yttria [143].

Since there is a broad range of coordination numbers of aluminium, one may expect broad O – Al – O bond angle distributions. For YAS+H, there are three peaks which are of importance i.e. 80º, 95º and 147º respectively (Figure 3.15), which correspond to 6, 5 and 4 coordinated aluminium atoms. From left to right, the peaks

show decreasing intensity. The bond-angle distributions of YAS+H are very broad, this is mainly due to there being a broad range of Al – O coordination numbers, which largely consist of four, five and six coordinated aluminium atoms.

C) Hydrogen

The mean bond length of H – OH is 1.00 Å in YAS+H. The experimental bond distance is 1.00 Å [150]. The H – OH bond distance found in YAS+H is in very good agreement to that of the bond length found in literature [150].

Figure 3.13: H - OH Pair distribution functions for YAS+H

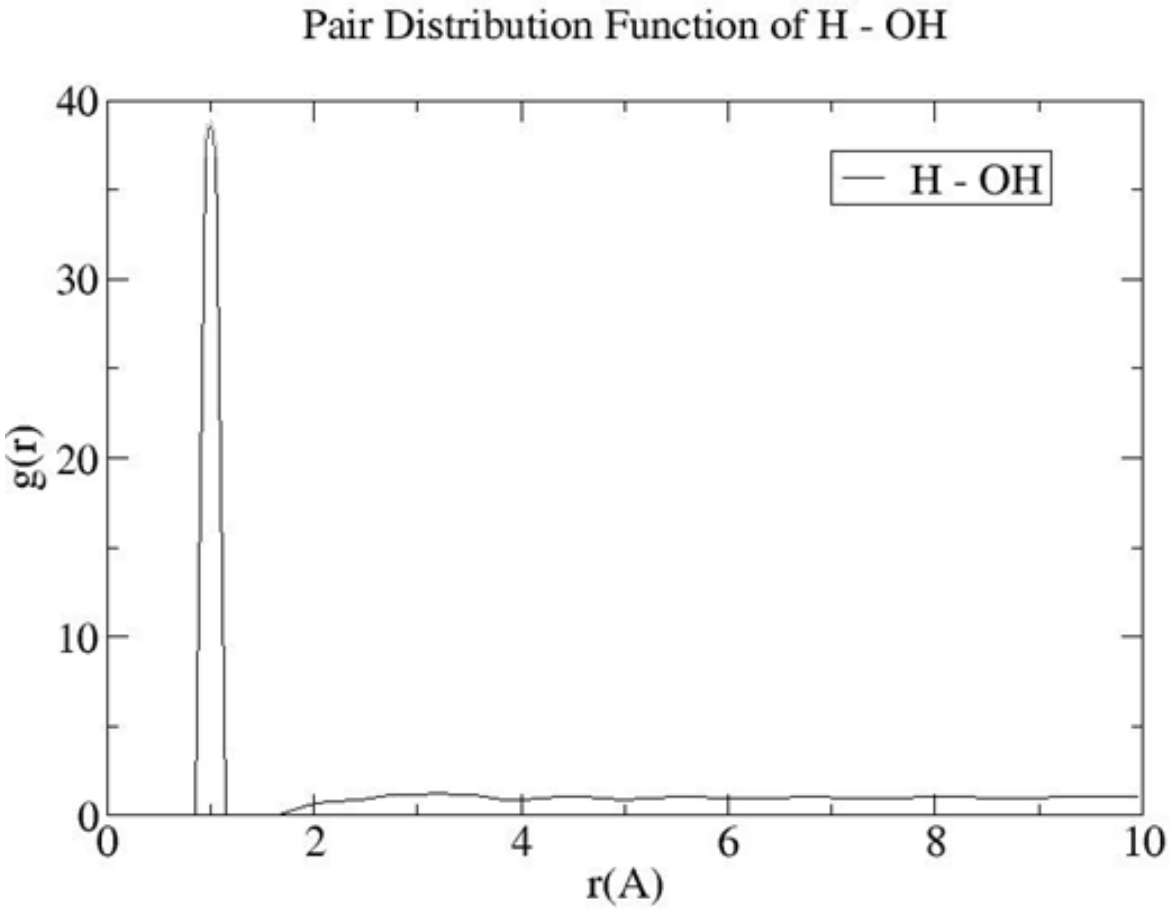

D) Yttrium

The Y – O bond length of YAS+H is 2.295 Å. The Y – O bond length has been reported at 2.391 Å for YAS17 in work by Christie and Tilocca [42]. The actual Y – O distance has not been measured experimentally for YAS glasses, however the mean distance received from the simulation of YAS+H are close to the work of Christie and Tilocca [42] as well as 2.32Å [147] and 2.28Å [148] for binary yttria-alumina glasses. The Y – OH bond length was calculated at 2.185Å.

Figure 3.14: Y – O / Y – OH Pair distributions functions for YAS+H

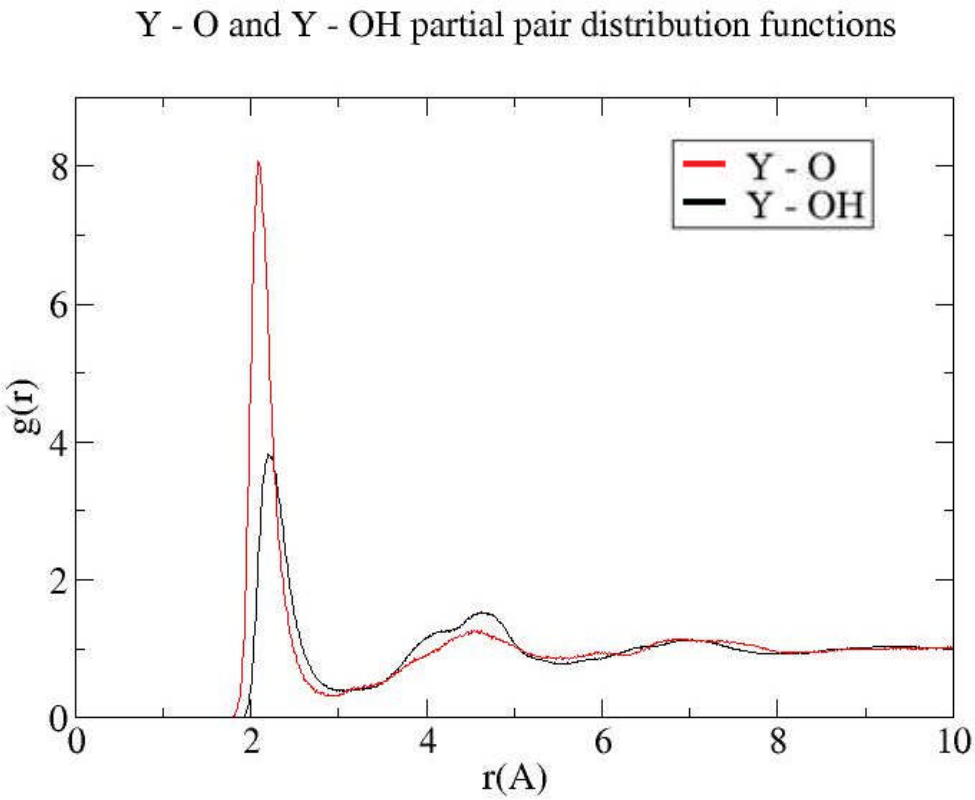

The Y – O coordination number found in YAS+H is 6.345. This coordination number compares well to binary yttria-alumina glasses experimentally measured, where coordination numbers of 6.9 +/- 0.4 [147] and 6.64 +/- 0.33 [148] were found. A wider range of bonding environments are observed for yttrium than for either silicon or aluminium. Here six-, seven- and eight-coordinated yttrium atoms are observed. Some yttrium atoms have been seen to have coordination numbers of as low as four and as high as ten (Table 3.17). The bond angle distribution of O – Y – O is seen with two main peaks at 78^{o} and 136^{o} respectively for YAS+H (Figure 3.15). Since a high number of Y coordination numbers are present, that range from three to ten, broad O – Y – O bond angle distribution peaks are expected.

Figure 3.15: O – Si – O / O – Al – O / O – Y – O Bond angle distributions

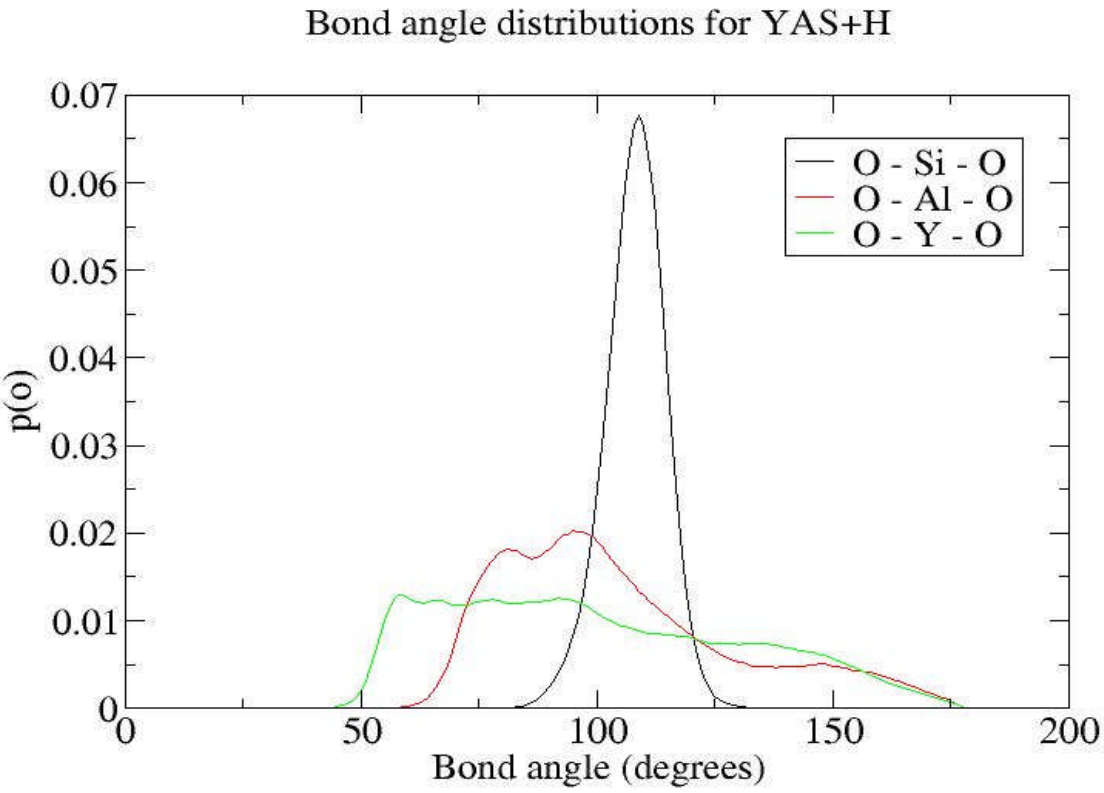

Figure 3.16: Si – O – H / Al – O – H / Y – O – H Bond angle distributions

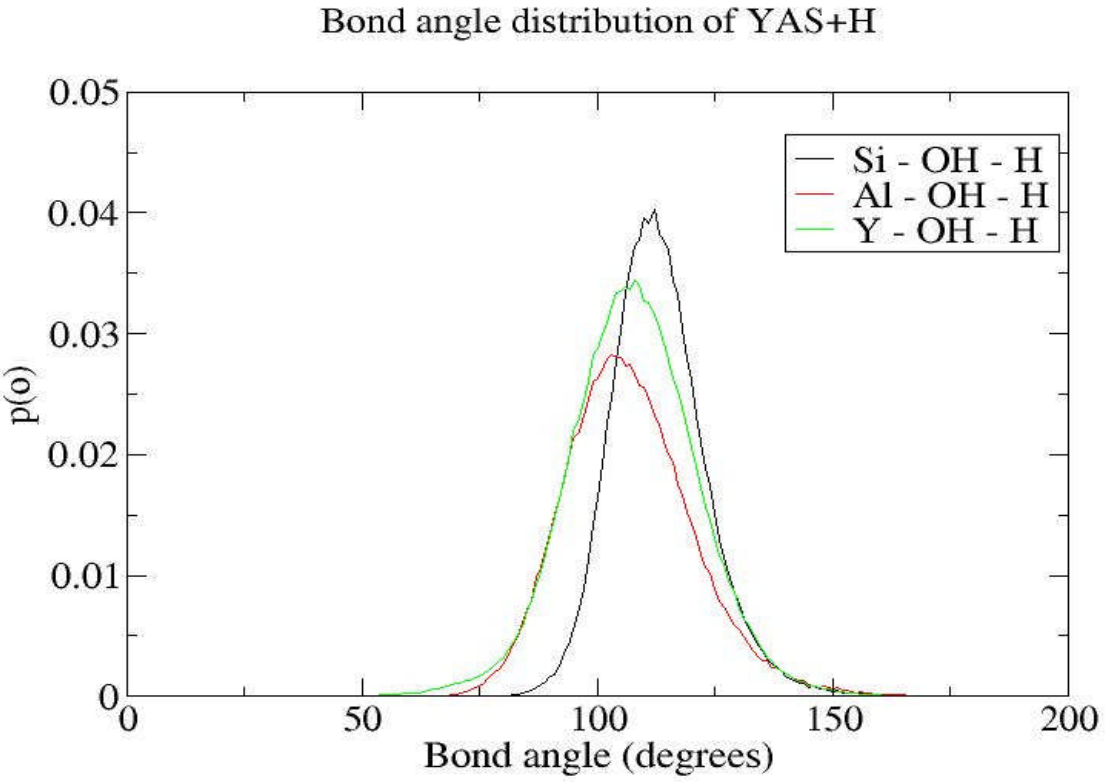

3.3.2 Medium-range structure

A) Aluminium and Silicon Q^n

The total Q^n distribution and network connectivity (Table 3.18) show that YAS+H has approximately the same silicon connectivity as YAS17 modelled via SM1 and SM2 (see section 3.1.2). The composition of YAS+H is very different to the composition of YAS17 modelled via SM1 or SM2. Although the compositions of YAS+H and YAS17 are different the total Q^n distributions of silicon are similar, which is intriguing. Hydrated YAS was hypothesised by us to decrease the Q^n distributions for Si and Al i.e. Q^0, Q^1 and Q^2 species were likely to predominate in YAS+H. The protons in this case may not only attach to bridging oxygen atoms but also to non-bridging oxygen atoms, in which case the Q^n speciation remains unaffected. The total Q^n distribution for Al changed in the way expected and is lower than that found in YAS17 modelled via SM1 / SM2 in Table 3.2a. The majority of aluminium in YAS+H are Q^4 whereas in YAS17 modelled via SM1/SM2 show the majority of aluminium being Q^5. The network connectivity for Al decreased from YAS17 (Table 3.2) to YAS+H (Table 3.18) which shows that the Al and Si connectivities are affected differently when YAS is hydrated.

Since a decrease in aluminium NC is seen from YAS17 to YAS+H, we infer that hydroxyl groups like to break the network created by aluminium in the structure of YAS+H thus decreasing the strength of the aluminium network. The silicon network connectivities remain largely unaffected as their values do not differ before hydration i.e. YAS17 modelled via SM1/SM2 (Table 3.6) or after hydration (3.18). This means hydroxyl groups avoid interfering with the network created by silicon and instead interfere with the network of aluminium. This would indicate that the strength of the aluminium network is inherently weaker than the network of silicon. Hydroxyl groups therefore find it easier to break Al – O – connections than Si – O – connections, probably due to the bond strengths between Si – O being greater than Al – O.

Table 3.18: Total Q^n distributions and network connectivities (NC) for Si and Al cations in YAS+H model.

n	Si Q^n (%)	Al Q^n (%)
0	0.33	0.00
1	2.79	0.00
2	20.12	4.57
3	45.96	23.28
4	30.79	40.38
5	0.00	28.07
6	0.00	3.49
7	0.00	0.22
NC	3.04	4.02

Table 3.19. Average Coordination Numbers for the Hydrogen Atoms.

	YAS+H
H – Si	0.56
H – Al	0.62
H – Y	1.55
Total	2.74

The average coordination numbers for the hydrogen atoms are shown in Table 3.19. The H – Si coordination number is smaller than the H – Al and H – Y coordination numbers. Yttrium clustering has been demonstrated in YAS17 [42]. Yttrium clustering has been seen visually in YAS+H also but yttrium has been seen to cluster around free hydroxyl groups present within the YAS+H structure (see figures 3.17a and 3.17b). The images show yttrium clustering taking place around hydroxyl groups. The presence of hydroxyl groups may enhance the amount of yttrium clustering taking place in YAS+H. This correlates with the H – Y coordination being high at ~1.55 compared to Si and Al. The large H – Y coordination is largely due to yttrium coordinating to free hydroxyl groups as well as interacting to surrounding hydroxyl groups already attached to either Si and or Al. In Figure 3.17, the hydroxyl group is shown by a red and purple spherical rod, where the red is oxygen and purple is hydrogen. The yttrium atoms are seen as white coloured spheres. Visually observing the glass structure it was seen that wherever an yttrium atom was found, very close by was a hydroxyl group. Wherever a hydroxyl group was seen then an yttrium atom was seen very close by. Further visual analysis of the glass showed that yttrium atoms close to hydroxyl groups was found continually from one yttrium atom to the next in a chain manner. We discuss this further in section 4.5

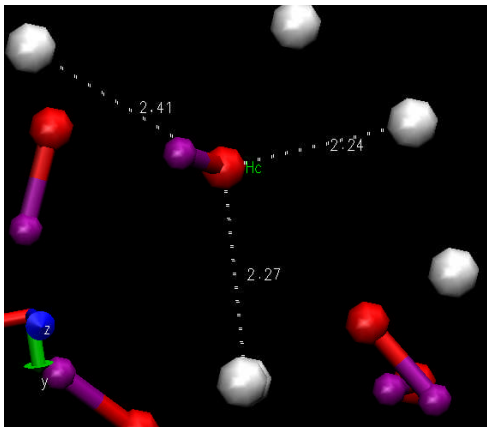

Figure 3.17a

Hydroxyl group near yttrium cations
View 1

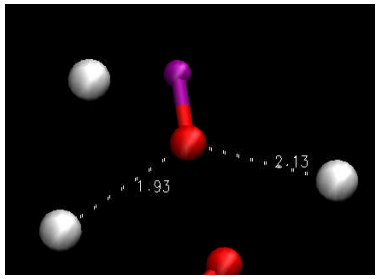

Figure 3.17b

Hydroxyl group near yttrium cations
View 2

4 Hydrated Yttrium Aluminosilicate Glasses

We have already carried out hydration tests on YAS17 earlier (section 3.3) which satisfied us as to the suitability of our methodology and interatomic potentials. This section will now thoroughly examine the effects of hydration on the bulk structure of YAS glasses. This section of work deals with simulating three different glass compositions YAS17, 24 and 30. These YAS glasses differ in yttrium and silicon content where the content with respect to aluminium remains more or less constant. Firstly, simulations of unhydrated yttrium aluminosilicate glasses 17, 24 and 30 were carried out. Each of the unhydrated YAS glasses were then hydrated at three increasing levels of hydration by adding hydroxyl groups into the bulk structure. The purpose of this was to investigate the effects of hydration on the structure of the glasses e.g. silicon, aluminium network connectivity, coordination numbers of network formers and modifiers etc.

The technique employed to hydrate a bulk glass such as YAS was taken from the idea found within the work of Mead and Mountjoy [152]. Here Mead and Mountjoy carried out MD simulations upon hydrated calcium silicate glasses. The technique used by Mead and Mountjoy was complex due to the number of network modifiers in their glasses. The hydration method therefore was modified and adapted for YAS glasses. The general method for hydrating YAS glasses was that for every one oxygen atom taken away from the total number of oxygens, two hydroxyl groups must be introduced e.g. if a total of 100 oxygens are present in a hypothetical bulk glass and we wanted to add two hydroxyl groups to the glass for the purpose of hydration, then one would simply decrease the total number of oxygens by one therefore leaving 99 oxygens. Here electroneutrality is observed and the glass is hydrated with two hydroxyl groups.

Molecular dynamics simulations were carried out upon yttrium aluminosilicates with simulation sizes of approx. 2000 atoms using DL_POLY. The data necessary for successfully simulating unhydrated YAS glasses has been given in the methodology, in section 2.5.1 (Tables 2.1 – 2.7). The Al – O Buckingham potential from Table 2.2 was used i.e. SM1 and the Y – O Buckingham potential from Table 2.3 was used i.e. SM2. This was after testing the SM1 and SM2 potentials upon YAS17 in section 3.1.3 where potentials were chosen on their good performance. Along with potentials and information used for unhydrated YAS glasses, the parameters in section 3.2 (Table 3.11) and section 3.3 (Tables 3.12 – 3.16) were required for simulating hydrated YAS glasses. YAS glasses were also simulated using three-body terms for each Si and Al i.e. Table 4.1a and 4.1b below.

Table 4.1a. Truncated three-body harmonic potentials

Truncated Three-body Harmonic Potential [133]					
Species	**k (eV rad^{-2})**	**θ_0 (deg)**	**Si $_{core}$ – O $_{shell}$ (Å)**	**ρ/Å**	**O $_{shell}$ – O $_{shell}$ (Å)**
O $_{shell}$ — Si $_{core}$ — O $_{shell}$	6.15	109.47	1.95	1.00	2.50
OH $_{shell}$ — Si $_{core}$ — O $_{shell}$	6.15	109.47	1.95	1.00	2.50
OH $_{shell}$ — Si $_{core}$ — OH $_{shell}$	6.15	109.47	1.95	1.00	2.50

Table 4.1b. Screened three-body harmonic potentials

Screened Three-body Harmonic Potential						
Species	**k (eV rad^{-2})**	**θ_0 (deg)**	**Si $_{core}$ – O $_{shell}$ (Å)**	**ρ_1/Å**	**ρ_2/Å**	**O $_{shell}$ – O $_{shell}$ (Å)**
O $_{shell}$ — Al $_{core}$ — O $_{shell}$	100	109.47	1.95	1.00	1.00	2.20
OH $_{shell}$ — Al $_{core}$ — O $_{shell}$	100	109.47	1.95	1.00	1.00	2.20
OH $_{shell}$ — Al $_{core}$ — OH $_{shell}$	100	109.47	1.95	1.00	1.00	2.20

Three body terms were not only used for simple oxygen shells but were also used for the incorporation of OHs i.e. hydrogen-bound oxygen shells. A process was followed in order to reach this stage of simulating YAS glasses. YAS glasses were simulated several times with and without the use of the three-body terms for aluminium. Different types of three-body terms were also tested i.e. truncated three-body terms and screened three-body terms.

Using the technique mentioned earlier, three bulk glasses were simulated i.e. YAS17, YAS24 and YAS30. Each glass was hydrated at three different levels where the

variable y, the level of hydration, was 0.1, 0.2 or 0.3. Here y=0.1 refers to low level hydration and y=0.3 is high level of hydration. The stoichiometries for each of the glasses are listed in Table 4.2. A range such as that chosen for this work would thoroughly examine the effects and role of hydration in YAS glasses.

The general rule: $SiO_2 : Al_2O_3 : (Y_2O_3)$-y . (OH) 2y

Table 4.2

Glass Type	Mol % Y_2O_3	Mol % Al_2O_3	Mol % SiO_2	Density (g/cm^3)
YAS17	17.0	18.9	64.1	3.20
YAS24	24.1	21.4	54.5	3.64
YAS30	30.0	20.0	50.0	4.00

Scaling for Hydration: y = OH fraction required to hydrate YAS

UNHYDRATED YAS17: 17.10 mol % Y_2O_3, 18.96 mol % Al_2O_3, and 63.94 mol % SiO_2

Scaled: 92 Y_2O_3, 102 Al_2O_3 and 344 SiO_2

YAS17_0.1 (y=0.1) [92 Y_2O_3, 102 Al_2O_3, 344 SiO_2] – 48 O from (Y_2O_3), +96 OH

YAS17_0.2 (y=0.2) [92 Y_2O_3, 102 Al_2O_3, 344 SiO_2] – 110 O from (Y_2O_3), +220 OH

YAS17_0.3 (y=0.3) [92 Y_2O_3, 102 Al_2O_3, 344 SiO_2] – 150 O from (Y_2O_3), +300 OH

UNHYDRATED YAS24: 24.10 mol % Y_2O_3, 21.40 mol % Al_2O_3, and 54.50 mol % SiO_2

Scaled: 121 Y_2O_3, 108 Al_2O_3 and 272 SiO_2

YAS24_0.1 (y=0.1) [121 Y_2O_3, 108 Al_2O_3, 272 SiO_2] – 50 O from (Y_2O_3), +100 OH

YAS24_0.2 (y=0.2) [121 Y_2O_3, 108 Al_2O_3, 272 SiO_2] – 100 O from (Y_2O_3), +200 OH

YAS24_0.3 (y=0.3) [121 Y_2O_3, 108 Al_2O_3, 272 SiO_2] – 150 O from (Y_2O_3), +300 OH

UNHYDRATED YAS30: 30.00 mol % Y_2O_3, 20.00 mol % Al_2O_3, and 50.00 mol % SiO_2

Scaled: 150 Y_2O_3, 100 Al_2O_3 and 250 SiO_2

YAS30_0.1 (y=0.1) [150 Y_2O_3, 100 Al_2O_3, 250 SiO_2] – 50 O from (Y_2O_3), +100 OH

YAS30_0.2 (y=0.2) [150 Y_2O_3, 100 Al_2O_3, 250 SiO_2] – 100 O from (Y_2O_3), +200 OH

YAS30_0.3 (y=0.3) [150 Y_2O_3, 100 Al_2O_3, 250 SiO_2] – 150 O from (Y_2O_3), +300 OH

4.1 *Short-range structure*

4.1.1 Radial Distribution Functions

Radial-distribution functions for cation-oxygen interactions for all compositions and levels of hydration are given in Figures 4.1 – 4.4.

Figure 4.1: Si – O and Si – OH radial distribution functions in hydrated YAS glasses

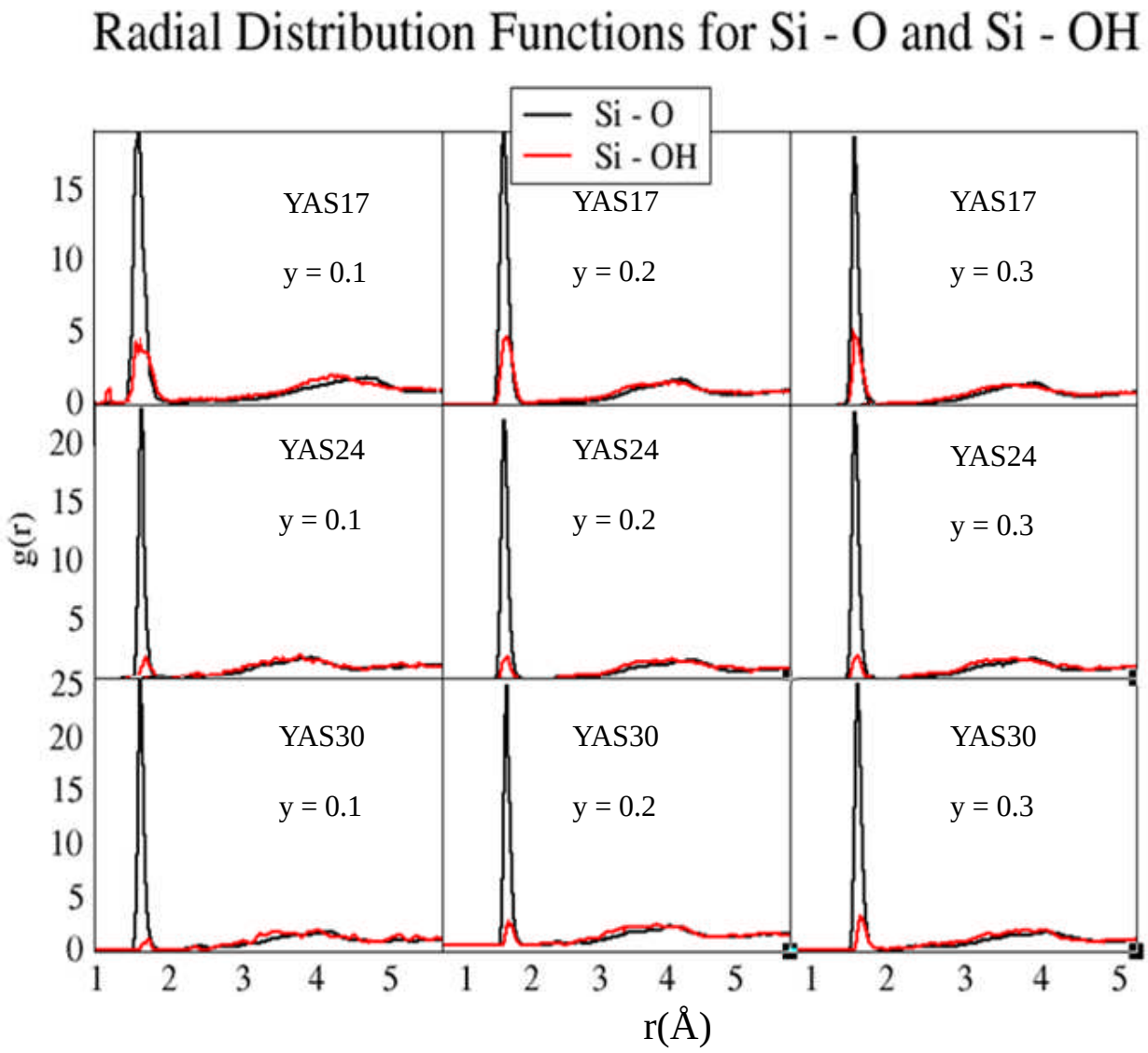

Figure 4.2: Al – O and Al – OH radial distribution functions in hydrated YAS glasses

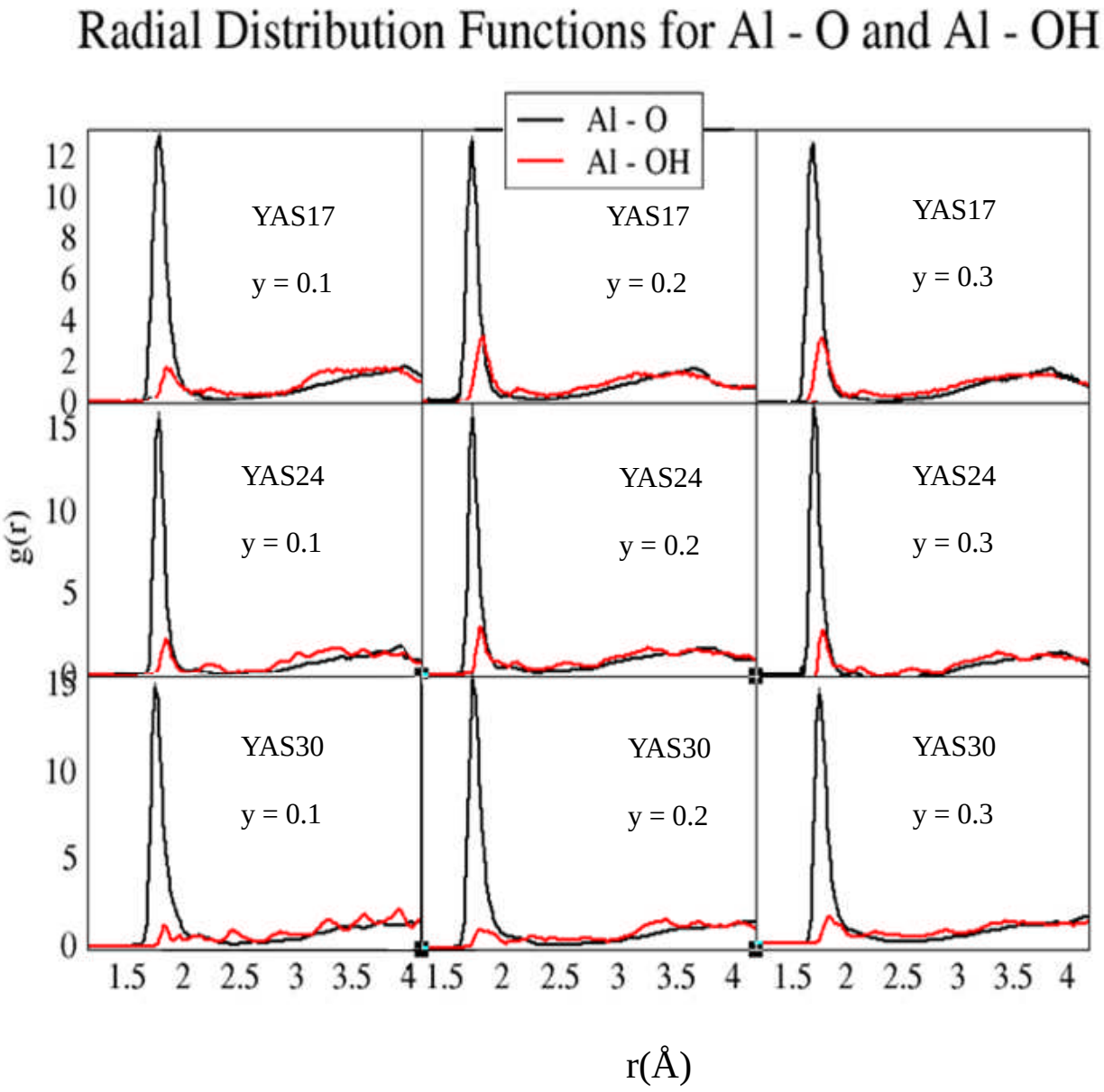

Figure 4.3: Y – O and Y – OH radial distribution functions in hydrated YAS glasses

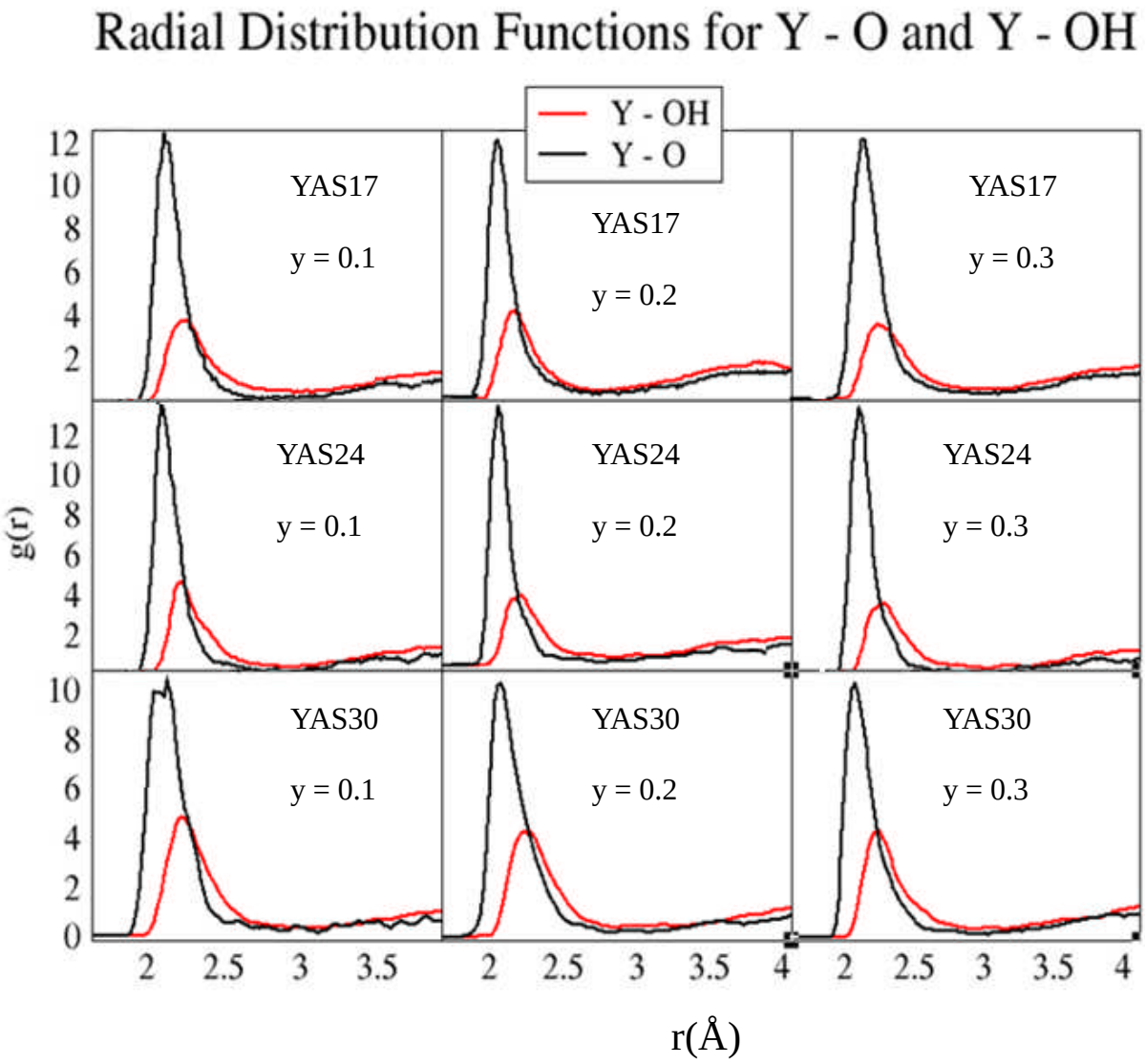

Figure 4.4: Si – O, Al – O and Y – O radial distribution functions in hydrated YAS glasses

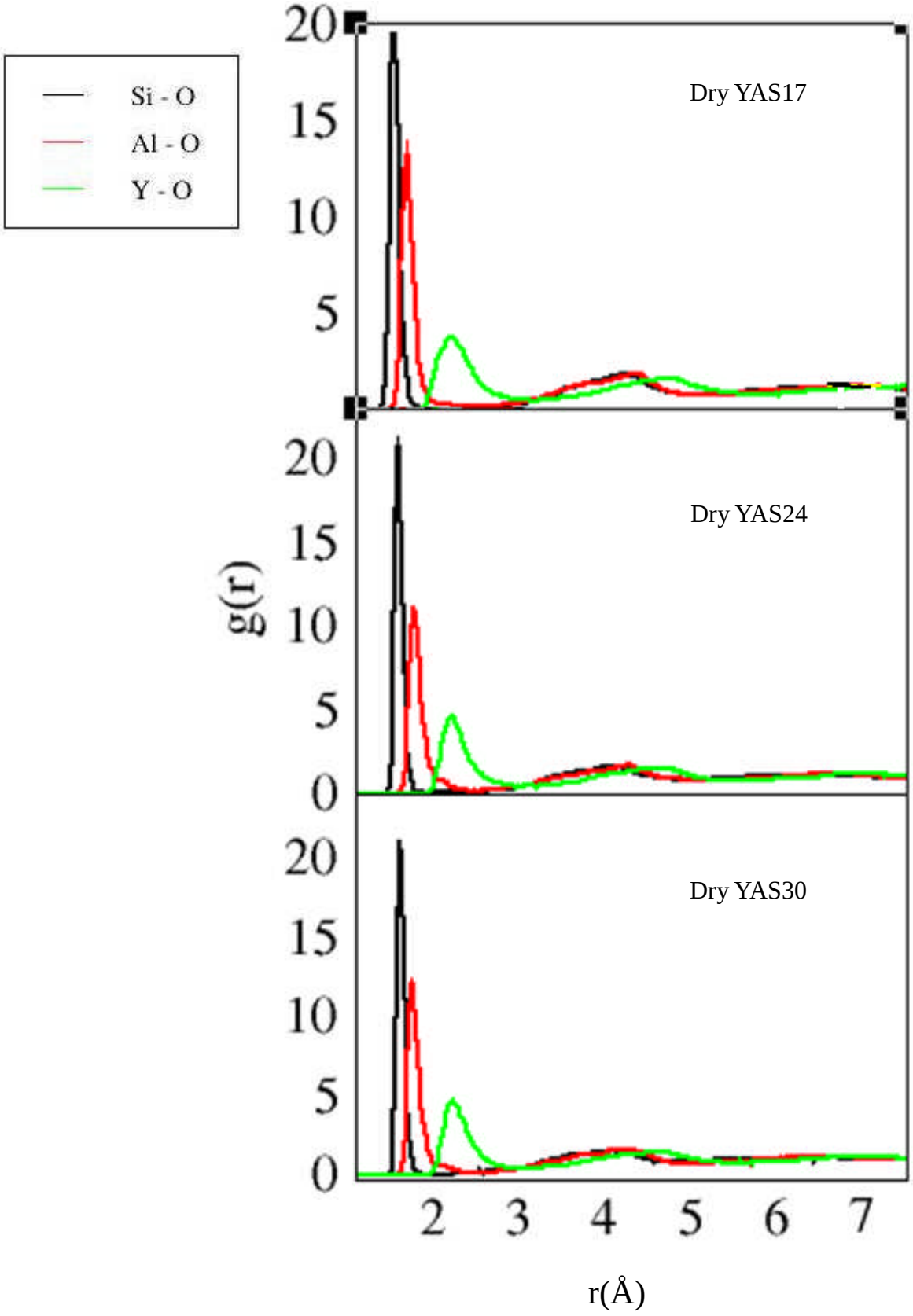

4.1.2 Bond Angles

Figure 4.5: O – Si – O / O – Al – O / O – Y – O bond angle distributions in hydrated YAS glasses

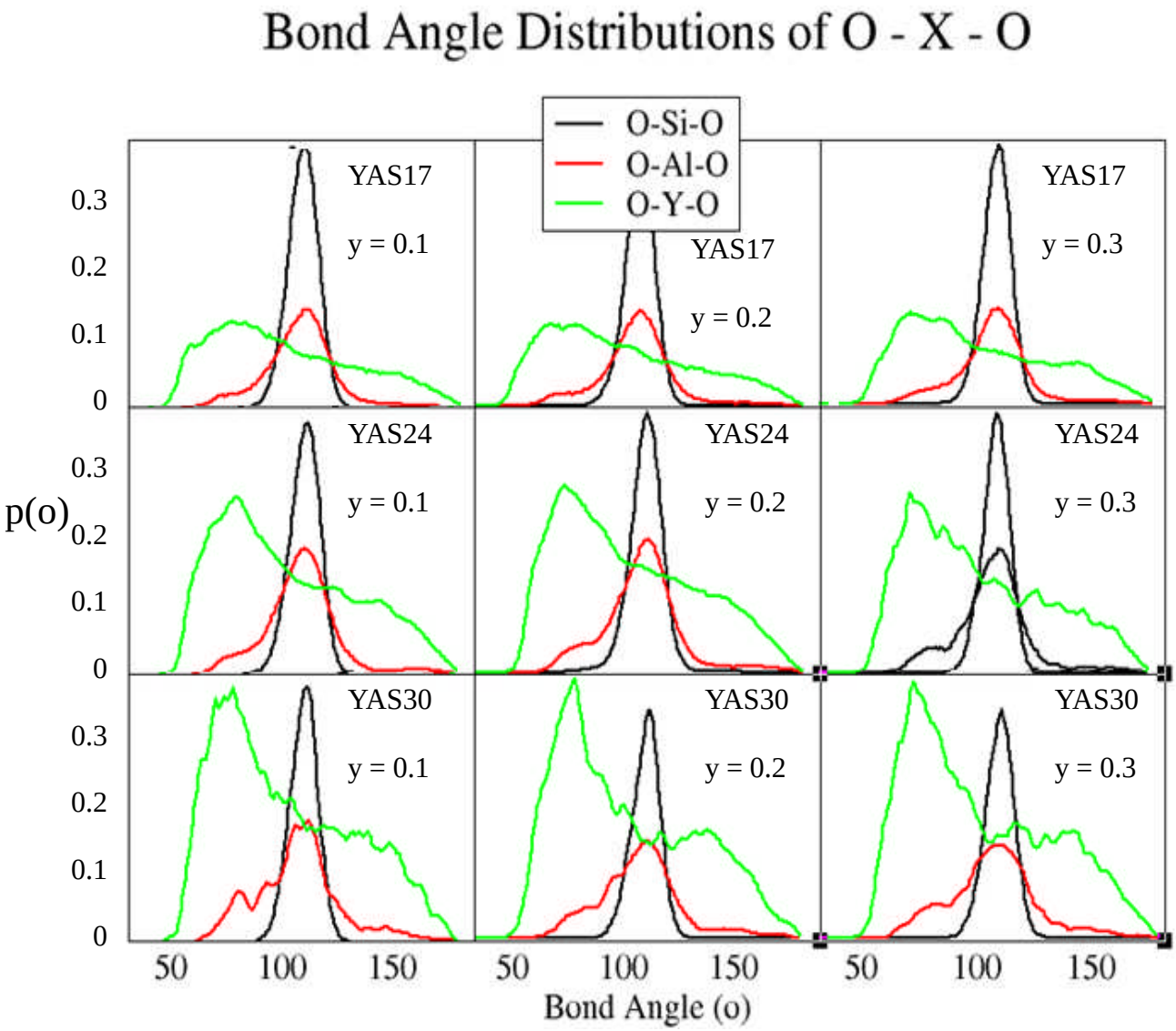

Figure 4.6: Si – O – H / Al – O – H / Y – O – H bond angle distributions in hydrated YAS glasses

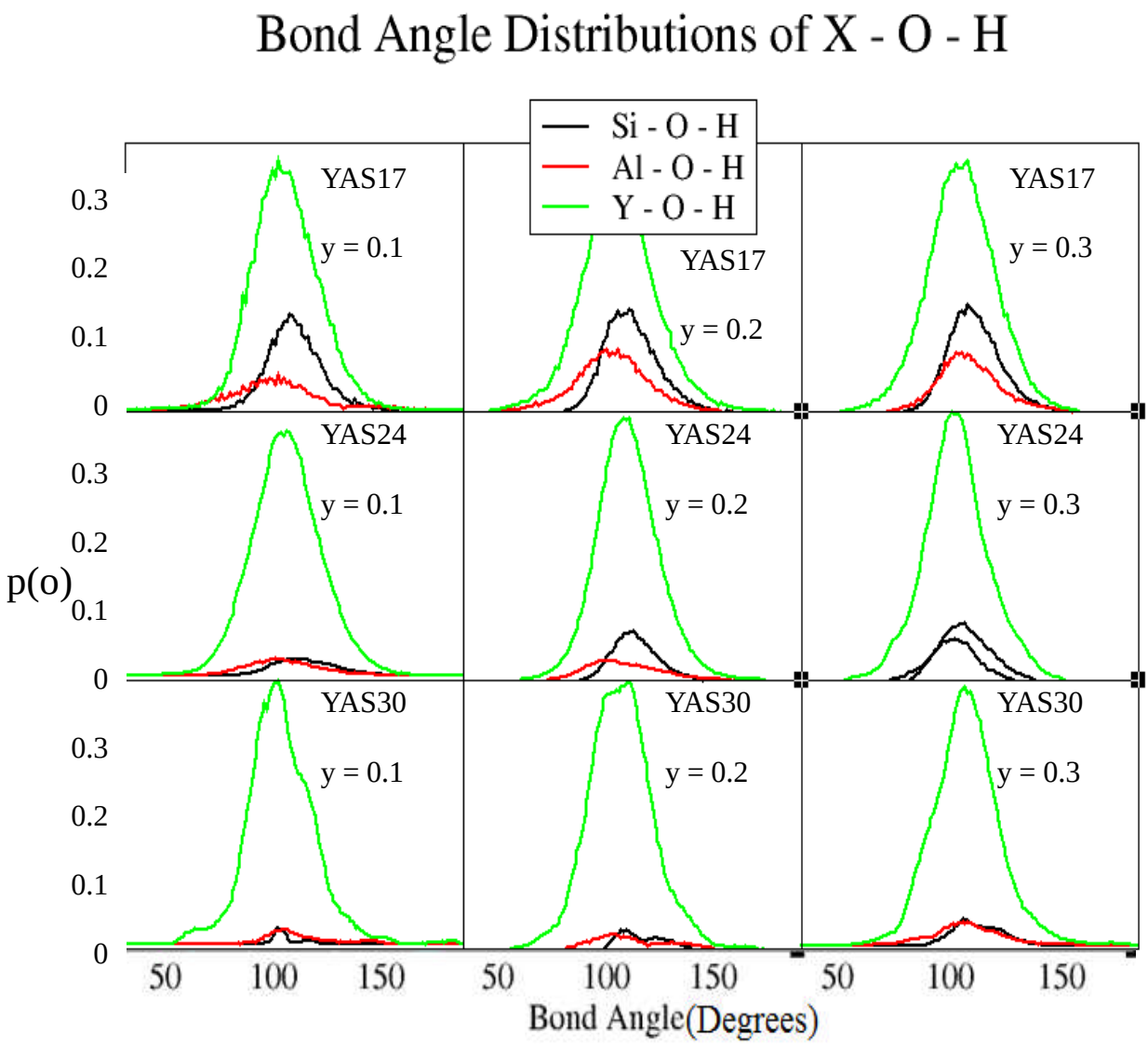

Figure 4.7: O – Si – O / O – Al – O / O – Y – O Bond Angle Distributions in unhydrated YAS Glasses

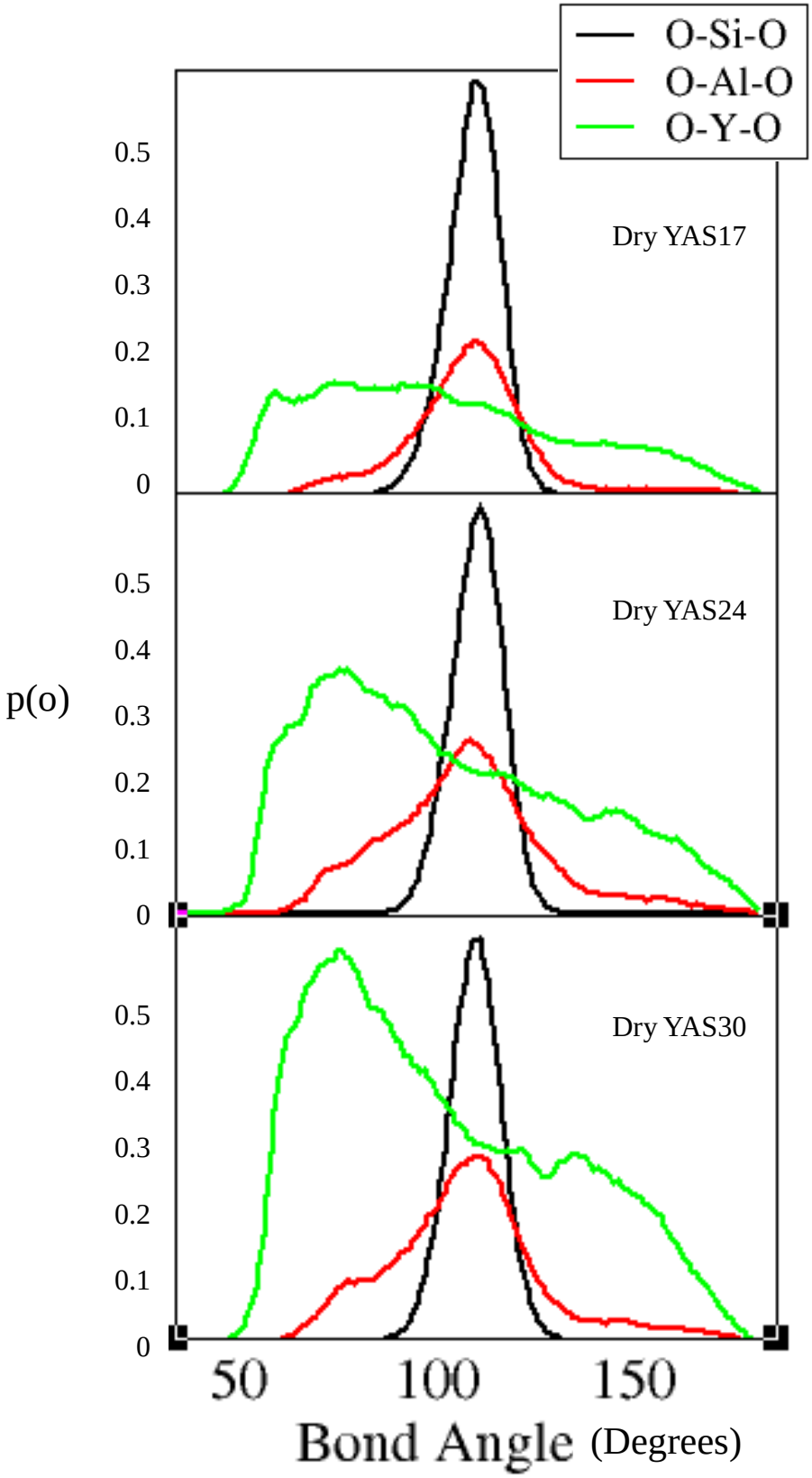

4.1.3 Coordination

1) Silicon

The total silicon coordination numbers for YAS17, 24 and 30 are given below in Figure 4.8a.

Figure 4.8a

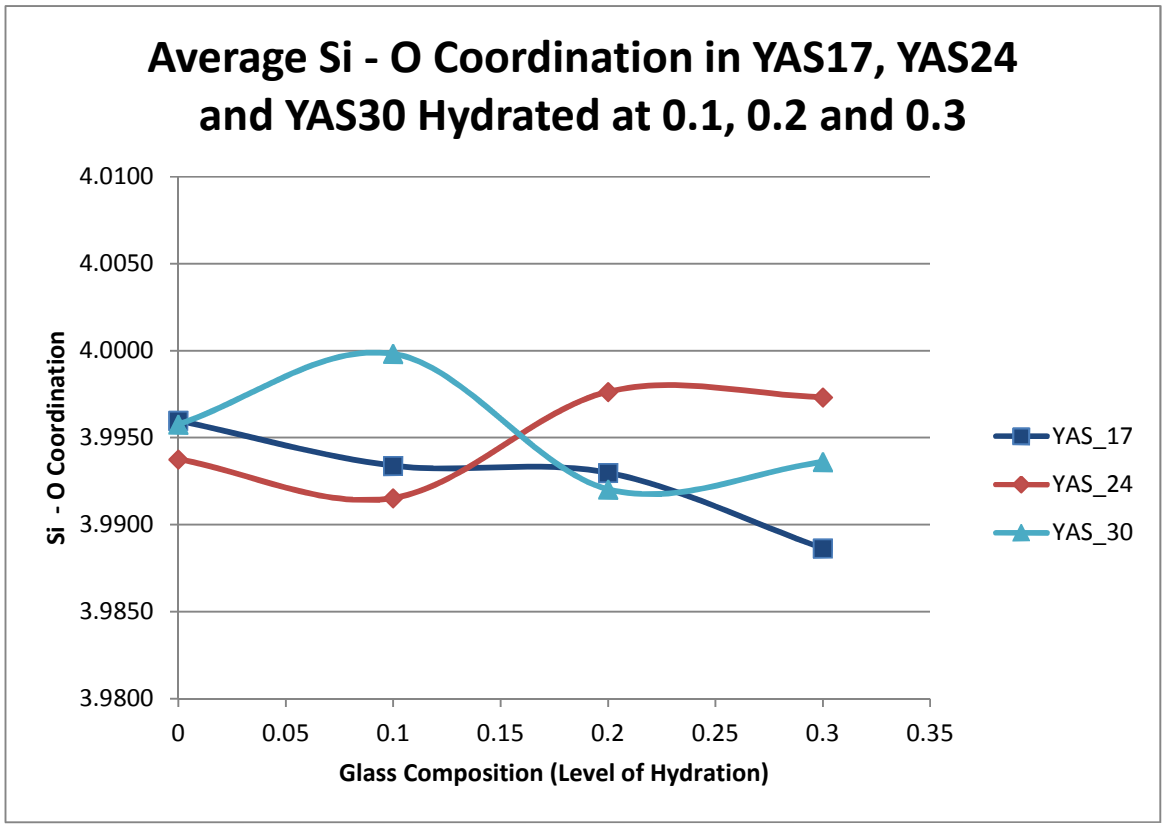

The mean Si - O bond length found in YAS17, 24 and 30 is 1.62 Å and is comparable to the work by Tilocca and Christie [42] where they found a bond length of 1.614 Å. Other MD and diffraction studies of YAS glasses have shown a bond length of 1.60 Å [142, 143]. The mean Si – OH bond length found for hydrated YAS17 (y=0.1, 0.2 and 0.3) was 1.62 Å. The mean Si – OH bond length found for hydrated YAS24 (y=0.1, 0.2 and 0.3) was 1.63 Å. The mean Si – OH bond length found for hydrated YAS30 (y=0.1, 0.2 and 0.3) was 1.64 Å.

There are virtually no silicon atoms with a coordination of five or higher, again which agrees with previous experimental and modelling data [42] which showed coordination numbers of 3.9 – 4.0. Silicon has a well-defined overall coordination of four and has the capacity to take up a maximum of four bonds to that of oxygen found from within the glass network. The graph above shows the total Si coordination for each

glass hydrated from concentrations of 0.1 to 0.3 and their derivatives i.e. non-hydrated glasses YAS17, 24 and 30. The general trend found for YAS24 and YAS30 is that by hydrating each of the glasses causes the overall silicon coordination to remain essentially constant. The same effect is found for YAS17 from hydrations of 0 – 0.2, but a very small decrease is found instead at hydration concentration of 0.3 for YAS17.

To further analyse the Si coordination to oxygen, the coordination contributions were split. We separate the coordination into silicon-oxygen coordination relating solely from the network former/modifier species i.e. Y_2O_3 / SiO_2 / Al_2O_3, and from those attached to hydrogen i.e. hydroxyl groups, which will give an insight as to why a constant silicon coordination is seen for all YAS glasses observed in Figure 4.8a.

The partial silicon coordination numbers are given below for YAS17, 24 and 30 without including hydroxyl groups in the silicon coordination sphere in Figure 4.8b.

Figure 4.8b

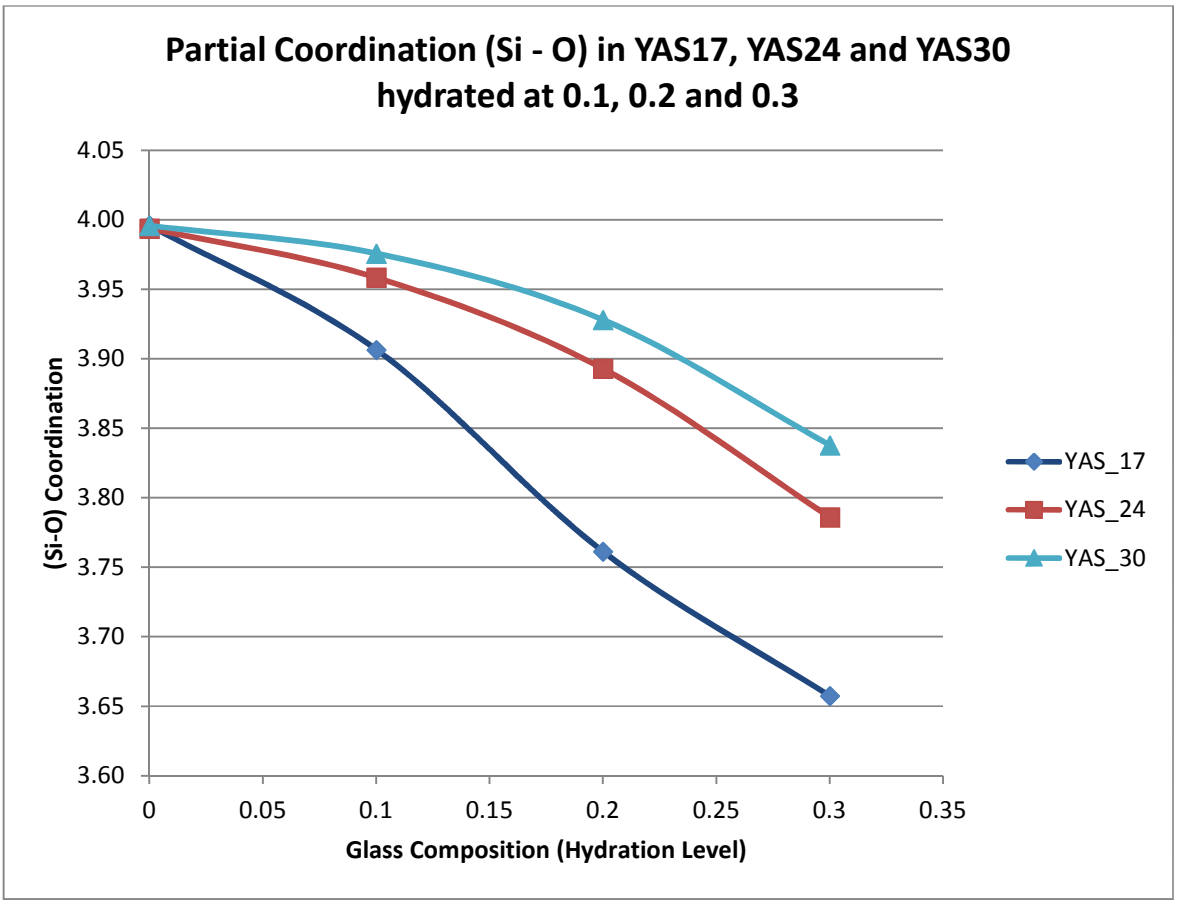

The general trend found for YAS17, 24 and 30 is that hydrating each of the glasses causes the partial Si – O coordination to decrease. Here YAS30 is least affected by hydroxyl groups being attached to silicon, whereas the opposite is found for YAS17 i.e. a greater decrease in coordination is seen and therefore shows that fewer oxygen atoms from the network cation species i.e. Y_2O_3 / SiO_2 / Al_2O_3, attach to Si in YAS17 than YAS30.

The partial silicon coordination numbers are given below for YAS17, 24 and 30 solely coordination of hydroxyl groups onto silicon excluding normal oxygens from the silicon coordination sphere in Figure 4.8c.

Figure 4.8c.

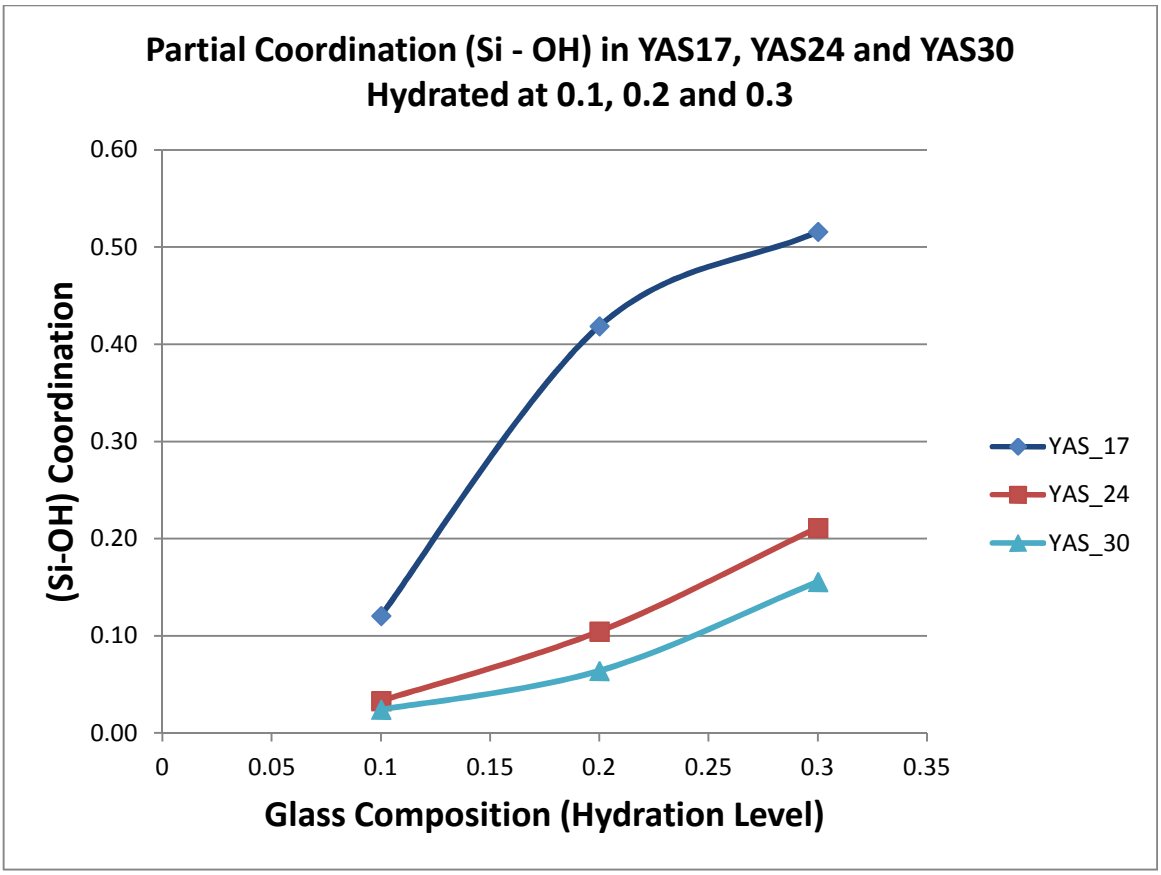

YAS17 is affected more by hydration than YAS30 i.e. more hydroxyls prefer to attach to silicon in YAS17 than YAS30. The general trend found was that for all glass compositions, gradual hydration caused a greater number of hydroxyl groups to coordinate to that of silicon. The main difference between YAS17 and YAS30 is the yttrium content at 17% and 30% respectively. We see that an yttrium aluminosilicate glass which has less yttrium content will in turn allow for hydroxyl groups to coordinate to silicon more than an yttrium aluminosilicate glass which has more yttrium content.

Mead and Mountjoy showed in their work on sol-gel derived calcium silicate glasses that hydroxyl groups affect silicon by forming a small contribution to Si – O coordination ($N_{Si\text{-}OH} \sim 0.4$) [152]. We see that this takes place for YAS glasses too. Dry YAS17 has a hydroxyl coordination of zero since hydration is absent, but if we were to hydrate YAS17 at y=0.3, this increases the silicon coordination where the contribution

from hydroxyl groups is ~ 0.4, see Figure 4.8c. The compositions used by Mead and Mountjoy are different to YAS glasses simulated in this work, but the way in which silicon is affected by hydration, more importantly, how many hydroxyl groups coordinate onto silicon is the same. Si – OH and Al – OH species have been reported for aluminosilicate glasses using NMR experiments by Xianyu Xue [153]. It had been demonstrated that hydroxyl groups coordinate onto silicon and aluminium for aluminosilicate glasses. For hydroxyl groups that have not attached to network-forming species, they would as a result be described as free hydroxyl groups with coordination to network-modifying species such as sodium [153] or yttrium in this work. These will be described in section 4.3.

2) Aluminium

The total aluminium coordination numbers for YAS17, 24 and 30 are given below in Figure 4.9a.

Figure 4.9a

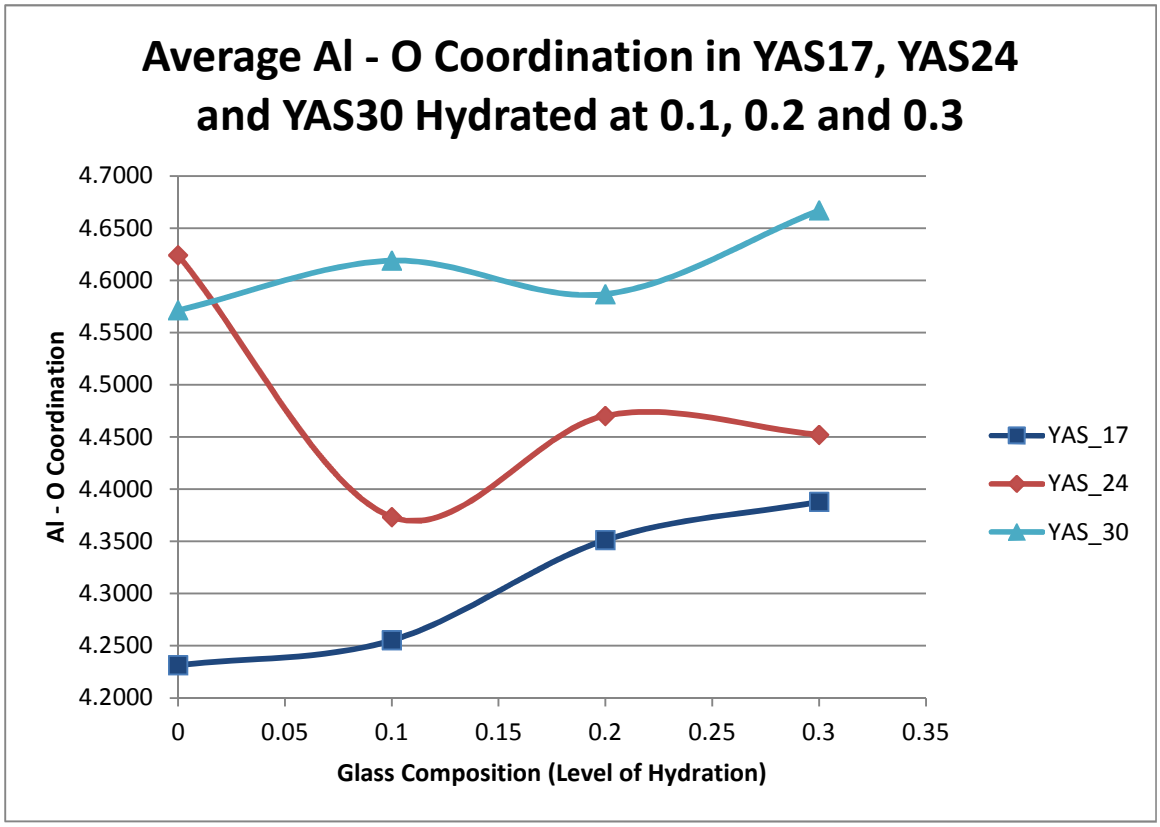

The average bond distance of Al – O found within YAS17, 24 and 30 is 1.78 Å. The value obtained is agreeable with 1.79 Å and 1.82 Å obtained in previous structural studies of YAS [142, 143]. The mean bond length for Al – OH found for hydrated YAS17, 24 and 30, was calculated to be 1.89 Å which is comparable to the values found by modelling techniques i.e. Al - O 1.79 Å and 1.82 Å [142, 143].

The total Al – O coordination for glass compositions YAS17, 24 and 30 both hydrated and unhydrated, range between 4.23 – 4.66. The coordination numbers coincide with diffraction experiments which gave 4.5 +/- 0.5 for glass with 11% yttria [143]. The general trend found from the above graph is that the total Al – O coordination increases gradually as hydration increases. What we can gather from solely observing Figure 4.9a is that YAS30 (which has the most yttrium content of 30%) has higher aluminium coordination numbers than YAS17 (which has the least yttrium content at 17%). It is still therefore seen that the more yttrium present in an yttrium aluminosilicate glass, the more likely aluminium will have higher coordination numbers

even when hydrated.

To further analyse the Al coordination to oxygen, the coordination contributions were split. We separate the coordination into aluminium-oxygen coordination relating solely from the network cations i.e. Y_2O_3 / SiO_2 / Al_2O_3 and those attached to hydrogen i.e. hydroxyl groups, which will give an insight as to why an overall increase in aluminium coordination is seen for all YAS glasses observed in Figure 4.9a.

The partial aluminium coordination numbers are given below for YAS17, 24 and 30 without including hydroxyl groups in the aluminium coordination sphere in Figure 4.9b.

Figure 4.9b

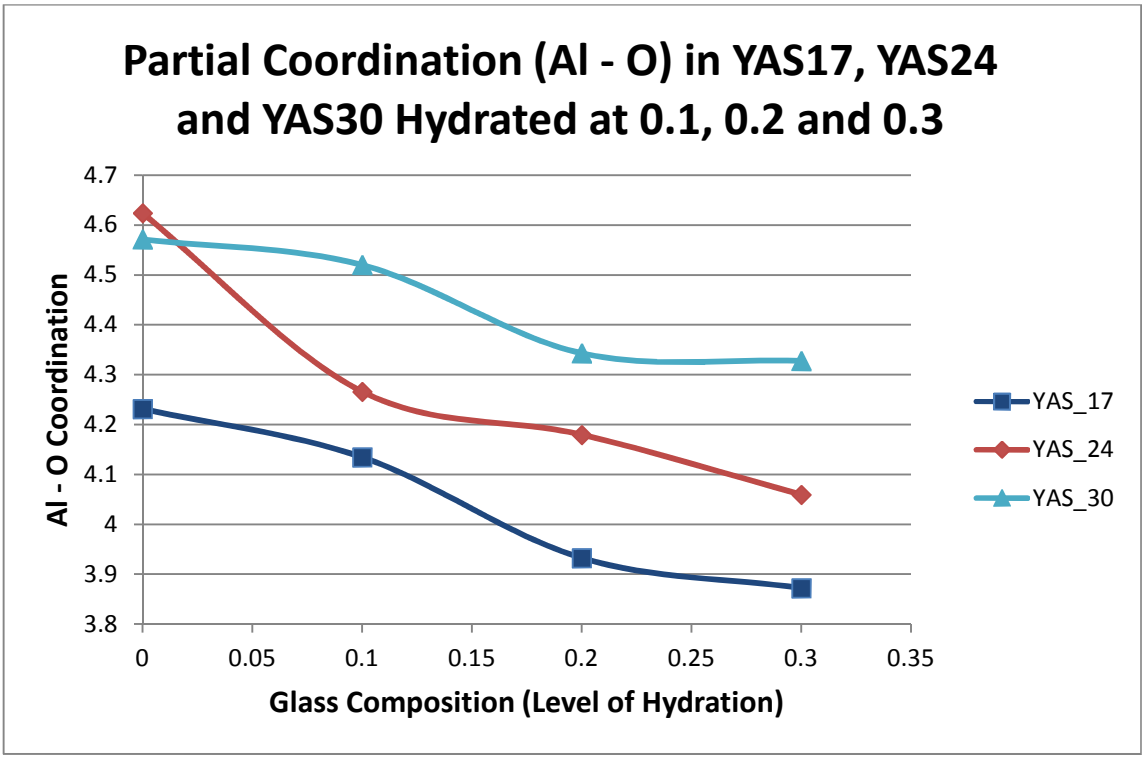

The general trend found for YAS17, 24 and 30 is that by hydrating each of the glasses causes the partial Al – O coordination to decrease. Since the yttrium content in unhydrated YAS30 is greater than in unhydrated YAS17 at 30% and 17% respectively, we see that aluminium generally has higher coordination numbers for an yttrium aluminosilicate glass with a greater yttrium content than compared to an yttrium aluminosilicate with lower yttrium content, whether hydrated or unhydrated as demonstrated in Figure 4.9b. The same trend is seen from the work by Tilocca and Christie [42] but the absolute values of coordination for unhydrated glasses YAS17 and 30 in this work are different as discussed in section 3.1.3.

The partial aluminium coordination numbers are given below for YAS17, 24 and 30 without including oxygen atoms in the silicon coordination sphere in Figure 4.9c. Figure 4.9c demonstrates solely coordination of hydroxyl groups onto aluminium.

Figure 4.9c

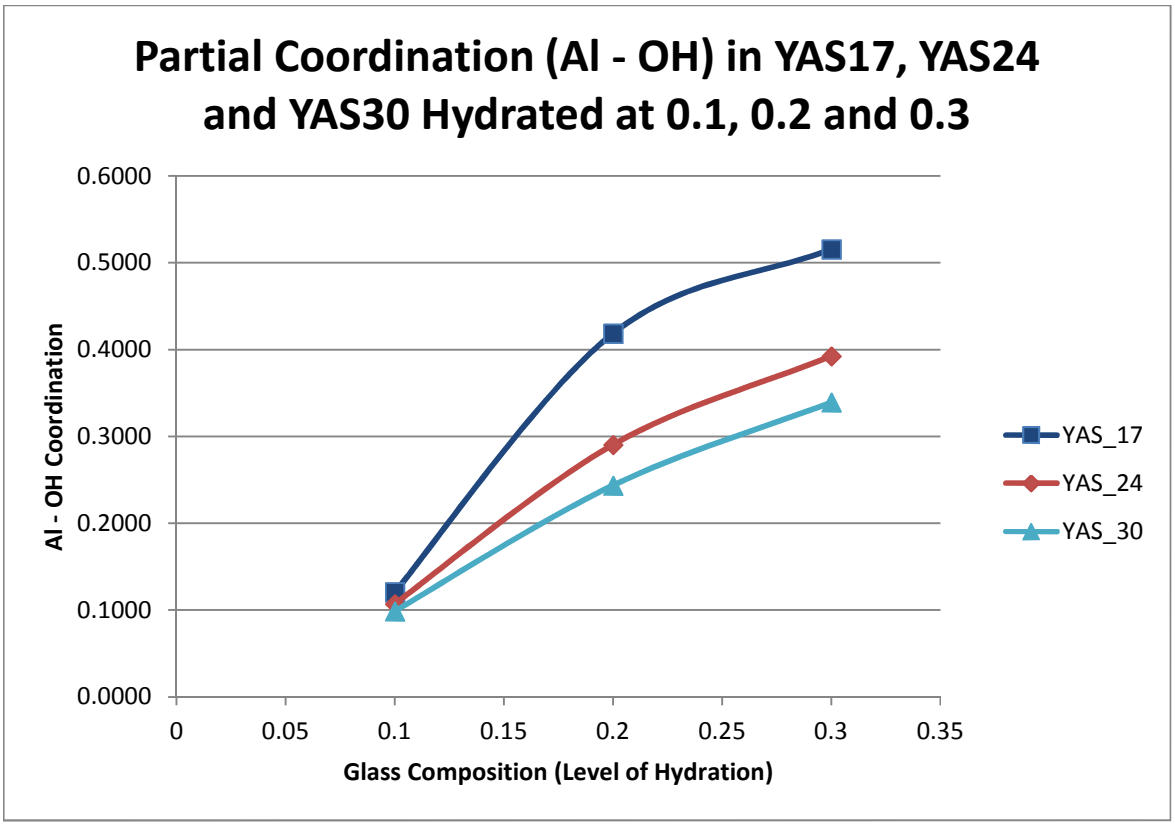

YAS17 was affected more by hydration than YAS30 i.e. more hydroxyl groups prefer to attach to Al in YAS17 than YAS30 at the same hydration level. The general trend found from the above graph, that for all glass compositions, gradual hydration caused a greater number of hydroxyl groups to coordinate to aluminium. By viewing Figure 4.8c, the range of hydroxyl groups coordinating onto silicon is 0.01 - 0.43, whereas in Figure 4.9c we see that the range for aluminium is 0.1 - 0.45, so the coordination numbers of hydroxyl groups onto aluminium in Figure 4.9c are very similar compared to hydroxyl coordination numbers onto silicon seen in Figure 4.8c. This shows hydroxyl groups have the ability to coordinate roughly equally to aluminium and silicon.

Mead and Mountjoy showed in their work on sol-gel derived calcium silicate glasses that hydroxyl groups affect silicon by forming a small contribution to Si – O coordination ($N_{Si\text{-}OH} \sim 0.4$) [152], and we saw that this takes place for YAS glasses too. Aluminium, similarly to silicon, is a network former, although it has a higher

coordination of approximately 4.5 due to the presence of a number of five- and six-coordinated aluminium atoms. If hydroxyl groups were seen and shown to attach to silicon in the work by Mead and Mountjoy, this would also support the assumption that association of hydroxyl groups onto aluminium would also occur since it is a second network former in YAS glasses. The silicon coordination solely due to hydroxyl groups is ~ 0.4 as seen in Figure 4.8c. The aluminium coordination solely due to hydroxyl groups is also ~ 0.4 as seen in Figure 4.9c. This means hydroxyl groups attach to silicon and aluminium by the same amounts yet aluminium loses coordination to normal oxygen species more than silicon (Figures 4.8b and 4.9b).

Si – OH and Al – OH species have been reported using NMR experiments by Xianyu Xue [153], and we have demonstrated that hydroxyl groups coordinate onto silicon and aluminium in aluminosilicate glasses.

3) Yttrium

The total yttrium coordination numbers for YAS17, 24 and 30 are given below in Figure 4.10a.

Figure 4.10a

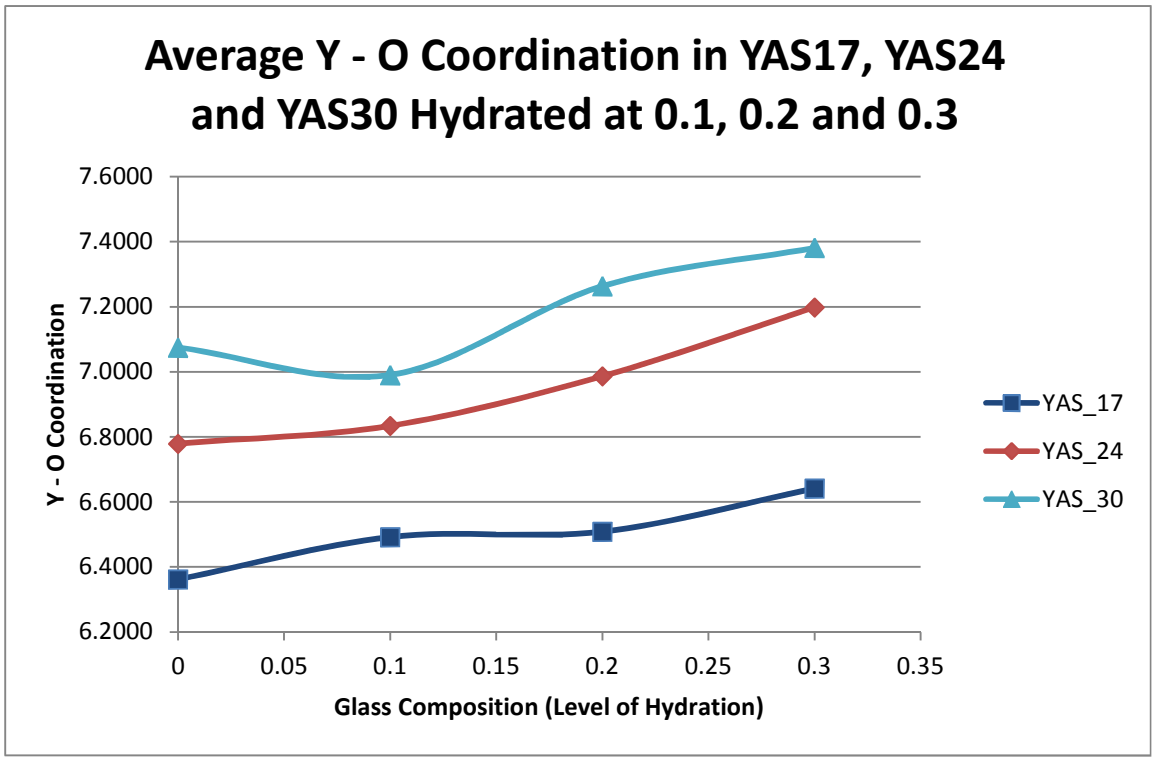

The total Y – O coordination for glass compositions YAS17, 24 and 30 ranged from 6.36 – 7.30. Such coordination numbers compare well enough to binary yttria-alumina glasses experimentally made, where coordination numbers of 6.9 +/- 0.4 [147] and 6.64 +/- 0.33 [148] were found. A wider range of bonding environments are observed for yttrium compared to either silicon or aluminium: here six- or seven-coordinated yttrium atoms are most dominant. Some yttrium atoms have been seen to have coordination numbers of as low as three and as high as ten. The general trend found from the above graph is that the total Y – O coordination increases gradually as hydration increases. An investigation is required to find out how many hydroxyls are able to attach to yttrium in each of the glasses and whether or not increased hydration improves the effect. Therefore partial Y – O and Y – OH contributions were shown in Figures 4.10b and 4.10c respectively.

What is evident from observing Figure 4.10a, is that the more yttrium a YAS glass has i.e. YAS30, the higher the coordination of yttrium will be and this is true even for hydrated glasses. YAS17 has lower yttrium content and the coordination numbers are lower.

The partial yttrium coordination numbers are given below for YAS17, 24 and 30 without including hydroxyl groups in the yttrium coordination sphere in Figure 4.10b.

Figure 4.10b

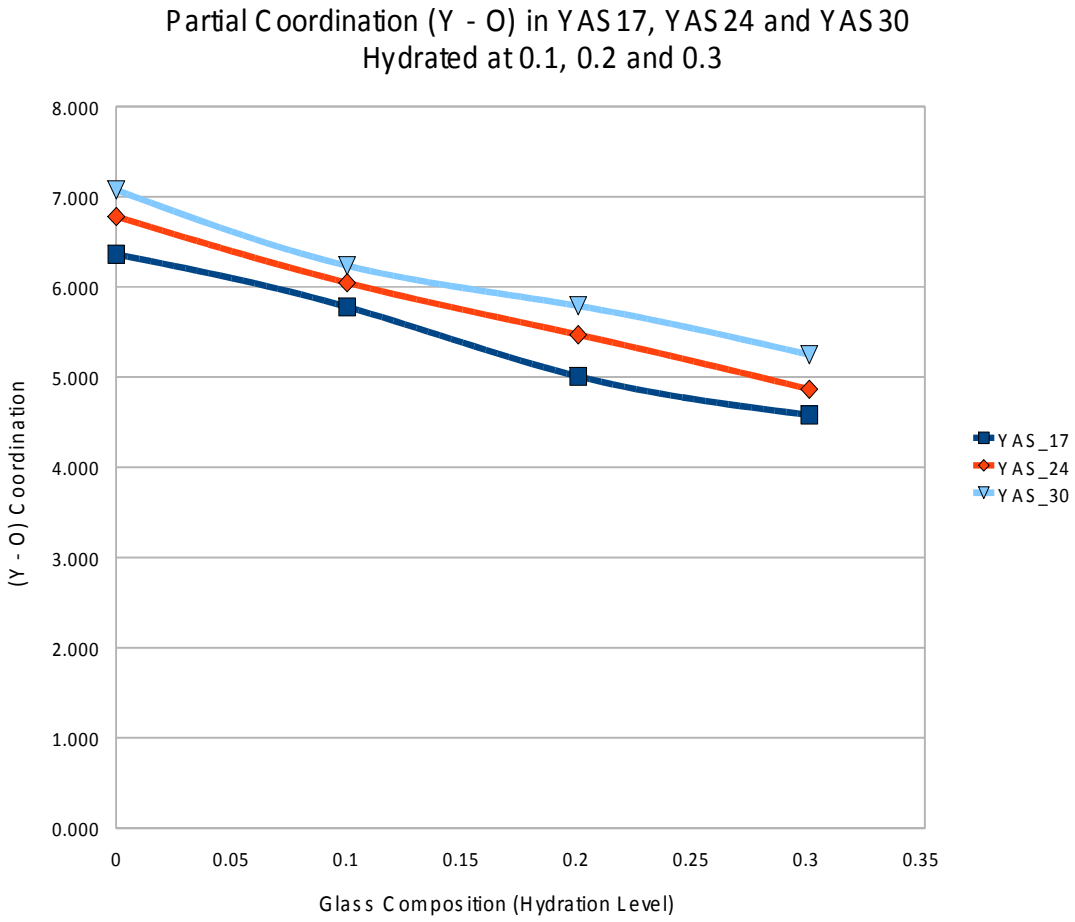

The graph above shows the partial Y - O coordination (exclusive of any hydroxyls that may be attached) for each glass YAS17, 24 and 30 hydrated from concentrations of 0.1 to 0.3. The general trend found for YAS17, 24 and 30 is that hydrating each of the glasses causes the partial Y – O coordination to decrease. Since the yttrium content in unhydrated YAS30 is greater than in unhydrated YAS17 at 30% and 17% respectively, we see that yttrium generally has higher coordination numbers for an yttrium aluminosilicate glass with a greater yttrium content than compared to an yttrium aluminosilicate with lower yttrium content. So an yttrium aluminosilicate glass with low yttrium content will give rise to lower overall yttrium coordination whether hydrated or not.

The partial yttrium coordination numbers are given below for YAS17, 24 and 30 without including oxygen atoms in the silicon coordination sphere in Figure 4.10c. Figure 4.10c demonstrates solely coordination of hydroxyl groups onto yttrium excluding normal oxygens from the yttrium coordination sphere.

Figure 4.10c

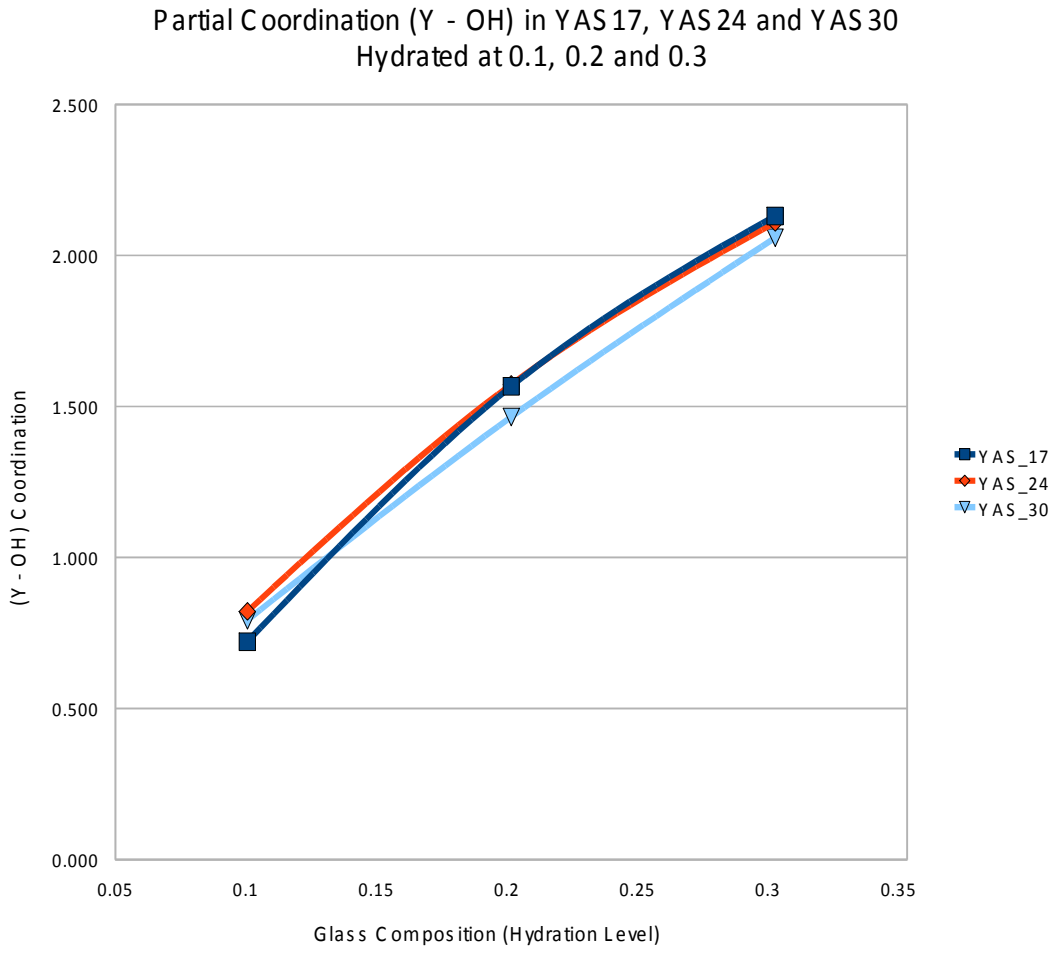

The general trend found from the above graph, that for all glass compositions, increasing hydration caused a greater number of hydroxyl groups to coordinate to yttrium. The more hydrated a glass becomes the greater number of hydroxyl groups will attach to yttrium. By viewing figure 4.10c we see that the range of coordination is 0.72 – 2.13. This shows hydroxyl groups having the ability to coordinate substantially more to yttrium and less with silicon or aluminium (Figure 4.8b and 4.9b). Yttrium has a wider range of coordination numbers than Si and Al thus giving rise to a greater capacity to welcome hydroxyl groups into the coordination sphere of yttrium. (Figures 4.8a, 4.9a and 4.10a).

Hydroxyl groups prefer to coordinate more to yttrium than to aluminium and silicon. Figures 4.8c, 4.9c and 4.10c show the coordination of hydroxyls to Si, Al and Y respectively. The coordination number is largest in Figure 4.10c of Y – OH. Silicon and aluminium are equally tied in being second highest in intensity found in Figure 4.8c and 4.9c respectively. This demonstrates that hydroxyl groups generally like to attach to yttrium more than aluminium and silicon for all YAS glass compositions.

Fig 4.11: $(Y - OH) > (Al - OH) \sim (Si - OH)$

Silicon is particular over what may enter the coordination sphere as it has a very well defined stable tetrahedral form. Once silicon has reached the maximum of four bonds onto oxygen and is tetrahedral in orientation it would no longer posses the ability to welcome anymore oxygen atoms. We have observed that silicon does not prefer hydroxyl groups into its coordination sphere; the opposite effect is observed by yttrium. Since hydroxyl groups coordinate less to silicon and aluminium they have one remaining area they can move towards i.e. to coordinate to yttrium.

For hydroxyl groups that have not attached to network-forming species, they would as a result be described as free hydroxyl groups with coordination to network-modifying species [153]. For hydrated YAS glasses, yttrium is the modifier which has coordination to free hydroxyl groups as well as hydroxyl groups that are coordinated to silicon and aluminium. The presence of free hydroxyl groups is discussed in section 4.3.

Table 4.3 below shows the coordination of hydroxyl groups onto silicon, aluminium and yttrium. The distribution of how many hydroxyl groups coordinate onto silicon, aluminium and yttrium are also given to support Figure 4.11.

Table 4.3: The coordination *n* and distribution of hydroxyl groups for silicon, aluminium and yttrium for YAS17, 24 and 30 hydrated at y=0.1, 0.2 and 0.3.

Si - OH (%)

n	YAS17_0.1		YAS17_0.2		YAS17_0.3		YAS24_0.1		YAS24_0.2		YAS24_0.3		YAS30_0.1		YAS30_0.2		YAS30_0.3	
	(%)	St.Dev	(%)	St.Dev	(%)	St.Dev	(%)	St.Dev	(%)	St.Dev	(%)	St.Dev	(%)	St.Dev	(%)	St.Dev	(%)	St.Dev
0.0	91.317	4.058	76.979	3.391	67.312	2.307	93.075	5.628	81.565	6.893	72.429	12.996	97.600	1.131	93.600	2.828	84.834	2.215
1.0	8.683	4.058	22.875	3.186	32.252	1.691	6.695	5.302	16.390	12.780	20.771	3.379	2.400	1.131	6.400	2.828	14.766	1.649
2.0	0.000	0.000	0.145	0.206	0.436	0.617	0.230	0.325	1.758	2.486	0.184	0.260	0.000	0.000	0.000	0.000	0.400	0.566
Coordination	0.087	0.041	0.232	0.036	0.331	0.029	0.033	0.005	0.105	0.044	0.211	0.039	0.024	0.011	0.064	0.028	0.156	0.028

Al – OH (%)

n	YAS17_0.1		YAS17_0.2		YAS17_0.3		YAS24_0.1		YAS24_0.2		YAS24_0.3		YAS30_0.1		YAS30_0.2		YAS30_0.3	
	(%)	St.Dev	(%)	St.Dev	(%)	St.Dev	(%)	St.Dev	(%)	St.Dev	(%)	St.Dev	(%)	St.Dev	(%)	St.Dev	(%)	St.Dev
0.0	87.935	3.004	63.992	8.915	55.823	10.855	89.504	0.578	73.875	3.983	67.052	5.393	90.122	1.471	78.458	5.663	69.557	2.480
1.0	12.065	3.004	30.921	7.242	37.776	10.961	10.266	0.253	23.429	2.825	27.437	5.444	9.877	1.472	18.713	4.112	27.220	2.015
2.0	0.000	0.000	4.309	1.277	5.402	0.607	0.230	0.325	2.465	1.486	4.713	0.235	0.001	0.001	2.830	1.552	2.954	0.792
3.0	0.000	0.000	0.778	0.396	0.999	0.714	0.000	0.000	0.232	0.328	0.798	0.185	0.000	0.000	0.000	0.000	0.268	0.328
Coordination	0.121	0.030	0.419	0.110	0.516	0.100	0.107	0.009	0.291	0.048	0.393	0.055	0.099	0.015	0.244	0.072	0.339	0.026

Y – OH (%)

n	YAS17_0.1		YAS17_0.2		YAS17_0.3		YAS24_0.1		YAS24_0.2		YAS24_0.3		YAS30_0.1		YAS30_0.2		YAS30_0.3	
	(%)	St.Dev	(%)	St.Dev	(%)	St.Dev	(%)	St.Dev	(%)	St.Dev	(%)	St.Dev	(%)	St.Dev	(%)	St.Dev	(%)	St.Dev
0.0	36.290	0.991	11.521	5.028	3.935	1.989	37.011	1.166	10.377	1.985	4.218	1.272	37.914	2.831	11.935	0.825	6.875	1.144
1.0	53.014	5.366	40.459	0.860	23.594	5.009	46.937	2.107	40.827	1.215	22.303	0.087	49.164	2.706	42.716	0.920	23.988	2.200
2.0	9.813	3.259	34.572	4.946	39.850	0.243	13.642	0.322	36.926	2.019	36.216	5.750	11.843	1.401	32.897	0.348	33.392	6.256
3.0	0.883	1.116	11.971	0.247	25.099	3.147	2.202	0.326	10.608	0.620	25.714	4.313	1.078	1.525	10.841	0.117	23.154	2.233
4.0	0.000	0.000	1.477	1.025	6.068	0.418	0.207	0.293	0.849	0.025	9.552	1.808	0.000	0.000	1.611	0.369	10.270	1.162
5.0	0.000	0.000	0.000	0.000	1.417	0.252	0.000	0.000	0.414	0.586	1.786	1.277	0.000	0.000	0.000	0.000	2.317	1.799
6.0	0.000	0.000	0.000	0.000	0.037	0.050	0.000	0.000	0.000	0.000	0.211	0.288	0.000	0.000	0.000	0.000	0.004	0.006
Coordination	0.753	0.045	1.514	0.074	2.102	0.041	0.817	0.007	1.520	0.075	2.203	0.132	0.761	0.045	1.475	0.014	2.129	0.101

A possible mechanism has been drawn of how hydroxyl groups coordinate onto yttrium in Figure 4.12.

Figure. 4.12

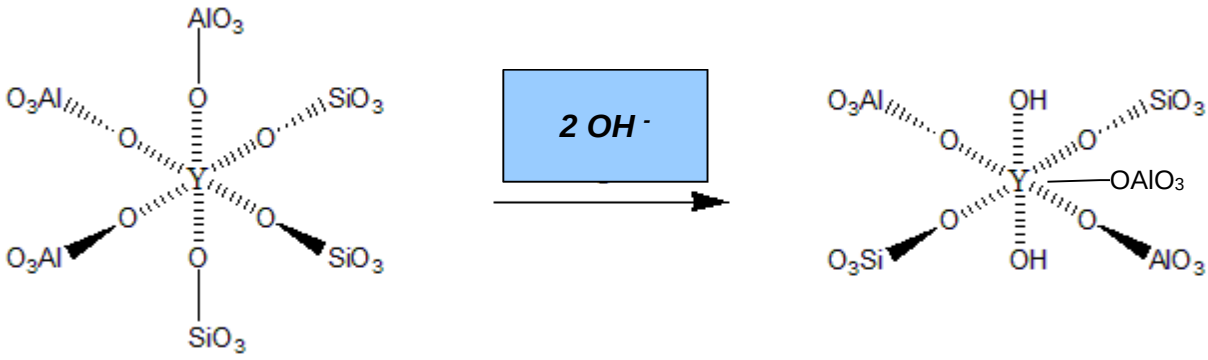

It is possible that aluminium and silicon tend to follow the same mechanism but since it has been seen that yttrium allows for more hydroxyls to coordinate into its coordination sphere, the mechanism has been created specifically for yttrium rather than for aluminium or silicon.

The mechanism we see is an addition process followed by substitution, where the first hydroxyl group will move into the yttrium coordination sphere (increasing coordination) and a second hydroxyl to break the interaction between Y – O – Si – O_3. For example in Figure 4.13.

Fig. 4.13

$$Y = = = O - Si - O_3 \xrightarrow{2\ OH^-} Y = = = OH + [HO - Si - O_3]---$$

Since we increase hydration for YAS glasses 17, 24 and 30 from 0.1 – 0.3 we as a result see further hydroxyl groups locating themselves into yttrium's coordination sphere who have already carried out substitution and thus gives rise to the latter part of the mechanism called addition (Figure 4.13). The [HO – Si – O_3]--- entity would as a result be put back into the glass structure and increase the network connectivity for silicon, as we discuss in section 4.4.

4.2 *Three-bonded Oxygen Species*

4.2.1 Species

1) Si-OH-Si

While calculating results for YAS glasses a code was developed for the detection of bridging or non-bridging hydroxyl groups between network-forming species Si and Al (Figure 4.14). There were no Si – OH – Si species seen in any of the hydrated YAS glasses of any composition. This shows that hydroxyl groups have a preference not to bridge between two silicon atoms because a silicon adjacent to another silicon is a charge balanced system i.e. Si – O – Si and if a proton bonded to the oxygen bridging the two silicons together, the proton would not be stabilising anything and would give the Si – O – Si a positive charge overall if Si – $^{+}$OH – Si formed. (Figure 4.14a)

Figure 4.14

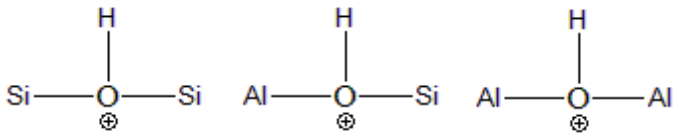

a b c

2) Si-OH-Al

A low number of species of the form Si – OH – Al were detected in each of the hydrated YAS glasses (YAS17, 24 and 30). This shows that hydroxyl groups have a preference to bridge between silicon and aluminium atoms than compared to a hydroxyl group bridging between two adjacent Si atoms, where none are seen (Figure 4.14b).

The number of these species i.e. Si – OH – Al seen in hydrated YAS glasses 17, 24 and 30 do not show any trends with respect to increasing hydration concentration, except for an increase at y=0.3 (Table 4.4a and 4.4b). More of these species are seen for YAS17 than YA24 and YAS30.

The numbers of Si – OH – Al species present in each of the hydrated glasses are shown in Table 4.4a. Normalisation of numbers in Table 4.4a give rise to Table 4.4b to remove any unnecessary effects of biasing with the number of hydroxyls used in each of the simulations. The normalisation method employed is:

NORMALISATION: No. of Si – OH – Al / Total No. of Hydroxyls in Simulation

E.g. for YAS17

(y=0.1) (y=0.2) (y=0.3)

Si – OH – Al = 3.5/96 Si – OH – Al = 8.0/220 Si – OH – Al = 15/300

Table 4.4a. The number of Si – OH – Al species in YAS glasses

Si – OH – Al						
Hydration Level	YAS17		YAS24		YAS30	
	Species No.	St dev	Species No.	St dev	Species No.	St dev
DRY	0.00	0.00	0.00	0.00	0.00	0.00
0.1	3.50	0.7071	1.50	0.7100	1.50	0.7100
0.2	8.00	1.4140	2.50	0.7100	3.50	0.7100
0.3	15.00	4.2430	8.50	0.7100	6.50	0.7100

Table 4.4b. The number of Si – OH – Al species in YAS glasses (normalized)

Normalized Si – OH – Al						
Hydration Level	YAS17		YAS24		YAS30	
	Species No.	St dev	Species No.	St dev	Species No.	St dev
DRY	0.00	0.00	0.00	0.00	0.00	0.00
0.1	0.0364	0.0073	0.0150	0.0071	0.0150	0.0071
0.2	0.0363	0.0064	0.0125	0.0032	0.0175	0.0032
0.3	0.0500	0.0141	0.0283	0.0023	0.0216	0.0023

3) Al-OH-Al

A code was developed for the detection of Al – OH – Al species (Figure 4.14c) in hydrated YAS glasses. Species which have the form of Al – OH – Al were detected in each of the hydrated YAS glasses (YAS17, 24 and 30). Roughly the same numbers of Al – OH – Al species were present in each of the hydrated YAS glasses compared to the number of Si – OH – Al found within each of the same glasses discussed earlier. As mentioned earlier, hydroxyl groups are not seen to bridge between two Si atoms. It may be possible that silicon does not allow for OH to move or exist in between two Si atoms as the proton H+ has nothing to stabilise.

The number of these species i.e. Al – OH – Al seen in hydrated YAS glasses 24 and 30 do not show any trends with respect to increasing hydration concentration except for YAS17 where they increase with respect to hydration. No trends are clear between YAS17, 24 and 30 with respect to yttrium content for each of the hydrated glasses.

The numbers of Al – OH – Al species present in each of the hydrated glasses are shown in Table 4.5a. Normalisation of numbers in Table 4.5a give rise to Table 4.5b to remove any unnecessary effects of biasing with the number of hydroxyls used in each of the simulations. The normalisation method employed is:

NORMALISATION: No. of Al – $^{+}$OH – Al / Total No. of Hydroxyls in Simulation

E.g. for YAS24

(y=0.1) Al – $^{+}$OH – Al = 4.5/100

(y=0.2) Al – $^{+}$OH – Al = 9.0/200

(y=0.3) Al – $^{+}$OH – Al = 17.5/300

Table 4.5a. The number of Al – OH – Al species in YAS glasses

Al – $^{+}$OH – Al						
Hydration Level	YAS17		YAS24		YAS30	
	Species No.	St dev	Species No.	St dev	Species No.	St dev
DRY	0.00	0.00	0.00	0.00	0.00	0.00
0.1	1.00	1.4142	4.50	0.7071	4.50	0.7071
0.2	8.50	0.7071	9.00	1.4142	8.50	0.7071
0.3	13.50	2.1210	17.50	0.7071	11.50	0.7071

Table 4.5b. The number of Al – OH – Al species in YAS glasses (Normalized)

Normalized Al – $^{+}$OH – Al						
Hydration Level	YAS17		YAS24		YAS30	
	Species No.	St dev	Species No.	St dev	Species No.	St dev
DRY	0.00	0.00	0.00	0.00	0.00	0.00
0.1	0.0104	0.0147	0.0450	0.0070	0.0450	0.0070
0.2	0.0386	0.0032	0.0450	0.0070	0.0425	0.0035
0.3	0.0450	0.0070	0.0583	0.0023	0.0383	0.0023

It is interesting that Al – OH – Al species exist whereas Si – OH – Si does not. It can be rationalised how Si – OH – Al species are formed due to charge stabilisation of Si and Al by a hydroxyl bridging between them, however the reason for Al – OH – Al to form is not due to the same reason. What makes this more complicated is that if Al – OH – Al is seen one would assume that Si – OH – Si would form also. It may be possible that silicon species in Si – OH – Si do not favour the formation of Si – OH – Si, but if one Si were replaced by Al i.e. Si – OH – Al then the species (Si – OH – Al) begin to form and if another Si is replaced by another Al atom i.e. Al – OH – Al then such species are also recognised. Silicon is very specific over what may enter its coordination shell as seen in Figure 4.8a, 4.8b and 4.8c. It may possibly be due to the complex nature and characteristics of silicon being selective over what can be nearby whereas aluminium is not as species such as Si – OH – Al and Al – OH – Si are seen. This may be a possibility as to why a decrease is seen in the aluminium network connectivity but not for silicon (section 4.4)

4.3 *Hydroxyl Groups*

This section deals with distinguishing between hydroxyl groups that are bonded to Si and/or Al. The remaining hydroxyl groups that are not bonded to Si and/or Al would be free and instead attach themselves to yttrium network-modifier ions. Tables 4.6a and 4.6b show how the number of hydroxyl groups bond to Si in hydrated YAS glass systems 17, 24 and 30.

Table 4.6a. The number of Si – OH species in YAS glasses

Si - OH						
Hydration Level	YAS17		YAS24		YAS30	
	No. Species	St dev	No. Species	St dev	No. Species	St dev
0.1	60.00	2.06	10.50	0.81	4.50	0.75
0.2	86.50	0.68	20.50	0.81	21.50	0.75
0.3	119.00	1.37	63.50	2.17	43.50	0.75

NORMALISATION: No. of OH attached to Si / Total No. of Si in Simulation

i.e. YAS17 → 0.1) Si = 60.00/344 0.2) Si = 86.5/344 3) Si = 119/344

Table 4.6b. The number of Si – OH species in YAS glasses (Normalized)

Si – OH Normalized						
Hydration Level	YAS17		YAS24		YAS30	
	No. Species	St dev	No. Species	St dev	No. Species	St dev
0.1	0.174	0.006	0.0386	0.003	0.018	0.003
0.2	0.251	0.002	0.0754	0.003	0.086	0.003
0.3	0.346	0.004	0.2335	0.008	0.174	0.003

Observing Table 4.6b we can see that for each glass composition YAS17, 24 and 30, as hydration in increased from 0.1 – 0.3 more hydroxyl groups coordinate onto silicon. For example, if we take YAS17 and hydrate the glass from 0.1, 0.2 and 0.3 the number of hydroxyls found coordinated to silicon increases to 0.174, 0.251 and 0.346 respectively. The opposite is seen when looking at a single hydration concentration across all three glasses YAS17, 24 and 30 i.e. a decrease in the number of OH groups coordinated to silicon when an increase in yttrium content is seen.

Tables 4.7a and 4.7b show the number of hydroxyl groups bonded to Al in hydrated YAS glass systems.

Table 4.7a. The number of Al – OH species in YAS glasses

Al – OH						
Hydration Level	YAS17		YAS24		YAS30	
	No. Species	St dev	No. Species	St dev	No. Species	St dev
0.1	33.00	2.04	26.50	0.64	17.50	0.80
0.2	68.50	6.12	58.50	0.64	42.50	0.80
0.3	87.50	2.04	91.50	2.14	72.00	5.60

NORMALISATION: No. of OH attached to Al / Total No. of Al in Simulation

i.e. YAS17 → 0.1) Al = 33.0/204 0.2) Al = 68.5/204 3) Al = 87.5/204

Table 4.7b. The number of Al – OH species in YAS glasses (normalized)

Al – OH Normalized						
Hydration Level	YAS17		YAS24		YAS30	
	No. Species	St dev	No. Species	St dev	No. Species	St dev
0.1	0.162	0.010	0.123	0.003	0.088	0.004
0.2	0.336	0.030	0.272	0.003	0.213	0.004
0.3	0.429	0.010	0.425	0.010	0.360	0.028

Observing Table 4.7b we can see that for each glass composition YAS17, 24 and 30, as hydration is increased from 0.1 – 0.3 more hydroxyl groups coordinate onto aluminium. For example, if we take YAS17 and hydrate the glass from 0.1, 0.2 and 0.3 the number of hydroxyls found coordinated to aluminium to increases to 0.162, 0.336 and 0.429 respectively. The opposite is seen when looking at a single hydration concentration across all three glasses YAS17, 24 and 30 i.e. a decrease in the number of OH groups coordinated to aluminium when an increase in yttrium content is seen. Free hydroxyl species (-OH) have been reported by Xianyu Xue [153]. For hydroxyl groups that have not attached to network-forming species, they would as a result be described as free hydroxyl groups with coordination to network-modifying species such as sodium [153]. Yttrium is the network modifier in YAS glasses and one would presume, on the basis of free hydroxyls attaching onto sodium, they would bond to yttrium in place of sodium for an yttrium aluminosilicate glass.

The number of free hydroxyl groups detected is shown in Table 4.8a, whereas the normalized numbers of numbers found in Table 4.8a are represented in Table 4.8b.

Table 4.8a. The number of free OH Species in YAS glasses

OH						
Hydration Level	YAS17		YAS24		YAS30	
	No. Species	St dev	No. Species	St dev	No. Species	St dev
0.1	51.00	4.22	63.00	1.40	78.00	1.40
0.2	65.00	5.06	121.00	4.80	136.00	3.40
0.3	93.50	4.20	145.00	6.60	184.50	6.30

NORMALISATION: No. of OH detected / Total No. of OH in Simulation

i.e. YAS17 → 0.1) OH = 51.0/96 0.2) OH = 65.0/220 3) OH = 93.5/300

Table 4.8b. The number of free OH Species in YAS glasses (Normalized)

OH Normalized						
Hydration Level	YAS17		YAS24		YAS30	
	No. Species	St dev	No. Species	St dev	No. Species	St dev
0.1	0.531	0.044	0.630	0.014	0.780	0.014
0.2	0.295	0.023	0.605	0.024	0.680	0.017
0.3	0.312	0.014	0.483	0.022	0.615	0.021

Observing Table 4.8b we can see that by progressively hydrating glass composition YAS30 from 0.1 – 0.3, fewer hydroxyl groups are seen to be free. That is, if we take YAS30 and hydrate the glass from 0.1, 0.2 and 0.3 causes the fraction of free hydroxyls to decrease from 0.780, 0.680 and 0.615 respectively. The opposite is seen when looking at a single hydration concentration across all three glasses (YAS17, 24 and 30), i.e. an increase in the number of OH groups is seen with respect to an increase in yttrium content. This evidence supports how hydroxyl groups coordinate to Y > Al ~ Si in this order as seen in section 4.1 (Figure 4.11). Generally the more a YAS glass is hydrated, the more hydroxyl groups will coordinate themselves to silicon and aluminium but as this takes place fewer free hydroxyl groups are seen. This shows silicon and aluminium cause this decrease in the number of free hydroxyl groups. The more a YAS glass is hydrated the less available hydroxyls are to be free in the glass system as silicon and aluminium are providing a home for hydroxyl groups.

4.4 *Medium-range structure*

4.4.1 Silicon Q^n

The silicon network connectivities for unhydrated and hydrated versions of YAS17, 24 and 30 are given below in Figure 4.15a.

Figure 4.15a.

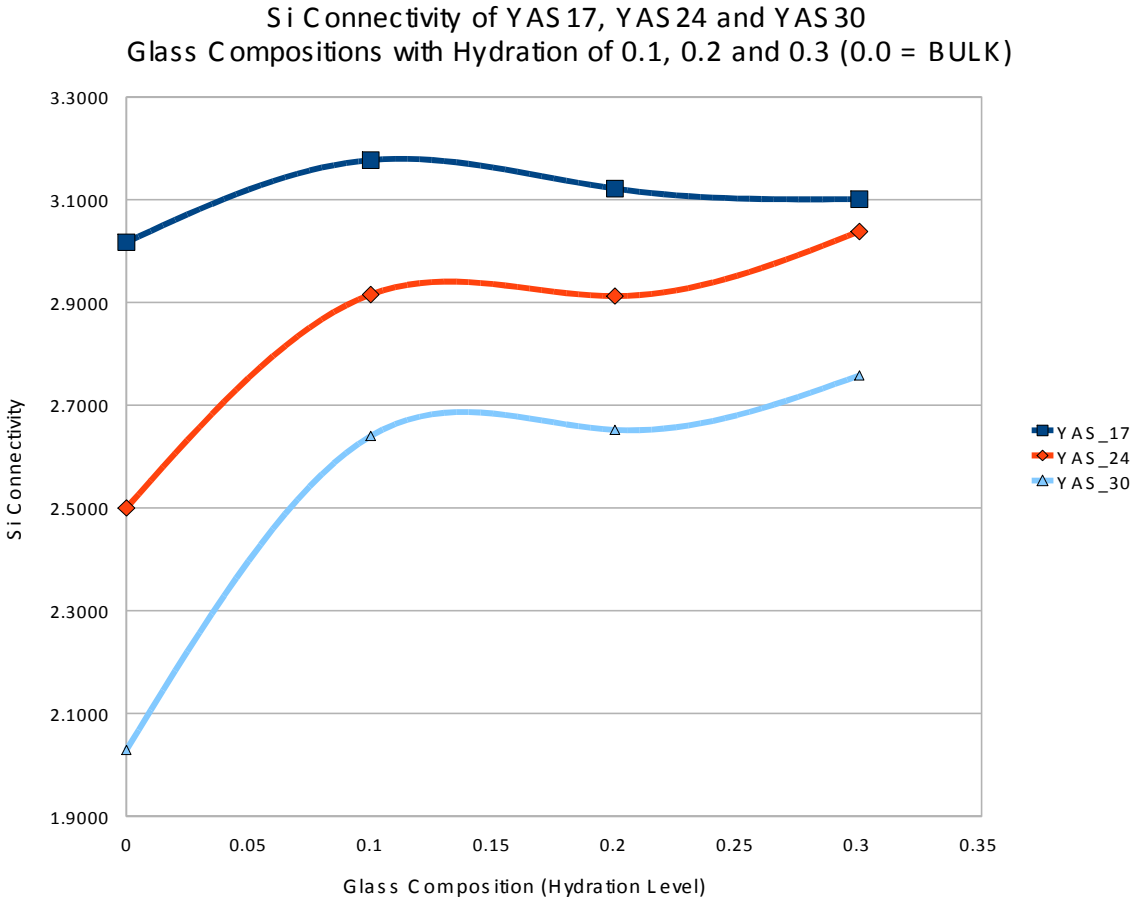

Observing Figure 4.15a we can see that for glass compositions YAS24 and 30 that as the glass is progressively hydrated from 0.1 – 0.3 the silicon network connectivity increases. A rise in silicon connectivities is seen for each of the glasses from dry to hydrated YAS at concentration of 0.1. The strength of the silicon network is increasing subject to increase in hydration from the dry forms of YAS glasses. This may be due to the hydroxyl groups substituting, Y --- O-Si-O_3 for Y --- OH which causes the movement of -[O-SiO_3] species back into the network causing this strengthening (Figures 4.12 and 4.13). What is seen after a hydration of 0.1 is a rough convergence in silicon network connectivities when hydrating each of the glasses from concentrations of 0.1 to 0.3. By first viewing the network connectivities of unhydrated YAS17, 24 and

30, we see that YAS17 has the highest network connectivity at 3.02, where YAS24 and 30 are 2.50 and 2.03 respectively. The differences between these three compositions is the amount of yttrium in each YAS glass, where YAS17 has the lowest yttrium content at 17%, YAS24 with 24% yttria and YAS30 with 30% yttria. We see that a change in yttrium content varies the way silicon connects itself in the glass structure. The silicon connectivity comprises of Si – O – Si and Si – O – Al connections, where oxygens in this situation are bridging between two like atoms of silicon and between two unlike atoms of silicon and aluminium. Aluminium plays the same role as the network former silicon. Yttrium is a network modifier in each of the glasses which would disturb such connections. The greater amount of yttrium in the YAS glass the more disruption to Si – O – Si and Si – O – Al connections.

Mead and Moutjoy [152] found that by increasing calcium content into their hydrated calcium silicate glasses caused the silicon network connectivity to decrease. The same was found to take place for YAS glasses [42]. As by increasing the yttrium content from 17 % to 30 % caused the silicon network connectivity to decrease. We can understand this as increasing yttrium content in YAS glasses causes yttrium ions to break Si – O – Si and Si – O – Al connections thus lowering the silicon network connectivity. A YAS glass with high yttrium content would make the glass more bioactive, with the durability of the glass decreased. Having a YAS with low durability containing radioactive yttrium ions would as a result allow, due to the low durability of the glass, radioactive yttrium to move out of the glass network and into surrounding healthy living tissue during treatment. This would be detrimental to the patient. The yttrium ions need to be harnessed in the glass network which needs to be durable enough to prevent leaching of yttrium ions outwards. After the full radioactivity of yttrium has depleted, used for radiotherapeutic use, then only is it safe to the patient for yttrium ions to be mobile outside of the glass network. A glass with low yttrium content would increase durability, be less bioactive and prevent yttrium ions leaching out of the glass network and into healthy surrounding tissues. Moreover hydration may enable the fine tuning of YAS with respect to silicon network connectivity. We see as YAS17 is hydrated progressively, higher silicon network connectivity is gained. This means that bioactivity is decreasing. This also means due to the strengthening of the silicon network that the YAS glass overall increases in durability. Some YAS glasses may be better suited to one organ than another according to durability. It would now be possible

to enhance and develop a YAS glass by engineering hydration levels specifically for use in different parts of the body.

The change in yttrium content is reflective of changes seen for silicon network connectivity (NC) for unhydrated YAS glasses (YAS17, 24 and 30). For YAS17, lower yttrium content causes a lower number of Q^2 and Q^1 Si species and a higher number of Q^3 species. This gives rise to a NC of 3.02 which is larger than the silicon NC for YAS24 and YAS30 whose yttrium content is greater. By having less yttrium in a YAS glass, like YAS17, causes oxygens, which would coordinate to yttrium to decrease. Oxygens that do not coordinate to yttrium instead coordinate to silicon and or aluminium atoms present in the glass structure, therefore giving rise to an increase in Si – O – Si and Si – O – Al connections, resulting in YAS17 having a high Si NC of 3.02. If an increase in yttrium content is seen i.e. YAS24 and 30, a greater number of Q^2 species would dominate over the number of Q^3 species thus giving rise to silicon NC's of 2.50 and 2.03 for YAS24 and 30 respectively. Yttrium in these glasses disturbs Si – O – Si and Si – O – Al bonds causing them to break, where oxygens would as a result coordinate onto yttrium itself if yttrium content is high. Yttrium is carrying out the task of modifying the network with respect to silicon thus being called a network modifier.

By hydrating each of the YAS glasses (YAS17, 24 and 30) we see the silicon network connectivities increasing. The general reason for this is due to the number of Q^2 species in hydrated YAS glasses decreasing and the number of Q^4 species increasing, where the number of Q^3 species remains more or less constant. The hydroxyl (hydration) groups are clearly causing the number of Si – O – Si and or Si – O – Al connections to increase. No hydroxyl groups are seen to bridge between two like atom pairs of silicon i.e. Si – $^+$OH – Si. We have instead seen evidence for the existence of Si – OH – Al species. This is possibly why a rise is seen in silicon NC is observed in Figure 4.15a. Hydration can affect the following species seen in Figure 4.16a and 4.16b.

Figure 4.16

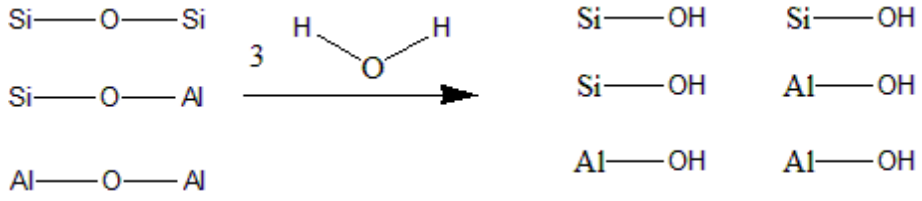

The partial A-B Q^n is defined in section 2.6.3. We remind the reader that each A-O-B linkage is counted, even if two or more share the same central oxygen atom. If three- and higher-coordinated oxygen atoms exist, this definition of partial Q^n can exceed the A-O coordination number, and that the sum of the partial Q^n is not equal to the total Q^n. The partial Si network connectivities were calculated i.e. Si – O – Si and Si – O – Al, in Figures 4.15b and 4.15c respectively. This is so a better understanding can be gained as to how progressively hydrating three different glass compositions YAS17, 24 and 30 can in turn increase the silicon connectivities (Q^n speciation) and what partial Si connectivity is responsible for this effect i.e. either or both of Si – O – Si / Si – O – Al.

Figure 4.15b.

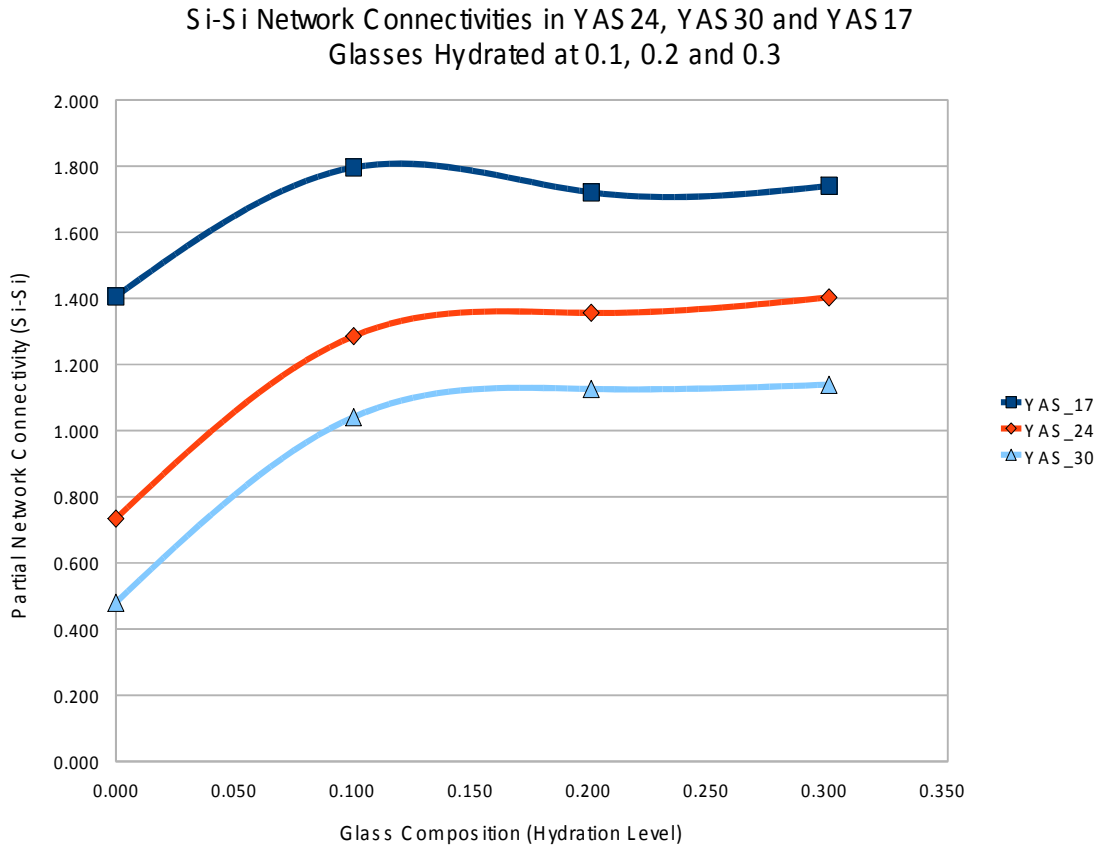

This graph shows the partial silicon connectivities for purely the Si – O – Si contributions present for each glass composition. Here a similar trend is found from that of Figure 4.15a earlier discussed. It is worth noting hydration largely does not affect the Si – O – Si contributions to connectivities after hydration of y=0.1. The hydroxyl groups are not breaking these connections with this connectivity type as one would imagine or predict to take place demonstrated in Figure 4.16. Instead the numbers of Si – O – Si connections are seen to increase.

Figure 4.15c

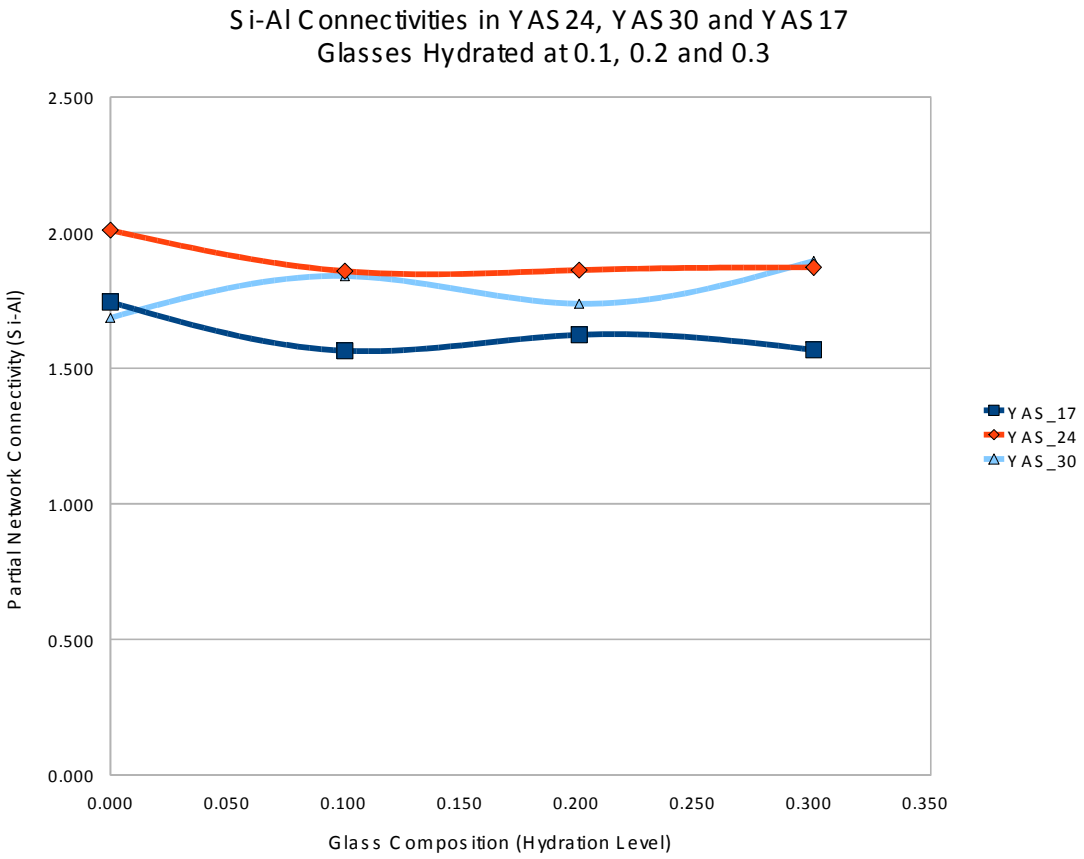

Figure 4.15c shows the partial silicon connectivities for purely Si – O – Al contributions present for each glass composition. Here a different trend is found, whereby hydrating YAS17 and YAS24 with concentration of 0.1 – 0.3, a general slight decrease is seen in the number of Si – O – Al species. This may be somewhat due to the fact that by hydrating the glass, the hydroxyl groups interfere with that of the Si – O – Al species in the glass network. For example, unhydrated YAS17 has a larger number of Si – O – Al species than hydrated YAS17 at a concentration of 0.1. The reason for this is that hydrating the glass causes the hydroxyl groups to integrate themselves into the Si – O – Al connectivities therefore splitting them apart and creating Si – OH and Al – OH. This is demonstrated by Figure 4.16b.

The Si – O – Al connections are seen to go up and down as we progressively hydrate each of the glass compositions in Figure 4.15c. The Si – O – Si connections are seen to increase as seen in Figure 4.15b. This shows that Si – O – Al links have weakness causing these connections to break i.e. Si – O – Al instead of Si – O – Si which are stronger and in fact increasing in number as hydration of any glass composition takes place. The hydroxyl groups break down the Si – O – Al connections more easily than Si – O – Si connections.

4.4.2 Aluminum Q^n

The aluminium network connectivities for dry and hydrated versions of YAS17, 24 and 30 are given below in Figure 4.17a.

Figure 4.17a.

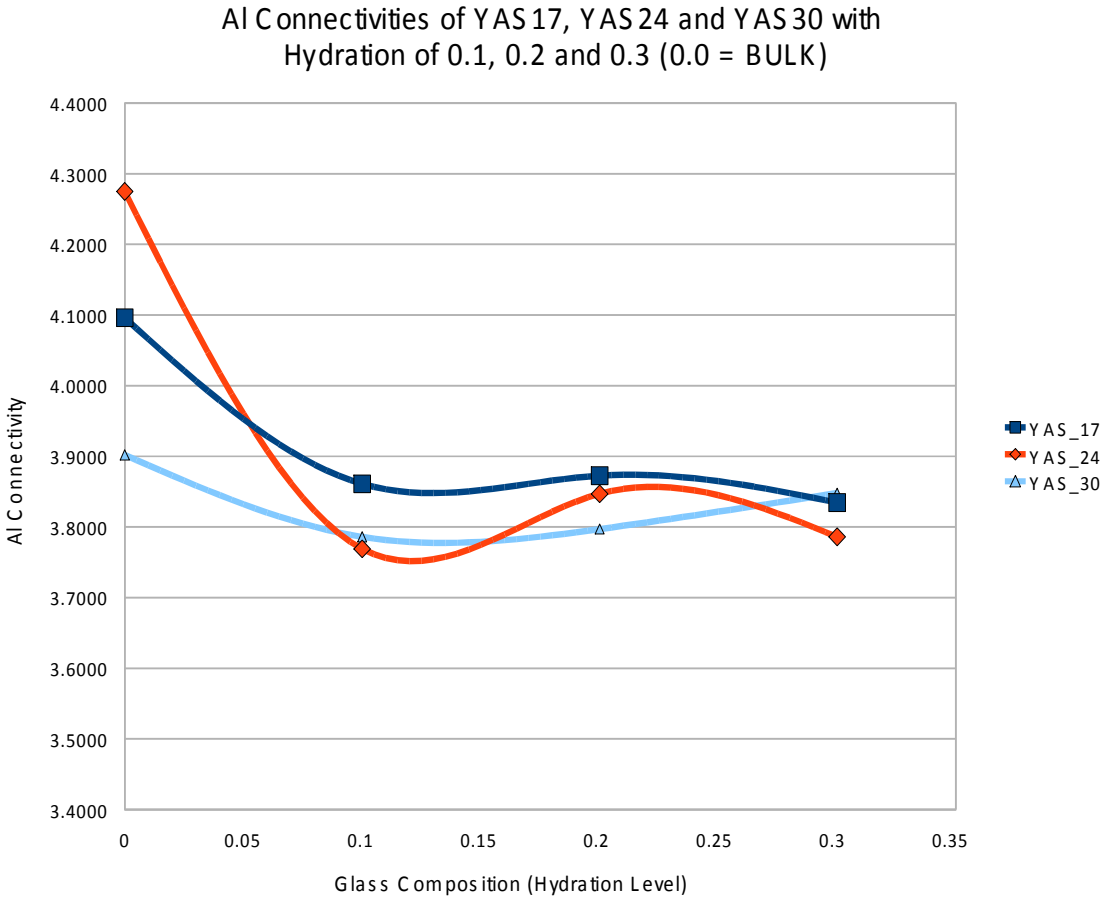

Observing Figure 4.17a we can see that for each glass composition YAS17, 24 and 30 progressively hydrated from 0.1 – 0.3, the aluminium network connectivity goes up and down. A decrease in Al NC is seen for each of the glasses from unhydrated to hydrated forms at concentrations of 0.1. The strength of the aluminium network is decreasing subject to increase in hydration from the dry forms of YAS glasses. What is seen after a hydration of 0.1 is a further smaller decrease if not a convergence (or slight increase) in aluminium network connectivities when hydrating each of the glasses from concentrations of 0.2 to 0.3. By first viewing the network connectivities of unhydrated YAS17, 24 and 30, we see that YAS24 has the highest network connectivity at 4.27, where YAS17 and 30 are 4.10 and 3.90 respectively. The Al connectivity comprises Al – O – Al and Si – O – Al connections, where oxygen atoms in this situation are bridging

between two like atoms of aluminium and between two unlike atoms of silicon and aluminium. Aluminium plays the same role as the network former silicon. Yttrium is a network modifier in each of the glasses which would disturb such connections. The trend i.e. increase in silicon NC with respect to decreasing amount of yttrium content in unhydrated YAS glasses (YAS17, 24 and 30) seen earlier in Figure 4.15a is not observed for the aluminium network connectivities in Figure 4.17a.

By hydrating each of the YAS glasses (YAS17, 24 and 30) we see the aluminium network connectivities are very random. Hydroxyl groups are seen to bridge between two like atom pairs of silicon i.e. Al – $^{+}$OH – Al in all hydrated YAS glasses 17, 24 and 30. We have also seen evidence for the existence of Si – OH – Al species. One would think that by seeing a number of Al – $^{+}$OH – Al and Si – OH – Al species, the NC for aluminium would increase, but an opposite trend is observed in Figure 4.17a. Possible ways in which hydration can affect aluminium NC can be viewed in Figure 4.16b and 4.16c.

The partial Al network connectivities were calculated i.e. Al – O – Al and Si – O – Al in Figures 4.16b and 4.16c respectively. This is to better the understanding of how progressively hydrating three different glass compositions YAS17, 24 and 30 can in turn decrease Al connectivities (Q^n speciation) and what partial Al connectivity is responsible for this effect i.e. either or both of Al – O – Al / Si – O – Al.

Figure 4.17b

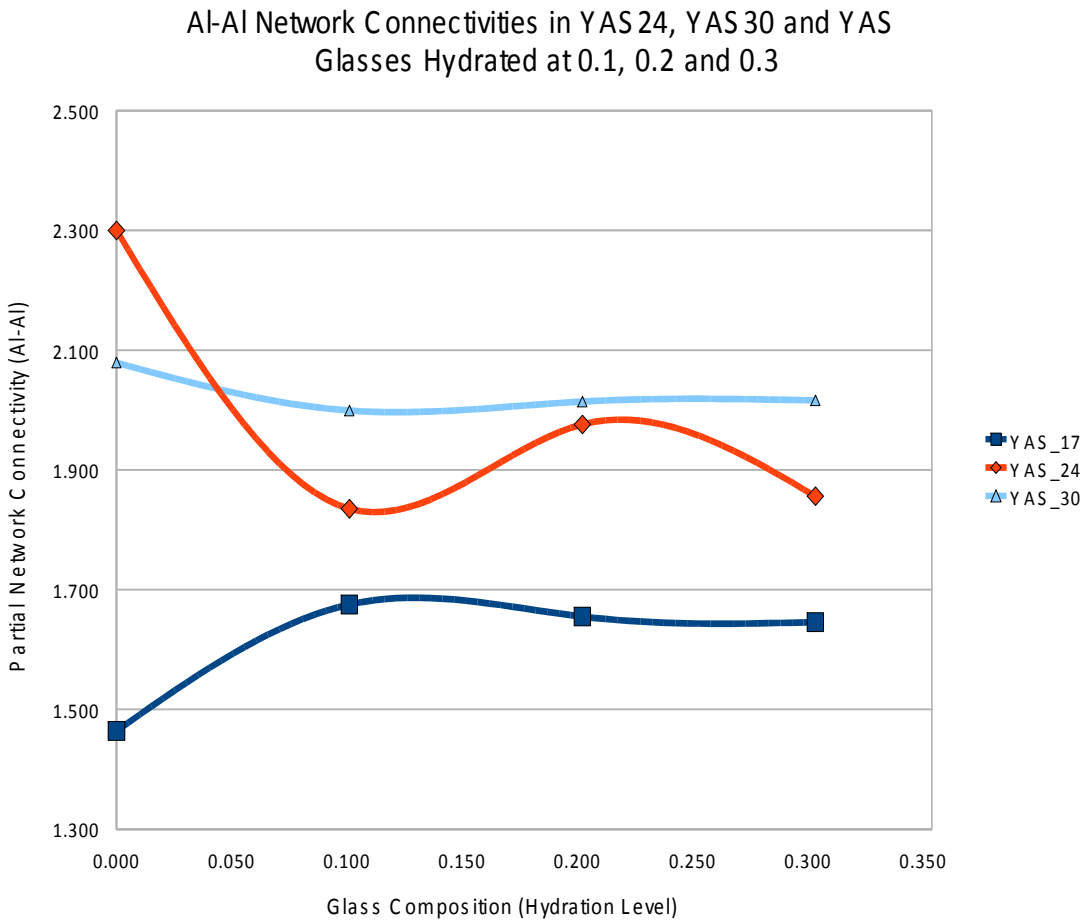

Figure 4.17b shows the partial aluminium connectivities for purely the Al – O – Al contributions present for each glass compositions. Here no obvious trend is found. Viewing Figure 4.16c it was thought that Al – O – Al connections may break down due to hydroxyl groups resulting in the formation of two Al – OH.

Figure 4.17c

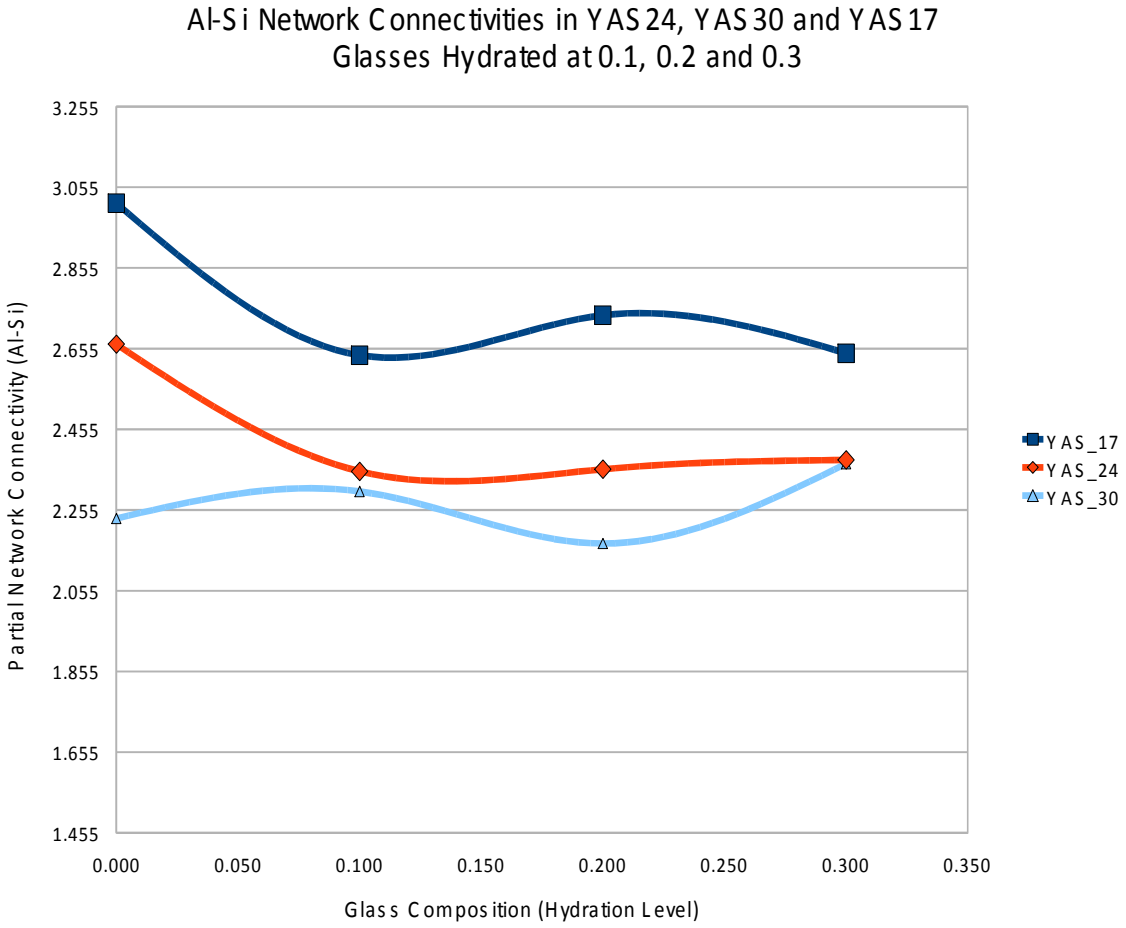

Figure 4.17c shows the partial aluminium connectivities for purely the Al – O – Si contributions present for each glass compositions. Generally the partial aluminium connectivities goes up and down and no overall trend is observed. Hydrating the glass, the hydroxyl groups interfere with that of the Al – O – Si species in the glass network. For example, dry YAS17 has a larger number of Al – O – Si species than compared to the same glass hydrated at a concentration of 0.1. The reason for this is that hydrating the glass causes the hydroxyl groups to integrate themselves into the Al – O – Si connectivities therefore splitting them apart and creating instead Al – OH and Si – OH as a result of hydration (Figure 4.16b).

4.5 *Clustering*

4.5.1 Si – OH

Figure 4.18a demonstrates how hydroxyl groups aggregate around silicon atoms with respect to varying yttrium content between YAS17, 24 and 30 as well as increasing hydration.

Figure 4.18a.

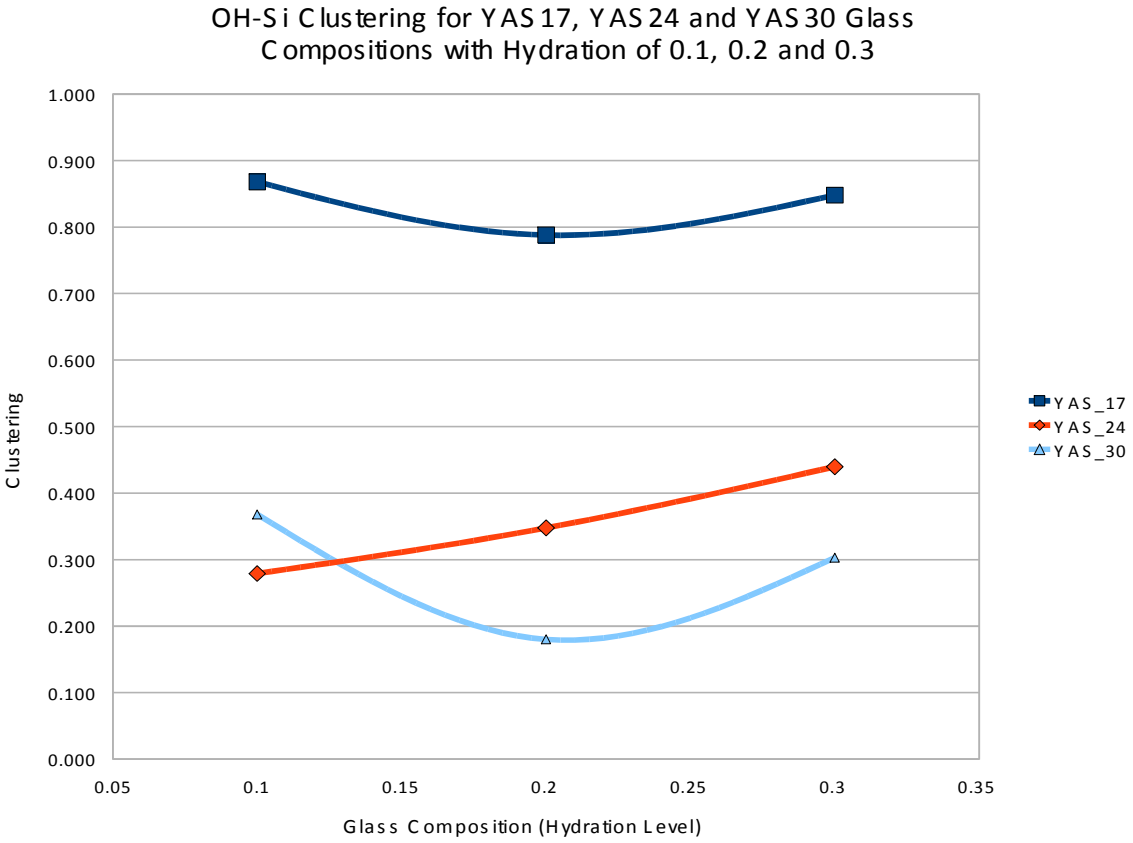

Figure 4.18a shows that hydroxyl groups do not aggregate around silicon atoms in YAS17 YAS24 or YAS30. From the Figure above we can understand that a glass with higher amounts of yttria will tend to cause fewer hydroxyl groups to aggregate around silicon. This is probably due to a higher yttria content attracting hydroxyl groups towards yttrium and thus lowering the tendency of hydroxyl groups to aggregate around silicon. One might think that the more hydration is increased would in turn cause hydroxyl groups to aggregate more around silicon but this is not the case. The clustering of hydroxyl groups around silicon does not increase with respect to increasing hydration concentration. The clustering ratios obtained with respect to hydroxyl groups clustering

around silicon are seen to be below a value of one. If clustering values were greater than one then clustering is taking place, but for all YAS glasses (YAS17, 24 and 30) show that no clustering takes place between hydroxyl groups and silicon. Even though all clustering values are below a value of one, for this case it is worth noting that if clustering were to take place more in one glass composition than another, it would be for YAS17 rather than YAS30 as seen from Figure 4.18a.

4.5.2 Al – OH

Figure 4.18b demonstrates how hydroxyl groups aggregate around aluminium atoms with respect to varying yttrium content between YAS17, 24 and 30 as well as increasing hydration.

Figure 4.18b

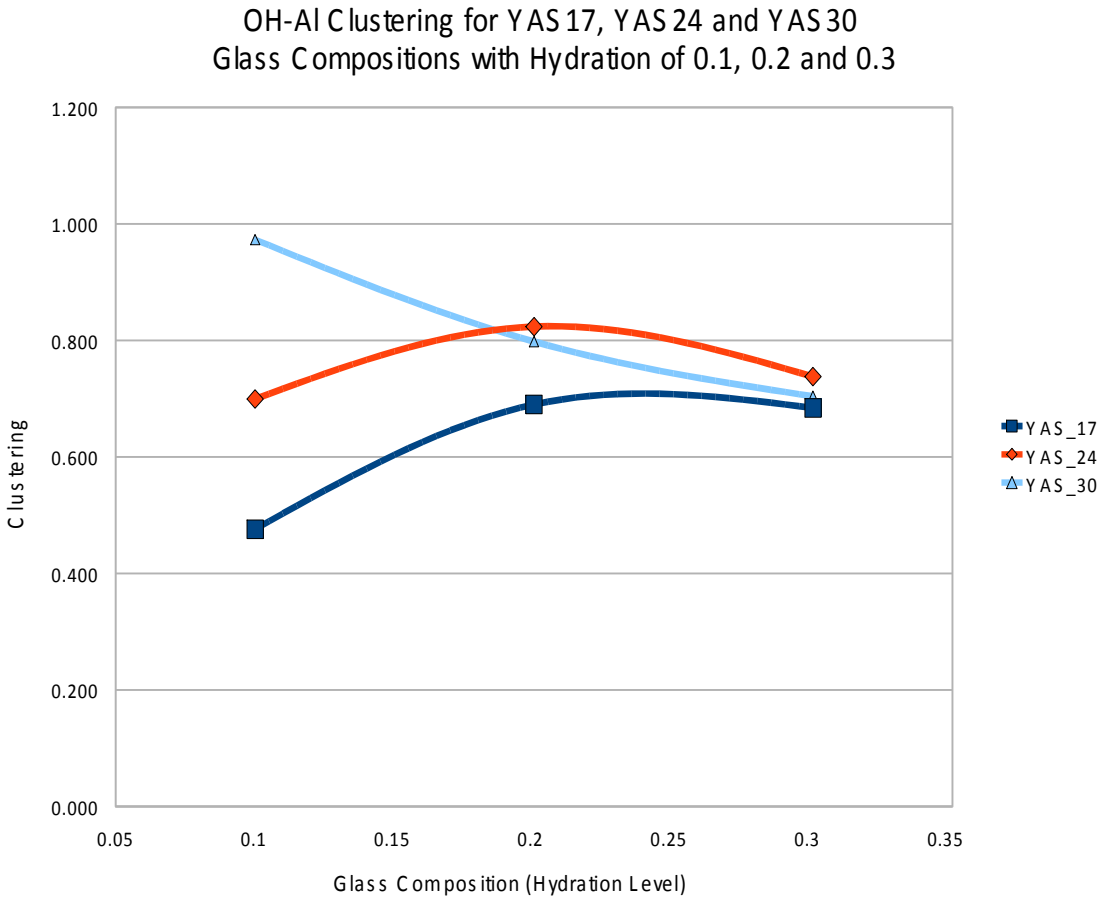

Figure 4.18b shows that hydroxyl groups do not aggregate around aluminium atoms in YAS17, 24 and 30 as hydration increases. From the Figure above we can understand that a glass with higher amounts of yttrium will cause more hydroxyl groups to aggregate around aluminium. One would think that the more hydration was increased would in turn cause hydroxyl groups to aggregate more around aluminium but this is not always the case. The clustering of hydroxyl groups around aluminium generally converges when all three YAS glasses reach a hydration of 0.3. The clustering values obtained with respect to hydroxyl groups clustering around aluminium are seen to be below a value of one. Even though all clustering values are below a value of one, for this case it is worth noting that if clustering were to take place more in one glass

composition than another, it would be for YAS30 rather than YAS17 especially at hydration concentration of 0.1, seen from Figure 4.18b.

4.5.3 Y – OH

Figure 4.18c demonstrates how hydroxyl groups aggregate around yttrium atoms with respect to varying yttrium content between YAS17, 24 and 30 as well increasing hydration.

Figure 4.18c

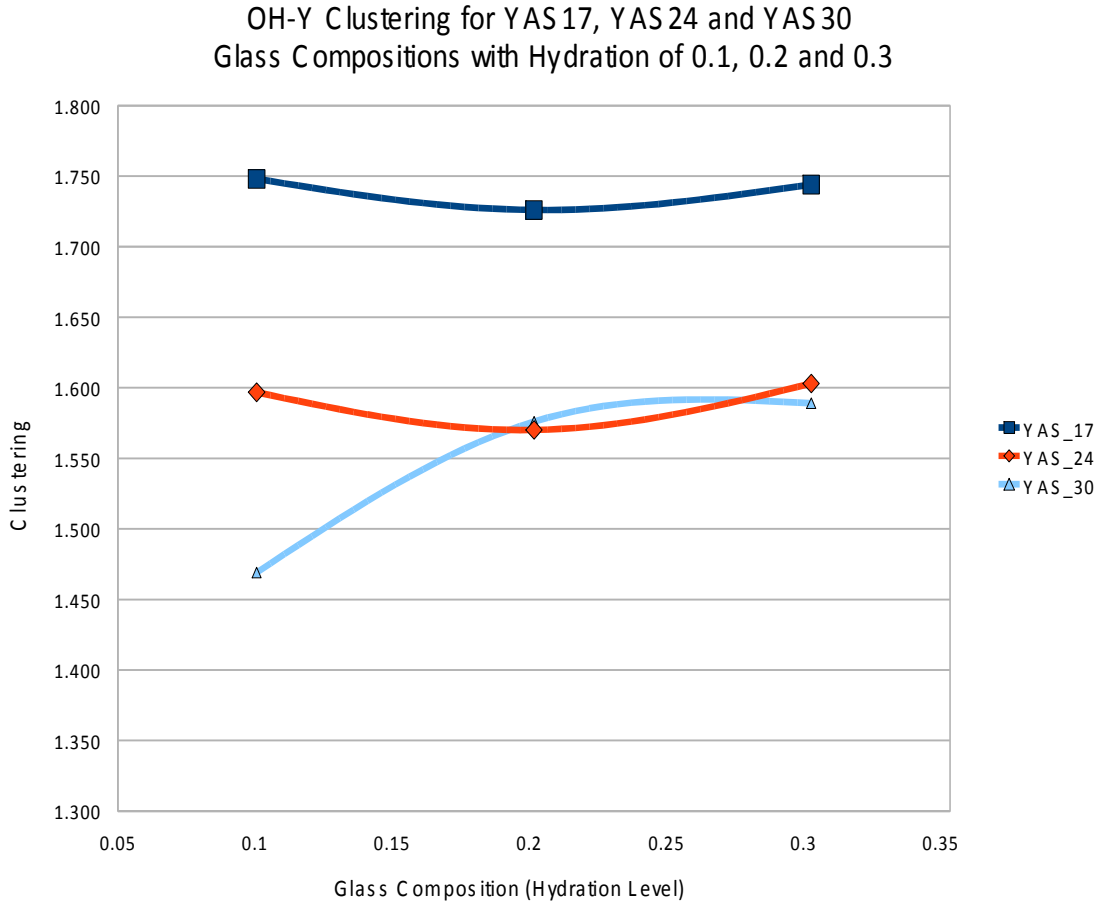

Figure 4.18c shows that hydroxyl groups aggregate around yttrium atoms more in YAS17 than in YAS30 or YAS24. From the Figure above we can understand that a glass with lower amount of yttria will tend to cause hydroxyl groups to aggregate around yttrium more. What was discussed earlier in Figure 4.18a for hydroxyl groups clustering around silicon atoms was, clustering of hydroxyl groups decrease as yttria content increases, instead the trend is not seen in Figure 4.18c for hydroxyl group aggregation around yttrium atoms. We expected more hydroxyl groups clustering around yttrium atoms for YAS30 since it has the highest content of yttrium compared to

YAS17. This is not seen. We instead see that hydroxyl groups prefer to cluster more around yttrium atoms in YAS17 than YAS30. One would think that the more hydration is increased would in turn cause hydroxyl groups to aggregate more around yttrium but this is not the case. The clustering of hydroxyl groups around yttrium does not increase with respect to increasing hydration concentration. The clustering values obtained for hydroxyl groups around yttrium are seen to be above a value of one. If clustering values are greater than one, as seen in Figure 4.18c, then clustering is taking place. All clustering values are above a value of one, for this case it is worth noting that more clustering occurs in YAS17 rather than YAS30 or YAS24 as seen from Figure 4.18c.

4.5.4 Cation – Cation Clustering

Tables 4.9a, 4.9b and 4.9c shows cation – cation clustering with respect to increasing hydration concentration for YAS17, 24 and 30 glass compositions respectively.

Table 4.9a: Cation – cation clustering for YAS17 hydrated at fractions y=0.1, 0.2 and 0.3

Cation - Cation Clustering for YAS17 (Dry and Hydrated (y=0.1, 0.2 and 0.3))

Species	**Dry YAS17**		**YAS17_0.1**		**YAS17_0.2**		**YAS17_0.3**	
	Ratio	St. Dev.	Ratio	St. Dev.	Ratio	St. Dev.	Ratio	St. Dev.
Y – Y	1.102	0.031	1.308	0.029	1.333	0.014	1.379	0.097
Y – Si	1.179	0.020	1.099	0.045	1.072	0.075	1.009	0.034
Y – Al	1.018	0.013	1.061	0.023	1.007	0.037	0.991	0.031
Si – Si	1.257	0.043	1.449	0.038	1.499	0.010	1.486	0.057
Si – Al	1.135	0.027	0.998	0.031	1.133	0.039	1.030	0.011
Al – Al	1.480	0.034	1.785	0.035	1.594	0.037	1.636	0.077

Table 4.9b: Cation – cation clustering for YAS24 hydrated at fractions y=0.1, 0.2 and 0.3

Cation - Cation Clustering for YAS24 (Dry and Hydrated (y=0.1, 0.2 and 0.3))

Species	**Dry YAS24**		**YAS24_0.1**		**YAS24_0.2**		**YAS24_0.3**	
	Ratio	St. Dev.	Ratio	St. Dev.	Ratio	St. Dev.	Ratio	St. Dev.
Y – Y	1.120	0.018	1.204	0.021	1.230	0.038	1.301	0.029
Y – Si	1.397	0.038	1.150	0.013	1.042	0.062	1.028	0.025
Y – Al	1.030	0.093	1.041	0.081	1.011	0.060	1.000	0.051
Si – Si	1.087	0.020	1.381	0.079	1.605	0.074	1.538	0.016
Si – Al	1.152	0.029	1.158	0.047	1.112	0.067	1.185	0.069
Al – Al	1.674	0.062	1.537	0.040	1.556	0.052	1.639	0.029

Table 4.9c: Cation – cation clustering for YAS30 hydrated at fractions y=0.1, 0.2 and 0.3

Cation - Cation Clustering for YAS30 (Dry and Hydrated (y=0.1, 0.2 and 0.3))

Species	**Dry YAS30**		**YAS30_0.1**		**YAS30_0.2**		**YAS30_0.3**	
	Ratio	St. Dev	Ratio	St. Dev	Ratio	St. Dev	Ratio	St. Dev
Y – Y	1.167	0.064	1.217	0.018	1.240	0.013	3.289	0.019
Y – Si	1.472	0.064	1.179	0.026	1.184	0.015	1.128	0.045
Y – Al	1.122	0.022	1.110	0.092	1.078	0.018	1.040	0.051
Si – Si	1.027	0.026	1.522	0.016	1.546	0.039	1.824	0.032
Si – Al	1.134	0.065	0.889	0.035	0.973	0.030	1.005	0.066
Al – Al	1.659	0.046	1.342	0.013	1.378	0.019	2.034	0.088

The clustering ratios seen above for dry YAS17, 24 and 30 compare well to simulation studies of yttrium aluminosilicates carried out by the work of Tilocca and Christie [42]. From the Tables above, hydration generally causes an increase in clustering for like pairs of cations and decreases clustering for unlike pairs of cations. The trend seen from the above table is that cation - cation clustering for like pairs i.e. Y-Y, Si-Si and Al-Al are seen to increase as YAS17 is hydrated. For example, we previously saw hydroxyl groups tending to cluster around yttrium, aluminium and silicon in this order. As we see that hydrating the dry form of YAS17 progressively causes the Y-Y clustering to increase. This shows that not only will one likely find a hydroxyl group near an yttrium cation but one will also likely find another yttrium cation to which it is close. The same effect is seen for other like pairs i.e. Al-Al and Si-Si. The extent of like cation pair clustering seen in YAS30 is greater than that seen in YAS17 (Table 4.9c and 4.9a respectively). This is likely to be due to the different amounts of yttrium between the two glasses where YAS17 and YAS30 have 17 mol % and 30 mol % of yttrium respectively.

Clustering ratios for unlike cation pairs i.e. Y-Si, Y-Al and Si-Al are seen to decrease as dry YAS is hydrated. For example, this shows that the yttrium cations tend to stay away from silicon cations. This is firstly because yttrium cations are already involved with hydroxyl group aggregation and secondly with themselves and so this therefore lessens their ability to be near silicon. The same effect is seen for other unlike cation pairs Y-Al and Si-Al. Simply put, a hydroxyl group will have a number of cations i.e. yttrium surrounding itself, to which hydroxyls then cause further attraction to cations i.e. yttrium, which therefore prevents unlike cation pairs from aggregating.

4.6 *Yttrium bridging oxygens vs. non-bridging oxygens*

The following set of data will represent the yttrium environment with respect to the percentage of bridging oxygens (BO) vs. the percentage of non-bridging oxygens (NBO) in its coordination shell. This is to better the understanding and description of how yttrium content causes a change with respect to the number of BOs vs. NBOs around yttrium and secondly the affect of hydration affecting the percentage of BOs vs. NBOs with respect to each glass composition.

By viewing Table 4.10a we see the percentage of bridging oxygens changing with respect to yttrium content. It is clear from Table 4.10a that as the yttrium content in an yttrium aluminosilicate glass increases, the percentage of bridging oxygens around yttrium will decrease as a result.

By viewing Table 4.10a, YAS24 or YAS30 shows that hydrating the glass system causes the percentage of bridging oxygens around yttrium to increase, whereas for YAS17 this stays roughly constant. Hydrating the glass has the opposite effect that increasing yttrium content has. Increasing yttrium content causes a lower percentage of bridging oxygens around yttrium ions whereas hydration instead increases the percentage of bridging oxygens around yttrium.

As the percentage of bridging oxygens decreases with respect to increasing yttrium content, the percentage of non-bridging oxygens around yttrium as a result increases. The overall effect of hydrating a glass composition progressively from 0.1 to 0.3 from the unhydrated form causes the number of bridging oxygens around yttrium to increase thus lowering the percentage of non-bridging oxygens around yttrium (Table 4.10b).

The reason for increasing yttrium content to decrease the number of bridging oxygens around itself is due to yttrium being a network modifier. The more yttrium in the glass, the more yttrium shall modify the glass structure by breaking T - O - T bonds, and removing bridging oxygens around itself thus lowering the percentage seen in the yttrium environment. Yttrium modifier ions favour non-bridging oxygens to form around it with respect to increasing yttrium content.

Table 4.10a: Bridging oxygens surrounding yttrium in hydrated and unhydrated YAS glasses 17, 24 and 30

BO	**YAS17**		**YAS24**		**YAS30**	
	%	St. Dev	%	St. Dev	%	St. Dev
DRY	46.13	2.27	37.97	1.88	30.84	0.95
0.1	44.07	1.70	38.70	1.60	32.66	0.82
0.2	42.56	0.40	43.08	4.42	35.30	0.39
0.3	43.94	1.82	42.04	1.38	36.97	2.14

From Table 4.10b, the number of non-bridging oxygens increases with respect to yttrium content.

Table 4.10b: Non-bridging oxygens surrounding yttrium in hydrated and unhydrated YAS glasses 17, 24 and 30

NBO	**YAS17**		**YAS24**		**YAS30**	
	%	St. Dev	%	St. Dev	%	St. Dev
DRY	53.87	2.04	62.03	1.91	69.16	1.24
0.1	52.94	2.61	55.95	0.76	58.93	1.04
0.2	54.57	1.67	52.04	2.99	56.31	0.23
0.3	52.19	1.75	51.35	1.61	54.20	3.08

Table 4.10c: Non-bridging and bridging oxygens surrounding yttrium in hydrated and unhydrated YAS glasses 17, 24 and 30

	YAS17		**YAS24**		**YAS30**	
	NBO+BO Total %	(OH) %	NBO+BO Total %	(OH) %	NBO+BO Total %	(OH) %
DRY	100	n/a	100	n/a	100	n/a
0.1	97.01	2.99	94.65	5.35	91.59	8.41
0.2	97.13	2.87	95.12	4.88	91.61	8.39
0.3	96.13	3.87	93.40	6.60	91.17	8.83

Mead and Mountjoy found [152] for calcium phosphate glass that a higher amount of non-bridging oxygens surrounded calcium similarly to how non-bridging oxygens surround yttrium in YAS glass (Table 4.10b). As calcium and yttrium are network modifiers, they share the same characteristics as to being present around non-bridging oxygens more than bridging oxygens. What they also found was with increasing

calcium content caused an increase in numbers of non-bridging oxygens surrounding calcium. The same effect is seen for YAS glasses.

Yttrium has high field strength, and because of this nature, it causes yttrium to be surrounded by a high percentage of non bridging oxygens. This was demonstrated by the work of Tilocca and Christie [115]. They modelled a glass with three network modifiers: yttrium, calcium and sodium. Yttrium had the highest field strength and sodium had the lowest. The high field strength of yttrium influenced the way in which a larger percentage of non-bridging oxygens to surround itself and sodium the least.

4.7 *Main Findings*

Coordination is seen to increase for Si, Al and Y as YAS glasses 17, 24 and 30 are progressively hydrated from 0.1 – 0.3 (Figures 4.8a, 4.9a and 4.10a). The order by which hydroxyl-oxygens coordinate to network-forming and modifying cations is shown below:

$$Y > Al \sim Si$$

Yttrium has the greatest ability in allowing hydroxyl-oxygen to coordinate to it, aluminium and silicon having lower coordination to hydroxyl-oxygen. The increase in coordination is due to hydration effects where hydroxyl groups squeeze themselves into the coordination spheres, most easily with yttrium, and then silicon and/or aluminium. The more a YAS glass is hydrated the more hydroxyl groups will fit themselves into the coordination spheres of yttrium firstly and then aluminium and silicon (Figures 4.8c, 4.9c and 4.10c).

The same order is observed as the coordination of silicon, aluminium and yttrium to non hydroxyl-oxygen decreases. Yttrium shows this effect the most and silicon the least, where coordination to non hydroxyl-oxygen decreases (Figures 4.8b, 4.9b and 4.10b)

As coordination of, for example, yttrium decreases with non hydroxyl-oxygen, the coordination of yttrium to hydroxyl-oxygen increases. Hydroxyl groups coordinate as a displacement to non hydroxyl-oxygens. Furthermore, the hydroxyl-oxygens not only displace non hydroxyl-oxygens but cause an overall increase in coordination. The same is seen for silicon and aluminium where the effect is not as marked as found for yttrium (Figures 4.8a, 4.9a and 4.10a).

The main difference between YAS glasses 17, 24 and 30 is the increase in yttrium content, and decrease in the silicon content. The content of aluminium between the YAS glasses 17, 24 and 30 remains roughly unchanged. It is seen that the more yttrium a YAS glass has i.e. YAS30, when progressively hydrated, causes yttrium, aluminium and silicon to generally hold higher coordination numbers than compared to a YAS glass that contains less yttrium i.e. YAS17 (Figures 4.8a, 4.9a and 4.10a). The same effect is seen for aluminium and silicon but the effect is least marked for silicon. Hydroxyl groups tend to favour associating themselves to yttrium first then aluminium and lastly silicon as YAS glasses 17, 24 and 30 are hydrated. The more yttrium a YAS

glass has the fewer hydroxyl groups would bind onto yttrium, aluminium and silicon. (Figures 4.8c, 4.9c and 4.10c).

Of the following species only B and C were observed in YAS glass 17, 24 and 30:

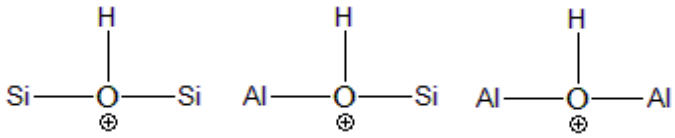

Figure 4.14 A B C

There is no correlation as to the number of species B and C increasing with respect to hydration concentration. What we do know is that these species do exist and they form from the presence of hydroxyl groups bridging between two aluminium atoms or a silicon and aluminium atom as demonstrated in B and C. Generally there were a greater number of B species that were found in YAS glasses 17, 24 and 30 than C species found in the same YAS glass systems. A possible reason as to why species B forms is rationalized by stabilizing the charge on silicon which therefore causes the hydroxyl group to place itself between an aluminium and silicon. The reason for a hydroxyl group to place itself between two aluminium atoms as seen in C cannot be due to the same reason given earlier of charge stabilization between Al and Si (B).

The overall silicon network connectivities are generally increasing with hydration as seen in Figure 4.15a which shows that the silicate network is strengthening itself as YAS glasses 17, 24 and 30 are hydrated. By viewing Figure 4.15b we realise that this effect seen in Figure 4.15a is due to the number of Si – O – Si and Si – O – Al bridges increasing with increasing hydration.

The overall aluminium network connectivities are generally decreasing with hydration as seen in Figure 4.17a which shows that the aluminate network is weakening itself as YAS glasses 17, 24 and 30 are hydrated. By viewing Figure 4.17b and 4.17c we realise that this affect seen in Figure 4.17a is due to the number of Al – O – Al and Al – O – Si bridges decreasing (Figures 4.16b and 4.16c).

The network connectivity of a glass has a central role in determining the glass dissolution rate: a fragmented network with a low connectivity will dissolve faster in an aqueous environment [42]. For example, low-silica bioactive glasses have NC of approximately 2, whereas loss of bioactivity has been associated to NC approaching 3

in higher silica compositions. The central importance of the network connectivity in this context makes it a key structural factor for the possible use of a silica-based glass composition to store radionuclides, either in nuclear waste disposal or for *in situ* cancer radiotherapy. The incorporation of water in the form of hydroxyl groups in a glass structure is in principle expected to disrupt the glass network: this is based on the assumption that protons act as additional network modifiers [154] and therefore the O_2^- → 2 OH^- substitution would break T – O − T bridges either directly (e.g., T – O − T + OH^- → T − O^- + T − OH) or indirectly (e.g., T – O ⋯ M + OH^- → T − OH + M^+, where M^+ is a free modifier cation which is able to break another T – O − T bridge). For example, the breakdown of the silica network (compared to melt-derived glasses) caused by the hydration process is often reported as one of the possible effects contributing to the extended range of bioactivity of sol−gel glasses [154]. Also, a more disrupted YAS network would be less stable in a physiological environment, affecting its performance for radiotherapy. In the short term, a faster yttrium release in the bloodstream from a rapidly dissolving glass would be a negative factor for the medical applications, which require the highest short-term durability to avoid releasing yttrium isotopes while they are radioactive. On the other hand, if short-term Y^{3+} release is not significantly affected, the possibility to enhance the long-term (post-radioactive decay of Y) biodegradation of YAS glasses into harmless products represents a very attractive option at present, since the long term effects of implanted YAS microparticles are not yet known. It is therefore important to investigate the effects of different hydration levels on the glass structure.

The earlier simulations show that the disruptive effect of OH^- on the glass network acts differently on the silicate and aluminate connectivity. Overall, the silicate NC increases with respect to hydration, while the Al NC decreases. This occurs because OH^- mainly happens to break Si − Al cross-links (possibly weaker than Si−Si and Al−Al), which dominate the Al connectivity, but not the Si connectivity. It seems as though the yttrium carries a driving force which draws hydroxyl groups towards itself. When hydroxyl groups move towards yttrium ions, it is possible that, for this reason, fewer hydroxyl groups are available to break down the network of the glass with respect to silicon or aluminum. This is unexpected where one simply thought hydroxyl groups would interfere with T – O − T bridges, instead because yttrium has an attraction for hydroxyl groups as they are drawn away to prevent the breakdown of T – O − T bridges, strengthening the network.

5 Yttrium-Bioglass (YBG)

5.1 *Yttrium-Bioglass (YBG) with Phosphorus*

We have already carried out hydration of YAS17, 24 and 30 earlier (section 3.4). This section will now thoroughly examine the effects of hydration on the bulk structure of YBG glasses. This work deals with simulating a different glass composition YBG that mainly deals with the same procedures employed upon YAS glasses 17, 24 and 30. The results will instead reflect that of YBG since YAS glasses 17, 24 and 30 has different characteristics and properties, furthermore YBG and YAS glasses have different uses and applications in radiotherapy. Firstly, simulations of unhydrated YBG were carried out. The unhydrated YBG glass was then hydrated at three increasing levels of hydration by adding hydroxyl groups into the bulk structure. The purpose of this was to investigate further the effects of hydration on the structure of the glasses e.g. silicon, phosphorus network connectivity, coordination numbers of network formers and modifiers etc.

Molecular dynamics simulations were carried out upon hydrated YBG with simulation sizes of approx 2000 atoms using DL_POLY. The potentials necessary for successfully simulating hydrated YBG glasses have been given in the methodology, in section 2.5.2 (Tables 2.8 – 2.13). Other data in section 3.2 (Table 3.11) were used also.

Using the technique mentioned earlier YBG was hydrated at three different levels where the variable y, the level of hydration, was 0.1, 0.2 or 0.3. Here y=0.1 refers to a low level of hydration and y=0.3 is a high level of hydration. The stoichiometries for each of the glasses are listed in Table. 5.1. This range thoroughly examines the effects and role of hydration in YBG glasses.

The general rule: $SiO_2 : P_2O_5 : CaO : Na_2O : (Y_2O_3)\text{-}y \,.\, (OH)\ 2y$

Table. 5.1

Glass Type	% Y_2O_3	% Na_2O	% P_2O_5	% CaO	% SiO_2	Density (g/cm^3)
YBG	4.68	15.85	1.0	16.12	62.35	2.730

Scaling for Hydration: y = OH fraction required to hydrate YBG

UNHYDRATED YBG: 4.68 mol % Y_2O_3, 1.00 mol % P_2O_5, 62.35 mol % SiO_2, 16.12 mol % CaO and 15.85 mol % Na_2O

Scaled: 32 Y_2O_3, 7 P_2O, 420 SiO_2, 108 CaO and 107 Na_2O

YBG_0.1 (y=0.1) [32 Y_2O_3, 7 P_2O, 420 SiO_2, 108 CaO and 107 Na_2O] – 50 O, + 100 OH

YBG_0.2 (y=0.2) [32 Y_2O_3, 7 P_2O, 420 SiO_2, 108 CaO and 107 Na_2O] – 100 O, + 200 OH

YBG_0.3 (y=0.3) [32 Y_2O_3, 7 P_2O, 420 SiO_2, 108 CaO and 107 Na_2O] – 150 O, + 300 OH

5.1.1 Short-range structure:

A) Bond Angles:

Figure 5.1: Hydrated yttrium bioglass (YBG) bond angle distributions for O – X – O, where X = Si, P, Y, Ca and Na

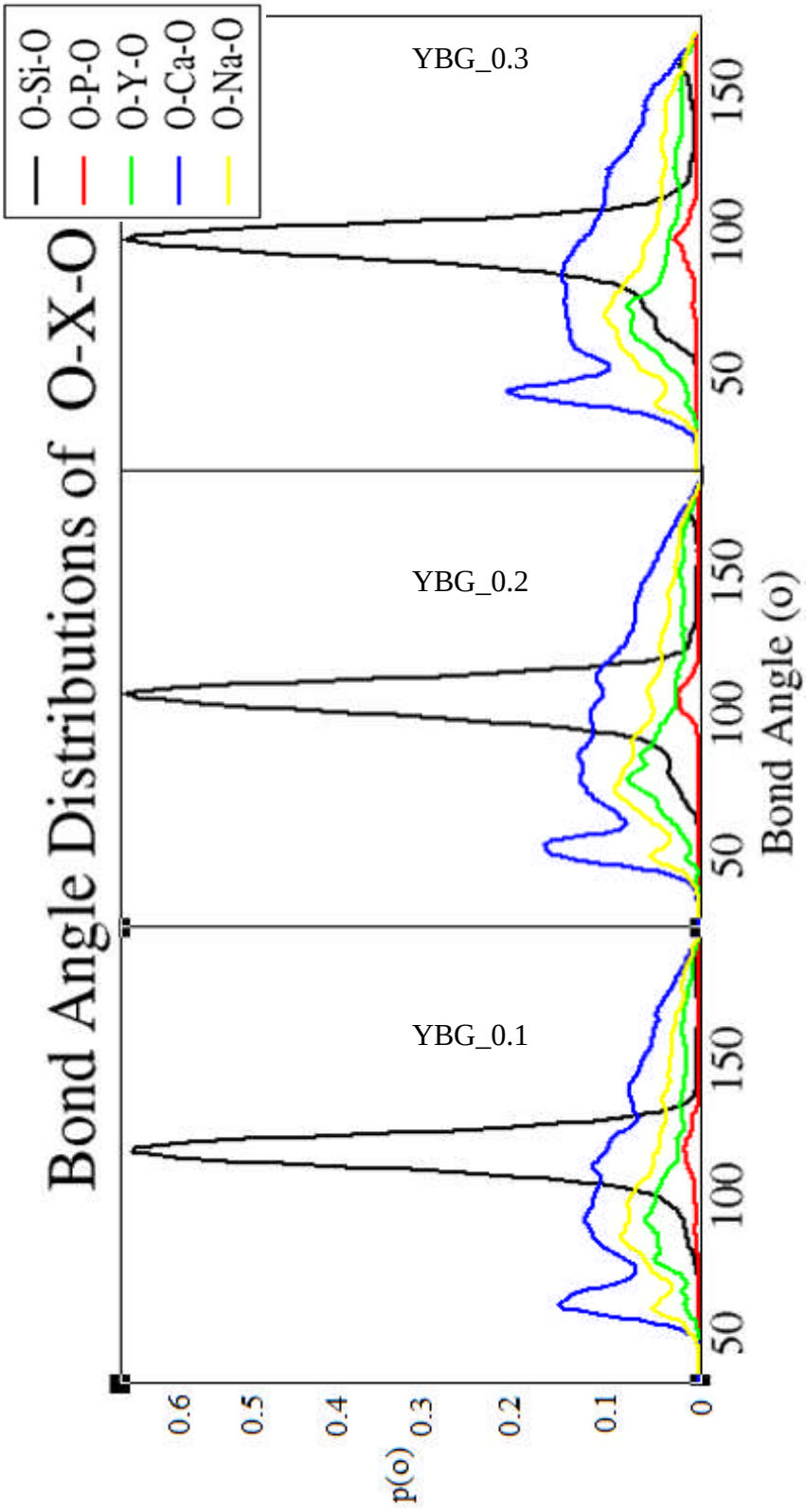

Figure 5.2: Hydrated yttrium bioglass (YBG) bond angle distributions for X – O – H, where X = Si, P, Y, Ca and Na

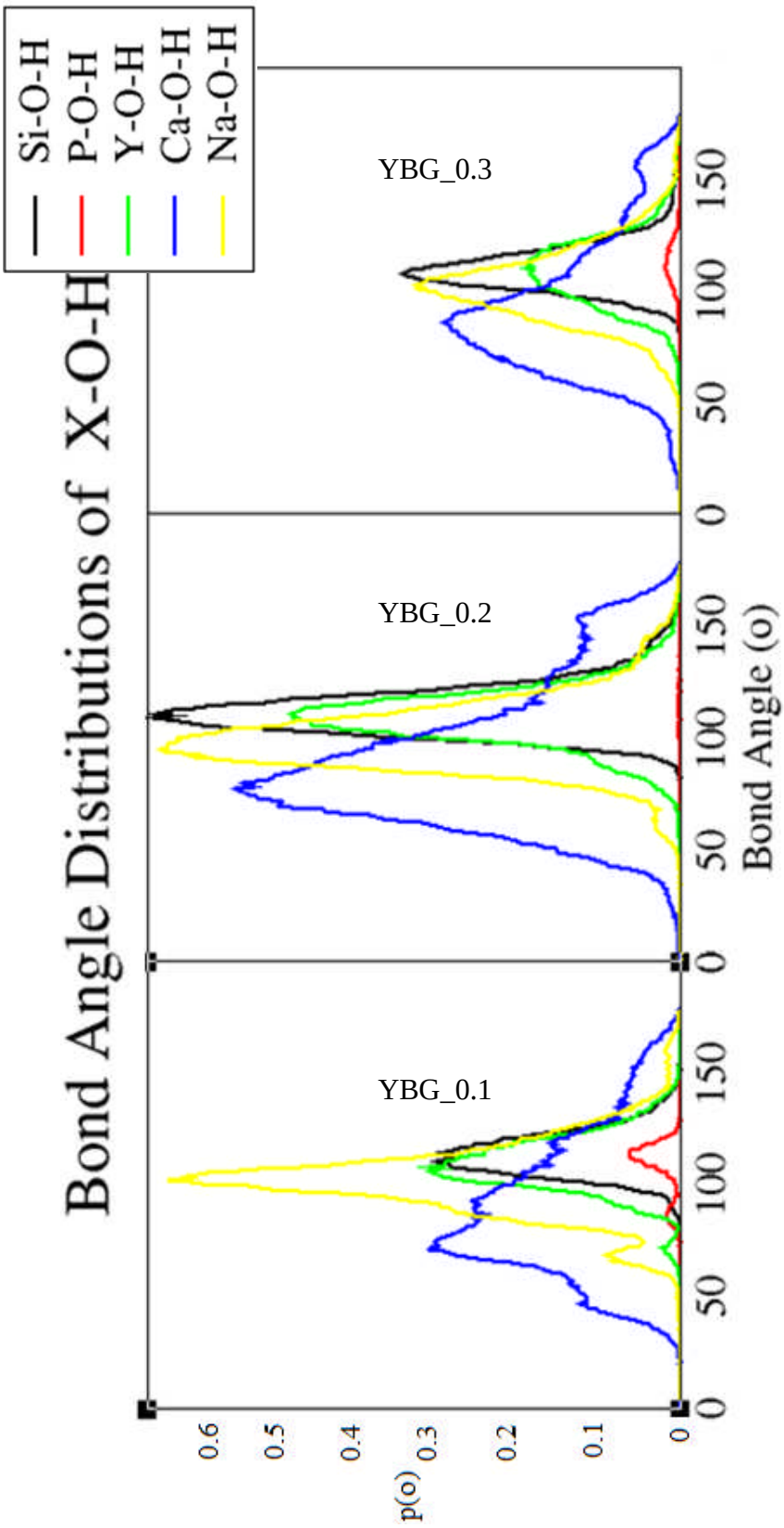

B) Coordination

1) Silicon

Table 5.2a. Total Coordination for Silicon (Oc + OHc) in dry and hydrated YBG glass

Si Coordination								
n	Dry YBG		YBG y=0.1		YBG y=0.2		YBG y=0.3	
	Distribution (%)	St. Dev	Distribution (%)	St. Dev	Distribution (%)	St. Dev	Distribution (%)	St. Dev
1	0.0000	0.0000	0.0000	0.0000	0.0000	0.0000	0.0000	0.0000
2	0.0000	0.0000	0.0000	0.0000	0.0000	0.0000	0.0000	0.0000
3	0.0003	0.0001	0.0289	0.0157	0.0208	0.0274	0.0001	0.0001
4	99.6775	0.3967	94.9332	0.6862	90.8076	0.0665	85.6681	0.2968
5	0.3222	0.3966	5.0379	0.6705	9.1679	0.0443	14.3151	0.2730
6	0.0000	0.0000	0.0000	0.0000	0.0037	0.0053	0.0167	0.0237
7	0.0000	0.0000	0.0000	0.0000	0.0000	0.0000	0.0000	0.0000
8	0.0000	0.0000	0.0000	0.0000	0.0000	0.0000	0.0000	0.0000
9	0.0000	0.0000	0.0000	0.0000	0.0000	0.0000	0.0000	0.0000
10	0.0000	0.0000	0.0000	0.0000	0.0000	0.0000	0.0000	0.0000
Average	**4.003**	0.0040	**4.050**	0.0065	**4.092**	0.0001	**4.144**	0.0032

Table 5.2a shows the silicon coordination. Oc refers to standard oxygen whereas OHc refers to oxygen attached to hydrogen atoms i.e. hydroxyl groups. There are virtually no silicon atoms with a coordination of five or higher, again which agrees with previous experimental and modelling data [115, 137] which showed coordination numbers of 3.9 – 4.0. Silicon has a well defined overall coordination of 4 and has the capacity to take up a maximum of 4 bonds to that of oxygen found from within the glass network. The table above shows the total Si coordination for hydrated YBG for hydration levels of 0.1 to 0.3 and for non-hydrated YBG glass. The general trend found is that by progressively hydrating YBG causes the overall silicon coordination to increase, due to the presence of a small percentage of 5-coordinated silicon species (Table 5.2a).

To analyse further the Si coordination to oxygen, the coordination contributions were split. The coordination of oxygen, both from the network modifier or former species (Na_2O/CaO/Y_2O_3/ SiO_2/P_2O_5) and from those attached to hydrogen (hydroxyl groups) were combined to form the overall silicon coordination seen in Table 5.2a. These contributions were then separated i.e. silicon oxygen coordination relating solely to the network modifier/former species i.e Na_2O/CaO/Y_2O_3/ SiO_2/P_2O_5 from those attached to hydrogen i.e. hydroxyl groups, to give an insight as to why a subtle increase in overall silicon coordination is seen for all YAS glasses observed in Table 5.2a.

The partial silicon coordination numbers are given below for yttrium bioglass (YBG) without calculating or including hydroxyl groups in the silicon coordination sphere in Table 5.2b.

Table 5.2b. Partial Coordination for Silicon (Oc) in hydrated YBG glass

Si Coordination						
n	YBG y=0.1		YBG y=0.2		YBG y=0.3	
	Distribution (%)	St. Dev	Distribution (%)	St. Dev	Distribution (%)	St. Dev
1	0.000	0.000	0.000	0.000	0.000	0.000
2	0.000	0.000	0.119	0.168	0.249	0.015
3	5.087	1.411	14.915	2.573	22.443	1.498
4	93.446	1.706	84.499	2.538	77.047	1.367
5	1.467	0.295	0.467	0.204	0.261	0.116
6	0.000	0.000	0.000	0.000	0.000	0.000
7	0.000	0.000	0.000	0.000	0.000	0.000
8	0.000	0.000	0.000	0.000	0.000	0.000
9	0.000	0.000	0.000	0.000	0.000	0.000
10	0.000	0.000	0.000	0.000	0.000	0.000
Average	**3.964**	0.011	**3.853**	0.031	**3.773**	0.016

The general trend found is that hydration causes the partial Si – O coordination to decrease. This shows that fewer oxygen atoms from the network modifier/former species i.e. $Na_2O/CaO/Y_2O_3/SiO_2/P_2O_5$ attach to Si in yttrium bioglass YBG.

The partial silicon coordination numbers are given below for YBG without including oxygen atoms in the silicon coordination sphere in Table 5.2c. Table 5.2c demonstrates solely coordination of hydroxyl groups onto silicon.

Table 5.2c. Partial Coordination for Silicon (OHc) in hydrated YBG glass

Si Coordination						
n	YBG y=0.1		YBG y=0.2		YBG y=0.3	
	Distribution (%)	St. Dev	Distribution (%)	St. Dev	Distribution (%)	St. Dev
0	91.495	0.637	78.388	2.333	68.607	0.741
1	8.380	13.135	19.382	12.932	25.877	16.117
2	0.125	1.372	2.230	1.183	5.397	3.162
3	0.000	0.000	0.000	0.000	0.119	0.168
4	0.000	0.000	0.000	0.000	0.000	0.000
5	0.000	0.000	0.000	0.000	0.000	0.000
6	0.000	0.000	0.000	0.000	0.000	0.000
7	0.000	0.000	0.000	0.000	0.000	0.000
8	0.000	0.000	0.000	0.000	0.000	0.000
9	0.000	0.000	0.000	0.000	0.000	0.000
10	0.000	0.000	0.000	0.000	0.000	0.000
Average	**0.086**	0.005	**0.238**	0.031	**0.370**	0.013

The general trend found was that for yttrium bioglass, gradual hydration caused a greater number of hydroxyl groups to coordinate to that of silicon. We saw that in Table 5.2b that the silicon to oxygen coordination decreases as the glass becomes hydrated, but at the same time the silicon oxygen coordination found from hydroxyl groups increases as seen in Table 5.2c.

Si – OH and Al – OH species have been reported by Xianyu Xue [153]. It had been demonstrated that hydroxyl groups have been seen to coordinate onto silicon and aluminium for aluminosilicate glasses.

From Table 5.2b, hydroxyl groups are the cause as to why a decrease is seen in the coordination of silicon with oxygen. While silicon coordination with oxygen decreases as hydration increases, hydroxyl groups replace those that were coordinated to silicon. Furthermore the overall silicon coordination is increased due to the presence of hydroxyl groups in its coordination sphere (Tables 5.2a and 5.2c).

From Figure 5.1 it is seen that as YBG glass is hydrated the bond angles shift towards the more acute bond angles very slightly for O - Si - O with respect to increasing hydration. A small peak is seen at the 70^{o} region, this is because hydration causes the overall coordination of silicon to increase as a very small number of 5 coordinated species are seen. Figure 5.2 shows the Si - O - H bond angles as YBG is

hydrated. The Si - O - H bond angles with respect to hydration of YBG remain unaffected. In Figure 5.3 silicon radial distribution functions in dry and hydrated YBG glasses are given. These show that the silicon oxygen interatomic distance is 1.63 Å. Also the silicon to hydroxyl-oxygen interatomic distance is 1.65 Å. The Si - O bond distances found for hydrated YBG are slightly larger than the typical bond distance of 1.60Å [42] which may be a possible reason as to why an increase in overall silicon coordination is seen. Hydroxyl groups being linear molecules may have a trajectory that allows for them to be inserted easily into the coordination sphere of silicon which therefore increases the overall silicon coordination.

Figure 5.3: Silicon radial distribution functions in dry and hydrated YBG glasses

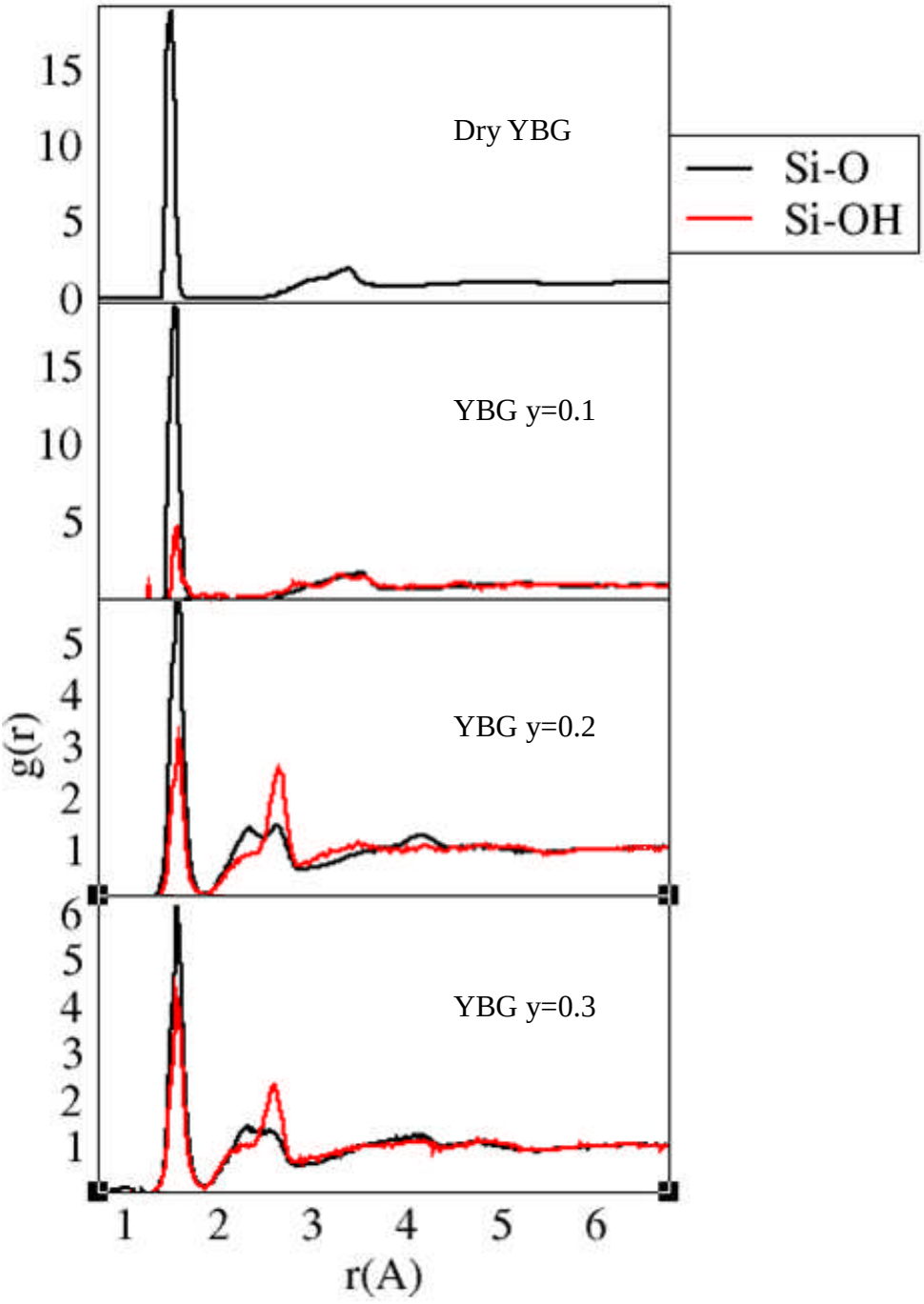

2) Phosphorus

Table 5.3a. Total Coordination for Phosphorus (Oc + OHc) in dry and hydrated YBG glass

P Coordination								
n	Dry YBG		YBG y=0.1		YBG y=0.2		YBGy=0.3	
	Distribution (%)	St. Dev	Distribution (%)	St. Dev	Distribution (%)	St. Dev	Distribution (%)	St. Dev
1	0.000	0.000	0.000	0.000	0.000	0.000	0.000	0.000
2	0.000	0.000	0.000	0.000	0.000	0.000	0.000	0.000
3	0.000	0.000	0.000	0.000	0.000	0.000	0.000	0.000
4	100.000	0.000	84.390	22.075	99.390	0.862	91.781	1.522
5	0.000	0.000	15.610	22.075	0.610	0.862	8.219	1.522
6	0.000	0.000	0.000	0.000	0.000	0.000	0.000	0.000
7	0.000	0.000	0.000	0.000	0.000	0.000	0.000	0.000
8	0.000	0.000	0.000	0.000	0.000	0.000	0.000	0.000
9	0.000	0.000	0.000	0.000	0.000	0.000	0.000	0.000
10	0.000	0.000	0.000	0.000	0.000	0.000	0.000	0.000
Average	**4.000**	0.000	**4.156**	0.221	**4.006**	0.009	**4.082**	0.015

Table 5.3a shows the phosphorus coordination. There are virtually no phosphorus atoms with a coordination of five or higher, except for YBG with y=0.1. Phosphorus typically has a well defined overall coordination of 4 and has the capacity to take up a maximum of 4 bonds to that of oxygen found from within the glass network. The table above shows the total P coordination for hydrated YBG from concentrations of 0.1 to 0.3 and its derivative i.e. non-hydrated glass YBG. Progressively hydrating YBG causes the overall phosphorus coordination to increase at concentration of 0.1.

To further analyse the P coordination to oxygen, the coordination contributions were split. The coordination of oxygen, whether from the network modifier/former species i.e. Na_2O/CaO/ Y_2O_3/SiO_2/P_2O_5 or from those attached to hydrogen i.e. hydroxyl groups were combined to form the overall phosphorus coordination seen in Table 5.3a. If these contributions were seperated i.e. phosphorus oxygen coordination relating solely to the network modifier/former species i.e. Na_2O/CaO/Y_2O_3/SiO_2/P_2O_5 from those attached to hydrogen i.e. hydroxyl groups, then this will give an insight as to why a subtle increase in overall phosphorus coordination is seen for yttrium biolgass observed in Table 5.3a.

The partial phosphorus coordination numbers are given for yttrium bioglass without including hydroxyl groups in the phosphorus coordination sphere in Table 5.3b.

Table 5.3b. Partial Coordination for Phosphorus (Oc) in hydrated YBG glass

P Coordination						
n	YBG y=0.1		YBG y=0.2		YBGy=0.3	
	Distribution (%)	St. Dev	Distribution (%)	St. Dev	Distribution (%)	St. Dev
1	0.000	0.000	0.000	0.000	0.000	0.000
2	0.000	0.000	0.000	0.000	0.000	0.000
3	14.286	0.000	3.571	5.051	28.571	20.203
4	78.343	10.425	95.819	4.189	70.881	20.978
5	7.371	10.425	0.610	0.862	0.548	0.774
6	0.000	0.000	0.000	0.000	0.000	0.000
7	0.000	0.000	0.000	0.000	0.000	0.000
8	0.000	0.000	0.000	0.000	0.000	0.000
9	0.000	0.000	0.000	0.000	0.000	0.000
10	0.000	0.000	0.000	0.000	0.000	0.000
Average	**3.931**	0.104	**3.970**	0.059	**3.720**	0.194

Phosphorus usually has a well-defined overall coordination of 4 and has the capacity to take up a maximum of 4 covalent bonds from oxygen found from within the glass system. The Table 5.3b shows the partial P – O coordination (exclusive of any hydroxyls that may be attached) for YBG hydrated from concentrations of 0.1 to 0.3. The general trend found is that hydration causes the partial P – O coordination to decrease.

The partial phosphorus coordination numbers are given for yttrium bioglass without including oxygen atoms in the phosphorus coordination sphere in Table 5.3c. Table 5.3c demonstrates solely coordination of hydroxyl groups onto phosphorus excluding normal oxygens from the phosphorus coordination sphere.

Table 5.3c. Partial Coordination for Phosphorus (OHc) in hydrated YBG glass

P Coordination						
n	YBG y=0.1		YBG y=0.2		YBG y=0.3	
	Distribution (%)	St. Dev	Distribution (%)	St. Dev	Distribution (%)	St. Dev
0	78.571	10.102	96.429	5.051	64.286	20.203
1	20.333	8.553	3.571	5.051	35.186	19.456
2	1.095	1.549	0.000	0.000	0.529	0.748
3	0.000	0.000	0.000	0.000	0.000	0.000
4	0.000	0.000	0.000	0.000	0.000	0.000
5	0.000	0.000	0.000	0.000	0.000	0.000
6	0.000	0.000	0.000	0.000	0.000	0.000
7	0.000	0.000	0.000	0.000	0.000	0.000
8	0.000	0.000	0.000	0.000	0.000	0.000
9	0.000	0.000	0.000	0.000	0.000	0.000
10	0.000	0.000	0.000	0.000	0.000	0.000
Average	**0.225**	0.117	**0.036**	0.051	**0.362**	0.210

The general trend found was that for yttrium bioglass, gradual hydration caused a greater number of hydroxyl groups to coordinate to that of phosphorus; the increase is seen especially at hydration concentration of 0.1. We saw that in Table 5.3b that the phosphorus to oxygen coordination decreases as the glass becomes hydrated, but at the same time the phosphorus-oxygen coordination found from hydroxyl groups increases as seen in Table 5.3c. The overall increase in coordination for phosphorus seen in Table 5.3a is due to the associated oxygens in hydroxyl groups taking precedence over normal oxygens from network modifier/former species i.e. $Na_2O/CaO/Y_2O_3/SiO_2/P_2O_5$.

Si – OH and Al – OH species have been reported by Xianyu Xue [153]. It had been demonstrated that hydroxyl groups have been seen to coordinate onto silicon and aluminium for aluminosilicate glasses.

From viewing Table 5.3b hydroxyl groups may be the cause as to why a decrease is seen in the coordination of phosphorus with oxygen. While phosphorus coordination with oxygen decreases as hydration increases, hydroxyl groups replace those that were coordinated to phosphorus. Furthermore the overall phosphorus coordination is increased due to the presence of hydroxyl groups in its coordination sphere. Tables 5.3a and 5.3c.

From Figure 5.1 it is seen that as YBG glass is hydrated the bond angles shift towards the more acute angles very slightly for O - P - O with respect to increasing hydration. A small peak is seen at the 72^{o} region, this is because hydration causes the overall coordination of phosphorus to increase as a very small number of 5 coordinated species are seen. Figure 5.2 shows the P - O - H bond angles as YBG is hydrated. The P - O - H bond angles with respect to hydration of YBG remain unaffected. In Figure 5.4 phosphorus radial distribution functions in dry and hydrated YBG glasses are given. These show that the phosphorus oxygen interatomic distance is 1.61 A. Also the phosphorus to hydroxyl-oxygen interatomic distance is 1.63 A.

Figure 5.4: Phosphorus radial distribution functions in dry and hydrated YBG Glasses

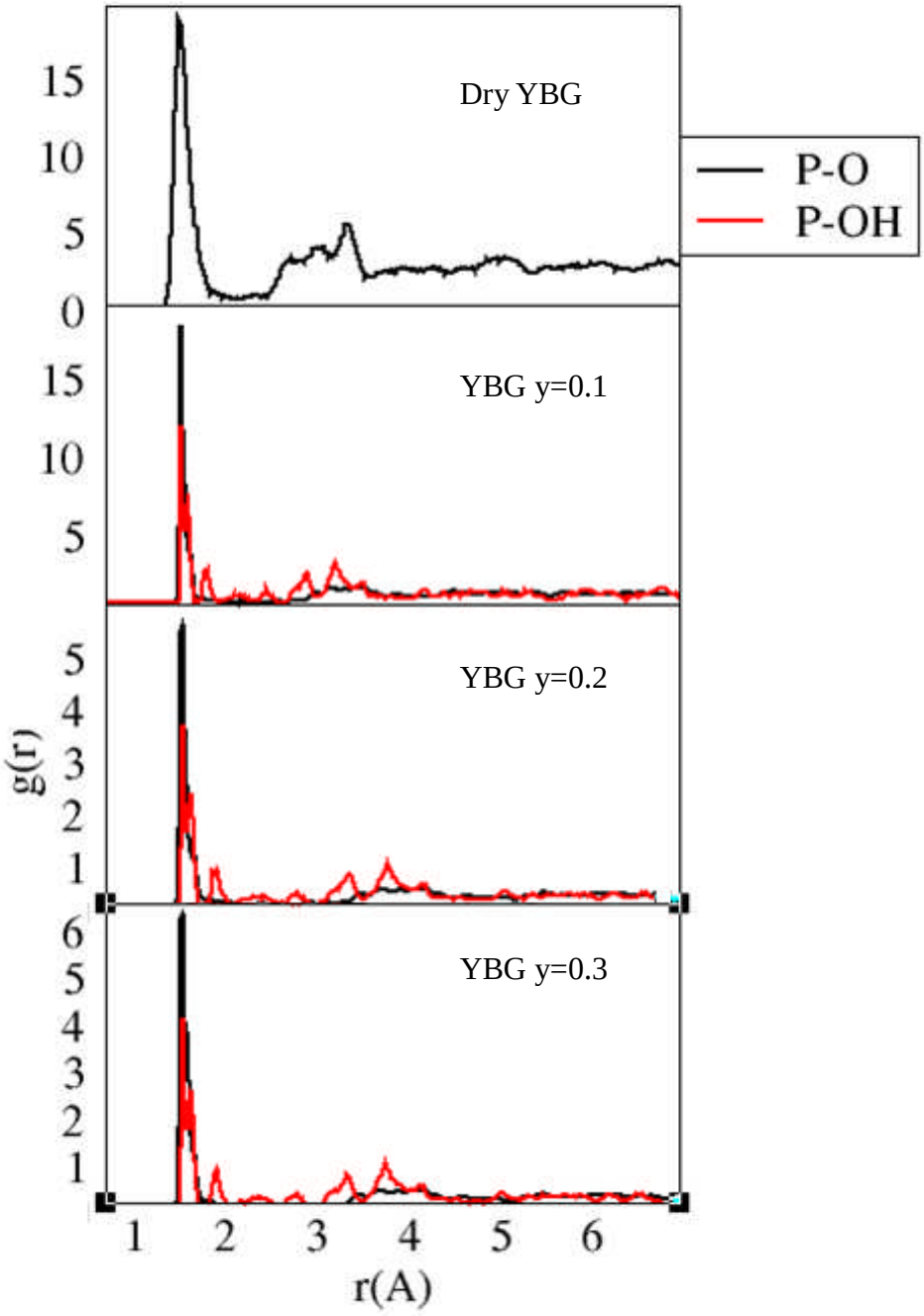

3) Yttrium

Table 5.4a. Total Coordination for Yttrium (Oc + OHc) in hydrated YBG glass

Y Coordination								
n	Dry YBG		YBG y=0.1		YBG y=0.2		YBG y=0.3	
	Distribution (%)	St. Dev	Distribution (%)	St. Dev	Distribution (%)	St. Dev	Distribution (%)	St. Dev
1	0.000	0.000	0.000	0.000	0.000	0.000	0.000	0.000
2	0.000	0.000	0.000	0.000	0.000	0.000	0.000	0.000
3	0.000	0.000	0.000	0.000	0.000	0.000	0.000	0.000
4	1.600	1.287	7.343	1.337	1.566	0.429	1.337	0.127
5	37.082	16.240	45.521	4.302	34.304	7.238	24.373	6.261
6	55.986	15.882	39.179	1.363	47.040	5.414	60.182	9.774
7	5.326	0.933	6.471	2.177	15.569	0.342	12.299	5.579
8	0.006	0.004	1.485	2.100	1.499	1.705	1.808	1.936
9	0.000	0.000	0.000	0.000	0.022	0.032	0.002	0.002
10	0.000	0.000	0.000	0.000	0.000	0.000	0.000	0.000
Average	**5.651**	0.127	**5.492**	0.134	**5.812**	0.095	**5.889**	0.043

The total Y – O coordination for yttrium bioglass ranged between 5.49 – 5.89. Such coordination numbers compare well to simulation studies of yttrium bioglass YBG carried out by the work of Tilocca and Christie [115, 137], where Y – O coordination for unhydrated YBG bioglass of 5.6 was found. A wider range of bonding environments are observed for yttrium compared to either silicon or phosphorus. Here five or six coordinated yttrium atoms are most commonly seen. Some yttrium atoms have been seen to have coordination numbers of as low as four and as high as nine. An investigation is required to find out exactly how many hydroxyls are able to bond to yttrium in each of the glasses and whether or not increased hydration increases the effect. Therefore partial Y – O and Y – OH contributions were shown in Tables 5.4b and 5.4c respectively.

The partial yttrium coordination numbers are given for yttrium bioglass without including hydroxyl groups in the yttrium coordination sphere in Table 5.4b.

Table 5.4b. Partial Coordination for Yttrium (Oc) in hydrated YBG glass

Y Coordination						
n	YBG y=0.1		YBG y=0.2		YBG y=0.3	
	Distribution (%)	St. Dev	Distribution (%)	St. Dev	Distribution (%)	St. Dev
1	0.000	0.000	0.000	0.000	1.563	0.000
2	1.022	1.445	1.565	2.205	8.510	0.756
3	10.487	2.823	16.120	6.038	29.047	4.632
4	29.213	7.363	39.733	13.199	41.486	5.496
5	35.312	4.354	33.628	5.978	14.518	0.071
6	18.446	1.104	7.873	1.864	4.677	0.096
7	4.808	2.277	1.081	1.525	0.198	0.276
8	0.711	1.006	0.000	0.000	0.000	0.000
9	0.000	0.000	0.000	0.000	0.000	0.000
10	0.000	0.000	0.000	0.000	0.000	0.000
Average	**4.769**	0.174	**4.334**	0.127	**3.737**	0.056

The table above shows the partial Y – O coordination (exclusive of any hydroxyls that may be attached) for yttrium bioglass hydrated from concentrations of 0.1 to 0.3. The general trend found is that hydration causes the partial Y – O coordination to decrease.

The partial yttrium coordinations are given below for yttrium bioglass without including oxygen atoms in the yttrium coordination sphere in Table 5.4c.

Table 5.4c. Partial Coordination for Yttrium (OHc) in dry and hydrated YBG glass

Y Coordination						
n	YBG y=0.1		YBG y=0.2		YBG y=0.3	
	Distribution (%)	St. Dev	Distribution (%)	St. Dev	Distribution (%)	St. Dev
0	41.775	6.211	3.906	1.105	3.125	2.210
1	44.161	8.422	53.804	1.307	16.256	3.527
2	14.064	2.211	34.404	2.819	49.216	0.828
3	0.000	0.000	6.324	0.407	26.715	2.144
4	0.000	0.000	1.563	0.000	3.113	0.017
5	0.000	0.000	0.000	0.000	1.575	0.018
6	0.000	0.000	0.000	0.000	0.000	0.000
7	0.000	0.000	0.000	0.000	0.000	0.000
8	0.000	0.000	0.000	0.000	0.000	0.000
9	0.000	0.000	0.000	0.000	0.000	0.000
10	0.000	0.000	0.000	0.000	0.000	0.000
Average	**0.723**	0.040	**1.478**	0.031	**2.152**	0.013

The general trend seen from the above table for yttrium bioglass, is that gradual hydration causes a greater number of hydroxyl groups to coordinate to yttrium. The coordinations of hydroxyl groups onto yttrium in Table 5.4c are raised and are of a wider range compared to hydroxyl coordinations onto silicon or phosphorus seen in Table 5.2c and 5.3c respectively. This shows hydroxyl groups have the ability to coordinate more to yttrium and less with silicon or phosphorus. We have already identified that silicon and phosphorus are typically well-defined in coordination at four and do not have the capacity to take up any more bonds to oxygen, whether they are from hydroxyl groups or from network former/modifier species i.e. $Na_2O/CaO/Y_2O_3/SiO_2/P_2O_5$. Yttrium on the other hand has a wider range of coordination numbers than Si and P thus giving rise to a greater capacity to welcome hydroxyl groups into its coordination sphere.

From viewing Table 5.4b hydroxyl groups may be the cause as to why a decrease is seen in the coordination of yttrium with oxygen. While yttrium coordination with oxygen decreases as hydration increases, hydroxyl groups replace those that were coordinated to yttrium. Furthermore the overall yttrium coordination is increased due to the presence of hydroxyl groups in its coordination sphere (Tables 5.4a and 5.4c).

From Figure 5.1 it is seen that as YBG glass is hydrated the bond angles shift towards the more acute angles for O - Y - O with respect to increasing hydration. Small peaks are seen at the 50^o region, this is because hydration causes the overall

coordination of yttrium to increase as a number of 5, 6 and 7 coordinated species are seen. Figure 5.2 shows the Y - O - H bond angles as YBG is hydrated. The Y - O - H bond angles with respect to hydration of YBG remain unaffected by hydration.

From Figure 5.5 yttrium radial distribution functions in dry and hydrated YBG glasses are given. These show that the yttrium-oxygen interatomic distance is 2.23 Å. Also the yttrium to hydroxyl-oxygen interatomic distance is 2.33 Å.

Figure 5.5: Yttrium radial distribution functions in dry and hydrated YBG Glasses

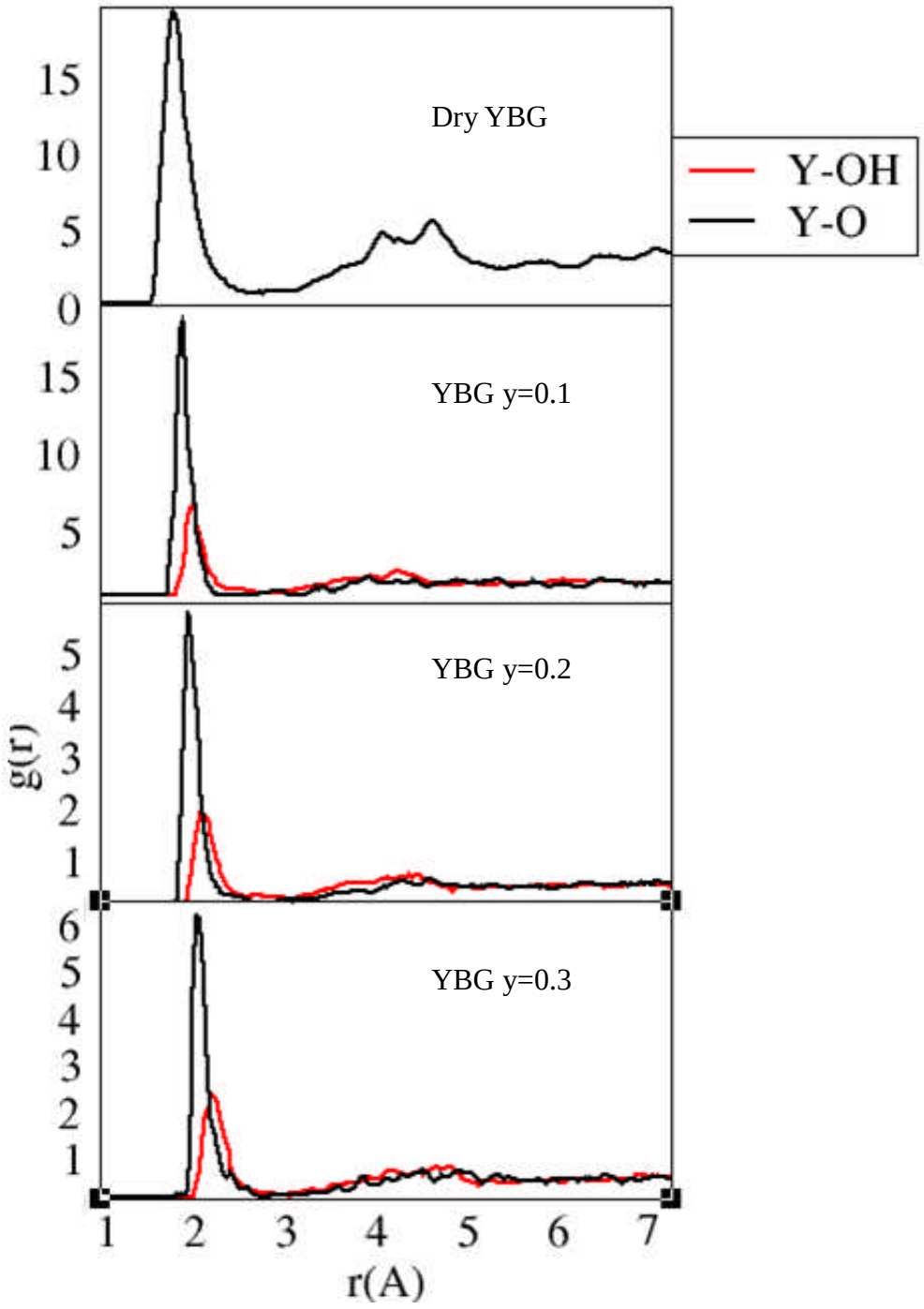

4) Calcium

Table 5.5a. Total Coordination for Calcium (Oc + OHc) in dry and hydrated YBG glass

Ca Coordination								
n	Dry YBG		YBG y=0.1		YBG y=0.2		YBG y=0.3	
	Distribution(%)	St. Dev	Distribution(%)	St. Dev	Distribution(%)	St. Dev	Distribution(%)	St. Dev
1	0.000	0.000	0.000	0.000	0.000	0.000	0.000	0.000
2	0.000	0.000	0.000	0.000	0.000	0.000	0.000	0.000
3	0.003	0.005	0.461	0.652	0.000	0.000	0.000	0.000
4	5.162	0.752	3.800	0.062	2.110	1.093	2.573	0.543
5	27.899	0.609	25.280	1.848	25.680	4.355	17.943	5.111
6	37.472	4.193	43.327	1.208	41.270	3.706	40.561	0.756
7	23.462	5.800	21.007	0.521	24.490	3.047	28.874	3.113
8	5.233	1.041	5.392	0.508	6.093	4.326	9.054	0.906
9	0.760	0.407	0.730	0.092	0.342	0.440	0.953	0.148
10	0.009	0.011	0.003	0.005	0.016	0.023	0.041	0.058
Average	**5.980**	0.034	**5.997**	0.010	**6.079**	0.136	**6.269**	0.083

The total Ca – O coordination for yttrium bioglass YBG ranged between 5.98 – 6.27. Such coordination numbers compare well enough to simulations studies of yttrium bioglass carried out by the work of Tilocca and Christie [115, 137], where Ca – O coordination for unhydrated YBG bioglass of ~6 was found. A wider range of bonding environments are observed for calcium compared to silicon, phosphorus and yttrium. Here five- six-, seven-coordinated calcium atoms are most commonly seen. Some calcium atoms have been seen to have coordination numbers of as low as three and as high as ten. The general trend found from the above graph is that the total Ca – O coordination increases gradually as hydration increases. An investigation is required to find out exactly how many hydroxyls are able to attach to calcium in each of the glasses and whether or not increased hydration improves the effect. Therefore partial Ca – O and Ca – OH contributions were shown in Tables 5.5b and 5.5c respectively.

The partial calcium coordination numbers are given for yttrium bioglass without including hydroxyl groups in the calcium coordination sphere in Table 5.5b.

Table 5.5b. Partial Coordination for Calcium (Oc) in hydrated YBG glass

Ca Coordination						
n	YBG y=0.1		YBG y=0.2		YBG y=0.3	
	Distribution(%)	St. Dev	Distribution(%)	St. Dev	Distribution(%)	St. Dev
1	0.000	0.000	0.405	0.572	0.978	0.063
2	0.002	0.003	2.367	2.046	8.369	1.025
3	3.750	0.680	14.964	4.517	21.471	4.850
4	27.204	1.508	28.776	2.746	30.789	8.700
5	32.798	4.277	34.207	0.781	24.044	1.946
6	23.842	5.896	15.191	8.745	11.664	0.218
7	10.214	1.430	3.797	0.023	1.877	1.632
8	1.878	0.210	0.292	0.331	0.798	1.128
9	0.312	0.431	0.000	0.000	0.010	0.014
10	0.000	0.000	0.000	0.000	0.000	0.000
Average	**5.164**	0.055	**4.562**	0.300	**4.151**	0.092

The general trend found is that hydration causes the partial Ca – O coordination to decrease.

The partial calcium coordination numbers are given below for yttrium bioglass without including oxygen atoms in the calcium coordination sphere in Table 5.5c.

Table 5.5c. Partial Coordination for Calcium (OHc) in hydrated YBG glass

Ca Coordination						
n	YBG y=0.1		YBG y=0.2		YBG y=0.3	
	Distribution(%)	St. Dev	Distribution(%)	St. Dev	Distribution(%)	St. Dev
0	31.604	5.041	8.297	3.686	3.880	2.643
1	53.964	6.173	44.740	4.498	27.460	2.881
2	13.969	1.787	36.317	4.275	33.945	3.457
3	0.463	0.655	8.331	3.254	23.404	4.708
4	0.000	0.000	2.315	0.655	10.730	0.371
5	0.000	0.000	0.000	0.000	0.148	0.032
6	0.000	0.000	0.000	0.000	0.432	0.611
7	0.000	0.000	0.000	0.000	0.000	0.000
8	0.000	0.000	0.000	0.000	0.000	0.000
9	0.000	0.000	0.000	0.000	0.000	0.000
10	0.000	0.000	0.000	0.000	0.000	0.000
Average	**0.833**	0.046	**1.516**	0.164	**2.118**	0.010

The general trend seen from the above table for yttrium bioglass, is that gradual hydration causes a greater number of hydroxyl groups to coordinate to calcium. The coordination of hydroxyl groups onto calcium are rather similar to that of yttrium seen in Table 5.5c. The coordination numbers of hydroxyl groups onto calcium in Table 5.5c are raised and are of a wider range compared to hydroxyl coordinations onto silicon or phosphorus seen in Table 5.2c and 5.3c respectively. This shows hydroxyl groups having the ability to coordinate more to calcium and less with silicon or phosphorus. We have already identified that silicon and phosphorus are well defined in coordination at four and shows they do not have the capacity to take up any more coordinations with oxygen, whether they are from hydroxyl groups or from network former/modifier species i.e. $Na_2O/CaO/Y_2O_3/SiO_2/P_2O_5$. Calcium, like yttrium, on the other hand has a wider range of coordination numbers than Si and P thus giving rise to a greater capacity to welcome hydroxyl groups into the coordination sphere of calcium.

From viewing Table 5.5b hydroxyl groups may be the cause as to why a decrease is seen in the coordination of calcium with oxygen. While calcium coordination with oxygen decreases as hydration increases, hydroxyl groups replace those that were coordinated to calcium. Furthermore the overall calcium coordination is increased due to the presence of hydroxyl groups in its coordination sphere (Tables 5.5a and 5.5c).

From Figure 5.1 it is seen that as YBG glass is hydrated the bond angles shift

towards more acute angles for O - Ca - O with respect to increasing hydration. A peak is seen at the 60^{o} region, this is because hydration causes the overall coordination of calcium to increase as a very small number of 5, 6 and 7 coordinated species are seen. Figure 5.2 shows the Ca - O - H bond angles as YBG is hydrated. The Ca - O - H bond angles with respect to hydration of YBG remain unaffected by hydration.

From Figure 5.6 calcium radial distribution functions in dry and hydrated YBG glasses are given. These show that the calcium-oxygen interatomic distance is 2.32 Å. Also the calcium to hydroxyl-oxygen interatomic distance is 2.34 Å.

Figure 5.6: Calcium radial distribution functions in dry and hydrated YBG Glasses

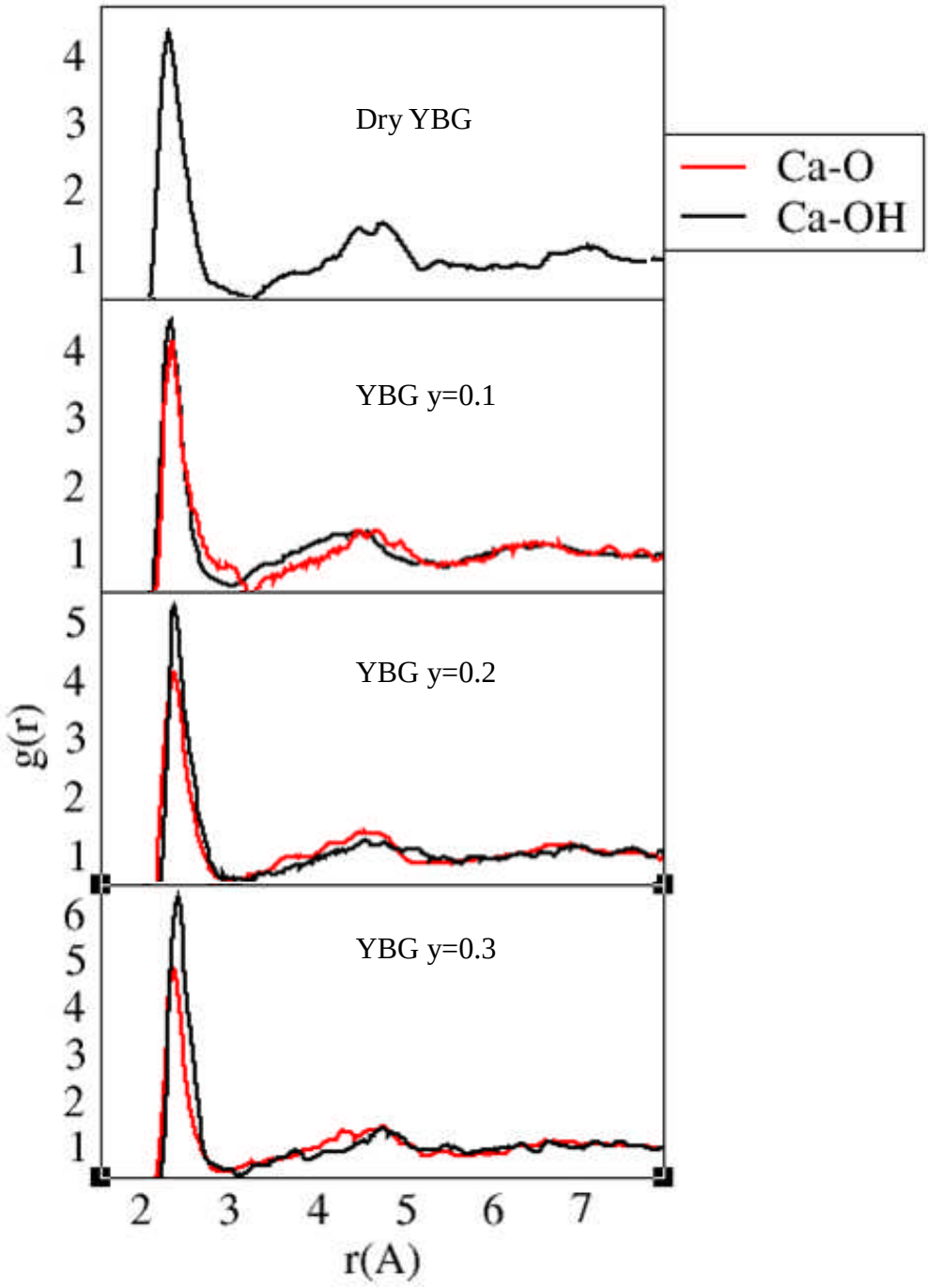

5) Sodium

Table 5.6a. Total Coordination for Sodium (Oc + OHc) in dry and hydrated YBG glass

Na Coordination								
n	Dry YBG		YBG y=0.1		YBG y=0.2		YBG y=0.3	
	Distribution(%)	St. Dev	Distribution(%)	St. Dev	Distribution(%)	St. Dev	Distribution(%)	St. Dev
1	0.000	0.000	0.000	0.000	0.000	0.000	0.000	0.000
2	0.000	0.000	0.000	0.000	0.004	0.005	0.000	0.000
3	0.437	0.244	1.280	0.533	0.064	0.059	0.020	0.028
4	5.645	0.351	7.840	0.971	5.150	0.139	4.037	1.929
5	23.739	0.298	25.630	0.067	24.070	0.539	20.802	1.338
6	38.727	3.015	37.652	1.802	32.192	1.013	32.816	0.419
7	23.475	2.332	19.387	1.110	27.657	1.198	28.416	2.344
8	7.304	0.549	6.975	0.048	8.836	0.535	11.538	3.299
9	0.626	0.301	1.228	0.695	1.757	0.002	2.099	1.660
10	0.044	0.023	0.008	0.001	0.228	0.193	0.255	0.236
Average	**6.038**	0.047	**5.919**	0.045	**6.167**	0.023	**6.298**	0.153

The total Na – O coordination for yttrium bioglass YBG ranged between 5.92 – 6.30. Such coordination numbers compare well enough to simulation studies of yttrium bioglass YBG carried out by the work of Tilocca and Christie [115, 137], where Na – O coordination for unhydrated YBG bioglass of ~6 was found. A wider range of bonding environments are observed for sodium compared to silicon, phosphorus, yttrium and calcium. Here five-, six and seven-coordinated sodium atoms are most commonly seen. Some sodium atoms have been seen to have coordination numbers of as low as three and as high as ten. The general trend found from the above graph is that the total Na – O coordination increases gradually as hydration increases. An investigation is required to find out exactly how many hydroxyls are able to attach to sodium in each of the glasses and whether or not increased hydration improves the effect. Therefore partial Na – O and Na – OH contributions were shown in Tables 5.6b and 5.6c respectively.

The partial sodium coordination numbers are given for yttrium bioglass without including hydroxyl groups in the sodium coordination sphere in Table 5.6b.

Table 5.6b. Partial Coordination for Sodium (Oc) in hydrated YBG glass

Na Coordination						
n	YBG y=0.1		YBG y=0.2		YBG y=0.3	
	Distribution(%)	St. Dev	Distribution(%)	St. Dev	Distribution(%)	St. Dev
1	0.000	0.000	0.000	0.000	0.110	0.156
2	0.000	0.000	0.914	0.078	2.233	1.827
3	4.797	1.366	7.990	2.251	12.845	3.098
4	15.972	2.834	21.054	0.098	28.183	3.940
5	35.050	1.724	32.290	0.104	32.190	2.064
6	28.079	1.497	25.348	3.070	16.120	2.704
7	11.929	0.426	10.200	0.265	7.202	1.054
8	3.441	0.217	1.912	0.375	1.053	0.519
9	0.725	0.769	0.250	0.191	0.062	0.034
10	0.007	0.002	0.042	0.059	0.000	0.000
Average	**5.396**	0.103	**5.129**	0.045	**4.729**	0.115

The general trend found is that hydration causes the partial Na – O coordination to decrease.

The partial sodium coordination numbers are given for yttrium bioglass without including oxygen atoms in the sodium coordination sphere in Table 5.6c.

Table 5.6c. Partial Coordination for Sodium (OHc) in hydrated YBG glass

Na Coordination						
n	YBG y=0.1		YBG y=0.2		YBG y=0.3	
	Distribution(%)	St. Dev	Distribution(%)	St. Dev	Distribution(%)	St. Dev
0	54.720	4.640	25.990	2.721	13.038	1.628
1	38.751	3.476	48.883	0.513	38.618	2.753
2	6.062	1.165	20.474	3.642	31.185	4.521
3	0.468	0.001	4.210	0.810	13.243	1.903
4	0.000	0.000	0.442	0.624	3.347	2.187
5	0.000	0.000	0.000	0.000	0.474	0.011
6	0.000	0.000	0.000	0.000	0.094	0.133
7	0.000	0.000	0.000	0.000	0.000	0.000
8	0.000	0.000	0.000	0.000	0.000	0.000
9	0.000	0.000	0.000	0.000	0.000	0.000
10	0.000	0.000	0.000	0.000	0.000	0.000
Average	**0.523**	0.058	**1.042**	0.029	**1.570**	0.041

The general trend seen from the above table for yttrium bioglass YBG, gradual hydration causes a greater number of hydroxyl groups to coordinate to sodium. The coordination of hydroxyl groups onto sodium are slightly lower than that of yttrium and calcium seen in Table 5.4c and 5.5c respectively. The coordination numbers of hydroxyl groups to sodium in Table 5.6c are raised and are of a wider range compared to hydroxyl coordinations to silicon or phosphorus seen in Table 5.2c and 5.3c respectively. This shows hydroxyl groups have the ability to coordinate more to sodium and less with silicon or phosphorus. We have already identified that silicon and phosphorus are too well-defined in coordination at four and shows they neither have the capacity to take up any more bonds with oxygen, whether they are from hydroxyl groups or from network former/modifier species i.e. $Na_2O/CaO/Y_2O_3/SiO_2/P_2O_5$. Sodium, like yttrium and calcium, has a wider range of coordination numbers than Si and P thus giving rise to a greater capacity to welcome hydroxyl groups into the coordination sphere of sodium.

From viewing Table 5.6b hydroxyl groups may be the cause as to why a decrease is seen in the coordination of sodium with oxygen. While sodium coordination with oxygen decreases as hydration increases, hydroxyl groups replace those that were coordinated to sodium. Furthermore the overall sodium coordination is increased due to the presence of hydroxyl groups in its coordination sphere (Tables 5.6a and 5.6c).

In Figure 5.1 it is seen that as YBG glass is hydrated the bond angles shift

towards more acute angles for O - Na - O with respect to increasing hydration. A peak is seen in the 60^{o} region, this is because hydration causes the overall coordination of sodium to increase as a number of 5, 6 and 7 coordinated species are seen. Figure 5.2 shows the Na - O - H bond angles as YBG is hydrated. The Na - O - H bond angles with respect to hydration of YBG remain unaffected by hydration.

From Figure 5.7 sodium radial distribution functions in dry and hydrated YBG glasses are given. These show that the sodium-oxygen interatomic distance is 2.34 Å. Also the sodium to hydroxyl-oxygen interatomic distance is 2.35 Å.

Figure 5.7: Sodium radial distribution functions in dry and hydrated YBG Glasses

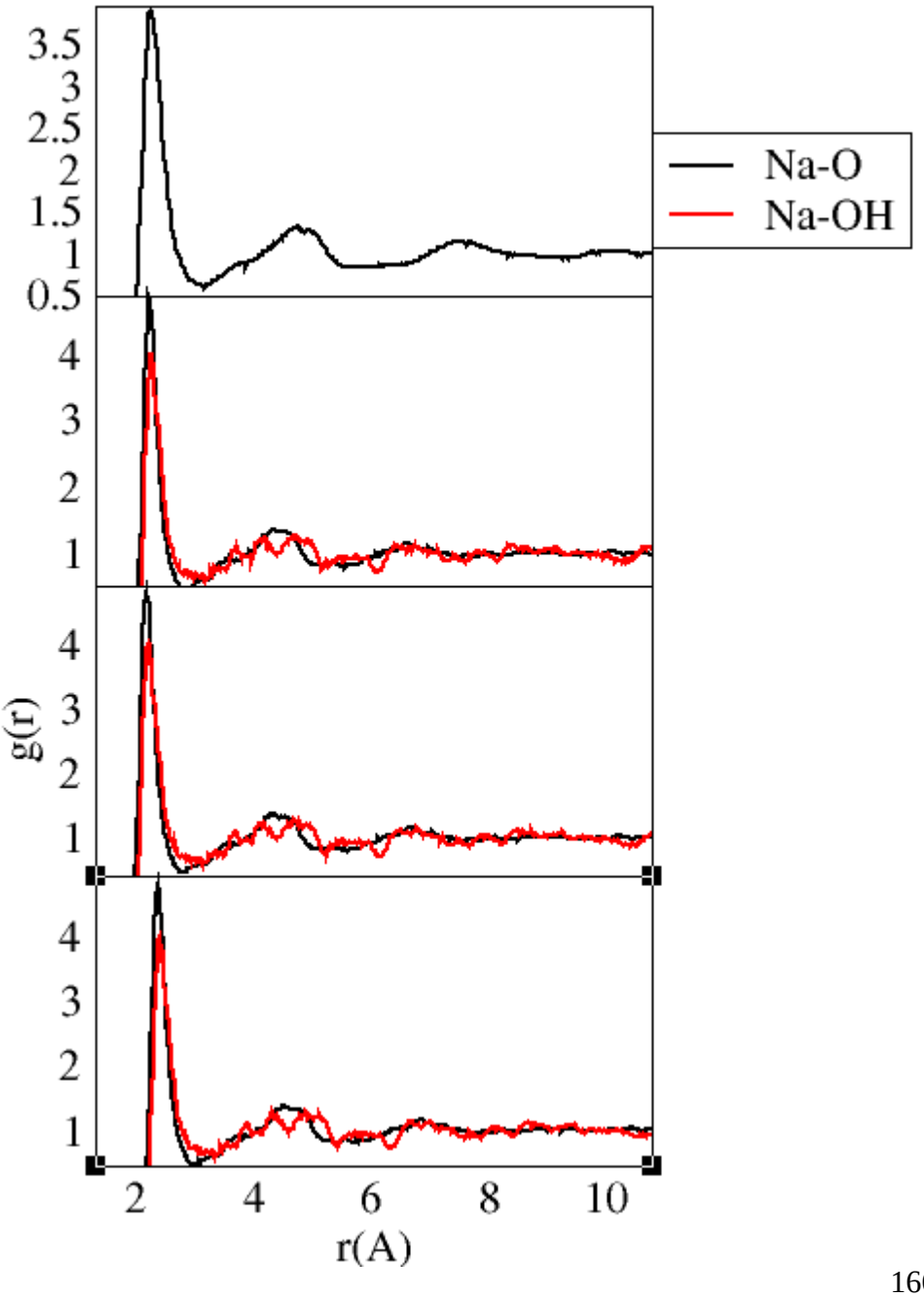

5.1.2 Preferential Attachment of –OH onto Network Formers

The number of OH species bonded to each network-forming cation, silicon and phosphorus, in hydrated yttrium bioglasses are shown in Table 5.7a and 5.7b. Table 5.7a shows the actual number of OH species that surround silicon or phosphorus. Normalisation of numbers in Table 5.7a give rise to Table 5.7b to remove unnecessary biasing due to the number of cations used in the simulation. The normalisation method employed is given below:

Table 5.7a: Number of hydroxyls attached to Si and P and those which are free

YBG	Si		P		Free OH	
	No. OH	St. Dev	No. OH	St. Dev	No. OH	St. Dev
0.1	36.246	0.707	3.153	1.414	60.601	1.414
0.2	100.136	9.899	0.500	0.707	99.364	1.237
0.3	155.517	4.243	5.074	2.828	139.409	1.325

NORMALISATION: No. of $^{-}$OH species attached to a cation/ Total no. of cations to which those hydroxyl groups are attached in simulation

e.g. for SILICON

(YBG y=0.1) OH on Si = 36.246/420 = 0.0863
(YBG y=0.2) OH on Si = 100.136/420 = 0.2384
(YBG y=0.3) OH on Si = 155.517/420 = 0.37027

Table 5.7b: Number of Hydroxyls attached to Si and P and those which are Free (normalized)

YBG	Si		P		Free OH	
	No. OH	St. Dev	No. OH	St. Dev	No. OH	St. Dev
0.1	0.086	0.002	0.225	0.101	0.606	0.0034
0.2	0.238	0.024	0.036	0.051	0.497	0.0029
0.3	0.370	0.010	0.362	0.202	0.465	0.0031

Hydroxyl groups prefer to coordinate to silicon and phosphorus by the same amount when yttrium bioglass is hydrated at concentrations of 0.2 and 0.3. As the glass is hydrated progressively from 0.1 - 0.3 the amount of hydroxyls attaching to silicon

rises. Phosphorus on the other hand is sporadic with respect to increasing hydration concentration as no correlation is found, this is due to poor statistics where low (14 atoms) amounts of phosphorus were present in YBG simulations. The more an yttrium bioglass is hydrated, the fewer free hydroxyl groups are seen. As hydroxyl groups attach to silicon the more it is hydrated, the less hydroxyl groups are available to be free in the glass as YBG is hydrated.

Figure 5.8 shows the order by which hydroxyl groups prefer to attach to silicon and then to phosphorus

Fig 5.8: (Si– OH) ~ (P – OH)

Phosphorus and silicon are equally as welcoming to hydroxyl groups. Hydroxyl groups that have not attached to network forming species, Si/P, would as a result be described as free hydroxyl groups with the ability to form coordination to network modifying species such as sodium in Xianyu Xue's paper [153]. Yttrium, calcium and sodium are the network modifiers in YBG glasses. Since free hydroxyls were seen to attach to sodium modifier ions [153] in other glasses, incorporating yttrium and calcium modifier ions would suggest that hydroxyl groups can bind to yttrium and calcium too in an yttrium bioglass (YBG), as we have seen.

5.1.3 Preferential Attachment of –OH onto Network Modifiers

The number of $^{-}$OH species present around each network modifying cation, yttrium, calcium and sodium, in hydrated yttrium bioglasses are shown in Table 5.8a and 5.8b. Table 5.8a shows the actual number of $^{-}$OH species that surround yttrium, calcium and sodium. Normalisation of numbers in Table 5.8a give rise to Table 5.8b to remove unnecessary biasing due to the number of cations used in the simulation. The normalisation method employed is:

Table 5.8a: Number of Hydroxyls attached to Y, Ca and Na

YBG	Y		Na		Ca	
	No. OH-	St. Dev	No. OH-	St. Dev	No. OH-	St. Dev
0.1	46.265	1.414	111.874	2.828	89.954	1.414
0.2	94.613	4.243	223.053	9.192	163.758	7.778
0.3	137.702	9.192	336.067	9.192	228.763	11.314

NORMALISATION: No. of OH- species attached to a cation/ Total no. of cations to which those hydroxyl groups are attached in simulation

e.g. for YTTRIUM

(YBG y=0.1) OH on Y = 46.265/64 = 0.723

(YBG y=0.2) OH on Y = 94.613/64 = 1.478

(YBG y=0.3) OH on Y = 137.702/64 = 2.152

Table 5.8b: Number of Hydroxyls attached to Y, Ca and Na (normalized)

YBG	Y		Na		Ca	
	No. OH-	St. Dev	No. OH-	St. Dev	No. OH-	St. Dev
0.1	0.723	0.022	0.523	0.013	0.833	0.013
0.2	1.478	0.066	1.042	0.043	1.516	0.072
0.3	2.152	0.144	1.570	0.043	2.118	0.105

Hydroxyl groups prefer to coordinate more to calcium, then to yttrium and then sodium in this order. Table 5.8a and 5.8b show the number of hydroxyls to Y, Ca and Na respectively. Figure 5.9 shows the order by which hydroxyl groups prefer to attach to yttrium, calcium and sodium.

Fig 5.9: (Ca – OH) > (Y – OH) > (Na – OH)

5.1.4 Medium-range structure

1) Silicon Q^n

Table 5.9a. Silicon Q^n Distribution and Network Connectivity in YBG Glasses

TOTAL Si								
n	Dry YBG		YBG y=0.1		YBG y=0.2		YBG y=0.3	
	Distribuion(%)	St. Dev	Distribuion(%)	St. Dev	Distribuion(%)	St. Dev	Distribuion(%)	St. Dev
0	0.120	0.167	3.580	0.154	3.687	0.326	3.571	0.163
1	5.357	0.503	4.727	0.791	5.595	1.070	5.385	0.530
2	38.106	0.631	24.384	0.569	25.717	2.171	24.147	2.220
3	47.235	0.501	45.157	2.186	43.964	3.191	42.827	0.788
4	9.018	0.406	21.184	3.463	20.717	0.012	23.931	1.848
5	0.165	0.200	0.967	0.072	0.319	0.365	0.139	0.049
6	0.000	0.000	0.000	0.000	0.000	0.000	0.000	0.000
7	0.000	0.000	0.000	0.000	0.000	0.000	0.000	0.000
8	0.000	0.000	0.000	0.000	0.000	0.000	0.000	0.000
9	0.000	0.000	0.000	0.000	0.000	0.000	0.000	0.000
10	0.000	0.000	0.000	0.000	0.000	0.000	0.000	0.000
Average	**2.602**	0.001	**2.785**	0.050	**2.734**	0.060	**2.786**	0.045

Table 5.9a shows that for yttrium bioglass (YBG) as we progressively hydrate from 0.1 – 0.3 the silicon network connectivity increases remains more or less constant. A rise in silicon connectivities are seen from dry YBG to hydrated YBG (y=0.1). The silicon network connectivity of the unhydrated form is 2.60. The silicon connectivity comprises both Si – O – Si and Si – O – P connections, where oxygen atoms in this situation are bridging between two like pair atoms of silicon and between two unlike pair of atoms silicon and phosphorus respectively. Yttrium, calcium and sodium are network modifiers in yttrium bioglass and therefore disturb such connections [115, 137]. As soon as the yttrium bioglass is hydrated, hydroxyl groups promote the increase in silicon network connectivities. The silicon network strengthens itself as a reaction towards the hydroxyl groups intergrating themselves into the yttrium bioglass structure. This may be due to the hydroxyl groups substituting, Y --- O-Si-O_3, Ca --- O-Si-O_3 and/or Na --- O-Si-O_3 for Y --- OH, Ca --- OH and/or Na --- OH which causes the movement of -[O-SiO_3] species back into the network causing this strengthening.

The Q^n speciation of the silicon atoms are given in the table above. By observing dry YBG, we see that the majority of silicon atoms in the glass network have a Q^n speciation of Q^2 and Q^3 speciation thus giving rise to a network connectivity of 2.602. As soon as we hydrate YBG with a hydration fraction of 0.1 (100 hydroxyl units), we see that the number of Q^2 species decreases and causes an increase in the number of Q^3 and Q^4 species which were not seen for dry YBG (Figure 5.10a).

Figure 5.10a

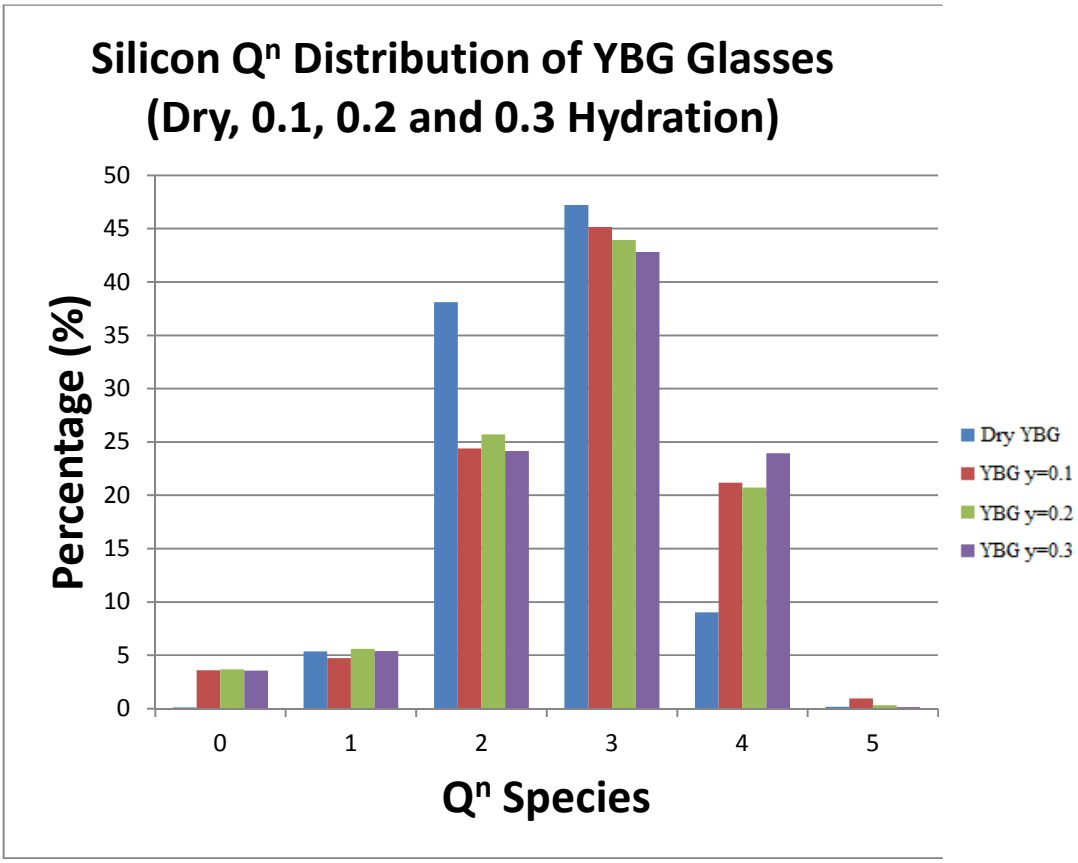
Silicon Qⁿ Distribution of YBG Glasses
(Dry, 0.1, 0.2 and 0.3 Hydration)
Percentage (%)
50
45
40
35
30
25
20
15
10
5
0
0
1
2
3
4
5
Qⁿ Species
Dry YBG
YBG y=0.1
YBG y=0.2
YBG y=0.3

2) Phosphorus Q^n

Table 5.9b. Phosphorus Q^n distribution and network connectivity in YBG glasses

	TOTAL P							
n	Dry YBG		YBG y=0.1		YBG y=0.2		YBG y=0.3	
	Distribution(%)	St. Dev	Distribution(%)	St. Dev	Distribution(%)	St. Dev	Distribution(%)	St. Dev
0	39.286	5.051	0.000	0.000	0.000	0.000	0.000	0.000
1	57.143	0.000	25.169	4.812	14.329	10.108	39.486	5.327
2	3.571	5.051	53.402	15.391	70.300	0.404	31.426	6.058
3	0.000	0.000	17.629	14.829	15.369	9.708	29.088	0.731
4	0.000	0.000	1.948	2.754	0.002	0.003	0.000	0.000
5	0.000	0.000	1.852	2.620	0.000	0.000	0.000	0.000
6	0.000	0.000	0.000	0.000	0.000	0.000	0.000	0.000
7	0.000	0.000	0.000	0.000	0.000	0.000	0.000	0.000
8	0.000	0.000	0.000	0.000	0.000	0.000	0.000	0.000
9	0.000	0.000	0.000	0.000	0.000	0.000	0.000	0.000
10	0.000	0.000	0.000	0.000	0.000	0.000	0.000	0.000
Average	**0.643**	0.101	**2.019**	0.330	**2.010**	0.198	**1.896**	0.046

Table 5.9b shows that for yttrium bioglass (YBG) as we progressively hydrate from 0.1 – 0.3 the phosphorus network connectivity remains more or less constant similarly to silicon in Table 5.9a. A substantial rise in phosphorus connectivities are seen from DRY_YBG to hydrated YBG at concentrations of 0.1 to 0.3. The network connectivity of phosphorus in DRY_YBG is 0.643. The phosphorus connectivity comprises of P – O – P and Si – O – P connections, where oxygen atoms in this situation are bridging between two like atoms of phosphorus and between two unlike atoms silicon and phosphorus respectively. Phosphorus plays the same role as the other network former silicon but since there are few phosphorus atoms in these models i.e. 14, there isn't much of a network to begin with. Yttrium, calcium and sodium are network modifiers in yttrium bioglass and therefore disturb such connections [115, 137]. As soon as the yttrium bioglass is hydrated, hydroxyl groups promote the increase in phosphorus network connectivities. According to the results it is seen that the phosphorus network strengthens itself as a reaction towards the hydroxyl groups integrating themselves into the yttrium bioglass structure thus increasing the number of Si – O – P connections. But it is worth mentioning that since such low amounts of phosphorus is present in these glasses, the network of phosphorus is very much nonexistent and so cannot really be called a phosphorus network.

Looking at dry YBG, we see the overall network connectivity is 0.64 and this is due to phosphorus having mainly Q^0 and Q^1 speciation. If we then hydrated YBG with a hydration fraction of 0.1 (100 hydroxyl units) then we see a shift in distribution of the

Q^n speciation. Here for y=0.1 a large number of Q^2 and Q^3 species predominate and therefore give rise to the large number of network connectivity of 2.02 (Figure 5.10b). The reason why phosphorus is so very well interconnected into the glass network remains open to debate.

Figure 5.10b

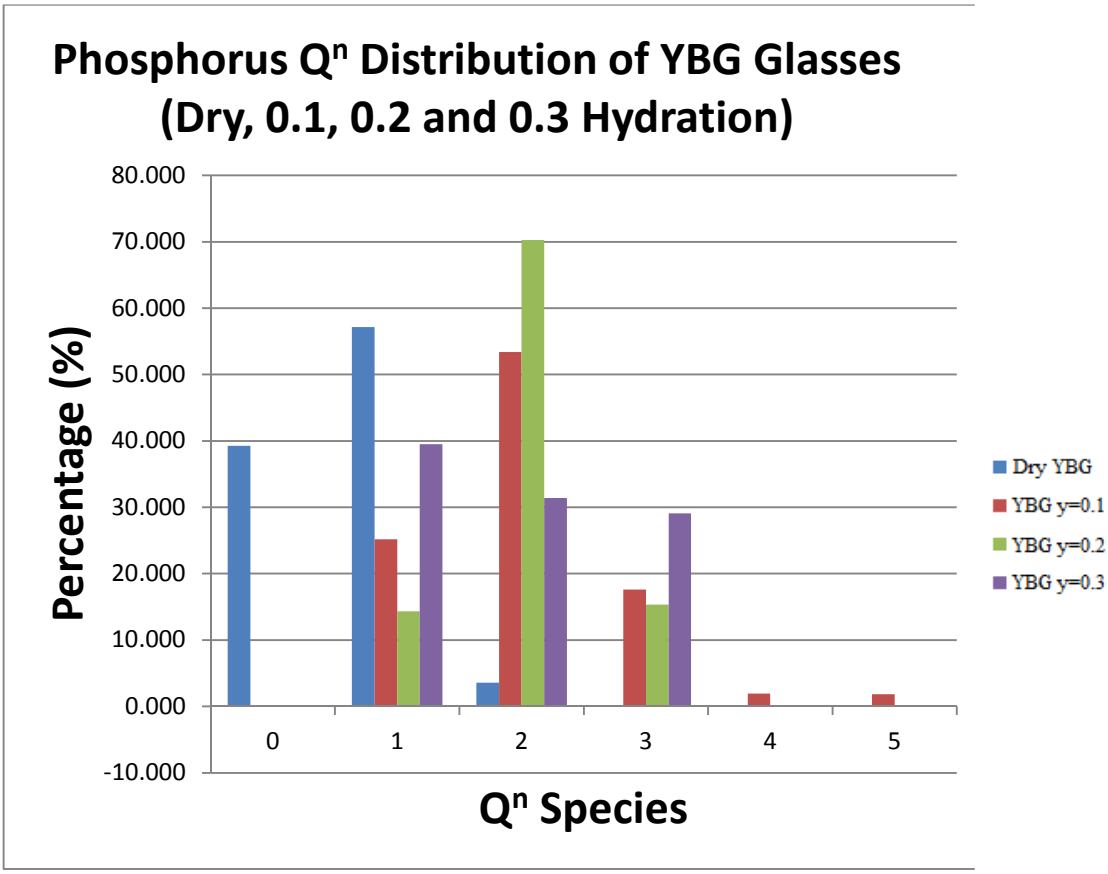

5.1.5 Clustering

Figure 5.11: Clustering ratios of hydroxyl groups surrounding cations Si, P, Na, Ca and Y

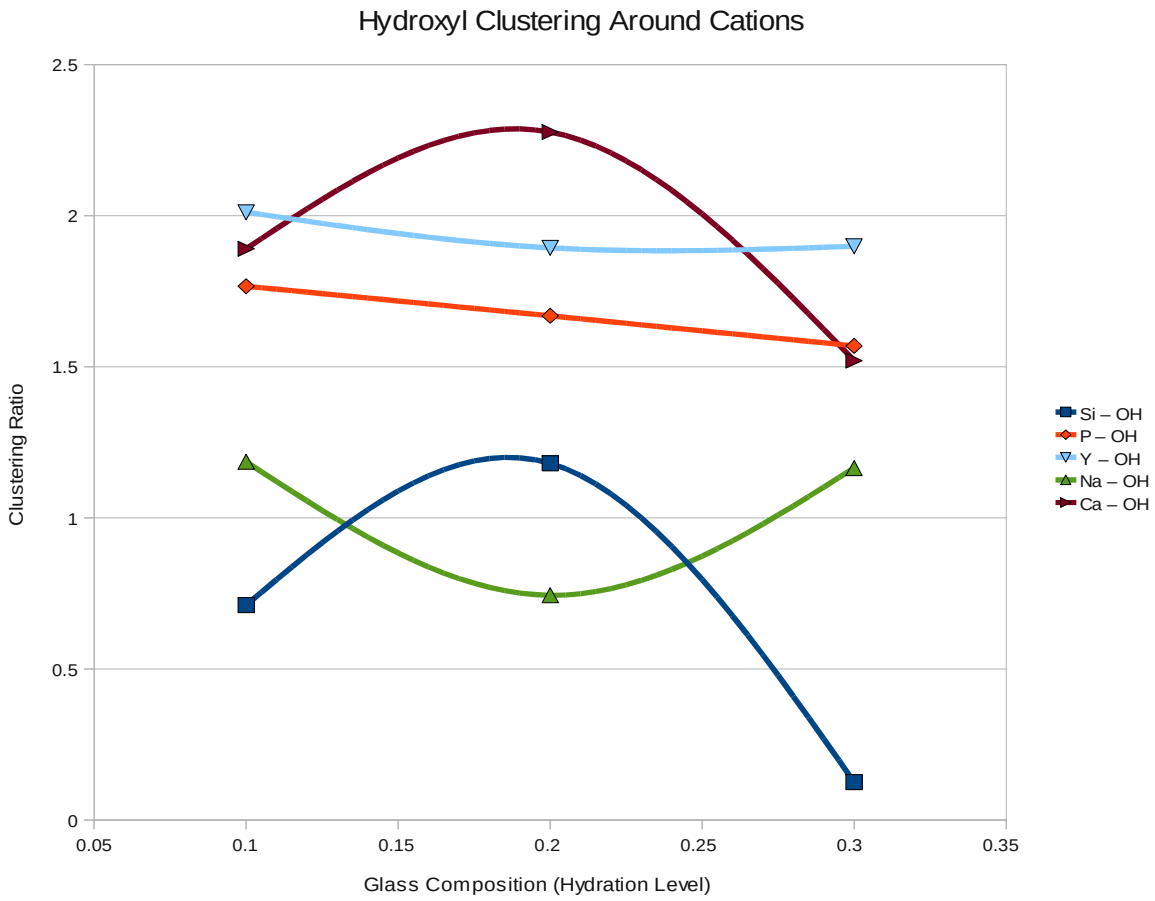

From Figure 5.11, the hydroxyl groups cluster around silicon, phosphorus, yttrium, calcium and sodium in the following order:

$$Ca - OH > Y - OH > P - OH > Na - OH > Si - OH$$

1) Si – OH

It is clear from Figure 5.11 that hydroxyl groups do not cluster around silicon atoms. We showed that very few hydroxyl groups coordinate to silicon. From the above Figure, hydroxyl groups seem to be evenly dispersed throughout the glass structure with respect to silicon in a homogenous fashion thus not favouring clustering around silicon even with increasing hydration. The clustering ratios are below the value of one.

2) Na – OH

From the above figure hydroxyl groups usually aggregate around sodium atoms more than silicon. It is known that hydroxyl groups do coordinate to sodium, more than to silicon and phosphorus, but these hydroxyl groups also seem to be evenly dispersed throughout the glass structure being attached to sodium in a homogenous fashion thus not favouring clustering around sodium even with respect to increasing hydration concentration. The clustering ratios are just above the value of one along the y-axis of the plot for hydration concentrations 0.1 and 0.3. This relates to the hydroxyls being almost homogeneously spread out through the glass structure with respect to sodium and/or hydration concentration. Clustering of hydroxyl groups around sodium ions is more marked than compared to hydroxyl groups aggregating around silicon ions.

3) P – OH

Clustering is taking place of hydroxyl groups around phosphorus ions. It is seen that hydroxyl groups do coordinate to phosphorus, which is less marked as silicon and sodium, but these hydroxyl groups seem to be less dispersed throughout the glass structure than for silicon or sodium. The ratios seen from the above graph are above the value of one and in being so they show that hydroxyl groups are surrounding phosphorus ions selectively more than silicon and sodium in this order.

4) Y – OH

It is evident from the above graph that clustering is taking place, where hydroxyl groups cluster around yttrium ions. It is seen that hydroxyl groups do coordinate to yttrium, which is more marked than silicon, phosphorus and sodium, but these hydroxyl groups seem to be less homogeneously dispersed throughout the glass structure as found for silicon, phosphorus or sodium. The ratios seen from the above graph are above the value of one and in being so they show that hydroxyl groups are surrounding yttrium ions selectively more than silicon, sodium and phosphorus in this order.

5) Ca – OH

Observing the above graph with respect to Ca – OH, clustering is clearly taking place, where hydroxyl groups cluster around calcium ions. It is seen that hydroxyl groups do coordinate to calcium, which is more marked than silicon, phosphorus, sodium and yttrium, but these hydroxyl groups seem to be less homogenously dispersed throughout the glass structure than silicon, phosphorus, sodium and yttrium. The ratios

seen from the above graph are above the value of one and in being so they show that hydroxyl groups are surrounding calcium ions selectively more than silicon, sodium, phosphorus and yttrium in this order.

The clustering ratios follow the same order by which hydroxyl groups coordinate to network-forming and modifying ions:

$$Ca - OH > Y - OH > P - OH > Na - OH > Si - OH$$

6) Cation – Cation Clustering

Table 5.10 shows cation – cation clustering with respect to increasing hydration concentration for YBG glass composition.

Table 5.10: Cation – cation clustering for YBG hydrated at fractions y=0.1, 0.2 and 0.3

Species	Dry YBG		YBG y=0.1		YBG y=0.2		YBG y=0.3	
Y – Y	**1.653**	0.098	**2.016**	0.092	**2.030**	0.007	**2.308**	0.032
Y – Na	**1.053**	0.038	**1.224**	0.014	**1.052**	0.002	**0.652**	0.620
Y – Ca	**0.776**	0.033	**1.177**	0.010	**1.290**	0.030	**0.701**	0.695
Na – Na	**1.244**	0.042	**1.729**	0.025	**1.798**	0.002	**1.595**	0.157
Na – Ca	**0.914**	0.028	**0.985**	0.012	**0.959**	0.000	**0.644**	0.516
Ca – Ca	**1.267**	0.065	**1.128**	0.023	**1.032**	0.011	**1.310**	0.199

The clustering ratios seen above for dry YBG compare well enough to simulation studies of yttrium bioglass YBG carried out by the work of Tilocca and Christie [115, 137]. From Table 5.10, hydration generally causes an increase in clustering for like pairs of cations and a decrease for unlike cation pairs. It seem as though the network-modifying species attract hydroxyl groups. Calcium is seen to do this the most, then yttrium and then sodium. By these modifying ions attracting the hydroxyls would cause them to be less available to silicon and phosphorus and do not allow for the breakage of T - O - T bridges.

5.1.6 Bridging oxygens vs. Non-bridging oxygens

Table 5.11a: Percentage of bridging oxygens around network modifier ions sodium, yttrium and calcium

BO	Y		Ca		Na	
	%	St. Dev	%	St. Dev	%	St. Dev
YBG_DRY	2.369	0.623	17.733	1.217	39.570	1.588
0.1	6.402	2.388	23.306	1.533	41.825	0.918
0.2	8.294	0.317	26.174	0.697	41.593	2.253
0.3	7.711	0.385	29.357	3.094	46.431	3.940

Table 5.11b: Percentage of non-bridging oxygens around network modifier ions sodium, yttrium and calcium

NBO	Y		Ca		Na	
	%	St. Dev	%	St. Dev	%	St. Dev
YBG_DRY	97.631	0.623	82.267	1.217	60.430	1.588
0.1	78.034	1.315	65.317	0.719	53.342	1.374
0.2	81.959	1.199	67.641	2.290	56.838	2.704
0.3	83.735	2.549	64.166	0.308	50.916	4.301

Table 5.11c: Percentage of non-bridging & bridging oxygens and free oxygens ($^{-}$OH) around network modifier ions sodium, yttrium and calcium

YBG	**Y**		**Ca**		**Na**	
	NBO+BO Total %	($^{-}$OH) %	NBO+BO Total %	($^{-}$OH) %	NBO+BO Total %	($^{-}$OH) %
DRY	100.000	n/a	100.000	n/a	100.000	n/a
0.1	84.437	15.563	88.623	11.377	95.168	4.832
0.2	90.253	9.747	93.815	6.185	98.432	1.568
0.3	91.446	8.554	93.523	6.477	97.347	2.653

1) Yttrium

From Table 5.11b it is seen that yttrium prefers to locate a large number of non-bridging oxygen species around itself for both hydrated and unhydrated forms of yttrium bioglass. Yttrium's coordination shell environment is dominated (97.6 %) by NBO's. Yttrium has an average coordination of 5.5 (unhydrated) to 5.9 (hydrated), the majority of these coordinated oxygen atoms are non-bridging oxygens. Yttrium cations have a +3 charge and the highest field strength of 0.6 compared to Ca and Na cations, which causes the preference for yttrium ions to be surrounded by non-bridging oxygen species in its coordination shell, as found in simulation studies of yttrium bioglass carried out by the work of Tilocca and Christie [115, 137]

After hydrating the yttrium bioglass, the percentage of non-bridging oxygens which surround yttrium decreases to ~80% when the yttrium bioglass is hydrated at 0.1. This shows yttrium, which still holds a total coordination of ~5.5 – 5.9, that non-bridging oxygen atoms are replaced by hydroxyl groups. The unhydrated form of YBG glass allowed 97% of NBO's to surround yttrium. The percentage of NBO's decreases and this is due to hydroxyl groups substituting ~20% of the NBO's in unhydrated YBG with hydroxyl groups where yttrium is still able to maintain, if not increase, its coordination as the bioglass is progressively hydrated (Table 5.4a, 5.4b and 5.4c).

2) Calcium

Calcium prefers to locate a large number of non-bridging oxygen species around itself for both hydrated and unhydrated forms of yttrium bioglass. Calcium has the second most dominant amount of NBO's in its coordination shell environment i.e. 82.30%. Calcium has an average coordination of 5.98 for unhydrated yttrium bioglass, to 6.30 (Table 5.5a, 5.5b and 5.5c), for the hydrated form of the same glass, and the majority of these coordinated atoms are of non-bridging oxygens which surround calcium ions. Calcium cations have a +2 charge and the second highest field strength of 0.33, higher than sodium cations. Calcium is less attractive to NBO's than yttrium is as yttrium has higher field strength causing more NBO's to locate themselves around yttrium ions.

After hydrating the yttrium bioglass, the percentage of non-bridging oxygen atoms which surround calcium decreases to ~65% when the yttrium bioglass is hydrated at 0.1. This shows calcium, which still holds a coordination of ~6, that non-bridging oxygen atoms are replaced by hydroxyl groups. The unhydrated form of YBG glass allowed 82% of NBO's to surround calcium. As soon as the same glass is hydrated at a concentration of 0.1, a drop in the percentage of NBO's surrounding calcium is seen. The percentage of NBO's decreases and this is due to hydroxyl groups substituting ~18% of the NBOs in unhydrated YBG with hydroxyl groups where calcium is still able to maintain, if not increase, its coordination as the bioglass is progressively hydrated (Table 5.5a, 5.5b and 5.5c).

3) Sodium

Sodium has the smallest preference to locate non bridging oxygen species around itself for both hydrated and unhydrated forms of yttrium bioglass YBG. Sodium is least dominant compared to calcium and yttrium with respect to the percentage of

NBO's in each of their coordination shells i.e. 60.43%. Sodium has an average coordination of 6.03 for unhydrated yttrium bioglass, to 6.30 (Table. 5.6a, 5.6b and 5.6c), for the hydrated form of the same glass, where 60.43% NBO's surround calcium ions. Sodium cations have a +1 charge and the lowest field strength of 0.19. It is for this reason of having the lowest field strength that causes sodium ions to be surrounded by the smallest number of non-bridging oxygen species which are found within the coordination shell environment of sodium. Sodium is less attractive to NBO's than calcium or yttrium as yttrium and calcium have higher field strength to cause more NBO's to locate themselves within their coordination shells.

After hydrating the yttrium bioglass, the percentage of non-bridging oxygens which surround sodium decreases to ~53% when the yttrium bioglass is hydrated at 0.1. This shows sodium, which still holds a coordination of ~6, that non-bridging oxygens are replaced by hydroxyl groups. The unhydrated form of YBG glass allowed 60% of NBO's to surround sodium. As soon as the same glass is hydrated at a concentration of 0.1, a drop in the percentage of NBO's surrounding sodium is seen. The percentage of NBO's decreases and this is due to hydroxyl groups substituting ~10% of the NBOs in unhydrated YBG with hydroxyl groups where sodium is still able to maintain, if not increase, its coordination as the bioglass is progressively hydrated. Although all three network modifying cations (Y, Ca and Na) drop in their percentage of BO or NBO's from dry YBG, the order (Y > Ca > Na) is preserved.

5.1.7 Main Findings

Coordination is seen to increase for silicon, phosphorus, yttrium, calcium and sodium as yttrium bioglass is progressively hydrated from 0.1 – 0.3 (Tables 5.2a, 5.3a, 5.4a, 5.5a and 5.6a). The preference by which hydroxyl-oxygens coordinate to network forming and modifying cations is shown below:

$$Ca > Y > Na > P \sim Si$$

Calcium has the greatest ability in allowing hydroxyl-oxygen to coordinate with itself, then yttrium, sodium, phosphorus and silicon having lower coordination to hydroxyl-oxygen. The increase in coordination is due to hydration effects where hydroxyl groups squeeze themselves into the coordination spheres, most easily with calcium, yttrium, sodium and then silicon and phosphorus. The more a YBG glass is hydrated the more hydroxyl groups will fit themselves into the coordination spheres of Ca, Y, Na, P and Si (Tables 5.2c, 5.3c, 5.4c, 5.5c and 5.6c).

The same order is observed as coordination of cations to non hydroxyl-oxygen decreases. Calcium shows this effect the most and silicon the least, where coordination to non hydroxyl-oxygen decreases (Tables 5.2b, 5.3b, 5.4b, 5.5b and 5.6b).

As coordination of, for example, calcium decreases with non hydroxyl-oxygen, the coordination of calcium to hydroxyl-oxygen increases. Hydroxyl groups coordinate as a displacement to non hydroxyl-oxygens. Furthermore, the hydroxyl-oxygens not only displace non hydroxyl-oxygens but cause an overall increase in coordination. The same is seen for Si, P, Na and Y (Tables 5.2a, 5.3a, 5.4a, 5.5a and 5.6a).

The overall silicon network connectivities are generally increasing as seen in Table 5.9a which shows that the silicate network is strengthening itself as yttrium bioglass is hydrated. By viewing Figure 5.10a we realise that this effect is due to a shift in Q^n species from Q^0, Q^1 and Q^2 to Q^1, Q^2 and Q^3 as hydration increases which causes this strengthening in silicon network.

The overall phosphorus network connectivities are generally increasing as seen in Table 5.9b which shows that the phosphate network is strengthening itself as yttrium bioglass is hydrated. By viewing figure 5.10b we realise that this effect seen in Table 5.9b is due to shift in Q^n species from Q^0, Q^1 to Q^1, Q^2 and Q^3 as hydration increases which causes this strengthening in phosphorus network.

The network connectivity of a glass has a central role in determining the glass

dissolution rate: a fragmented network with a low connectivity will dissolve faster in an aqueous environment [42]. For example, low-silica bioactive glasses have NC of approximately 2, whereas loss of bioactivity has been associated to NC approaching 3 in higher silica compositions. The central importance of the network connectivity in this context makes it a key structural factor for the possible use of a silica-based glass composition to store radionuclides, either in nuclear waste disposal or for in situ cancer radiotherapy. The incorporation of water in the form of hydroxyl groups in a glass structure is in principle expected to disrupt the glass network: this is based on the assumption that protons act as additional network modifiers [154] and therefore the O_2^- → 2 OH^- substitution would break T – O − T bridges either directly (e.g., T – O − T + OH^- → T − O^- + T − OH) or indirectly (e.g., T – O ⋯ M + OH^- → T − OH + M^+, where M^+ is a free modifier cation which is able to break another T – O − T bridge). For example, the breakdown of the silica network (compared to melt-derived glasses) caused by the hydration process is often reported as one of the possible effects contributing to the extended range of bioactivity of sol−gel glasses [154].

A more disrupted YBG network would be less stable in a physiological environment, affecting its performance for radiotherapy. In the short term, a faster yttrium release in the bloodstream from a rapidly dissolving glass would be a negative factor for their medical applications, which requires the highest short-term durability to avoid releasing yttrium isotopes while they are radioactive. On the other hand, if short-term Y^{3+} release is not significantly affected, the possibility to enhance the long-term (post-radioactive decay of Y) biodegradation of YBG glasses into harmless products represents a very attractive option at present. It is therefore important to investigate the effects of different hydration levels on the glass structure. The earlier simulations show that the disruptive effect of OH^- on the glass network acts differently on the silicate and phosphate connectivity. Overall, the silicate and phosphate NC generally increases with respect to hydration where the phosphate NC is heavily affected. The reason why phosphorus is so very well interconnected into the glass network remains open to debate.

5.2 *Yttrium-Bioglass (YBG-P) without Phosphorus*

We have already carried out hydration of YAS17, 24 and 30 earlier (section 3.4) . This section will now thoroughly examine the effects of hydration on the bulk structure of YBG without phosphorus. The same procedures that were employed upon YAS glasses 17, 24 and 30 and YBG earlier are followed through here. The results will instead reflect that of YBG but without phosphorus. Initially (section 5.1.4) the overall phosphorus network connectivities were seen to increase as seen in Table 5.9b, which showed that the phosphate network was strengthening itself as YBG was hydrated. By viewing Figure 5.10b we realise that this effect seen in Table 5.9b was due to shift in Q^n species from Q^0, Q^1 to Q^1, Q^2 and Q^3 with respect to hydration which caused this strengthening in phosphorus network. The reason why phosphorus was so very well interconnected into the glass network remains open to debate. For this reason phosphorus was removed to see whether or not YBG glass without phosphorus had any impact on the glass structure i.e. whether silicon network connectivity, network-former or modifier coordination, cation-oxygen bond distances etc. are affected.

Firstly, simulations of unhydrated YBG-P were carried out. The unhydrated YBG-P glass was then hydrated at three increasing levels of hydration by adding hydroxyl groups into the bulk structure. The purpose of this was to investigate further the effects of hydration on the structure of the glasses e.g. silicon network connectivity, coordination numbers of network former and modifiers etc, without the presence of the highly interconnected phosphorus species.

Molecular dynamics simulations were carried out upon hydrated YBG-P with simulation sizes of approx 2000 atoms using DL_POLY. The data necessary for successfully simulating hydrated YBG-P glasses have been given in the methodology, in section 2.5.2 (Tables 2.8 – 2.13). Other data in section 3.2 (Table 3.11) were used also.

Using the technique mentioned earlier YBG-P was hydrated at three different levels where variable y, the level of hydration, was 0.1, 0.2 or 0.3. Here y=0.1 refers to a low level hydration and y=0.3 is a high level of hydration. The stoichiometries for each of the glasses are listed in Table 5.12. A range such as that chosen for this work would thoroughly examine the effects and role of hydration in YBG-P glasses.

The general rule: $SiO_2 : CaO : Na_2O : Y_2O\text{-}y.\ (OH)2y$

Table. 5.12

Glass Type	% Y_2O_3	% Na_2O	% CaO	% SiO_2	Density (g/cm^3)
YBG-P	4.68	15.85	16.12	62.35	2.730

Scaling for Hydration: y = OH fraction required to hydrate YBG-P

UNHYDRATED YBG-P: 4.68 mol % Y_2O_3, 62.35 mol % SiO_2, 16.12 mol % CaO and 15.85 mol % Na_2O

Scaled: 32 Y_2O_3, 420 SiO_2, 108 CaO and 107 Na_2O

YBG-P (y=0.1) [32 Y_2O_3, 420 SiO_2, 108 CaO and 107 Na_2O] – 50 O, + 100 OH

YBG-P (y=0.2) [32 Y_2O_3, 420 SiO_2, 108 CaO and 107 Na_2O] – 100 O, + 200 OH

YBG-P (y=0.3) [32 Y_2O_3, 420 SiO_2, 108 CaO and 107 Na_2O] – 150 O, + 300 OH

5.2.1 Short-range structure:

A) Bond Angles

Figure 5.12 shows the bond angles of O - X - O species for dry YBG-P glass, where X=Si, Y, Ca, and Na.

Figure 5.12: Unhydrated yttrium bioglass (YBG-P) bond angle distributions for O – X – O, where X = Si, Y, Ca and Na

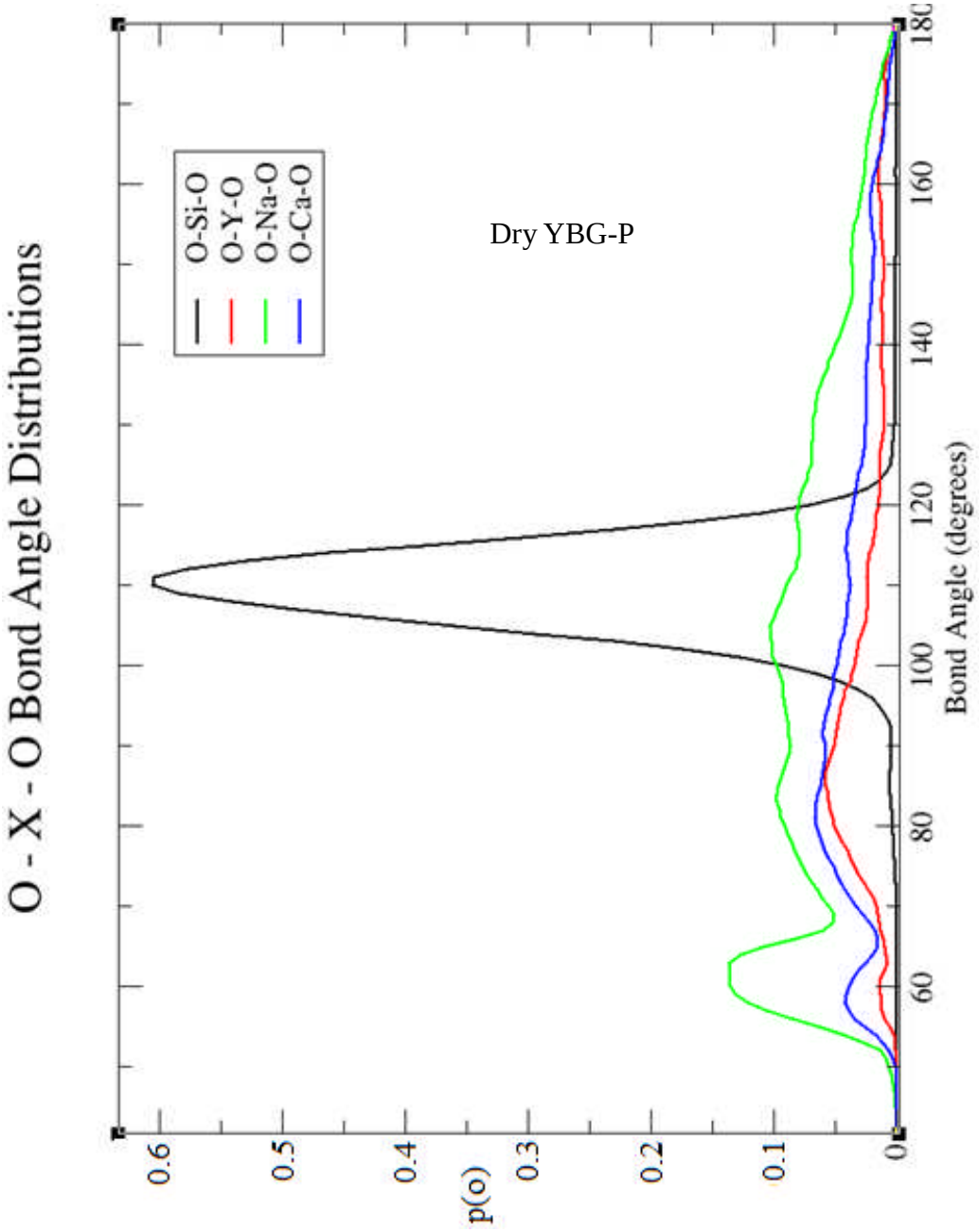

Figure 5.13: Hydrated Yttrium Bioglass (YBG-P) Bond Angle Distributions for O – X – O, where X = Si, Y, Ca and Na

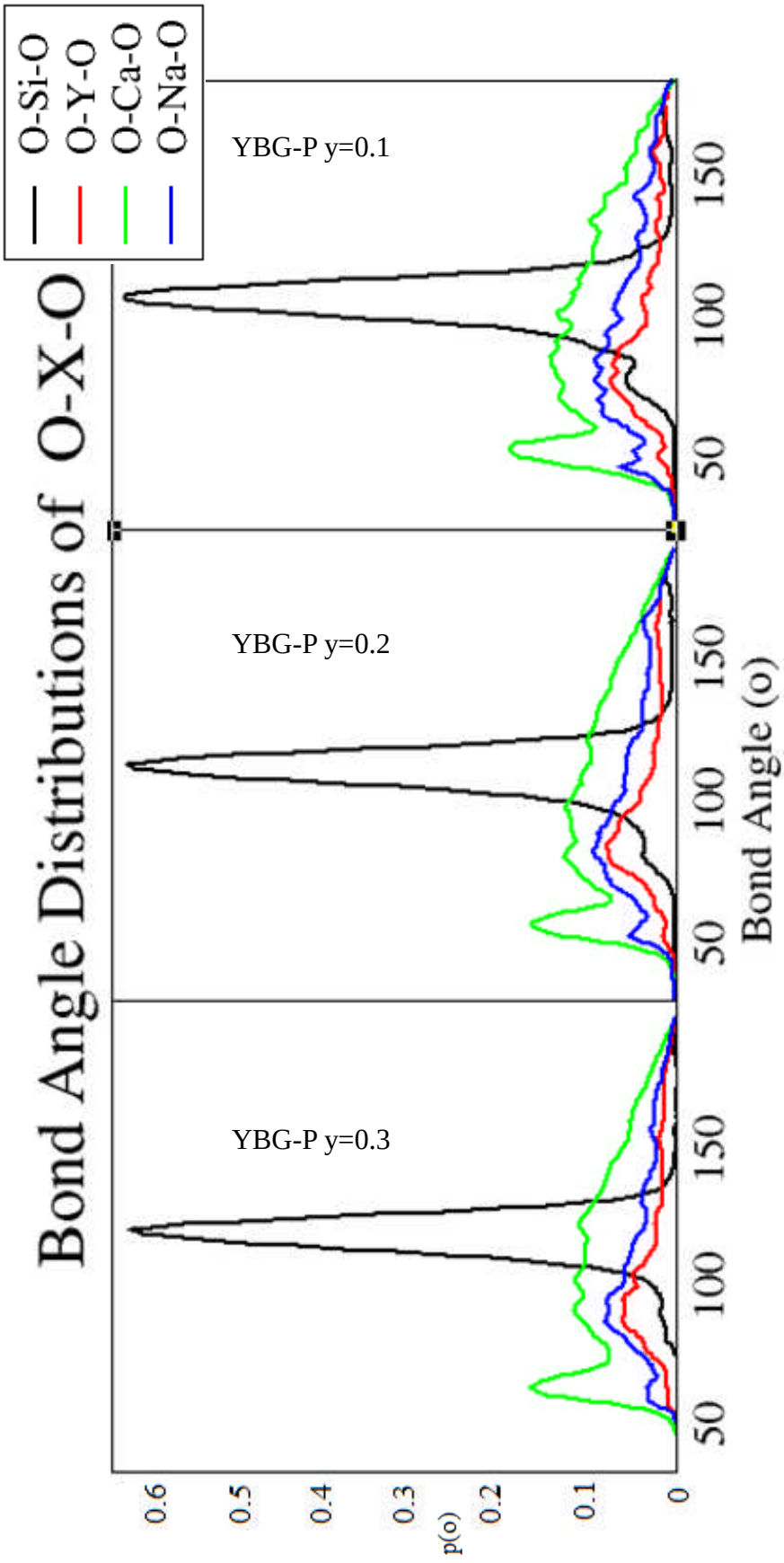

Figure 5.14: Hydrated Yttrium Bioglass (YBG-P) Bond Angle Distributions for X – O – H, where X = Si, Y, Ca and Na

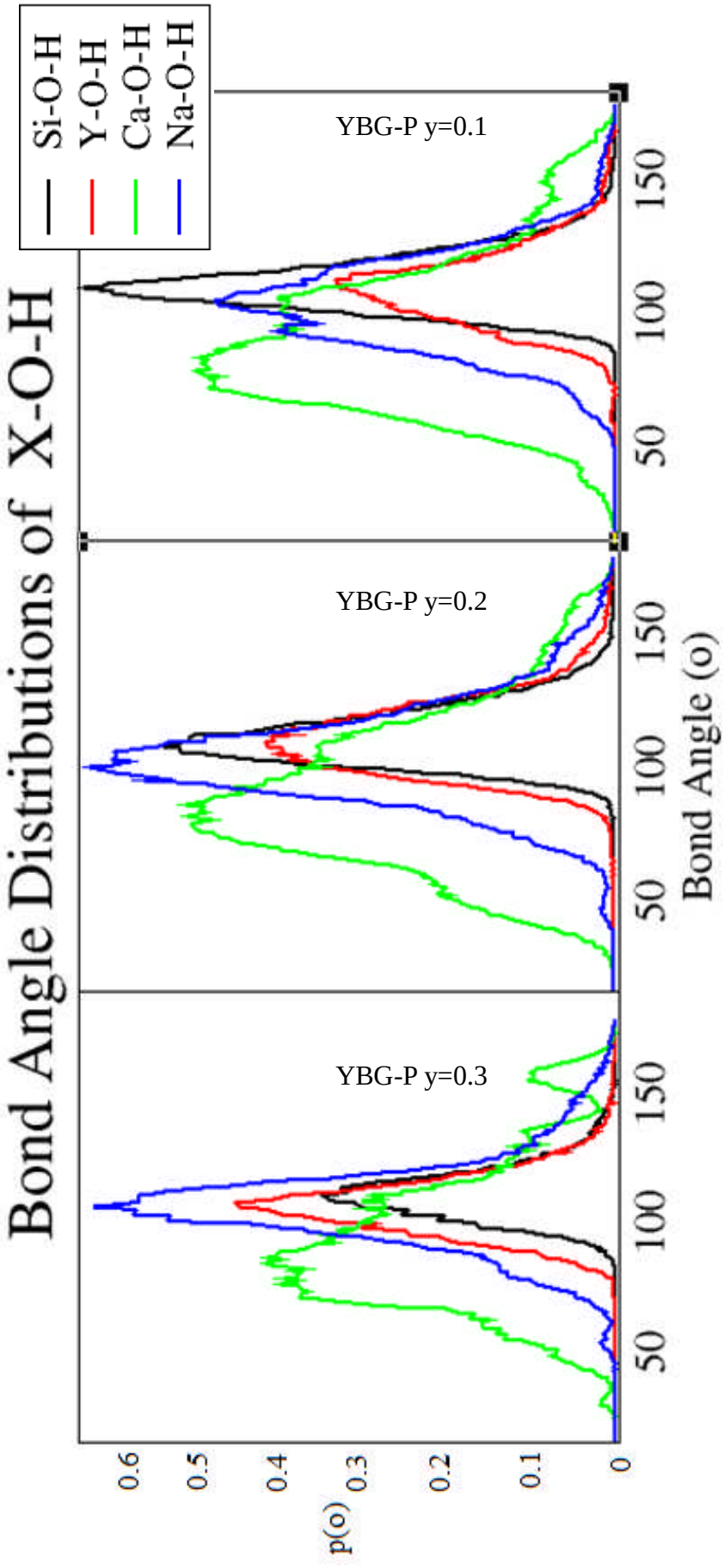

B) Coordination

1) Silicon

Table 5.13a: Total coordination for silicon (Oc + OHc) in dry and hydrated YBG-P glass

Si Coordination								
n	Dry YBG		YBG y=0.1		YBG y=0.2		YBG y=0.3	
	Distribution (%)	St. Dev	Distribution (%)	St. Dev	Distribution (%)	St. Dev	Distribution (%)	St. Dev
1	0.0000	0.0000	0.0000	0.0000	0.0000	0.0000	0.0000	0.0000
2	0.0000	0.0000	0.0000	0.0000	0.0000	0.0000	0.0000	0.0000
3	0.0015	0.0012	0.0165	0.0216	0.0000	0.0000	0.0006	0.0004
4	99.0142	0.0194	95.7266	0.9700	90.5892	1.7178	85.5399	0.3548
5	0.9843	0.0182	4.2100	0.9254	9.1913	1.7364	14.1182	0.1243
6	0.0000	0.0000	0.0468	0.0662	0.2195	0.0185	0.3413	0.4796
7	0.0000	0.0000	0.0000	0.0000	0.0000	0.0000	0.0000	0.0000
8	0.0000	0.0000	0.0000	0.0000	0.0000	0.0000	0.0000	0.0000
9	0.0000	0.0000	0.0000	0.0000	0.0000	0.0000	0.0000	0.0000
10	0.0000	0.0000	0.0000	0.0000	0.0000	0.0000	0.0000	0.0000
Average	**4.010**	0.0002	**4.0429**	0.0108	**4.0963**	0.0170	**4.1480**	0.0084

There are virtually no silicon atoms with a coordination of five or higher, again which agrees with previous experimental and modelling data [115, 137] which showed coordination numbers of 3.9 – 4.0. Silicon has a well-defined overall coordination of four and has the capacity to take up a maximum of four bonds to that of oxygen found from within the glass network. The table above shows the total Si coordination for hydrated YBG-P for hydration levels of 0.1 to 0.3 and for non-hydrated YBG-P glass. The general trend found is that progressively hydrating YBG-P causes the overall silicon coordination to increase. The more a YBG-P glass is hydrated, the more the overall coordination will increase due to the presence of an increasing percentage of five-coordinated silicon species seen in Table 5.13a.

To further analyse the Si coordination to oxygen, the coordination contributions were split. The coordination of oxygen, whether from the network modifier/former species ($Na_2O/CaO/Y_2O_3/SiO_2$) or from those attached to hydrogen (hydroxyl groups), were combined to form the overall silicon coordination seen in Table 5.13a. If these contributions were separated i.e. silicon oxygen coordination relating solely to the network modifier/former species i.e. ($Na_2O/CaO/Y_2O_3/SiO_2$) from those attached to hydrogen i.e. hydroxyl groups, then this will give an insight as to why a slight increase in overall silicon coordination is seen for all YBG-P glasses observed in Table 5.13a.

The partial silicon coordination numbers are given for yttrium bioglass without including hydroxyl groups in the silicon coordination sphere in Table 5.13b.

Table 5.13b: Partial coordination for silicon (Oc) in hydrated YBG-P glass

Si Coordination						
n	YBG-P y=0.1		YBG-P y=0.2		YBG-P y=0.3	
	Distribution (%)	St. Dev	Distribution (%)	St. Dev	Distribution (%)	St. Dev
1	0.000	0.000	0.000	0.000	0.000	0.000
2	0.000	0.001	0.117	0.166	0.000	0.001
3	6.741	1.773	13.476	3.158	22.671	2.747
4	91.916	1.507	86.100	2.934	76.972	2.899
5	1.343	0.266	0.307	0.390	0.356	0.151
6	0.000	0.000	0.000	0.000	0.000	0.000
7	0.000	0.000	0.000	0.000	0.000	0.000
8	0.000	0.000	0.000	0.000	0.000	0.000
9	0.000	0.000	0.000	0.000	0.000	0.000
10	0.000	0.000	0.000	0.000	0.000	0.000
Average	**3.946**	0.020	**3.866**	0.039	**3.777**	0.026

Silicon has a well defined overall coordination of four and has the capacity to take up a maximum of 4 covalent bonds from oxygen found from within the glass system. The table above shows the partial Si – O coordination (exclusive of any hydroxyls that may be attached) for YBG-P hydrated from concentrations of 0.1 to 0.3. The general trend found is that hydration causes the partial Si – O coordination to decrease.

The partial silicon coordination numbers are given for yttrium bioglass without including oxygen atoms in the silicon coordination sphere in Table 5.13c.

Table 5.13c: Partial coordination for silicon (OHc) in hydrated YBG-P glass

Si Coordination						
n	YBG-P y=0.1		YBG-P y=0.2		YBG-P y=0.3	
	Distribution(%)	St. Dev	Distribution(%)	St. Dev	Distribution(%)	St. Dev
0	90.412	1.098	78.945	1.439	67.502	3.238
1	9.489	7.328	19.179	13.837	28.208	17.821
2	0.098	0.000	1.773	1.770	3.961	3.074
3	0.000	0.000	0.103	0.000	0.329	0.465
4	0.000	0.000	0.000	0.000	0.000	0.000
5	0.000	0.000	0.000	0.000	0.000	0.000
6	0.000	0.000	0.000	0.000	0.000	0.000
7	0.000	0.000	0.000	0.000	0.000	0.000
8	0.000	0.000	0.000	0.000	0.000	0.000
9	0.000	0.000	0.000	0.000	0.000	0.000
10	0.000	0.000	0.000	0.000	0.000	0.000
Average	**0.097**	0.010	**0.230**	0.022	**0.371**	0.018

The general trend found was that for yttrium bioglass, gradual hydration caused a greater number of hydroxyl groups to coordinate to that of silicon. We saw that in

Table 5.13b that the silicon to oxygen coordination decreases as the glass becomes hydrated, but at the same time the silicon-oxygen coordination found from hydroxyl groups increases as seen in Table 5.13c. The overall increase in coordination for silicon seen in Table 5.13a is due to the associated oxygen atoms in hydroxyl groups taking precedence over normal oxygens from network modifier/former species i.e. $Na_2O/CaO/Y_2O_3/SiO_2$.

Si – OH and Al – OH species have been reported by Xianyu Xue [153]. It had been demonstrated that hydroxyl groups have been seen to coordinate onto silicon/aluminium for aluminosilicate glasses.

From Table 5.13b, hydroxyl groups may be the cause as to why a decrease is seen in the coordination of silicon with oxygen. While silicon coordination with oxygen decreases as hydration increases, hydroxyl groups replace those that were coordinated to silicon. Furthermore the overall silicon coordination is increased due to the presence of hydroxyl groups in its coordination sphere (Tables 5.13a and 5.13c).

From Figure 5.13 it is seen that as YBG-P glass is hydrated the bond angles shift very slightly to more acute angles for O - Si - O with respect to increasing hydration. A small peak is seen at the 70^o region, this is because hydration causes the overall coordination of silicon to increase as a very small number of 5 coordinated species are seen. Figure 5.14 shows the Si - O - H bond angles as YBG-P is hydrated. The Si - O - H bond angles with respect to hydration of YBG-P remain unaffected.

In Figure 5.15, silicon radial distribution functions in dry and hydrated YBG-P glasses are given. These show that the silicon oxygen interatomic distance is 1.62 Å. Also the silicon to hydroxyl-oxygen interatomic distance is 1.65 Å. The Si - O bond distances found for hydrated YBG-P are slightly larger than the typical bond distance of 1.60Å [42] which may be a possible reason as to why an increase in overall silicon coordination is seen. Hydroxyl groups being linear molecules may have a trajectory that allows for them to be easily inserted into the coordination sphere of silicon which therefore increases the overall silicon coordination.

Figure 5.15: Silicon radial distribution functions in dry and hydrated YBG-P Glasses

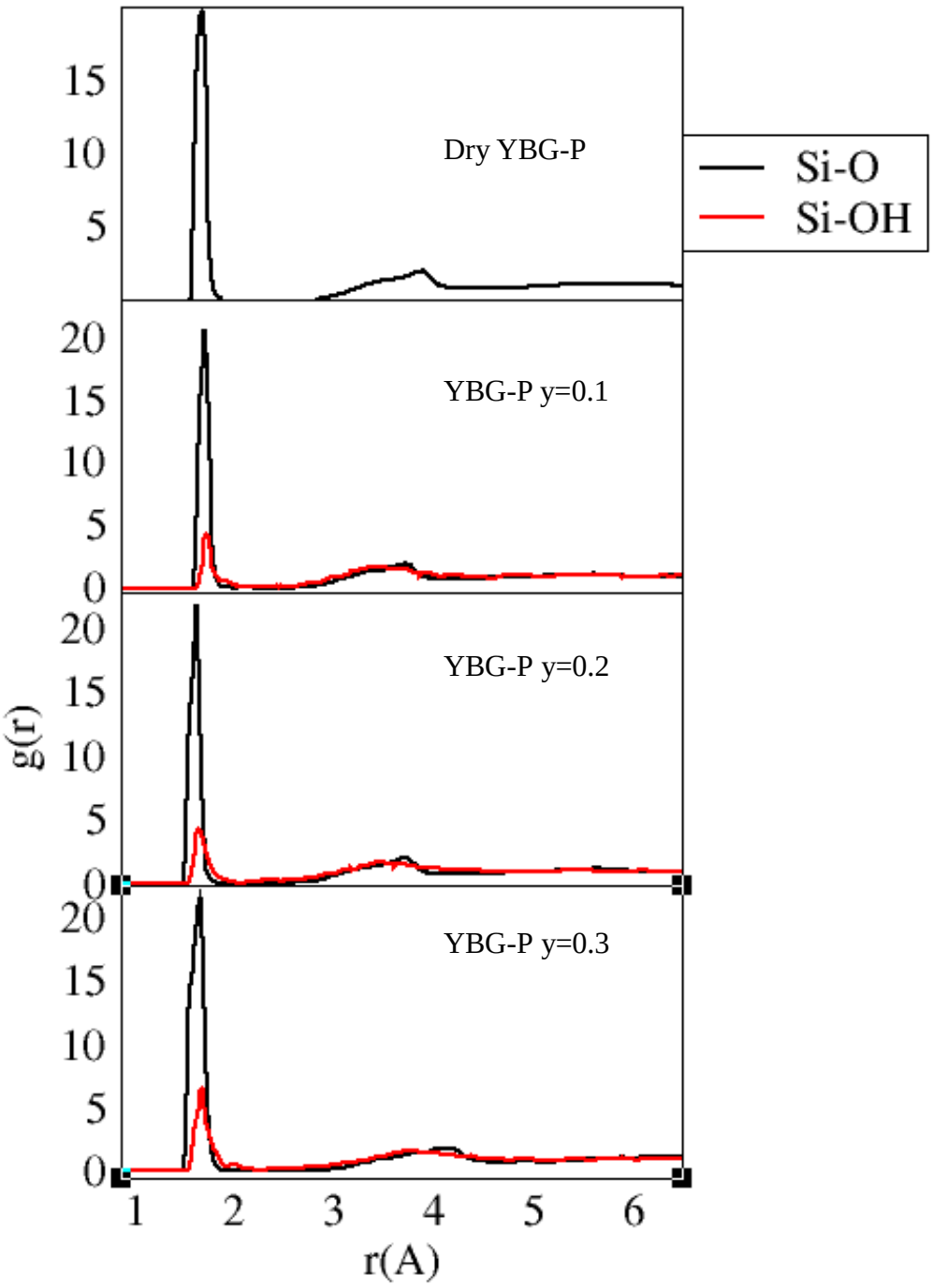

2) Yttrium

Table 5.14a: Total coordination for Yttrium (Oc + OHc) in dry and hydrated YBG-P glass

Y Coordination								
n	Dry YBG-P		YBG-P y=0.1		YBG-P y=0.2		YBG-P y=0.3	
	Distribution (%)	St. Dev	Distribution (%)	St. Dev	Distribution (%)	St. Dev	Distribution (%)	St. Dev
1	0.000	0.000	0.000	0.000	0.000	0.000	0.000	0.000
2	0.000	0.000	0.000	0.000	0.000	0.000	0.000	0.000
3	0.000	0.000	0.000	0.000	0.000	0.000	0.000	0.000
4	4.042	1.965	3.853	0.514	0.800	1.108	0.469	0.018
5	27.156	7.565	24.511	2.756	24.407	5.240	24.966	7.983
6	56.080	3.689	51.557	2.886	45.570	4.064	51.135	8.070
7	10.819	6.705	17.176	6.799	22.957	0.768	21.884	0.219
8	1.820	2.467	2.901	1.672	6.043	1.292	1.546	0.289
9	0.083	0.117	0.001	0.001	0.223	0.224	0.000	0.000
10	0.000	0.000	0.000	0.000	0.000	0.000	0.000	0.000
Average	**5.795**	0.156	**5.908**	0.052	**6.097**	0.115	**5.991**	0.077

The total Y – O coordination for yttrium bioglass ranged between 5.80 – 6.10. Such coordination numbers compare well enough to simulation studies of yttrium bioglass YBG-P carried out by the work of Tilocca and Christie [115, 137], where Y – O coordination for unhydrated YBG-P bioglass of 5.6 was found. A wider range of bonding environments are observed for yttrium compared to either silicon or phosphorus. Here six or seven coordinated yttrium atoms are most commonly seen. Some yttrium atoms have been seen to have coordination numbers of as low as three and as high as nine. An investigation is required to find out exactly how many hydroxyls are able to attach to yttrium in each of the glasses and whether or not increased hydration improves the effect. Therefore partial Y – O and Y – OH contributions are shown in Tables 5.14b and 5.14c respectively.

The partial yttrium coordination numbers are given for yttrium bioglass without including hydroxyl groups in the yttrium coordination sphere in Table 5.14b.

Table 5.14b: Partial Coordination for Yttrium (Oc) in hydrated YBG-P glass

Y Coordination						
n	YBG-P y=0.1		YBG-P y=0.2		YBG-P y=0.3	
	Distribution(%)	St. Dev	Distribution(%)	St. Dev	Distribution(%)	St. Dev
1	0.000	0.000	0.000	0.000	0.163	0.209
2	0.000	0.000	0.000	0.000	2.857	2.332
3	2.111	0.326	15.238	1.659	33.454	6.034
4	24.134	3.720	30.388	0.221	35.668	7.220
5	44.318	0.258	29.984	1.669	22.247	0.829
6	24.694	4.714	21.150	3.391	5.601	1.752
7	4.743	1.062	2.673	0.121	0.010	0.015
8	0.000	0.000	0.568	0.278	0.000	0.000
9	0.000	0.000	0.000	0.000	0.000	0.000
10	0.000	0.000	0.000	0.000	0.000	0.000
Average	**5.058**	0.057	**4.673**	0.075	**3.938**	0.128

The table above shows the partial Y – O coordination (exclusive of any hydroxyls that may be attached) for yttrium bioglass YBG-P hydrated from concentrations of 0.1 to 0.3. The general trend found is that hydration causes the partial Y – O coordination to decrease.

The partial yttrium coordination numbers are given below for yttrium bioglass without including oxygen atoms in the yttrium coordination sphere in Table 5.15c.

Table 5.14c: Partial Coordination for Yttrium (OHc) in hydrated YBG-P glass

Y Coordination						
n	YBG-P y=0.1		YBG-P y=0.2		YBG-P y=0.3	
0	27.543	2.650	6.969	5.616	2.518	1.404
1	60.754	3.724	50.945	2.052	20.548	2.790
2	10.922	0.031	34.836	1.949	50.791	10.658
3	0.781	1.105	7.250	5.719	21.455	14.854
4	0.000	0.000	0.000	0.000	4.689	0.001
5	0.000	0.000	0.000	0.000	0.000	0.000
6	0.000	0.000	0.000	0.000	0.000	0.000
7	0.000	0.000	0.000	0.000	0.000	0.000
8	0.000	0.000	0.000	0.000	0.000	0.000
9	0.000	0.000	0.000	0.000	0.000	0.000
10	0.000	0.000	0.000	0.000	0.000	0.000
Average	**0.849**	0.005	**1.424**	0.190	**2.052**	0.204

The general trend seen from the above table for yttrium bioglass, is that gradual hydration causes a greater number of hydroxyl groups to coordinate to yttrium. The coordination numbers of hydroxyl groups onto yttrium in Table 5.14c are raised and are of a wider range compared to hydroxyl coordinations onto silicon seen in Table 5.13c.

This shows hydroxyl groups have the ability to coordinate more to yttrium and less with silicon. We have already identified that silicon is well-defined in coordination at four and does not have the capacity to take up anymore coordinations with oxygen, whether they are from hydroxyl groups or from network former/modifier species i.e. $Na_2O/CaO/Y_2O_3/SiO_2$. Yttrium on the other hand has a wider range of coordination numbers than Si thus giving rise to a greater capacity to welcome hydroxyl groups into its coordination sphere.

From viewing Table 5.14b hydroxyl groups may be the cause as to why a decrease is seen in the coordination of yttrium with oxygen. While yttrium coordination with oxygen decreases as hydration increases, hydroxyl groups replace those that were coordinated to yttrium. Furthermore the overall yttrium coordination is increased due to the presence of hydroxyl groups in its coordination sphere (Tables 5.14a and 5.14c).

From Figure 5.13 it is seen that as YBG-P glass is hydrated the bond angles shift towards more acute bond angles for O - Y - O with respect to increasing hydration. A small peak is seen at the 60^o region, this is because hydration causes the overall coordination of yttrium to increase as a number of 5, 6 and 7 coordinated species are seen. Figure 5.14 shows the Y - O - H bond angles as YBG-P is hydrated. The Y - O - H bond angles with respect to hydration of YBG-P remain unaffected.

In Figure 5.16, yttrium radial distribution functions in dry and hydrated YBG-P glasses are given. These show that the yttrium-oxygen interatomic distance is 2.23 Å. Also the yttrium to hydroxyl-oxygen interatomic distance is 2.33 Å. Hydroxyl groups being linear molecules may have a trajectory that allows for them to be easily inserted into the coordination sphere of yttrium which therefore increases the overall yttrium coordination.

Figure 5.16: Yttrium radial distribution functions in dry and hydrated YBG-P Glasses

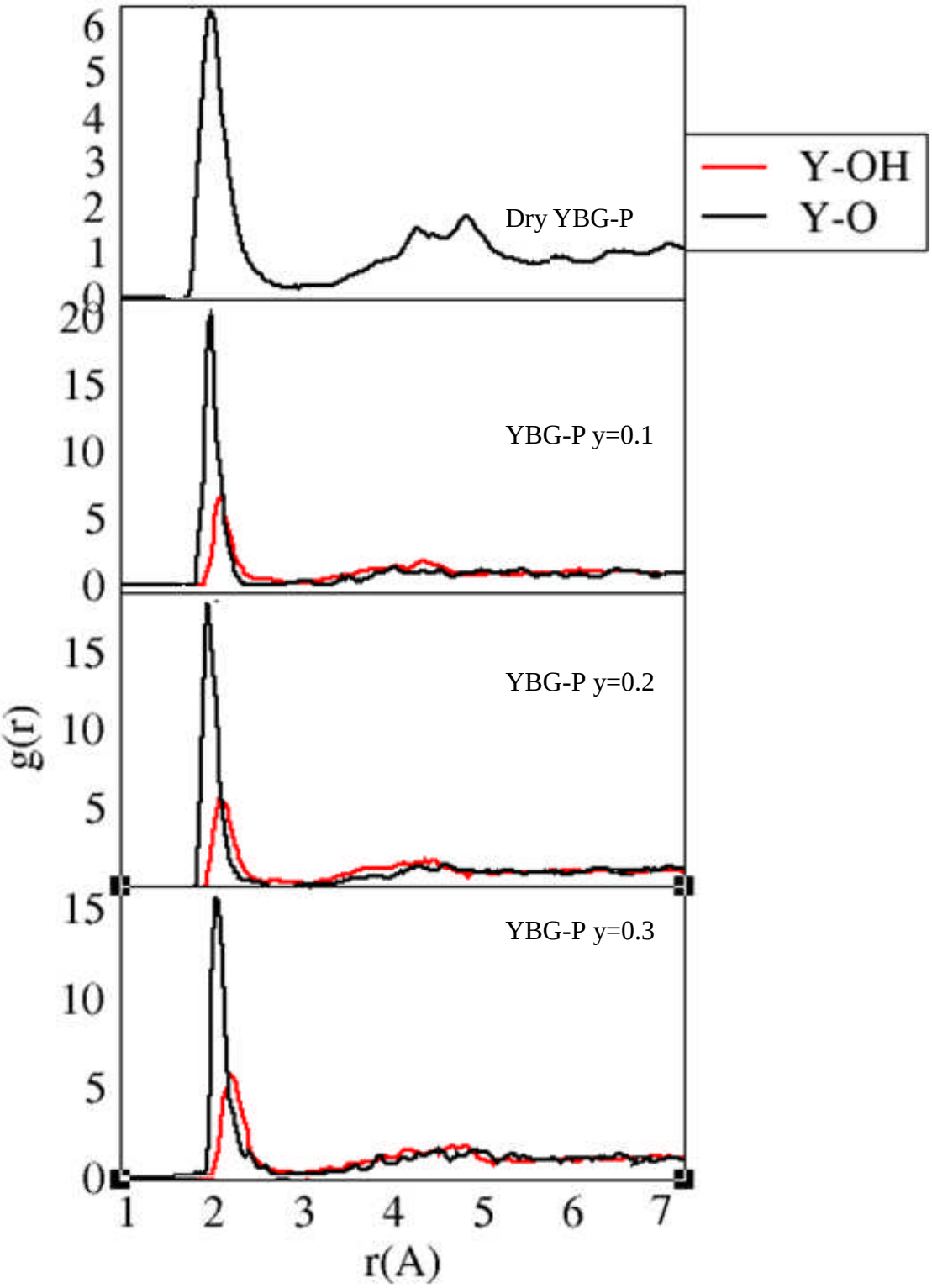

3) Calcium

Table 5.15a: Total coordination for calcium (Oc + OHc) in dry and hydrated YBG-P glass

Ca Coordination								
n	Dry YBG-P		YBG-P y=0.1		YBG-P y=0.2		YBG-P y=0.3	
	Distribution(%)	St. Dev	Distribution(%)	St. Dev	Distribution(%)	St. Dev	Distribution(%)	St. Dev
1	0.000	0.000	0.000	0.000	0.000	0.000	0.000	0.000
2	0.000	0.000	0.000	0.000	0.000	0.000	0.000	0.000
3	0.000	0.000	0.002	0.003	0.000	0.000	0.000	0.000
4	7.390	0.849	7.268	0.964	3.906	0.363	1.540	1.259
5	28.760	1.516	29.510	0.720	21.028	0.154	21.792	0.439
6	36.282	3.367	41.469	2.696	38.153	3.761	42.036	0.277
7	22.176	4.265	17.788	2.013	27.103	5.951	27.693	1.907
8	4.395	1.240	3.762	1.270	8.460	0.230	6.522	0.937
9	0.997	0.227	0.199	0.269	1.344	1.439	0.417	0.425
10	0.000	0.000	0.002	0.003	0.005	0.005	0.001	0.002
Average	**5.904**	0.106	**5.819**	0.024	**6.192**	0.020	**6.171**	0.008

The total Ca – O coordination for yttrium bioglass YBG-P ranged between 5.82 – 6.19. Such coordination numbers compare well to simulation studies of yttrium bioglass carried out by Tilocca and Christie [115, 137], where Ca – O coordination for unhydrated YBG-P bioglass of ~6 was found. A wider range of bonding environments are observed for calcium compared to silicon, phosphorus and yttrium. Here five-, six and seven-coordinated calcium atoms are most commonly seen. Some calcium atoms have been seen to have coordination numbers of as low as three and as high as ten. The general trend found from the above graph is that the total Ca – O coordination increases gradually as hydration increases. An investigation is required to find out exactly how many hydroxyls are able to attach to calcium in each of the glasses and whether or not increased hydration improves the effect. Therefore partial Ca – O and Ca – OH contributions were shown in Tables 5.15b and 5.15c respectively.

The partial calcium coordination numbers are given for yttrium bioglass without including hydroxyl groups in the calcium coordination sphere in Table 5.15b.

Table 5.15b: Partial coordination for calcium (Oc) in hydrated YBG-P glass

Ca Coordination						
n	YBG-P y=0.1		YBG-P y=0.2		YBG-P y=0.3	
	Distribution(%)	St. Dev	Distribution(%)	St. Dev	Distribution(%)	St. Dev
1	0.099	0.141	0.000	0.000	2.259	3.194
2	1.727	0.113	2.322	0.329	9.454	2.102
3	4.063	2.146	13.952	1.992	23.651	0.268
4	23.780	2.375	26.257	5.105	31.830	0.538
5	39.154	6.566	31.193	4.212	23.321	3.221
6	22.120	4.642	18.155	0.647	6.427	1.196
7	7.673	1.141	7.348	2.134	2.898	2.239
8	1.381	0.580	0.687	0.324	0.160	0.226
9	0.002	0.003	0.086	0.110	0.000	0.000
10	0.000	0.000	0.000	0.000	0.000	0.000
Average	**5.041**	0.108	**4.741**	0.164	**3.962**	0.220

The table above shows the partial Ca – O coordination (exclusive of any hydroxyls that may be attached) for yttrium bioglass YBG-P hydrated from concentrations of 0.1 to 0.3. The general trend found is that hydration causes the partial Ca – O coordination to decrease.

The partial calcium coordination numbers are given for yttrium bioglass without including oxygen atoms in the calcium coordination sphere in Table 5.15c.

Table 5.15c: Partial Coordination for Calcium (OHc) in hydrated YBG-P glass

Ca Coordination						
n	YBG-P y=0.1		YBG-P y=0.2		YBG-P y=0.3	
	Distribution(%)	St. Dev	Distribution(%)	St. Dev	Distribution(%)	St. Dev
0	36.715	8.452	9.998	3.874	2.753	0.377
1	49.449	4.599	47.240	1.024	20.637	1.301
2	13.229	2.995	31.351	2.005	42.514	10.793
3	0.607	0.858	10.485	8.212	22.901	3.724
4	0.000	0.000	0.927	1.309	9.397	5.450
5	0.000	0.000	0.000	0.000	1.798	2.543
6	0.000	0.000	0.000	0.000	0.000	0.000
7	0.000	0.000	0.000	0.000	0.000	0.000
8	0.000	0.000	0.000	0.000	0.000	0.000
9	0.000	0.000	0.000	0.000	0.000	0.000
10	0.000	0.000	0.000	0.000	0.000	0.000
Average	**0.777**	0.132	**1.451**	0.144	**2.209**	0.228

The general trend seen from the above table for YBG-P, gradual hydration causes a greater number of hydroxyl groups to coordinate to calcium. The coordination of hydroxyl groups onto calcium are rather similar to that of yttrium seen in Table 5.14c. The coordination numbers of hydroxyl groups onto calcium in Table 5.15c are raised and are of a wider range compared to hydroxyl coordination onto silicon in Table 5.13c respectively. This shows hydroxyl groups having the ability to coordinate more to calcium and less with silicon. We have already identified that silicon is well defined in coordination at four and does not have the capacity to take up any more coordination with oxygen, whether they are from hydroxyl groups or from network former/modifier species i.e. $Na_2O/CaO/Y_2O_3/SiO_2$. Calcium, like yttrium, on the other hand has a wider range of coordination numbers than Si thus giving rise to a greater capacity to welcome hydroxyl groups into the coordination sphere of calcium.

From viewing Table 5.15b, hydroxyl groups may be the cause as to why a decrease is seen in the coordination of calcium with oxygen. While calcium coordination with oxygen decreases as hydration increases, hydroxyl groups replace those that were coordinated to calcium. Furthermore the overall calcium coordination is increased due to the presence of hydroxyl groups in its coordination sphere (Tables 5.15a and 5.15c).

From Figure 5.13 it is seen that as YBG-P glass is hydrated the bond angles shift towards more acute bond angles for O - Ca - O with respect to increasing hydration. A

small peak is seen at the 65° region, this is because hydration causes the overall coordination of calcium to increase as a number of 5, 6 and 7 coordinated species are seen. Figure 5.14 shows the Ca - O - H bond angles as YBG-P is hydrated. The Ca - O - H bond angles with respect to hydration of YBG-P remain unaffected.

In Figure 5.17, calcium radial distribution functions in dry and hydrated YBG-P glasses are given. These show that the calcium-oxygen interatomic distance is 2.36 Å. Also the calcium to hydroxyl-oxygen interatomic distance is 2.37 Å. Hydroxyl groups being linear molecules may have a trajectory that allows for them to be easily inserted into the coordination sphere of yttrium which therefore increases the overall yttrium coordination.

Figure 5.17: Calcium radial distribution functions in dry and hydrated YBG-P glasses

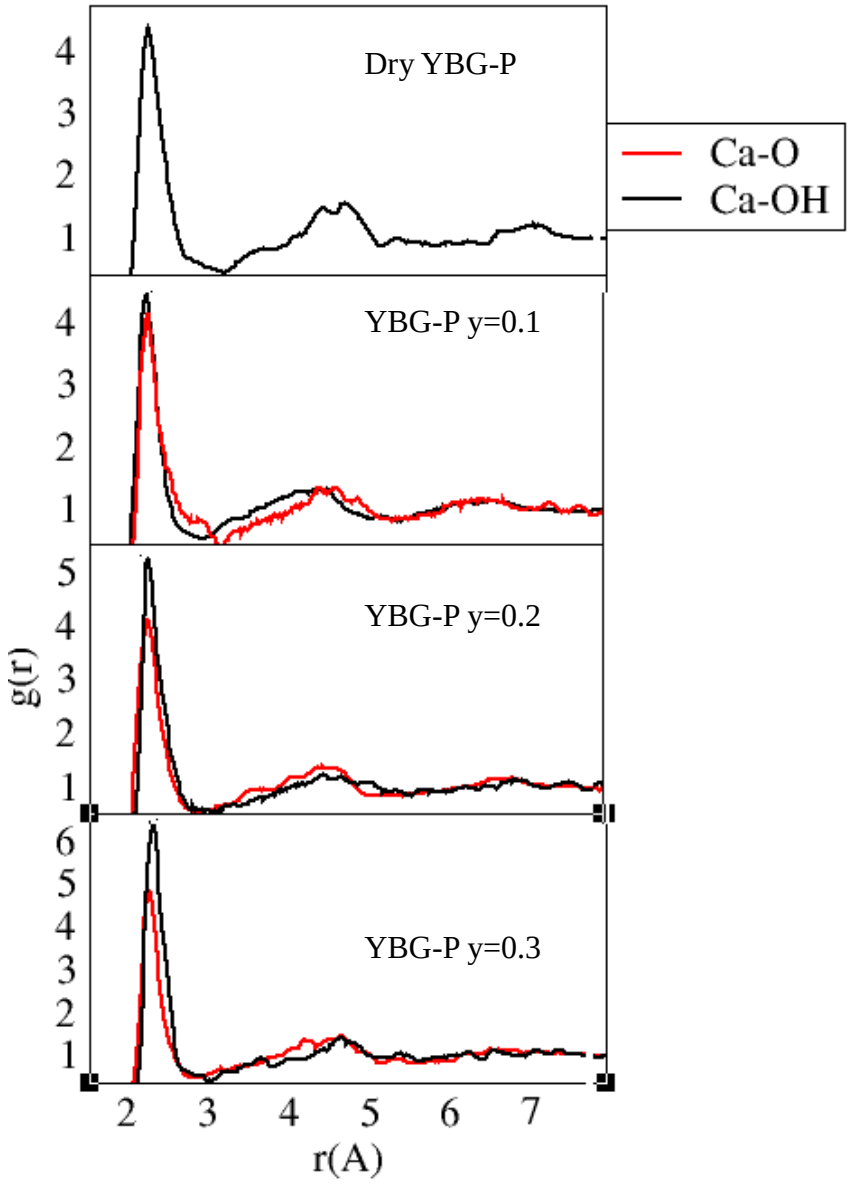

4) Sodium

Table 5.16a: Total Coordination for Sodium (Oc + OHc) in dry and hydrated YBG-P glass

Na Coordination								
n	Dry YBG-P		YBG-P y=0.1		YBG-P y=0.2		YBG-P y=0.3	
1	0.000	0.000	0.000	0.000	0.000	0.000	0.000	0.000
2	0.000	0.000	0.000	0.000	0.000	0.000	0.000	0.000
3	0.612	0.398	1.077	0.232	0.361	0.326	0.248	0.340
4	5.457	0.106	5.806	1.629	5.190	0.048	4.252	2.177
5	25.594	0.248	24.351	1.850	22.264	1.323	20.965	1.133
6	39.133	7.929	37.252	0.919	37.318	0.578	37.650	2.497
7	22.751	4.566	23.177	3.345	23.288	2.754	24.862	1.027
8	5.891	2.106	7.332	0.025	9.540	0.620	9.551	1.520
9	0.540	0.476	0.989	0.776	1.848	0.200	2.038	1.348
10	0.021	0.030	0.016	0.021	0.191	0.155	0.428	0.053
Average	**5.979**	0.087	**6.017**	0.102	**6.149**	0.037	**6.215**	0.063

The total Na – O coordination for yttrium bioglass YBG-P ranged between 5.98 – 6.21. Such coordination numbers compare well enough to simulation studies of yttrium bioglass YBG-P carried out by the work of Tilocca and Christie [115, 137], where Na – O coordination for unhydrated YBG-P bioglass of ~6 was found. Here five-, six-, and seven-coordinated sodium atoms are seen. Some sodium atoms have been seen to have coordination numbers of as low as three and as high as ten. The general trend found from the above graph is that the total Na – O coordination increases gradually as hydration increases. An investigation is required to find out exactly how many hydroxyls are able to attach to sodium in each of the glasses and whether or not increased hydration improves the effect. Therefore partial Na – O and Na – OH contributions were shown in Tables 5.16b and 5.16c respectively.

The partial sodium coordination numbers are given for yttrium bioglass without including hydroxyl groups in the sodium coordination sphere in Table 5.16b.

Table 5.16b: Partial coordination for sodium (Oc) in hydrated YBG-P glass

Na Coordination						
n	YBG-P y=0.1		YBG-P y=0.2		YBG-P y=0.3	
1	0.000	0.000	0.191	0.271	0.000	0.000
2	0.521	0.584	0.569	0.367	3.081	0.085
3	4.097	0.146	10.229	2.097	15.097	5.367
4	13.315	1.543	24.302	1.532	28.775	2.905
5	33.960	1.454	30.055	4.668	29.376	5.012
6	29.076	0.792	21.483	1.750	17.326	3.626
7	15.490	3.680	11.394	1.753	5.495	0.273
8	3.521	0.845	1.726	0.630	0.730	0.125
9	0.021	0.005	0.050	0.066	0.115	0.107
10	0.000	0.000	0.000	0.000	0.007	0.008
Average	**5.476**	0.127	**5.024**	0.048	**4.628**	0.171

The table above shows the partial Na – O coordination (exclusive of any hydroxyls that may be attached) for yttrium bioglass YBG-P hydrated from concentrations of 0.1 to 0.3. The general trend found is that hydration causes the partial Na – O coordination to decrease.

The partial sodium coordination numbers are given for yttrium bioglass without including oxygen atoms in the sodium coordination sphere in Table 5.16c.

Table 5.16c: Partial coordination for sodium (OHc) in hydrated YBG-P glass

Na Coordination						
	YBG-P y=0.1		YBG-P y=0.2		YBG-P y=0.3	
0	53.988	0.518	25.010	4.796	10.748	2.771
1	38.523	0.836	44.400	2.982	39.234	1.270
2	6.943	0.775	24.503	0.100	32.994	0.271
3	0.545	0.579	5.225	1.574	14.680	3.446
4	0.000	0.000	0.862	0.140	2.160	0.518
5	0.000	0.000	0.000	0.000	0.184	0.194
6	0.000	0.000	0.000	0.000	0.000	0.000
7	0.000	0.000	0.000	0.000	0.000	0.000
8	0.000	0.000	0.000	0.000	0.000	0.000
9	0.000	0.000	0.000	0.000	0.000	0.000
10	0.000	0.000	0.000	0.000	0.000	0.000
Average	**0.540**	0.024	**1.125**	0.084	**1.588**	0.107

The general trend seen from the above table for YBG-P, gradual hydration causes a greater number of hydroxyl groups to coordinate to sodium. The coordination numbers of hydroxyl groups onto sodium are rather similar to that of yttrium and calcium seen in Table 3.48c and 3.49c respectively. Sodium, like yttrium and calcium, has a wider range of coordination numbers than Si thus giving rise to a greater capacity to welcome hydroxyl groups into the coordination sphere of sodium.

From viewing Table 5.16b hydroxyl groups may be the cause as to why a decrease is seen in the coordination of sodium with oxygen. While sodium coordination with oxygen decreases as hydration increases, hydroxyl groups replace those that were coordinated to sodium. Furthermore the overall sodium coordination is increased due to the presence of hydroxyl groups in its coordination sphere (Tables 5.15a and 5.15c).

From Figure 5.13 it is seen that as YBG-P glass is hydrated the bond angles shift towards more acute bond angles for O - Na - O with respect to increasing hydration. A small peak is seen at the 69^{o} region, this is because hydration causes the overall coordination of sodium to increase as a number of 5, 6 and 7 coordinated species are seen. Figure 5.14 shows the Na - O - H bond angles as YBG-P is hydrated. The Na - O - H bond angles with respect to hydration of YBG-P remain unaffected.

In Figure 5.18, sodium radial distribution functions in dry and hydrated YBG-P glasses are given. These show that the sodium oxygen interatomic distance is 2.34 Å. Also the sodium to hydroxyl-oxygen interatomic distance is 2.35 Å. Hydroxyl groups being linear molecules may have a trajectory that allows for them to be easily inserted

into the coordination sphere of yttrium which therefore increases the overall yttrium coordination.

Figure 5.18: Sodium Radial Distribution Functions in dry and hydrated YBG-P Glasses

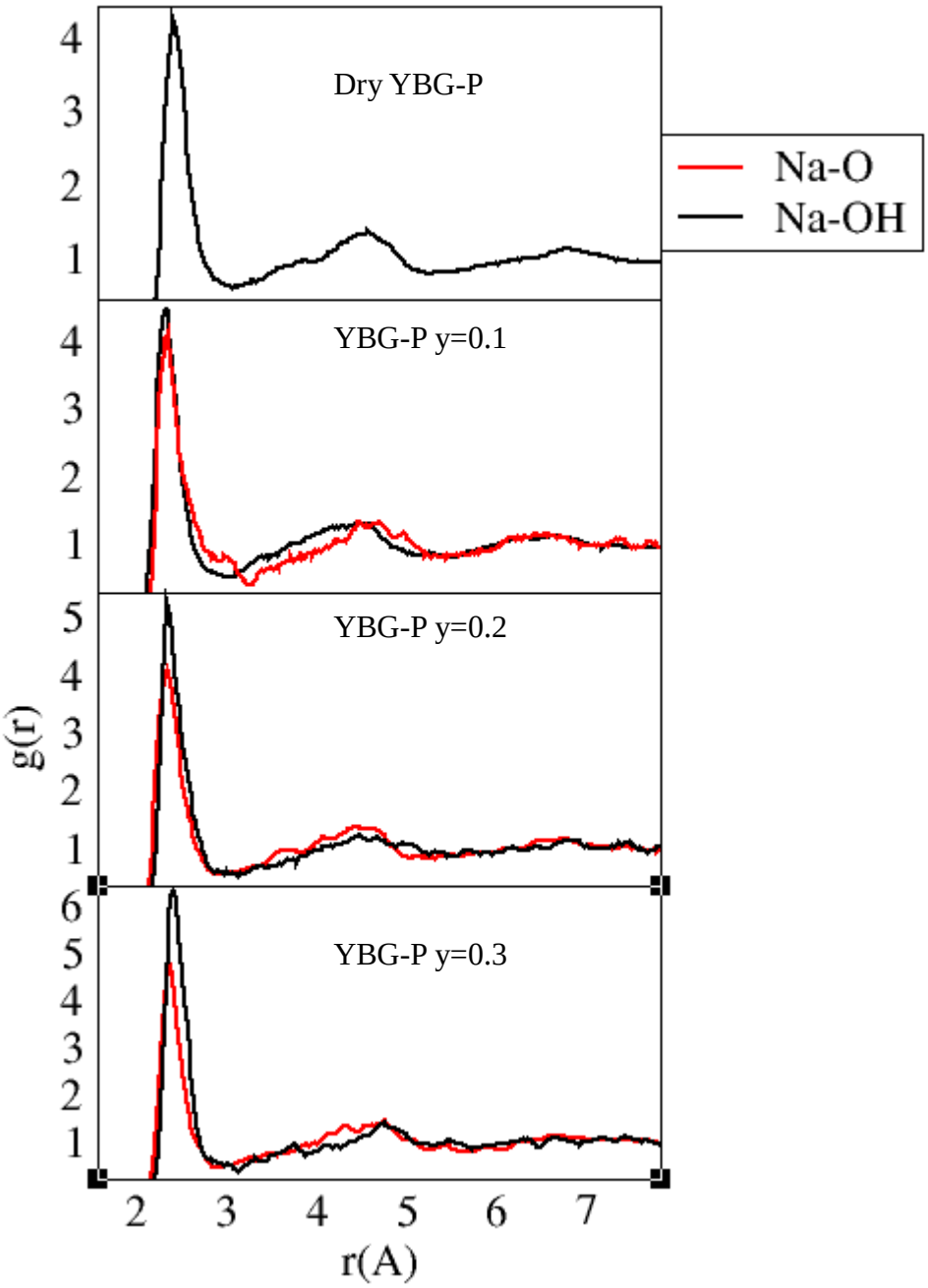

5.2.2 Preferential Attachment of –OH onto Network Former

The number of OH species present around silicon in hydrated yttrium bioglasses are shown in Table 5.17a and 5.17b. Table 5.17a shows the actual number of $^{-}$OH species that surround silicon. Normalisation of numbers in Table 5.17a gives rise to Table 5.17b to remove unnecessary biasing due to the number of cations used in the simulation. The normalisation method employed is given below:

Table 5.17a: Number of hydroxyls attached to Si and those which are free

YBG	Si		Free OH	
	No. OH	St. Dev	No. OH	St. Dev
0.1	39.500	0.807	60.500	0.725
0.2	80.000	0.923	120.000	0.639
0.3	156.501	0.975	43.499	0.824

NORMALISATION: No. of $^{-}$OH species attached to a cation/ total no. of cations to which those hydroxyl groups are attached in simulation

e.g. for Silicon

(YBG-P y=0.1) OH on Si = 39.500/420 = 0.094

(YBG-P y=0.2) OH on Si = 80.000/420 = 0.190

(YBG-P y=0.3) OH on Si = 156.500/420 = 0.372

Table 5.17b: Number of hydroxyls attached to Si and those which are free (normalized)

YBG	Si		Free OH	
	No. OH	St. Dev	No. OH	St. Dev
0.1	0.094	0.002	0.605	0.007
0.2	0.190	0.002	0.600	0.003
0.3	0.372	0.002	0.145	0.003

Hydroxyl groups prefer to coordinate more to silicon when the yttrium bioglass is hydrated from concentrations 0.1 - 0.3. The more an yttrium bioglass is hydrated the fewer free hydroxyl groups are seen.

Si – OH and Al – OH species have been reported by Xianyu Xue [153]. It had been demonstrated that hydroxyl groups have been seen to coordinate onto silicon and aluminium for aluminosilicate glasses.

Hydroxyl groups that have not attached to the network-forming species silicon, would as a result be described as free hydroxyl groups with the ability to form coordination to network modifying species such as sodium in Xianyu Xue's paper [153]. Yttrium, calcium and sodium are the network modifiers in YBG-P glasses. Since free hydroxyls were seen to attach to sodium modifier ions [153], incorporating yttrium and calcium modifier ions would allow for hydroxyl groups to attach to yttrium and calcium too in an yttrium bioglass (YBG-P).

5.2.3 Preferential Attachment of –OH onto Network Modifiers

The number of OH species present around each cation, yttrium, calcium and sodium, in hydrated yttrium bioglasses are shown in Table 5.18a and 5.18b. Table 5.18a shows the actual number of OH species that surround yttrium, calcium and sodium. Normalisation of numbers in Table 5.18a give rise to Table 5.18b to remove unnecessary biasing due to the number of cations used in the simulation. The normalisation method employed is given below.

Table 5.18a: Number of hydroxyls attached to Y, Ca and Na

YBG-P	Y		Ca		Na	
	No. OH	St. Dev	No. OH	St. Dev	No. OH	St. Dev
0.1	42.500	0.707	63.500	0.707	47.500	0.707
0.2	76.500	2.121	55.900	1.414	104.000	1.414
0.3	108.000	4.243	163.500	4.950	140.000	4.243

NORMALISATION: No. of OH species attached to a cation / total no. of cations to which those hydroxyl groups are attached in simulation

e.g. for Yttrium

(YBG-P y=0.1) OH on Y = 42.50/64 = 0.664

(YBG-P y=0.2) OH on Y = 76.50/64 = 1.195

(YBG-P y=0.3) OH on Y = 108.00/64 = 1.688

Table 5.18b Number of Hydroxyls attached to Y, Ca and Na (normalized)

YBG-P	Y		Ca		Na	
	No. OH	St. Dev	No. OH	St. Dev	No. OH	St. Dev
0.1	0.664	0.011	0.588	0.007	0.222	0.003
0.2	1.195	0.033	0.518	0.013	0.486	0.013
0.3	1.688	0.066	1.514	0.046	0.654	0.040

Hydroxyl groups prefer to coordinate more to calcium than yttrium and sodium in this order. Table 5.18a and 5.18b show the number of hydroxyls attaching to Y, Ca and Na respectively. Figure 5.19 shows the order by which hydroxyl groups prefer to attach to yttrium, then calcium and sodium.

Fig 5.19: (Y– OH) > (Ca – OH) > (Na – OH)

5.2.4 Medium-range structure

1) Silicon Q^n

Table 5.19: Silicon Q^n Distribution and Network Connectivity

TOTAL Si								
n	Dry YBG-P		YBG-P y=0.1		YBG-P y=0.2		YBG-P y=0.3	
	Distribution(%)	St. Dev	Distribution(%)	St. Dev	Distribution(%)	St. Dev	Distribution(%)	St. Dev
0	3.809	1.418	0.466	0.004	0.468	0.331	0.234	0.331
1	16.637	1.644	5.295	0.515	6.319	1.331	4.910	0.646
2	38.679	7.154	30.132	0.577	25.495	0.359	25.127	1.061
3	34.279	1.056	45.356	0.681	45.543	3.202	46.973	3.552
4	6.597	3.036	18.114	0.374	21.902	4.210	22.409	3.630
5	0.000	0.000	0.637	0.041	0.272	0.350	0.347	0.162
6	0.000	0.000	0.000	0.000	0.000	0.000	0.000	0.000
7	0.000	0.000	0.000	0.000	0.000	0.000	0.000	0.000
8	0.000	0.000	0.000	0.000	0.000	0.000	0.000	0.000
9	0.000	0.000	0.000	0.000	0.000	0.000	0.000	0.000
10	0.000	0.000	0.000	0.000	0.000	0.000	0.000	0.000
Average	**2.232**	0.026	**2.773**	0.021	**2.829**	0.069	**2.875**	0.045

Observing Table 5.19 we can see that for yttrium bioglass (YBG-P) as one progressively hydrates from 0.1 – 0.3 the silicon network connectivity increases. A large rise in silicon connectivities are seen from dry YBG-P to hydrated forms at concentrations of 0.1. What is seen after is a further rise in silicon network connectivities but not as large as that from unhydrated to hydrated form of 0.1. The silicon network connectivity of the unhydrated glass is 2.23. The silicon connectivity comprises Si – O – Si connections, where oxygens in this situation are bridging between two like pair atoms of silicon. All network connections for silicon in this glass are of Si – O – Si because there is no phosphorus. As soon as the yttrium bioglass is hydrated, hydroxyl groups promote the increase in silicon network connectivities. The silicon network strengthens itself as a reaction towards the hydroxyl groups integrating themselves into the yttrium bioglass structure. This may be due to the hydroxyl groups substituting, Y --- O-Si-O_3, Ca --- O-Si-O_3 and/or Na --- O-Si-O_3 for Y --- OH, Ca --- OH and/or Na --- OH which causes the movement of -[$^-$O-SiO_3] species back into the silicon network causing this strengthening. Figure 5.20 below was originally hypothesized for how hydration would break the network connectivity of silicon, by replacing a single oxygen for two hydroxyl groups to cause the breakage in silicon network.

Figure 5.20 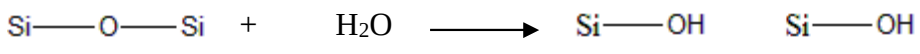

Figure 5.21: Q^n Distributions of Silicon with respect to hydrated YBG-P glasses

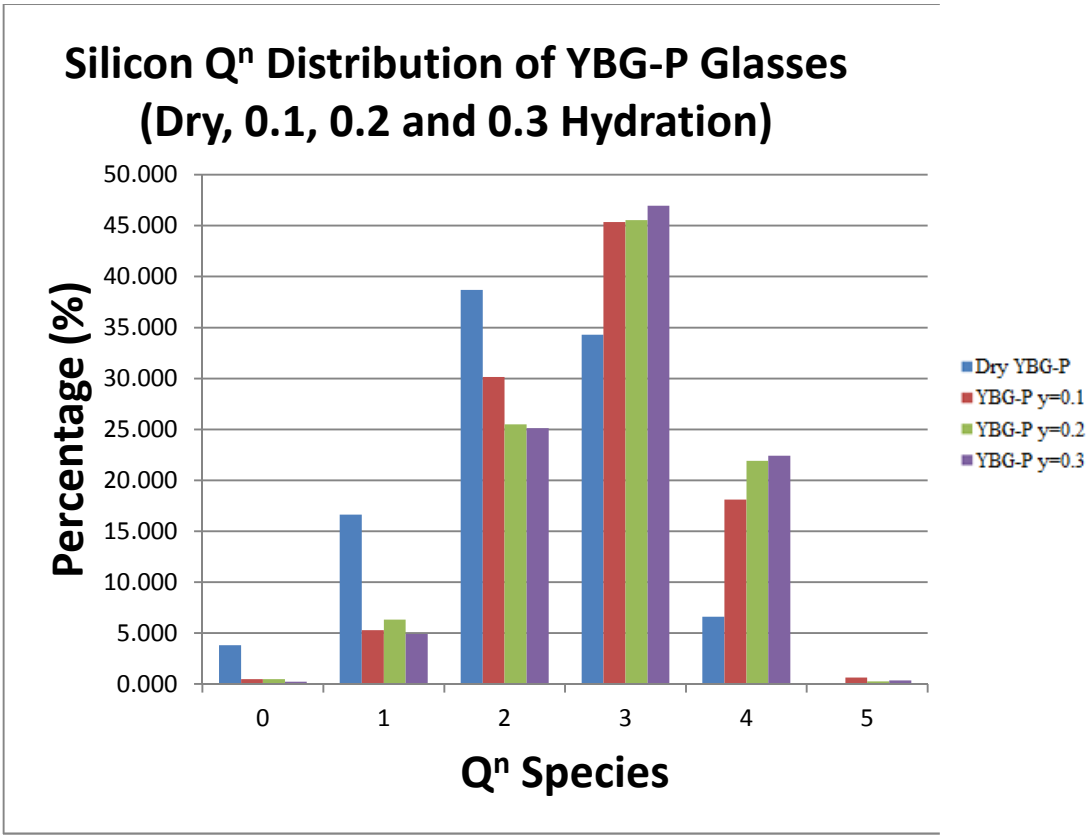

The Q^n speciation of the silicon is given in Table 5.19 and Figure 5.21. By observing the dry YBG-P, we see that the majority of silicon atoms in the glass network have a Q^n speciation of Q^2 and Q^3 thus giving rise to a network connectivity of 2.23. As soon as we hydrated YBG-P with a concentration of 0.1, we see that the amount of Q^1 and Q^2 species decreases and results in the increase of Q^3 and Q^4 species which were less observed in dry yttrium bioglass. This is also why the network connectivity increases with respect to hydration of YBG-P glasses.

Having a YBG with low durability containing radioactive yttrium ions would as a result allow, due to the low durability of the glass, yttrium to move out of the glass network and into surrounding healthy living tissue. This would be detrimental to the patient. The yttrium ions need to be harnessed in the glass network which needs to be durable enough to prevent leaching of yttrium ions. After the full radioactivity of yttrium has depleted, used for radiotherapeutic use, then only is it safe to the patient for yttrium ions to be mobile outside of the glass network. For this reason YBG-P glass with increased durability that is less bioactive would prevent yttrium ions leaching out

of the glass network and into healthy surrounding tissues. Moreover hydration enables the fine tuning of YBG-P with respect to silicon network connectivity. We see as dry YBG-P is hydrated progressively, higher silicon network connectivity is gained. This means that bioactivity is decreasing. This also means due to the strengthening of the silicon network that the glass overall increases in durability. Some YBG-P glasses may be better suited to one organ than another according to durability. It would be now possible to enhance further and develop a YBG-P glass with respect to hydration which can be engineered for its use in different parts of the body where radiotherapy can be given more effectively.

5.2.5 Clustering

Figure 5.22: Clustering ratios of hydroxyl groups surrounding cations Si, Na, Ca and Y

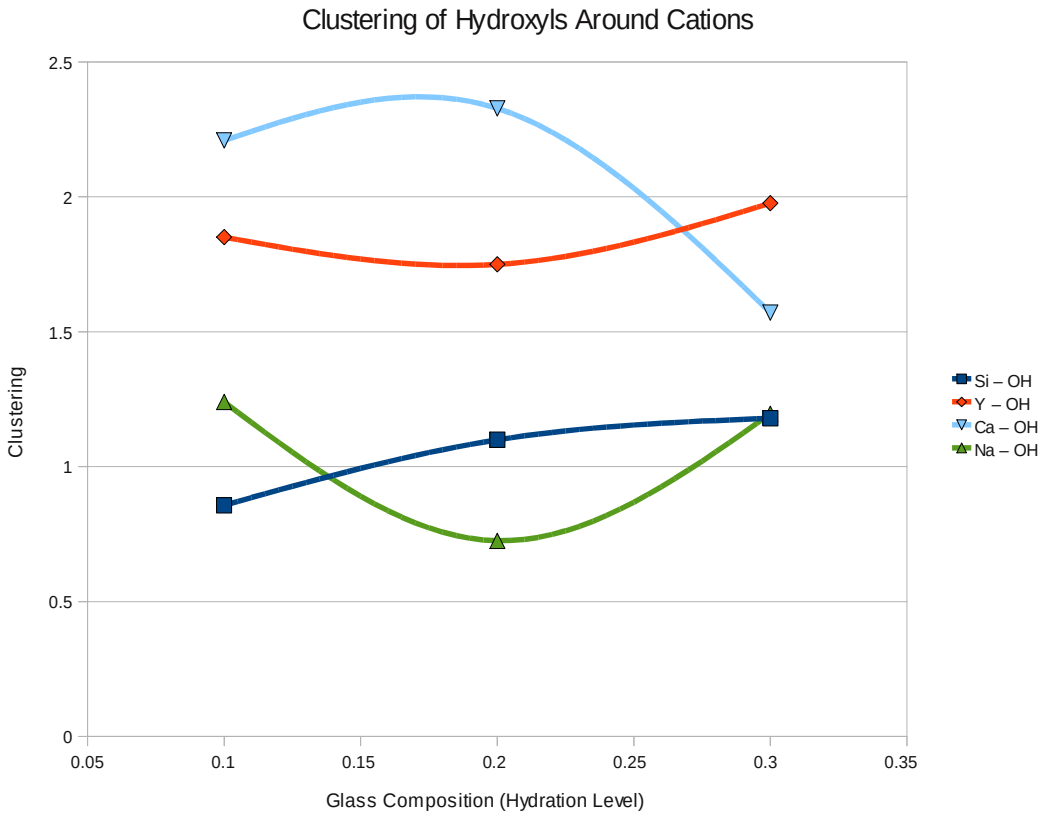

From the Figure above, the hydroxyl groups cluster around silicon, yttrium, calcium and sodium in the following order:

$$Ca - OH > Y - OH > Na - OH > Si - OH$$

1) Si – OH

It is clear from the above Figure that hydroxyl does cluster around silicon atoms as hydration is increased upon dry YBG-P. It is known that very few hydroxyl groups coordinate to silicon. From the above Figure, hydroxyl groups seem to be evenly dispersed throughout the glass structure with respect to silicon in a homogenous fashion thus not favouring clustering around silicon at low levels of hydration. As the YBG glass is further hydrated some clustering is occurring as they are above the clustering ratio of one.

2) Na – OH

From the above Figure hydroxyl groups seem to aggregate around sodium atoms. Na – OH clustering at hydration concentration of 0.2 is an anomaly where clustering is not taking place. It is known that hydroxyl groups do coordinate to sodium, more than to silicon, but these hydroxyl groups also seem to be evenly dispersed throughout the glass structure being attached to sodium in a homogenous fashion thus not favouring clustering around sodium with respect to hydration concentration of 0.2. The clustering ratios are just above the value of one along the y-axis of the plot for hydration concentrations 0.1 and 0.3. This relates to the hydroxyls being almost homogeneously spread out through the glass structure with respect to sodium and hydration concentration.

4) Y – OH

It is evident from the above graph that clustering is taking place, where hydroxyl groups cluster around yttrium ions. It is seen that hydroxyl groups do coordinate to yttrium, which is more marked than silicon and sodium, but these hydroxyl groups also seem to be less homogeneously dispersed throughout the glass structure as found for silicon or sodium. The ratios seen from the above graph are above the value of one and in being so they show that hydroxyl groups are surrounding yttrium ions selectively more than silicon, sodium and phosphorus in this order.

5) Ca – OH

Observing the above graph with respect to Ca – OH, clustering is clearly taking place, where hydroxyl groups cluster around calcium ions. It is seen that hydroxyl groups do coordinate to calcium, which is more marked than silicon, sodium and yttrium, but these hydroxyl groups seem to be less homogeneously dispersed throughout the glass structure as found for silicon, sodium and yttrium. The ratios seen from the above graph are above the value of one and in being so they show that hydroxyl groups are surrounding calcium ions selectively more than silicon, sodium and yttrium in this order.

5) Cation – Cation Clustering

Table 5.20 shows cation – cation clustering with respect to increasing hydration concentration for YBG glass composition.

Table 5.20: Cation – cation clustering for YBG hydrated at fractions y=0.1, 0.2 and 0.3 and dry YBG

Species	Dry YBG-P		YBG-P y=0.1		YBG-P y=0.2		YBG-P y=0.3	
	Ratio	St.Dev	**Ratio**	St.Dev	**Ratio**	St.Dev	**Ratio**	St.Dev
Y – Y	**1.174**	0.048	**1.811**	0.095	**1.782**	0.056	**1.903**	0.066
Y – Na	**0.495**	0.070	**1.007**	0.025	**0.872**	0.054	**0.882**	0.051
Y – Ca	**0.381**	0.054	**1.064**	0.077	**1.140**	0.073	**1.084**	0.077
Na – Na	**0.675**	0.060	**1.180**	0.048	**1.216**	0.022	**1.145**	0.025
Na – Ca	**0.465**	0.066	**1.011**	0.067	**0.964**	0.070	**1.006**	0.024
Ca – Ca	**1.005**	0.072	**1.551**	0.033	**1.437**	0.031	**1.621**	0.043

The clustering ratios seen above for dry YBG compare well enough to simulation studies of yttrium bioglass YBG carried out by the work of Tilocca and Christie [115, 137]. From the table above, hydration generally causes an increase in clustering both for like pairs of cations and for unlike cation pairs. The trend seen from the above table is that cation - cation clustering for like pairs i.e. Y – Y, Na – Na and Ca – Ca are seen to increase as YBG is hydrated. As we see that hydrating the dry form of YBG progressively causes the Y – Y clustering to increase. This shows that not only will one typically find a hydroxyl group near an yttrium cation but also one will typically find another yttrium cation to which it is close. The same effect is seen for other like pairs i.e. Ca – Ca and Na – Na.

It seems as though the network-modifying species attract hydroxyl groups. Calcium is seen to do this the most, then yttrium and then sodium. Because these modifying ions attract the hydroxyls, this would cause them to be less available to silicon and allow for the breakage of fewer T - O - T bridges.

5.2.6 Bridging oxygens vs. Non-bridging oxygens

Table 5.21a: Percentage of bridging oxygens around network modifier ions sodium, yttrium and calcium

BO	Y		Ca		Na	
	%	St. Dev	%	St. Dev	%	St. Dev
Dry YBG-P	14.213	0.070	25.938	1.367	37.079	0.162
0.1	11.938	0.088	21.927	3.197	41.077	1.122
0.2	13.058	1.267	25.713	1.079	48.783	3.551
0.3	12.443	0.800	29.487	1.936	48.656	2.882

Table 5.21b: Percentage of non-bridging oxygens around network modifier ions sodium, yttrium and calcium

NBO	Y		Ca		Na	
	%	St. Dev	%	St. Dev	%	St. Dev
Dry YBG-P	85.787	3.254	74.062	4.208	62.921	2.796
0.1	79.519	2.856	71.214	3.452	56.287	0.556
0.2	77.905	2.581	69.105	1.294	48.828	3.829
0.3	77.268	2.346	66.418	2.196	48.370	1.623

Table 5.21c: Percentage of non-bridging & bridging oxygens and free oxygen ($^{-}$OH) around network modifier ions sodium, yttrium and calcium

YBG-P	Y		Ca		Na	
	NBO+BO Total %	(OH) %	NBO+BO Total %	(OH) %	NBO+BO Total %	(OH) %
DRY	100.000	n/a	100.000	n/a	100.000	n/a
0.1	91.457	8.543	93.141	6.859	97.364	2.636
0.2	90.963	9.037	94.818	5.182	97.610	2.390
0.3	89.711	10.289	95.904	4.096	97.026	2.974

1) Yttrium

From Table 5.21b it is seen that yttrium prefers to locate itself around a large number of non-bridging oxygen species for both hydrated and unhydrated forms of yttrium bioglass. Yttrium's coordination shell environment is dominated (85.8 %) by NBO's. Yttrium has an average coordination of 5.5 (unhydrated) to 6.1 (hydrated): the majority of these coordinated oxygen atoms are non-bridging oxygens. Yttrium cations have a +3 charge and the highest field strength of 0.6 compared to Ca and Na cations, which causes the preference for yttrium ions to be surrounded by non-bridging oxygen species in its coordination shell. This trend is seen in simulation studies of yttrium bioglass carried out by the work of Tilocca and Christie [115, 137].

After hydrating the yttrium bioglass, the percentage of non-bridging oxygens which surrounds yttrium decreases to ~80% when the yttrium bioglass is hydrated at 0.1. This shows yttrium, which still holds a total coordination of ~5.5 – 6.1, that non-bridging oxygen atoms are replaced by hydroxyl groups. The unhydrated form of YBG glass allowed ~86% of NBO's to surround yttrium. The percentage of NBO's decreases and this is due to hydroxyl groups substituting ~15% of the NBO's in unhydrated YBG with hydroxyl groups where yttrium is still able to maintain, if not increase, its coordination as the bioglass is progressively hydrated.

2) Calcium

Calcium prefers to locate itself around a large number of non-bridging oxygen species for both hydrated and unhydrated forms of yttrium bioglass. Calcium has the second most dominant amount of NBO's in its coordination shell environment i.e. 74%. Calcium has an average coordination of 5.98 for unhydrated yttrium bioglass, to 6.30 (Tables 5.15a, 5.15b and 5.15c), for the hydrated form of the same glass: the majority of these coordinated atoms are of non-bridging oxygens which surround calcium ions. Calcium cations have a +2 charge and the second highest field strength of 0.33, higher than sodium cations. Calcium is less attractive to NBO's than yttrium is as yttrium has higher field strength causing more NBO's to locate themselves around yttrium ions.

After hydrating the yttrium bioglass, the percentage of non-bridging oxygen atoms which surround calcium decreases to ~71 % when the yttrium bioglass is hydrated at 0.1. This shows calcium, which still holds a coordination of ~6, that non-bridging oxygen atoms are replaced by hydroxyl groups. The unhydrated form of YBG glass allowed 74 % of NBO's to surround calcium. As soon as the same glass is hydrated at a concentration of 0.1, a drop in the percentage of NBO's surrounding calcium is seen. The percentage of NBO's decreases and this is due to hydroxyl groups substituting ~5% of the NBOs in unhydrated YBG with hydroxyl groups where calcium is still able to maintain, if not increase, its coordination as the bioglass is progressively hydrated.

3) Sodium

Sodium has the smallest preference to locate itself around non-bridging oxygen species for both hydrated and unhydrated forms of yttrium bioglass. Sodium is least dominant compared to calcium and yttrium with respect to the percentage of NBO's in

each of their coordination shells i.e. 62 %. Sodium has an average coordination of 6.03 for unhydrated yttrium bioglass, to 6.30 (Tables 5.16a, 5.16b and 5.16c), for the hydrated form of the same glass, where 56 % NBO's surround calcium ions. Sodium cations have a +1 charge and the lowest field strength of 0.19. Having a low field strength of 0.19 causes the least attractive behaviour of sodium ions to be surrounded by non-bridging oxygen species which are found within the coordination shell environment of sodium. Sodium is less attractive to NBO's than calcium or yttrium is as yttrium and calcium have higher field strength to cause more NBO's to locate themselves within their coordination shells.

After hydrating the yttrium bioglass, the percentage of non-bridging oxygens which surround sodium decreases to ~56% when the yttrium bioglass is hydrated at 0.1. This shows sodium, which still holds a coordination of ~6, that non-bridging oxygens are replaced by hydroxyl groups. The unhydrated form of YBG glass allowed ~52% of NBO's to surround sodium. As soon as the same glass is hydrated at a concentration of 0.1, a drop in the percentage of NBO's surrounding sodium is seen. The percentage of NBO's decreases and this is due to hydroxyl groups substituting ~6% of the NBOs in unhydrated YBG with hydroxyl groups where sodium is still able to maintain, if not increase, its coordination as the bioglass is progressively hydrated.

5.2.7 Main Findings

Coordination is seen to increase for silicon, yttrium, calcium and sodium as yttrium bioglass is progressively hydrated from 0.1 – 0.3 (Tables 5.13a, 5.14a, 5.15a and 5.16a). The preference by which hydroxyl-oxygens coordinate to network-forming and modifying-cations is shown below:

$$Ca > Y > Na > Si$$

Calcium has the greatest ability in allowing hydroxyl-oxygen to coordinate to it, with yttrium, sodium and silicon having lower coordination to hydroxyl-oxygen. The increase in coordination is due to hydration effects where hydroxyl groups squeeze themselves into the coordination spheres, most easily with calcium, yttrium, sodium and then silicon. The more a YBG glass is hydrated the more hydroxyl groups will fit themselves into the coordination spheres of Ca, Y, Na and Si (Tables 5.13c, 5.14c, 5.15c and 5.16c).

The same order is observed as coordination of silicon, aluminium and yttrium with non hydroxyl-oxygen decreases. Calcium shows this effect the most and silicon the least, where coordination to non hydroxyl-oxygen decreases (Tables 5.13b, 5.14b, 5.15b and 5.16b)

As coordination of, for example, calcium decreases with non hydroxyl-oxygen, the coordination of calcium to hydroxyl-oxygen increases. Hydroxyl groups coordinate as a displacement to non hydroxyl-oxygens. Furthermore, the hydroxyl-oxygens not only displace non hydroxyl-oxygens but cause an overall increase in coordination. The same is seen for Si, Na and Y. (Tables 5.13a, 5.14a, 5.15a and 5.16a).

The overall silicon network connectivities are generally increasing as seen in Table 5.19 which shows that the silicate network is strengthening itself as yttrium bioglass is hydrated. By viewing Figure 5.20 we realise that this effect seen in Table 5.19 is due to shift in Q^n species from Q^0, Q^1 and Q^2 to Q^1, Q^2 and Q^3 with respect to hydration (Table 5.19).

The main intentions of simulating hydrated YBG-P glasses was to see if by removing phosphorus would change the glass characteristics in any shape or form. Initially (section 5.1.4) the overall phosphorus network connectivities were seen to increase as seen in Table 5.9b, which showed that the phosphate network was strengthening itself as YBG was hydrated. By viewing Figure 5.10b we realise that this

effect seen in Table 5.9b was due to shift in Q^n species from Q^0, Q^1 to Q^1, Q^2 and Q^3 with respect to hydration which caused this strengthening in phosphorus network. The reason why phosphorus was so very well interconnected into the glass network remains open to debate. For this reason we modelled glass compositions in which the phosphorus was removed since it showed high network connectivities that could not be explained and to see whether or not YBG glass without phosphorus had any impact on the glass i.e. whether silicon network connectivity, network-former or modifier coordination, cation-oxygen bond distances etc. were affected. After having simulated YBG-P (without phosphorus) the trends and results did not change with respect to YBG containing phosphorus. This shows that by removing phosphorus from a dry or hydrated YBG-P glass does not have any impact on the short range or medium range structure of the glass.

6 Conclusions

The express purpose of this thesis was to investigate how the hydration of various kinds of yttrium silicate glasses can modify the glass structure i.e. network connectivity and clustering and how these changes affect the glasses suitability for in situ radiotherapy . Results and further information gained from the deep probing of the glass structure allowed us to gain a meaningful insight as to how hydration affects these glasses, which are beyond the reach of current experimental techniques. In order to achieve this classical molecular dynamics simulations using DL_POLY were carried out on yttrium silicate glasses. Amongst the results from this investigation, the most important are now summarized.

Firstly, coordination is seen to increase for network formers and modifiers in all yttrium silicate glasses (YAS17, 24 and 30 / YBG / YBG-P) which are progressively hydrated. Generally, the more an yttrium silicate is hydrated the more the network formers and modifiers for each of the respective glasses will increase their overall coordination towards oxygen. The order by which hydroxyl-oxygens coordinate to network forming and modifying cations is shown below:

YAS	→	Y > Al ~ Si
YBG	→	Ca > Y > Na > Si ~ P
YBG-P	→	Ca > Y > Na > Si

In general it is seen that hydroxyl-oxygen prefers to coordinate with network-modifier cations rather than network-forming cations. The increase in coordination to network-modifier cations is due to hydration effects led by hydroxyl groups, which are linear, squeezing themselves into the coordination spheres, most easily with network-modifier cations than with network-forming cations. The more an yttrium silicate glass is hydrated the more hydroxyl groups will fit themselves into the coordination spheres of modifier cations than network-forming cations.

The same order is observed as coordination of network-forming cations and network-modifier cations with non hydroxyl-oxygen decreases. Modifiers show this effect the most and formers the least. It is realised that hydroxyl groups, prefer to be free in the glass environment and occupy space around network modifying cations instead.

As coordination of, for example, yttrium decreases with non hydroxyl-oxygen,

the coordination of yttrium to hydroxyl-oxygen increases. Hydroxyl groups coordinate as a displacement to non hydroxyl-oxygens. Furthermore, the hydroxyl-oxygens not only displace non hydroxyl-oxygens but cause an overall increase in coordination. The same is seen for other network modifier ions i.e. calcium and sodium where the effect is seen to a lesser extent. The same effect is also seen for network forming cations i.e. silicon, aluminium and phosphorus, where the effect is not as marked as found for network modifiers.

The difference between YAS glasses 17, 24 and 30 is the respective increase in yttrium content, where the silicon content decreases. The content of aluminium between the YAS glasses 17, 24 and 30 remains largely unchanged. It is seen that the more yttrium a YAS glass has when progressively hydrated, causes yttrium, aluminium and silicon to generally hold higher coordination numbers than compared to a YAS glass that contains less yttrium e.g. YAS17 (Figures 4.8a, 4.9a and 4.10a). The same effect is seen for aluminium and silicon but the effect is least marked for silicon. Hydroxyl groups tend to favour associating themselves to yttrium first then aluminium and lastly silicon as YAS glasses 17, 24 and 30 are hydrated. The more yttrium a YAS glass has the fewer hydroxyl groups would attach themselves onto yttrium, aluminium and silicon than compared to a YAS glass that has low yttrium content.

Of the following species only B and C were only observed in YAS glass:

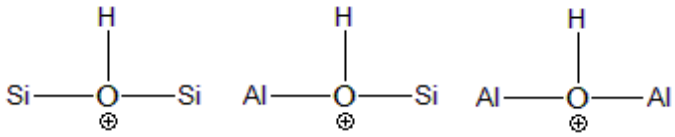

Figure 4.14 A B C

There is no correlation as to the number of species B and C increasing with respect to hydration concentration. What we do know is that these species do exist and they form from the presence of hydroxyl groups bridging between two aluminium atoms or a silicon and aluminium atom as demonstrated in B and C. Generally there were a greater number of B species than C species found in the YAS glass systems. A possible reason as to why species B forms is rationalized by stabilizing the charge on silicon which therefore causes the hydroxyl group to place itself between an aluminium and silicon. The reason for a hydroxyl group to place itself between two aluminium atoms as seen in C cannot be due to the same reason given earlier of charge stabilization

between Al and Si (B).

The overall silicon network connectivities of yttrium silicate glasses are seen to increase which shows that the silicate network is strengthening itself as YAS glasses or yttrium bioglasses (with and without phosphorus) are hydrated. This is due to the number of T – O – T (Si – O – Si) (where T = network-former species) bridges increasing with respect to hydration which causes this strengthening in silicon network found in YAS and YBG / YBG-P.

For YAS glasses, the overall aluminium network connectivities are generally decreasing which shows that the aluminate network is weakening itself as YAS glasses are hydrated. This is due to the number of (T – O – T) (Al – O – Al) (where T = network-former species) bridges decreasing with respect to hydration which causes the weakening of aluminium network in YAS glasses 17, 24 and 30.

For yttrium bioglass (YBG) hydroxyl groups promote the increase in phosphorus network connectivities. The phosphorus network strengthens itself as a reaction towards the hydroxyl groups integrating themselves into the yttrium bioglass structure thus increasing the number of T – O – T connections (where T = network-former specie). This is mainly due to phosphorus having mainly Q^0 and Q^1 speciation when not hydrated. Once YBG is hydrated, we then see a shift in distribution of the Q^n speciation to a large number of Q^2 and Q^3 species which gives rise to the overall increase in network connectivity. The reason why phosphorus is so very well interconnected into the glass network remains open to debate.

Having simulated YBG-P (without phosphorus) the trends and results did not change with respect to YBG containing phosphorus. This showed that by removing phosphorus from a dry or hydrated YBG-P glass has only minimal impact on the short range or medium range structure of the glass.

The network connectivity of a glass has a central role in determining the glass dissolution rate: a fragmented network with a low connectivity will dissolve faster in an aqueous environment [42]. For example, low-silica bioactive glasses have NC of approximately 2, whereas loss of bioactivity has been associated to NC approaching 3 in higher silica compositions. The central importance of the network connectivity in this context makes it a key structural factor for the possible use of a silica-based glass composition to store radionuclides, either in nuclear waste disposal or for *in situ* cancer radiotherapy. The incorporation of water in the form of hydroxyl groups in a glass

structure was in principle expected to disrupt the glass network: this is based on the assumption that protons act as additional network modifiers [154] and therefore the O_2^- → 2 OH^- substitution would break T – O − T bridges either directly (e.g., T – O − T + OH^- → T − O^- + T − OH) or indirectly (e.g., T – O ⋯ M + OH^- → T − OH + M^+, where M^+ is a free modifier cation which is able to break another T – O − T bridge). For example, the breakdown of the silica network (compared to melt-derived glasses) caused by the hydration process is often reported as one of the possible effects contributing to the extended range of bioactivity of sol−gel glasses [154]. The opposite effect is seen in hydrated yttrium silicate glasses in general (YAS17, 24 and 30 / YBG / YBG-P). What is seen in this work is that by modelling hydrated yttrium silicate glasses causes the strengthening of the glass network.

A more disrupted YAS or YBG network would be less stable in a physiological environment, affecting its performance for radiotherapy. In the short term, a faster yttrium release in the bloodstream from a rapidly dissolving glass would be a negative factor for the medical applications, which require the highest short-term durability to avoid releasing yttrium isotopes while they are radioactive. On the other hand, if short-term Y^{3+} release is not significantly affected, the possibility to enhance the long-term (post-radioactive decay of Y) biodegradation of YAS and YBG glasses into harmless products represents a very attractive option at present, since the long term effects of implanted YAS microparticles are not yet known. It was therefore important to investigate the effects of different hydration levels on the glass structure.

The earlier simulations show that the disruptive effect of OH^- on the glass network acts differently on the silicate and aluminate connectivity. For YAS and YBGP/YBG-P glasses the silicate NC increases slightly with respect to hydration, while the Al NC decreases for YAS glasses. This occurs for YAS glasses because OH^- mainly breaks Si − Al cross-links (possibly weaker than Si−Si and Al−Al), which dominate the Al connectivity, but not the Si connectivity. Another reason why the network breakdown is less than expected (instead strengthening) has to do with the presence of “free” OH groups highlighted by the simulations: as these are not directly bonded to either Si or Al, free hydroxyl groups do not affect the Si / Al ability to form T – O − T bridges. The driving force leading to the presence of free hydroxyl groups is the strong network modifier − OH interaction, which leads to the formation of stable aggregates of modifier and OH^- ions, separated from the aluminosilicate network. The marked modifier − OH

association with formation of nanosegregated modifier − OH regions could in principle accelerate the dissolution process of “solvated” modifier ions such as yttrium and their release from the glass matrix into the surrounding environment.

The relatively high abundance of free hydroxyl species that was detected in YAS and YBG+P/YBG-P also agrees with the experimental suggestion that their number increases when the glass contains modifier cations of higher field strength, such as Y^{3+} [155, 156]. The simulations also highlighted significant clustering of the free OH species but was not detected in experimental studies [157]. The high modifier − OH affinity appears to be the driving force for the separation of OH clusters in the YAS and YBG case: the nature of the modifier cations may be the key factor in determining the tendency to form free –OH domains in the glass.

In conclusion, the present simulations have highlighted that the incorporation of OH groups in an yttrium-doped silicate glass matrix introduces structural effects which may influence the dissolution behaviour of the glass in non-obvious ways. On one hand, the uneven distribution of OH groups between network former ions and their effects on T − O − T bridges increases the silicate network strength for YAS and YBG and disrupts the Al network for YAS glasses. At the same time, the formation of modifier – OH rich regions separated from the silicate matrix results in a significant portion of “free” OH groups which do not directly alter the strength of the glass network and the corresponding biodegradability but could affect the yttrium release rate. The identification of these fundamental effects is the first step toward a rationalization of the properties of hydrated YAS glasses for biomedical applications.

References

[1] Elliott S.R., Physics of Disordered Materials, Theory and Applications, 2nd edn. Longman, Essex, UK (1990)

[2] Zallen R., Physics of Amorphous Solids, Wiley, New York (1983)

[3] Drabold D.A., European physical journal. **B68**, 1434-6028 (2009)

[4] Hench L. L., Splinter R. J., Allen W. C., Greenlee Jr T. K. J., Biomed. Mater. Res. **2**, 117–141 (2001)

[5] Hench L. L., Polak J. M., Science. **295**, 1014–1017 (2002)

[6] Takada A., Cormack A. N., Phys. Chem. Glasses. **49**, 127–135 (2008)

[7] Herba M.J., Illescas F.F., Thirlwell M.P., Rosenthall L., Smith P., Radiology. **169,** 311 (1988)

[8] Herba M.J., Illescas F.F., Smith M.P., Cancer. **61,** 1336 (1983)

[9] Houle S., Yip T.K., Shepherd F.A., Rotstein L.E., Sniderman K.W., Theis E., Cawthorn R.H., Richmond-Cox K., Radiology. **172,** 857 (1989)

[10] Anderson J.H., Goldberg J.A., Bessent R.G., Kerr D.J., Mckllop J .H., Stewart I., Cooks T.G., Meardle C.S., Radiotherapy Oncol. **25,** 137 (1992)

[11] Burton M.A., Gray B.N., Jones C., Coletti A., Nucl. Med. Biol. **16,** 495 (1992)

[12] Shepherd F.A., Lotstein L.E., Houle S., Yip T.K., Paul K., Sniderman K.W., Cancer. **70,** 2250 (1992)

[13] Andrews J.C., Walker S.C., Ackermann R.J., Cotton L.A., Newsmonger W.D., Shapiro B., J. Nucl. Med. **35,** 1637 (1994)

[14] Ho S., Lau W. Y., Leung T. W. T., Johnson P. J., Cancer (N. Y.). **83**, 1894 (1998)

[15] Ehrhardt G.J., Day D.E., Nucl. Med. Bio. **14**, 233 (1987)

[16] Araki N., Nagata Y., Fujiwara K., Aoki T., Mitsumori M., Kimura H., Itasaka S., Saitou H., Hiraoka M., Kawashita M., Kokubo T., Nucl, Int. J. Radiat. Oncol. Biol. Phys. **14,** 459 (2001)

[17] Hyatt M.J., Day D.E., J .Am. Ceram. Soc. **70**, 283 (1987)

[18] Erbe E.M., Day D.E., J. Biomed. Mater. Res. **27**, 1301 (1993)

[19] Weast R.C., Lide D.R., Astle M.J., Beyer W.H., CRC Handbook of Chemistry and Physics, vol. B-28, CRC, Boca Raton FL, p. 231 (1989)

[20] Mantravadi R.V.P, Spignos D.G., Tan W.S., Felix E.L., Radiology. **142**, 783 (1982).

[21] Herba M.J., Illescas F.F., Thirlwell M.P., Rosenthall L., Smith P., Radiology. **169,** 311 (1988)

[22] Herba M.J., Illescas F.F., Smith M.P., Cancer. **61,** 1336 (1983)

[23] Yip T.K., Shepherd F.A., Cawthorn R.H., Richmond-Cox K., Radiology. **163**, 739 (1989)

[24] Kerr D.J., Mckllop J .H., Stewart I., Cooks T.G., Meardle C.S., Radiotherapy Oncol. **17**, 241 (1993).

[25] Jones C., Coletti A., Nucl. Med. Biol. **19**, 628 (1994)

[26] Houle S., Yip T.K., Paul K., Sniderman K.W., Cancer. **54**, 1728 (1994)

[27] Day D.E., Day T.E., An Introduction to Bioceramics, in: Hench L.L., Wilson J. (Eds.), World Sconce, Singapore,. p. 305 (1993)

[28] Ackermann R.J., Cotton L.A., Newsmonger W.D., Shapiro B., J. Nucl. Med. **24,** 1826 (1992)

[29] Li R., Clark A.E., Hench L.L., An investigation of bioactive glass powders by sol-gel processing. J. Appl. Biomater., **2**, 231–9 (1991)

[30] Brinker C.J., Scherer G.W. Sol–gel science. San Diego, CA: Academic Press (1990)

[31] Avnir D., Braun S. Biochemical aspects of sol-gel science and technology: a special issue of the journal o sol-gel science and technology. New York: Springer-Verlag, (1996)

[32] Nieto A., Areva S., Wilson T., Viitala R, Vallet-Regí M. Cell viability in a wet silica gel. Acta. Biomater. **5**, 3478–87 (2009)

[33] Zhong J., Greenspan D.C. Processing and properties of sol–gel bioactive glasses. J. Biomed. Mater. Res. **53**, 694–701 (2006)

[34] Hamadouche M., Meunier A., Greenspan D.C., Blanchat C., Zhong J.P., LaTorre G.P., et al. J. Biomed. Mater. Res. **54**, 560–6 (2004)

[35] Vallet-Regí M., Dalton. Trans. **44**, 5211–20 (2006)

[36] Vallet-Regí M., Balas F., Arcos D., Angew. Chem. Int. Ed. **46**, 7548–58 (2006)

[37] Du J., J. Am. Ceram. Soc. **92**, 87–95 (2009)

[38] Florian P., Sadiki N., Massiot D., Coutures J. P., J. Phys. Chem. B, **111**, 9747–9757 (2007)

[39] Erratum: Du J., Cormack A. N., J. Non-Cryst. Solids. **351**, 956 (2005)

[40] Pozdnyakova I., Sadiki N., Hennet L., Cristiglio V., Bytchkov A., Cuello G. J., Coutures J. P., Price D. L., J. Non-Cryst. Solids. **354**, 2038–2044 (2008)

[41] Tilocca A., Cormack A. N., J. Phys. Chem. C, **112**, 11936 (2008)

[42] Tilocca A., Christie. J. K., Chem. Mater. **22**, 3725–3734 (2010)

[43] Tilocca A., de Leeuw N. H., Cormack A. N., Phys. Rev. B: Condens. Matter. **73**, 104209 (2006)

[44] Tilocca A., Cormack A. N., de Leeuw N. H., Chem. Mater. **19**, 95–103 (2007)

[45] Pedone A., Malavasi G., Menziani M. C., J. Phys. Chem. C, **113**, 15723 (2009)

[46] Tilocca A., J. Chem. Phys., **129**, 084504 (2008)

[47] Gale J. D., Rohl A. L., Mol. Simul. **29**, 291 (2003)

[48] Christie J. K., Pedone A., Menziani M. C., Tilocca A., J. Phys. Chem. B, **115**, 2038 (2011)

[49] Priven A. I., Glass Technol. **45**, 244 (2004)

[50] Wilding M. C., Benmore C. J., McMillan P. F., J. Non-Cryst. Solids. **297**, 143–155 (2002)

[51] Tilocca A., J. Chem. Phys. **133**, 014701 (2010)

[52] Cormack A. N., Du J., Zeitler T. R., J. Non-Cryst. Solids. **323**, 147 (2003)

[53] Tilocca A., de Leeuw N. H., J. Phys. Chem. B, **110**, 25810 (2006)

[54] O'Donnell M. D., Hill R. G., Acta Biomater. **6**, 2382 (2010)

[55] Strnad Z., Biomaterials. **13**, 317 (1992)

[56] Jund P., Kob W., Jullien R., Phys. Rev. B: Condens. Matter. **64**, 134303 (2001)

[57] Huang C., Cormack A. N., J. Chem. Phys. **95**, 3634 (1991)

[58] Greaves G. N., J. Non-Cryst. Solids. **71**, 203 (1985)

[59] Wu H.-F., Lin C.-C., Shen P., J. Non-Cryst. Solids. **209**, 76 (1997)

[60] Li R., Clark A.E., Hench L. L., J. App. Biomat. **2**, 231-239 (1991)

[61] Ahmad M., Jones J. R., Hench L. L., Biomed. Mater. **2** , 6-10 (2007)

[62] Pereira M. M., Jones J. R., Hench L.L., Advances in Applied Ceramics. **104**, 35-42 (2005)

[63] Skipper L. J., Sowrey F. E., Pickup D. M., J. Mater. Chem. **15**, 2369-2374 (2005)

[64] Shirtliff V. J., Hench L. L., Bioceramics 16, Key Engineering Materials. **254**, 989-992 (2004)

[65] Saravanapavan P., Hench L. L., J. Non-Crystalline Solids. **318**, 1-13 (2003)

[66] Jones J. R., Hench L.L., Bioceramics 15 Key Engineering Materials. **240**, 209-212 (2003)

[67] Jones J. R., Sepulveda P., Hench L. L., Bioceramics 14 Key Engineering Materials. **218**, 299-302 (2002)

[68] Bellantone M., Hench L. L., Bioceramics 12 Key Engineering Materials. **192**, 617-620 (2000)

[69] Powers K. W., Hench L. L., Sol-Gel Synthesis and Processing Ceramic Transactions. **95** 173-182 (1998)

[70] Hench L. L., Current Opinion In Solid State & Materials Science. **2**, 604-610 (1997)

[71] Li R.N., Clark A.E., Hench L. L., Chemical Processing Of Advanced Materials. **24**, 627-633 (1992)

[72] Li R.N., Clark A.E., Hench L. L., J. Applied Biomater. **2**, 231-239 (1991)

[73] Hench L. L., West J. K., Chemical Reviews. **90**, 33-72 (1990)

[74] Newport R. J., Skipper L. J., Carta D., J. Mater. Sci-Mater. Medic. **17**, 1003-1010 (2006)

[75] Tilocca A., Cormack A. N., de Leeuw N. H., Chem. Mater. **19**, 95–103 (2007).

[76] Frenkel D., Smit B., Understanding Molecular Simulations: From Algorithms to Applications, 2nd ed. Academic Press: New York (1996)

[77] Car R., Parrinello M., Phys. Rev. Lett. **55**, 2471–2474. 509 (1985)

[78] Ispas S., Benoit M., Jund P., Jullien R., Phys. Rev. B, **64**, 214206 (2001)

[79] Donadio D., Bernasconi M., Tassone F., Phys. Rev. B, **70**, 214205 (2004)

[80] Massobrio C., Celino M., Pasquarello A., Phys. Rev. B, **70**, 174202 (2004)

[81] Tilocca A., de Leeuw N. H., J. Phys. Chem. B, **110**, 25810 (2006)

[82] Tilocca A., Phys. Rev. B, **76**, 224202 (2007)

[83] Tilocca. A., Cormack A. N., J. Phys. Chem. B, **111**, 14256 (2007)

[84] Tilocca A., Proc. R. Soc. A, **465**, 1003–1027 (2009)

[85] Tilocca A., Cormack A. N., Nuovo. Cimento. B, **123**, 1415 (2008)

[86] Lammert H., Heuer A., Phys. Rev. B, **72**, 214202 (2005)

[87] Woodcock L. V., Angell C. A., Cheeseman P. J., Chem. Phys. **65**, 1565–1577 (1976)

[88] Huang C., Cormack A. N. J., Chem. Phys. **95**, 3634–3642 (1991)

[89] Smith W., Greaves G. N., Gillan M. J., J. Chem. Phys. **103**, 3091–3097 (1995)

[90] Tilocca A., de Leeuw N. H., J. Phys. Chem. B**, 110**, 25810–25816 (2006)

[91] Lammert H., Heuer A., Phys. Rev. B**, 72**, 214202 (2005)

[92] Mead R. N., Mountjoy G. J., Phys. Chem. B, **110**, 14273–14278 (2006)

[93] Van Beest B.W. H., Kramer G. J., Van Santen R. A., Phys. Rev. Lett. **64**, 1955–1958 (2001)

[94] Vollmayr K., Kob J., Binder W., W. Phys. Rev. B**, 54**, 15808–15827 (1996)

[95] Yuan X., Cormack A. N., J. Non-Cryst. Solids. **283**, 69–87 (2001)

[96] Machacek J., Gedeon O., Phys. Chem. Glasses. **44**, 308–312 (2003)

[97] Yu H., van Gunsteren W. F., Comp. Phys. Commun. **172**, 69–85 (2002)

[98] Hench L.L., West J.K., Chem. Rev. **90**, 33–72 (1990)

[99] Zarzycki J., J. Sol-Gel. Sci. Technol. **8**, 1–6 (1997)

[100] Zyrina N. V., Antipova V. N., Zheleznaya L. A., Microbio. Lett. **351**, 1-6 (2014)

[101] Kangawa Y., Akiyama T., Ito T., Materials. **6**, 3309-3360 (2013)

[102] Maris P., Vary J. P. International Journal Of Modern Physics. **22**, 13 (2007)

[103] Woodruff D. P., Chemical Reviews. **113**, 3863-3886 (2013)

[104] Rimola A., Costa D., Sodupe M.,. Chemical Reviews. **113**, 4216-4313 (2013)

[105] Barrett B. R., Navratil P., Vary J. P., Progress In Particle And Nuclear Physics. **69**, 131-181 (2013)

[106] Duerr M., Hoefer U., Progress In Surface Science. **88,** 61-101 (2013)

[107] Mirabella S., De Salvador D., Napolitani E., J. Appl. Phys. **113**, 3 (2013)

[108] Haag M. P., Reiher M., Inter. J. Quant. Chem. **113**, 8-20 (2013)

[109] Hill J. G., Inter. J. Quant. Chem. **113**, 21-34 (2013)

[110] Ho S., Lau W. Y., Leung T. W. T., Johnson P. J., Cancer. **83**, 1894 (1998)

[111] Hench L. L., Day D. E., Holand W., Rheinberger V. M., Int. J. Appl. Glass Sci. **1**, 104 (2010)

[112] Roberto W. S., Pereira M. M., Campos T. P. R., Artif. Organs. **27**, 432 (2003)

[113] Hench L. L., J. Am. Ceram. Soc. **81**, 1705–1728 (1998)

[114] Tilocca A., J. Mater. Chem., **20**, 6848 (2010)

[115] Malik J., Christie J. K., Tilocca A., J Phys. Chem. Chem. Phys. **13**, 17749-17755 (2011)

[116] Tilocca A., de Leeuw N. H., Cormack A. N., Phys. Rev. B**, 73**, 104209 (2006)

[117] Jensen F., Introduction to Computational Chemistry, Wiley, Second Edition (2007)

[118] Gale J. D., Bush T. S., Catlow C. R. A., J. Mater. Chem. **4**, 831–837 (1994)

[119] Tilocca A., Proc. Royal Soc. A**, 465**, 1003–27 (2009)

[120] Hertz A., Bruce I. J., Nanomedicine. **2**, 899–918 (2007)

[121] Cerruti M., Greenspan D., Powers K., Biomaterials. **26**, 1665–1674 (2005)

[122] Sanbonmatsu K. Y., Tung C. S., J. Struc. Biol. **157**, 470–480 (2007)

[123] Schulz R., Lindner B., Petridis L., Smith J. C., J. Chem. Theory Comput. **5**, 2798–2808 (2009)

[124] Allen M. P., Tildesley D. J., Computer Simulations of Liquids Oxford University Press (1989)

[125] Frenkel D., Smit B. J. Understanding Molecular Simulation: From Algorithms to Applications Academic Press, San Diego, California (2001)

[126] Freddolino P. L., Arkhipov A. S., Larson S. B., McPherson A., Schulten K., Structure.

14, 437–449 (2006)

[127] Tilocca A., Cormack A. N., J. Phys. Chem. C, **112**, 11936–11945 (2006)

[128] Dick B. G., Overhauser A. W., Phys Rev. **112**, 90-103 (1958)

[129] Smith W., Forester T. R., DL_POLY_2.0: A general-purpose parallel molecular dynamics simulation package. J. Mol. Graphics, **14**, 136−141 (1996)

[130] Kerisit S., Parker S. C., J. Am. Chem. Soc. **126**, 10152–10161 (2004)

[131] Spangberg D., Hermansson K. J., Chem. Phys. **120**, 4829–4843 (2004)

[132] Rosen J., Warschkow O., McKenzie D. R., Bilek M., J. Chem. Phys. **126**, 204709 (2007)

[133] Tilocca A., de Leeuw N. H., Cormack A. N., Phys. Rev. B, **73**, 104209 (2006)

[134] Sanders M. J., Leslie M., Catlow C. R. A., J. Chem. Soc., Chem. Commun. 1273 (1984)

[135] Gale J. D., Rohl A. L., Mol. Simul. **29**, 291 (2003)

[136] Schröder K. P., Sauer J., Leslie M., Catlow C. R. A., Chem. Phys. Lett. **188**, 320 (1992)

[137] Tilocca A. Christie J. K., Chem. Mater. Chem., **22,** 12023 (2012)

[138] Du Z., de Leeuw N. H., Dalton Trans. **12**, 2623–2634 (2006)

[139] Tilocca A., Cormack A. N., de Leeuw N. H., Chem. Mater. **19**, 95–103 (2007)

[140] Tilocca A., Cormack A. N., J. Phys. Chem. B, **111**, 14256 (2007)

[141] Mead R. N., Mountjoy G., J. Phys. Chem. B, **110**, 14273–14278 (2006)

[142] Du J., J. Am. Ceram. Soc. **92**, 87–95 (2009)

[143] Pozdnyakova I., Sadiki N., Hennet L., Cristiglio V., Bytchkov A., Cuello G. J., Coutures J. P., Price D. L., J. Non-Cryst. Solids, **354**, 2038–2044 (2008)

[144] Florian P., Sadiki N., Massiot D., Coutures J. P., J. Phys. Chem. B, **111**, 9747–9757 (2007)

[145] Schaller T., Stebbins J. F., J. Phys. Chem. B, **102**, 10690–10697 (1998)

[146] Sen S., Youngman R. E., J. Phys. Chem. B, **108**, 7557–7564 (2004)

[147] Du J., Benmore C. J., Corrales R., Hart R. T., Weber J. K. R., J. Phys. Condens. Matter, **21**, 205102 (2009)

[148] Wilding M. C., Benmore C. J., McMillan P. F., J. Non-Cryst. Solids. **297**, 143–155 (2002)

[149] Tilocca A., Proc. R. Soc. A, **465**, 1027 (2009)

[150] McCarthy M. C., Woon D. E., Tamassia F., Chemical Physics. **128**, 184301 (2008)

[151] Jones J. R., Smith M. E., Lin, Pike. J. K., J. Mater. Chem. **19**, 1276–1282 (2009)

[152] Mead R. N., Mountjoy G., Chem. Mater. **18**, 3956–3964 (2006)

[153] Xue X., Amer. Mineral. **94**, 395–398 (2009)

[154] Jones J. R., Sol-Gel Derived Glasses for Medicine. In Bio-Glasses, John Wiley & Sons, Ltd: Chichester, 29−44 (2012)

[155] Xue X., Kanzaki M., Solid State Nucl. Magn. Reson. **31**, 10−27 (2007)

[156] Zeng Q., Nekvasil H., Grey C. P., J. Phys. Chem. B, **103**, 7406−7415 (1999)

[157] Eckert H., Yesinowski J. P., Silver L. A., Stolper E. M., J. Phys. Chem. **92**, 2055−2064 (1988)

Appendix

1a) Supplementary Material – YAS17

Here, listed in tables are other relevant information regarding the simulations whereby YAS17 was hydrated.

1) Silicon Q^n Distribution

Si Qn (%)								
n	**YAS17_SM2**		**YAS17 y=0.1**		**YAS17 y=0.2**		**YAS17 y=0.3**	
0.0	0.0023	0.0033	0.0000	0.0000	0.0039	0.0055	0.0000	0.0000
1.0	3.2308	1.4315	2.0029	0.3659	3.0291	0.1883	2.2859	1.1760
2.0	21.2093	0.0296	14.9221	4.5008	17.9116	1.7110	18.2771	3.5805
3.0	46.1413	2.2257	46.4236	2.2337	42.8950	1.7047	46.3866	3.9047
4.0	29.4163	0.7680	36.6514	2.6330	36.1566	0.1773	33.0440	1.5093
5.0	0.0000	0.0000	0.0000	0.0000	0.0000	0.0008	0.0064	0.0090
6.0	0.0000	0.0000	0.0000	0.0000	0.0000	0.0000	0.0000	0.0000
7.0	0.0000	0.0000	0.0000	0.0000	0.0000	0.0000	0.0000	0.0000
8.0	0.0000	0.0000	0.0000	0.0000	0.0000	0.0000	0.0000	0.0000
9.0	0.0000	0.0000	0.0000	0.0000	0.0000	0.0000	0.0000	0.0000
10.0	0.0000	0.0000	0.0000	0.0000	0.0000	0.0000	0.0000	0.0000
NC	3.0174	0.0211	3.1772	0.0787	3.1216	0.0118	3.1021	0.0026

2) Silicon Q^n Distribution – Si - O - Al

SiQn (%)								
n	**YAS17_SM2**		**YAS17 y=0.1**		**YAS17 y=0.2**		**YAS17 y=0.3**	
0.0	12.4244	0.2352	18.0990	1.9911	14.8326	1.2152	14.9963	0.8422
1.0	30.4738	0.3790	33.0690	2.5116	36.7948	2.2981	35.6029	1.7554
2.0	34.0797	0.7556	30.0085	2.0512	25.9359	2.1199	32.9849	0.1250
3.0	17.1994	3.5150	13.2953	2.9764	17.0126	0.6279	11.6215	1.0434
4.0	4.9093	1.9141	4.2981	0.5235	4.6496	1.0930	3.6318	0.1261
5.0	0.9122	0.2294	1.0684	0.1099	0.6052	0.8378	1.1560	0.3768
6.0	0.0012	0.0016	0.1610	0.2278	0.1694	0.1540	0.0066	0.0044
7.0	0.0000	0.0000	0.0006	0.0008	0.0000	0.0000	0.0000	0.0000
8.0	0.0000	0.0000	0.0000	0.0000	0.0000	0.0000	0.0000	0.0000
9.0	0.0000	0.0000	0.0000	0.0000	0.0000	0.0000	0.0000	0.0000
10.0	0.0000	0.0000	0.0000	0.0000	0.0000	0.0000	0.0000	0.0000
NC	1.7444	0.0016	1.5648	0.0104	1.6235	0.0105	1.5678	0.0022

3) Silicon Q^n Distribution – Si - O - Si

SiQn (%)								
n	**YAS17_SM2**		**YAS17 y=0.1**		**YAS17 y=0.2**		**YAS17 y=0.3**	
0.0	16.7151	3.3875	9.3200	2.9038	8.3512	1.1396	7.8308	0.0255
1.0	39.4285	4.7697	27.3539	0.8611	33.1370	1.3876	32.6390	2.0235
2.0	30.8593	1.6559	40.6583	4.1689	38.2048	1.6661	39.5481	0.7674
3.0	12.5663	0.4720	19.7605	0.8156	18.7126	2.9372	17.6473	1.9563
4.0	0.4308	0.1982	2.9074	0.4117	1.5944	1.0231	2.3349	0.8091
5.0	0.0000	0.0000	0.0000	0.0000	0.0000	0.0000	0.0000	0.0000
6.0	0.0000	0.0000	0.0000	0.0000	0.0000	0.0000	0.0000	0.0000
7.0	0.0000	0.0000	0.0000	0.0000	0.0000	0.0000	0.0000	0.0000
8.0	0.0000	0.0000	0.0000	0.0000	0.0000	0.0000	0.0000	0.0000
9.0	0.0000	0.0000	0.0000	0.0000	0.0000	0.0000	0.0000	0.0000
10.0	0.0000	0.0000	0.0000	0.0000	0.0000	0.0000	0.0000	0.0000
NC	1.4057	0.0208	1.7958	0.0668	1.7206	0.0000	1.7402	0.0555

4) Aluminium Q^n Distribution

Al Qn (%)

n	YAS17_SM2		YAS17 y=0.1		YAS17 y=0.2		YAS17 y=0.3	
0.0	0.0000	0.0000	0.0000	0.0000	0.0000	0.0000	0.0000	0.0000
1.0	0.0000	0.0000	0.2451	0.3466	0.4902	0.0000	0.2451	0.3466
2.0	0.2186	0.3092	2.3480	1.5321	6.1105	1.2982	5.2971	0.8139
3.0	9.3412	0.6101	24.7526	1.9499	23.1431	0.7196	26.5056	1.2890
4.0	71.6127	2.6801	56.7605	5.2765	48.3490	4.9220	48.3614	1.1961
5.0	18.2559	3.0627	15.5016	4.3928	19.7072	2.1361	17.8902	2.9643
6.0	0.5716	0.5366	0.3853	0.1095	2.2000	0.7681	1.7007	0.9465
7.0	0.0000	0.0000	0.0069	0.0097	0.0000	0.0000	0.0000	0.0000
8.0	0.0000	0.0000	0.0000	0.0000	0.0000	0.0000	0.0000	0.0000
9.0	0.0000	0.0000	0.0000	0.0000	0.0000	0.0000	0.0000	0.0000
10.0	0.0000	0.0000	0.0000	0.0000	0.0000	0.0000	0.0000	0.0000
NC	4.0962	0.0536	3.8611	0.0472	3.8727	0.0036	3.8346	0.0177

5) Aluminium Q^n Distribution – Al - O - Si

Al Qn (%)

n	YAS17_SM2		YAS17 y=0.1		YAS17 y=0.2		YAS17 y=0.3	
0.0	0.9794	0.6946	1.6765	0.4021	2.3353	0.5962	1.9922	0.0444
1.0	6.2029	1.8565	12.7101	0.8259	11.8807	4.1368	12.7673	0.2431
2.0	21.2922	0.8014	32.2199	1.6827	25.9719	4.0060	31.0124	2.4300
3.0	41.1176	3.1889	32.3346	4.8518	36.4578	1.1605	33.4353	2.3931
4.0	24.2873	0.9137	16.4673	1.2885	17.7464	2.3524	15.7225	0.2787
5.0	4.5265	0.2371	3.8624	1.5533	4.2608	0.7237	4.2500	1.0274
6.0	1.5176	0.0055	0.5761	0.1197	1.1585	0.1835	0.6072	0.7672
7.0	0.0765	0.0804	0.1529	0.2163	0.1886	0.1863	0.2131	0.2320
8.0	0.0000	0.0000	0.0000	0.0000	0.0000	0.0000	0.0000	0.0000
9.0	0.0000	0.0000	0.0000	0.0000	0.0000	0.0000	0.0000	0.0000
10.0	0.0000	0.0000	0.0000	0.0000	0.0000	0.0000	0.0000	0.0000
NC	3.0156	0.0074	2.6386	0.0176	2.7376	0.0177	2.6437	0.0036

6) Aluminium Q^n Distribution – Al - O - Al

Al Qn (%)

n	YAS17_SM2		YAS17 y=0.1		YAS17 y=0.2		YAS17 y=0.3	
0.0	16.8618	3.5480	13.7549	0.0277	16.3261	0.9363	12.5294	2.8617
1.0	38.2520	4.2579	31.0209	4.3360	31.1650	2.2040	36.2366	1.1933
2.0	29.6431	0.6406	33.6206	1.5820	30.8984	4.1128	31.6771	2.6602
3.0	12.3333	1.8163	17.4252	2.8594	14.6408	1.8473	14.3176	2.1047
4.0	2.6627	0.1192	3.9147	0.4506	6.2275	0.1081	4.1748	0.4293
5.0	0.2471	0.3466	0.2637	0.3730	0.7422	0.7667	1.0556	0.2681
6.0	0.0000	0.0000	0.0000	0.0000	0.0000	0.0000	0.0088	0.0125
7.0	0.0000	0.0000	0.0000	0.0000	0.0000	0.0000	0.0000	0.0000
8.0	0.0000	0.0000	0.0000	0.0000	0.0000	0.0000	0.0000	0.0000
9.0	0.0000	0.0000	0.0000	0.0000	0.0000	0.0000	0.0000	0.0000
10.0	0.0000	0.0000	0.0000	0.0000	0.0000	0.0000	0.0000	0.0000
NC	1.4642	0.0230	1.6752	0.0747	1.6550	0.0475	1.6457	0.0731

7) Total Silicon Coordination (OH+O)

TOTAL (Oc+OHc) Si - O (%)

n	**YAS17_SM2**		**YAS17 y=0.1**		**YAS17 y=0.2**		**YAS17 y=0.3**	
1.0	0.0000	0.0000	0.0000	0.0000	0.0000	0.0000	0.0000	0.0000
2.0	0.0000	0.0000	0.0000	0.0000	0.0000	0.0000	0.0000	0.0000
3.0	0.4017	0.3560	0.6605	0.1118	0.7025	0.0677	1.1422	0.3366
4.0	99.5983	0.3560	99.3395	0.1118	99.2969	0.0669	98.8514	0.3456
5.0	0.0000	0.0000	0.0000	0.0000	0.0006	0.0008	0.0064	0.0090
6.0	0.0000	0.0000	0.0000	0.0000	0.0000	0.0000	0.0000	0.0000
7.0	0.0000	0.0000	0.0000	0.0000	0.0000	0.0000	0.0000	0.0000
8.0	0.0000	0.0000	0.0000	0.0000	0.0000	0.0000	0.0000	0.0000
9.0	0.0000	0.0000	0.0000	0.0000	0.0000	0.0000	0.0000	0.0000
10.0	0.0000	0.0000	0.0000	0.0000	0.0000	0.0000	0.0000	0.0000
AVERAGE	3.9960	0.0036	3.9934	0.0011	3.9930	0.0007	3.9886	0.0033

8) Partial Silicon Coordination (O)

Oc Si - O (%)

n	**YAS17 y=0.1**		**YAS17 y=0.2**		**YAS17 y=0.3**	
1.0	0.0000	0.0000	0.0000	0.0000	0.0000	0.0000
2.0	0.0238	0.0337	0.1488	0.2105	0.4360	0.6167
3.0	9.2959	4.1020	23.5704	3.1072	33.3880	2.0183
4.0	90.6802	4.1358	76.2808	3.3177	66.1760	2.6349
5.0	0.0000	0.0000	0.0000	0.0000	0.0000	0.0000
6.0	0.0000	0.0000	0.0000	0.0000	0.0000	0.0000
7.0	0.0000	0.0000	0.0000	0.0000	0.0000	0.0000
8.0	0.0000	0.0000	0.0000	0.0000	0.0000	0.0000
9.0	0.0000	0.0000	0.0000	0.0000	0.0000	0.0000
10.0	0.0000	0.0000	0.0000	0.0000	0.0000	0.0000
AVERAGE	3.9066	0.0417	3.7613	0.0353	3.6574	0.0325

9) Partial Silicon Coordination (OH)

Ohc Si - O (%)

n	**YAS17 y=0.1**		**YAS17 y=0.2**		**YAS17 y=0.3**	
0.0	91.3169	4.0576	76.9793	3.3911	67.3118	2.3074
1.0	8.6831	4.0576	22.8754	3.1855	32.2521	1.6908
2.0	0.0000	0.0000	0.1453	0.2056	0.4360	0.6167
3.0	0.0000	0.0000	0.0000	0.0000	0.0000	0.0000
4.0	0.0000	0.0000	0.0000	0.0000	0.0000	0.0000
5.0	0.0000	0.0000	0.0000	0.0000	0.0000	0.0000
6.0	0.0000	0.0000	0.0000	0.0000	0.0000	0.0000
7.0	0.0000	0.0000	0.0000	0.0000	0.0000	0.0000
8.0	0.0000	0.0000	0.0000	0.0000	0.0000	0.0000
9.0	0.0000	0.0000	0.0000	0.0000	0.0000	0.0000
10.0	0.0000	0.0000	0.0000	0.0000	0.0000	0.0000
AVERAGE	0.0868	0.0406	0.2317	0.0360	0.3312	0.0292

10) Total Aluminium Coordination (OH+O)

TOTAL (Oc+OHc) Al – O (%)

n	**YAS17_SM2**		**YAS17 y=0.1**		**YAS17 y=0.2**		**YAS17 y=0.3**	
1.0	0.0000	0.0000	0.0000	0.0000	0.0000	0.0000	0.0000	0.0000
2.0	0.0000	0.0000	0.0000	0.0000	0.0000	0.0000	0.0000	0.0000
3.0	0.0000	0.0000	0.0000	0.0000	0.0010	0.0014	0.0029	0.0042
4.0	77.4294	3.4468	75.2438	4.0023	67.4065	6.5682	65.5758	2.6186
5.0	21.9980	2.9116	23.9977	4.3901	30.0565	4.7885	30.0729	1.0958
6.0	0.5725	0.5352	0.7516	0.3975	2.5340	1.7839	4.3239	1.5616
7.0	0.0000	0.0000	0.0069	0.0097	0.0020	0.0028	0.0245	0.0347
8.0	0.0000	0.0000	0.0000	0.0000	0.0000	0.0000	0.0000	0.0000
9.0	0.0000	0.0000	0.0000	0.0000	0.0000	0.0000	0.0000	0.0000
10.0	0.0000	0.0000	0.0000	0.0000	0.0000	0.0000	0.0000	0.0000
AVERAGE	4.2314	0.0398	4.2552	0.0362	4.3513	0.0835	4.3879	0.0412

11) Partial Aluminium Coordination (O)

Oc Al – O (%)

n	**YAS17 y=0.1**		**YAS17 y=0.2**		**YAS17 y=0.3**	
1.0	0.0000	0.0000	0.0000	0.0000	0.0000	0.0000
2.0	0.0000	0.0000	0.9941	0.9400	1.7333	0.6017
3.0	4.3458	3.0512	18.6693	2.6657	22.3824	6.7938
4.0	78.6114	0.9118	67.8085	4.1918	63.4487	5.6102
5.0	16.2905	4.3586	11.1422	0.7390	11.8092	0.8384
6.0	0.7454	0.4053	1.3859	1.3250	0.6265	0.2565
7.0	0.0069	0.0097	0.0000	0.0000	0.0000	0.0000
8.0	0.0000	0.0000	0.0000	0.0000	0.0000	0.0000
9.0	0.0000	0.0000	0.0000	0.0000	0.0000	0.0000
10.0	0.0000	0.0000	0.0000	0.0000	0.0000	0.0000
AVERAGE	4.1346	0.0663	3.9326	0.0263	3.8721	0.0592

12) Partial Aluminium Coordination (OH)

Ohc Al – O (%)

n	**YAS17 y=0.1**		**YAS17 y=0.2**		**YAS17 y=0.3**	
0.0	87.9346	3.0040	63.9922	8.9151	55.8225	10.8548
1.0	12.0654	3.0040	30.9209	7.2421	37.7761	10.9611
2.0	0.0000	0.0000	4.3088	1.2770	5.4020	0.6073
3.0	0.0000	0.0000	0.7781	0.3961	0.9993	0.7136
4.0	0.0000	0.0000	0.0000	0.0000	0.0000	0.0000
5.0	0.0000	0.0000	0.0000	0.0000	0.0000	0.0000
6.0	0.0000	0.0000	0.0000	0.0000	0.0000	0.0000
7.0	0.0000	0.0000	0.0000	0.0000	0.0000	0.0000
8.0	0.0000	0.0000	0.0000	0.0000	0.0000	0.0000
9.0	0.0000	0.0000	0.0000	0.0000	0.0000	0.0000
10.0	0.0000	0.0000	0.0000	0.0000	0.0000	0.0000
AVERAGE	0.1207	0.0300	0.4187	0.1098	0.5158	0.1003

13) Total Yttrium Coordination (OH+O)

TOTAL (Oc+OHc) Y – O (%)

n	YAS17_SM2		YAS17 y=0.1		YAS17 y=0.2		YAS17 y=0.3	
1.0	0.0000	0.0000	0.0000	0.0000	0.0000	0.0000	0.0000	0.0000
2.0	0.0000	0.0000	0.0000	0.0000	0.0000	0.0000	0.0000	0.0000
3.0	0.0000	0.0000	0.0000	0.0000	0.0000	0.0000	0.0000	0.0000
4.0	2.1446	0.5949	0.5315	0.5580	0.2337	0.3305	0.6348	0.1015
5.0	15.3152	0.0922	12.6446	1.9077	11.4957	1.5864	9.8453	2.0194
6.0	38.0391	1.9184	38.7167	0.1486	40.4659	1.9379	34.0301	1.3584
7.0	33.9717	2.5210	34.8909	1.8943	34.1982	0.8859	38.7525	0.1809
8.0	9.7630	0.7317	11.6746	0.4468	12.2366	2.9611	14.0091	2.8894
9.0	0.7652	0.5565	1.5188	0.2757	1.3207	1.0499	2.4496	0.0436
10.0	0.0011	0.0015	0.0228	0.0292	0.0493	0.0687	0.2786	0.3653
AVERAGE	6.3619	0.0190	6.4918	0.0108	6.5087	0.0939	6.6412	0.0977

Oc Y – O (%)

n	YAS17 y=0.1		YAS17 y=0.2		YAS17 y=0.3	
1.0	0.0000	0.0000	0.0000	0.0000	0.6384	0.9028
2.0	0.2717	0.3843	0.5819	0.6938	4.8388	1.3317
3.0	0.5250	0.0753	10.4094	0.4806	13.4772	0.5857
4.0	10.1029	2.0793	25.3065	1.1498	30.1330	2.2694
5.0	32.0442	0.8598	30.1482	1.0212	29.0167	0.3177
6.0	33.0848	1.5556	22.3938	2.2407	16.5308	2.0255
7.0	19.5920	0.4099	8.8634	1.7222	4.5207	0.3828
8.0	3.9257	0.6707	1.9931	0.8060	0.8446	0.4658
9.0	0.4536	0.1373	0.3036	0.2787	0.0000	0.0000
10.0	0.0000	0.0000	0.0000	0.0000	0.0000	0.0000
AVERAGE	5.7389	0.0558	4.9944	0.0199	4.5395	0.0571

14) Partial Yttrium Coordination (O)

Ohc Y – O (%)

n	YAS17 y=0.1		YAS17 y=0.2		YAS17 y=0.3	
0.0	36.2902	0.9915	11.5207	5.0281	3.9348	1.9891
1.0	53.0141	5.3663	40.4594	0.8598	23.5942	5.0092
2.0	9.8130	3.2588	34.5721	4.9462	39.8504	0.2434
3.0	0.8826	1.1160	11.9710	0.2470	25.0986	3.1471
4.0	0.0000	0.0000	1.4768	1.0248	6.0678	0.4176
5.0	0.0000	0.0000	0.0000	0.0000	1.4170	0.2516
6.0	0.0000	0.0000	0.0000	0.0000	0.0373	0.0497
7.0	0.0000	0.0000	0.0000	0.0000	0.0000	0.0000
8.0	0.0000	0.0000	0.0000	0.0000	0.0000	0.0000
9.0	0.0000	0.0000	0.0000	0.0000	0.0000	0.0000
10.0	0.0000	0.0000	0.0000	0.0000	0.0000	0.0000
AVERAGE	0.7529	0.0450	1.5142	0.0739	2.1017	0.0406

15) Partial Yttrium Coordination (OH)

16) YAS17 Dry and Hydrated Clustering Ratios

Clustering R = N(obs)/N(hom)								
Species	**YAS17_SM2**		**YAS17+H y=0.1**		**YAS17+H y=0.2**		**YAS17+H y=0.3**	
OH – Si			**0.868**	0.0819	**0.788**	0.0166	**0.848**	0.0466
OH – Al			**0.476**	0.0691	**0.690**	0.0671	**0.684**	0.0832
OH – Y			**1.748**	0.0585	**1.726**	0.0179	**1.744**	0.0138
Y – Y	1.102	0.0032	**1.308**	0.0292	**1.333**	0.0145	**1.379**	0.0010
Y – Si	1.179	0.2059	**1.099**	0.0005	**1.072**	0.0076	**1.009**	0.0343
Y – Al	1.018	0.0138	**1.061**	0.0231	**1.007**	0.0038	**0.991**	0.0314
Si – Si	1.257	0.0044	**1.449**	0.0389	**1.499**	0.0104	**1.486**	0.0575
Si – Al	1.135	0.0276	**0.998**	0.0031	**1.133**	0.0039	**1.030**	0.1118
Al – Al	1.480	0.0340	**1.785**	0.0355	**1.594**	0.0038	**1.636**	0.0078

17) A) Partial Yttrium Coordination due to Hydroxyls

B) Hydroxyl Coordination to Yttrium (Free OH)

C) Hydroxyls Coordinated to Yttrium attached to Si or Al

A) Ohc Y – O (%)						
n	**YAS17+H y=0.1**		**YAS17+H y=0.2**		**YAS17+H y=0.3**	
1.0	53.014	5.366	40.459	0.860	23.594	5.009
2.0	9.813	3.259	34.572	4.946	39.850	0.243
3.0	0.883	1.116	11.971	0.247	25.099	3.147
4.0	0.000	0.000	1.477	1.025	6.068	0.418
5.0	0.000	0.000	0.000	0.000	1.417	0.252
6.0	0.000	0.000	0.000	0.000	0.037	0.050
7.0	0.000	0.000	0.000	0.000	0.000	0.000
8.0	0.000	0.000	0.000	0.000	0.000	0.000
9.0	0.000	0.000	0.000	0.000	0.000	0.000
10.0	0.000	0.000	0.000	0.000	0.000	0.000
AVERAGE	**0.753**	0.045	**1.514**	0.074	**2.102**	0.041
	0.75288042		1.51423908		2.10170653	
B) FREE ONLY Ohc Y – O (%)						
n	**YAS17+H y=0.1**		**YAS17+H y=0.2**		**YAS17+H y=0.3**	
1.0	0.275	0.388	1.570	0.683	2.114	1.363
2.0	21.586	5.329	35.029	2.575	48.971	2.903
3.0	2.914	0.761	6.814	4.268	9.112	3.187
4.0	0.000	0.000	0.007	0.009	0.099	0.140
5.0	0.000	0.000	0.000	0.000	0.000	0.000
6.0	0.000	0.000	0.000	0.000	0.000	0.000
7.0	0.000	0.000	0.000	0.000	0.000	0.000
8.0	0.000	0.000	0.000	0.000	0.000	0.000
9.0	0.000	0.000	0.000	0.000	0.000	0.000
10.0	0.000	0.000	0.000	0.000	0.000	0.000
AVERAGE	**0.522**	0.080	**0.921**	0.084	**1.278**	0.173
C) Si/Al ONLY Ohc Y – O (%)						
n	**YAS17+H y=0.1**		**YAS17+H y=0.2**		**YAS17+H y=0.3**	
1.0	17.899	0.773	47.414	1.272	68.028	10.089
2.0	2.458	1.157	5.635	0.139	6.758	0.976
3.0	0.095	0.134	0.214	0.190	0.280	0.396
4.0	0.000	0.000	0.000	0.000	0.000	0.000
5.0	0.000	0.000	0.000	0.000	0.000	0.000
6.0	0.000	0.000	0.000	0.000	0.000	0.000
7.0	0.000	0.000	0.000	0.000	0.000	0.000
8.0	0.000	0.000	0.000	0.000	0.000	0.000
9.0	0.000	0.000	0.000	0.000	0.000	0.000
10.0	0.000	0.000	0.000	0.000	0.000	0.000
AVERAGE	**0.231**	0.035	**0.593**	0.010	**0.824**	0.132

1b) Supplementary Material – YAS24

Here, listed in tables are other relevant information regarding the simulations whereby YAS24 was hydrated.

1) Silicon Q^n Distribution

Si Qn (%)

n	**YAS-24**		**YAS-24 y=0.1**		**YAS-24 y=0.2**		**YAS-24 y=0.3**	
0.0	1.8449	0.5251	0.0007	0.0010	0.1860	0.2568	0.0000	0.0000
1.0	11.2838	3.2506	4.8765	0.3951	7.7064	4.6686	4.4123	1.9168
2.0	35.3515	0.7737	25.4569	3.1834	18.3505	1.7314	18.2733	2.2936
3.0	38.0551	2.5737	42.8934	1.0700	48.9093	0.5508	46.3900	0.6347
4.0	13.4647	0.4284	26.7725	1.7192	25.0294	2.1296	30.9245	4.8451
5.0	0.0000	0.0000	0.0000	0.0000	0.0000	0.0000	0.0000	0.0000
6.0	0.0000	0.0000	0.0000	0.0000	0.0000	0.0000	0.0000	0.0000
7.0	0.0000	0.0000	0.0000	0.0000	0.0000	0.0000	0.0000	0.0000
8.0	0.0000	0.0000	0.0000	0.0000	0.0000	0.0000	0.0000	0.0000
9.0	0.0000	0.0000	0.0000	0.0000	0.0000	0.0000	0.0000	0.0000
10.0	0.0000	0.0000	0.0000	0.0000	0.0000	0.0000	0.0000	0.0000
NC	2.5001	0.0773	2.9156	0.0412	2.9125	0.0897	3.0383	0.1097

CROSS SiQn (%)

n	**YAS-24**		**YAS-24 y=0.1**		**YAS-24 y=0.2**		**YAS-24 y=0.3**	
0.0	11.0478	1.3716	8.9993	2.8433	12.9718	0.2631	10.3527	0.1723
1.0	25.3684	0.2527	31.0397	1.8302	27.8615	1.3085	28.3542	1.5255
2.0	30.9360	1.5088	33.9390	5.6697	31.2716	5.0905	34.0610	3.4111
3.0	21.2110	0.1279	18.9235	0.0042	18.6968	2.7442	19.4162	0.9054
4.0	7.8676	0.3910	5.5363	1.0780	6.9108	0.9026	6.9684	1.3085
5.0	3.0441	0.3764	1.3642	0.3258	1.7272	0.6707	0.5897	0.3113
6.0	0.3463	0.2714	0.1980	0.2399	0.4681	0.1435	0.1907	0.2503
7.0	0.1787	0.2527	0.0000	0.0000	0.0922	0.1289	0.0672	0.0950
8.0	0.0000	0.0000	0.0000	0.0000	0.0000	0.0000	0.0000	0.0000
9.0	0.0000	0.0000	0.0000	0.0000	0.0000	0.0000	0.0000	0.0000
10.0	0.0000	0.0000	0.0000	0.0000	0.0000	0.0000	0.0000	0.0000
NC	2.0089	0.0243	1.8584	0.0537	1.8623	0.0456	1.8716	0.0193

2) Silicon Q^n Distribution – Si - O - Al

LIKE SiQn (%)

n	YAS-24		YAS-24 y=0.1		YAS-24 y=0.2		YAS-24 y=0.3	
0.0	42.2154	2.2908	18.8998	0.7192	17.8358	3.8988	14.5297	1.3106
1.0	44.0838	2.8804	43.3907	3.6146	39.3672	0.0409	42.3306	1.4659
2.0	11.9346	0.1321	29.0586	5.7390	33.0544	3.5979	32.5439	1.2898
3.0	1.5824	0.4617	7.5480	1.8038	8.8468	0.4870	9.4929	0.9667
4.0	0.1838	0.2600	1.1029	1.0399	0.8958	0.7470	1.1029	0.5199
5.0	0.0000	0.0000	0.0000	0.0000	0.0000	0.0000	0.0000	0.0000
6.0	0.0000	0.0000	0.0000	0.0000	0.0000	0.0000	0.0000	0.0000
7.0	0.0000	0.0000	0.0000	0.0000	0.0000	0.0000	0.0000	0.0000
8.0	0.0000	0.0000	0.0000	0.0000	0.0000	0.0000	0.0000	0.0000
9.0	0.0000	0.0000	0.0000	0.0000	0.0000	0.0000	0.0000	0.0000
10.0	0.0000	0.0000	0.0000	0.0000	0.0000	0.0000	0.0000	0.0000
NC	0.7344	0.0072	1.2856	0.0171	1.3560	0.0876	1.4031	0.0609

3) Silicon Q^n Distribution – Si - O - Si

4) Aluminium Qn Distribution

Al Qn (%)

n	YAS-24		YAS-24 y=0.1		YAS-24 y=0.2		YAS-24 y=0.3	
0.0	0.0000	0.0000	0.0000	0.0000	0.0000	0.0000	0.0000	0.0000
1.0	0.0000	0.0000	1.6279	0.9867	0.9302	0.3289	0.4651	0.0000
2.0	1.9953	0.9880	5.9054	1.4046	6.2660	1.7532	4.7513	2.0983
3.0	15.1507	0.3407	27.2447	2.9565	25.0847	1.6216	30.1219	3.2577
4.0	40.4205	0.5157	45.8812	4.0225	43.9343	0.4394	46.4710	0.4056
5.0	38.1963	0.3960	17.8781	0.4609	22.4657	1.3607	16.7963	0.9042
6.0	4.2372	2.2404	1.4558	0.1776	1.3191	0.7240	1.3944	0.6608
7.0	0.0000	0.0000	0.0068	0.0096	0.0000	0.0000	0.0000	0.0000
8.0	0.0000	0.0000	0.0000	0.0000	0.0000	0.0000	0.0000	0.0000
9.0	0.0000	0.0000	0.0000	0.0000	0.0000	0.0000	0.0000	0.0000
10.0	0.0000	0.0000	0.0000	0.0000	0.0000	0.0000	0.0000	0.0000
NC	4.2753	0.0640	3.7687	0.0196	3.8470	0.0099	3.7857	0.0129

5) Aluminium Qn Distribution – Al - O - Si

CROSS Al Qn (%)

n	YAS-24		YAS-24 y=0.1		YAS-24 y=0.2		YAS-24 y=0.3	
0.0	3.3591	1.8115	5.3336	0.3521	4.4192	0.3280	4.1330	0.0759
1.0	13.1777	0.9761	17.9017	2.7605	19.2105	2.3846	19.4127	1.1287
2.0	28.2586	1.2945	32.5479	1.0073	33.5727	1.2436	31.1665	1.8093
3.0	31.6167	5.3043	28.8220	0.6766	27.0983	4.3010	29.1234	0.7871
4.0	17.1423	2.4785	11.5216	1.0853	11.1343	0.2885	12.8809	1.8510
5.0	5.4140	2.5916	3.6784	0.7170	4.0431	0.6775	2.4533	0.1737
6.0	0.8102	1.1143	0.1947	0.2754	0.4561	0.6407	0.8301	0.1337
7.0	0.2214	0.0053	0.0000	0.0000	0.0657	0.0930	0.0000	0.0000
8.0	0.0000	0.0000	0.0000	0.0000	0.0000	0.0000	0.0000	0.0000
9.0	0.0000	0.0000	0.0000	0.0000	0.0000	0.0000	0.0000	0.0000
10.0	0.0000	0.0000	0.0000	0.0000	0.0000	0.0000	0.0000	0.0000
NC	2.6660	0.0265	2.3511	0.0680	2.3560	0.0577	2.3789	0.0088

6) Aluminum Qn Distribution – Si - O - Si

LIKE Al Qn (%)

n	YAS-24		YAS-24 y=0.1		YAS-24 y=0.2		YAS-24 y=0.3	
0.0	6.8186	1.6602	11.5460	1.1147	10.0586	2.9034	11.1609	1.3173
1.0	20.5237	6.0134	26.3584	4.3185	25.7891	4.1799	30.6620	2.6394
2.0	32.1712	3.1836	36.7352	0.7678	31.9873	3.3323	31.1569	1.4677
3.0	20.6493	0.4604	18.7132	4.0457	23.2037	2.3803	17.3916	2.3513
4.0	16.2205	3.8664	5.7163	0.0127	7.1181	0.4561	8.2335	3.0867
5.0	3.4307	0.8446	0.9305	0.6065	1.2819	0.0079	0.8648	0.3977
6.0	0.1860	0.2394	0.0003	0.0004	0.5612	0.1394	0.5302	0.1921
7.0	0.0000	0.0000	0.0000	0.0000	0.0000	0.0000	0.0000	0.0000
8.0	0.0000	0.0000	0.0000	0.0000	0.0000	0.0000	0.0000	0.0000
9.0	0.0000	0.0000	0.0000	0.0000	0.0000	0.0000	0.0000	0.0000
10.0	0.0000	0.0000	0.0000	0.0000	0.0000	0.0000	0.0000	0.0000
NC	2.2997	0.2010	1.8349	0.1244	1.9762	0.0363	1.8559	0.0186

7) Total Silicon Coordination (OH+O)

TOTAL (Oc+OHc) Si - O (%)

n	YAS-24		YAS-24 y=0.1		YAS-24 y=0.2		YAS-24 y=0.3	
1.0	0.0000	0.0000	0.0000	0.0000	0.0000	0.0000	0.0000	0.0000
2.0	0.0000	0.0000	0.0000	0.0000	0.0000	0.0000	0.0000	0.0000
3.0	0.6235	0.3847	0.8466	0.3612	0.2358	0.2676	0.2469	0.1936
4.0	99.3765	0.3848	99.1534	0.3612	99.7642	0.2676	99.7481	0.1866
5.0	0.0000	0.0000	0.0000	0.0000	0.0000	0.0000	0.0000	0.0000
6.0	0.0000	0.0000	0.0000	0.0000	0.0000	0.0000	0.0000	0.0000
7.0	0.0000	0.0000	0.0000	0.0000	0.0000	0.0000	0.0000	0.0000
8.0	0.0000	0.0000	0.0000	0.0000	0.0000	0.0000	0.0000	0.0000
9.0	0.0000	0.0000	0.0000	0.0000	0.0000	0.0000	0.0000	0.0000
10.0	0.0000	0.0000	0.0000	0.0000	0.0000	0.0000	0.0000	0.0000
AVERAGE	3.9938	0.0038	3.9915	0.0036	3.9976	0.0027	3.9973	0.0017

8) Partial Silicon Coordination (O)

Oc Si - O (%)

n	YAS-24 y=0.1		YAS-24 y=0.2		YAS-24 y=0.3	
1.0	0.0000	0.0000	0.0000	0.0000	0.0000	0.0000
2.0	0.0000	0.0000	0.0000	0.0000	0.1838	0.2600
3.0	4.1578	0.1553	10.6890	4.1168	21.0221	3.5667
4.0	95.8422	0.1553	89.3060	4.1239	78.7941	3.8267
5.0	0.0000	0.0000	0.0000	0.0000	0.0000	0.0000
6.0	0.0000	0.0000	0.0000	0.0000	0.0000	0.0000
7.0	0.0000	0.0000	0.0000	0.0000	0.0000	0.0000
8.0	0.0000	0.0000	0.0000	0.0000	0.0000	0.0000
9.0	0.0000	0.0000	0.0000	0.0000	0.0000	0.0000
10.0	0.0000	0.0000	0.0000	0.0000	0.0000	0.0000
AVERAGE	3.9584	0.0016	3.8929	0.0415	3.7861	0.0409

Ohc Si - O (%)

n	**YAS-24 y=0.1**		**YAS-24 y=0.2**		**YAS-24 y=0.3**	
0.0	93.0746	5.6277	81.5653	6.8927	72.4286	12.9960
1.0	6.6954	5.3023	16.3896	12.7798	20.7711	3.3789
2.0	0.2301	0.3254	1.7578	2.4859	0.1838	0.2600
3.0	0.0000	0.0000	0.0000	0.0000	0.0000	0.0000
4.0	0.0000	0.0000	0.0000	0.0000	0.0000	0.0000
5.0	0.0000	0.0000	0.0000	0.0000	0.0000	0.0000
6.0	0.0000	0.0000	0.0000	0.0000	0.0000	0.0000
7.0	0.0000	0.0000	0.0000	0.0000	0.0000	0.0000
8.0	0.0000	0.0000	0.0000	0.0000	0.0000	0.0000
9.0	0.0000	0.0000	0.0000	0.0000	0.0000	0.0000
10.0	0.0000	0.0000	0.0000	0.0000	0.0000	0.0000
AVERAGE	0.0331	0.0052	0.1046	0.0439	0.2114	0.0390

9) Partial Silicon Coordination (OH)

10) Total Aluminium Coordination (OH+O)

TOTAL (Oc+OHc) Al – O (%)

n	**YAS-24**		**YAS-24 y=0.1**		**YAS-24 y=0.2**		**YAS-24 y=0.3**	
1.0	0.0000	0.0000	0.0000	0.0000	0.0000	0.0000	0.0000	0.0000
2.0	0.0000	0.0000	0.0000	0.0000	0.0000	0.0000	0.0000	0.0000
3.0	0.0000	0.0000	0.0000	0.0000	0.0000	0.0000	0.0000	0.0000
4.0	42.9460	1.1800	65.5851	2.5390	57.3752	1.7501	58.0465	2.7662
5.0	51.6949	0.5762	31.4896	2.7942	38.2226	2.1628	39.0090	3.1161
6.0	5.3591	1.7563	2.9184	0.2649	4.4022	0.4126	2.6304	0.0943
7.0	0.0000	0.0000	0.0068	0.0096	0.0000	0.0000	0.3141	0.4442
8.0	0.0000	0.0000	0.0000	0.0000	0.0000	0.0000	0.0000	0.0000
9.0	0.0000	0.0000	0.0000	0.0000	0.0000	0.0000	0.0000	0.0000
10.0	0.0000	0.0000	0.0000	0.0000	0.0000	0.0000	0.0000	0.0000
AVERAGE	4.6241	0.0294	4.3735	0.0229	4.4703	0.0134	4.4521	0.0197

Oc Al – O (%)

n	YAS-24 y=0.1		YAS-24 y=0.2		YAS-24 y=0.3	
1.0	0.0000	0.0000	0.0000	0.0000	0.0000	0.0000
2.0	0.0000	0.0000	0.2093	0.2960	0.6174	0.2153
3.0	3.3389	0.3456	8.8468	1.1809	11.4695	1.3283
4.0	68.6016	3.1170	64.5895	0.8819	70.1467	0.1811
5.0	26.1662	3.8168	25.4698	0.5139	16.8729	0.9292
6.0	1.8865	1.0551	0.8847	1.1090	0.8936	0.4333
7.0	0.0068	0.0096	0.0000	0.0000	0.0000	0.0000
8.0	0.0000	0.0000	0.0000	0.0000	0.0000	0.0000
9.0	0.0000	0.0000	0.0000	0.0000	0.0000	0.0000
10.0	0.0000	0.0000	0.0000	0.0000	0.0000	0.0000
AVERAGE	4.2662	0.0139	4.1797	0.0348	4.0596	0.0355

11) Partial Aluminium Coordination (O)

Ohc Al – O (%)

n	YAS-24 y=0.1		YAS-24 y=0.2		YAS-24 y=0.3	
0.0	89.5039	0.5780	73.8747	3.9835	67.0524	5.3929
1.0	10.2660	0.2526	23.4288	2.8249	27.4369	5.4437
2.0	0.2301	0.3254	2.4648	1.4861	4.7129	0.2355
3.0	0.0000	0.0000	0.2316	0.3276	0.7978	0.1846
4.0	0.0000	0.0000	0.0000	0.0000	0.0000	0.0000
5.0	0.0000	0.0000	0.0000	0.0000	0.0000	0.0000
6.0	0.0000	0.0000	0.0000	0.0000	0.0000	0.0000
7.0	0.0000	0.0000	0.0000	0.0000	0.0000	0.0000
8.0	0.0000	0.0000	0.0000	0.0000	0.0000	0.0000
9.0	0.0000	0.0000	0.0000	0.0000	0.0000	0.0000
10.0	0.0000	0.0000	0.0000	0.0000	0.0000	0.0000
AVERAGE	0.1073	0.0090	0.2905	0.0481	0.3926	0.0553

12) Partial Aluminium Coordination (OH)

13) Total Yttrium Coordination (OH+O)

TOTAL (Oc+OHc) Y – O (%)

n	YAS-24		YAS-24 y=0.1		YAS-24 y=0.2		YAS-24 y=0.3	
1.0	0.0000	0.0000	0.0000	0.0000	0.0000	0.0000	0.0000	0.0000
2.0	0.0000	0.0000	0.0000	0.0000	0.0000	0.0000	0.0000	0.0000
3.0	0.0000	0.0000	0.0000	0.0000	0.0000	0.0000	0.0000	0.0000
4.0	0.1220	0.1725	0.0041	0.0059	0.1851	0.2617	0.0000	0.0000
5.0	5.0100	1.8320	5.2437	0.4342	3.9220	1.2738	2.3074	1.5894
6.0	34.0008	4.4938	31.2819	0.0845	25.9906	1.5789	18.3095	5.0587
7.0	41.3535	1.2335	40.9970	3.3659	41.2971	1.7686	43.1719	1.6425
8.0	16.7485	1.7229	19.8188	4.0556	24.2943	0.1393	30.0492	3.3126
9.0	2.7261	0.4307	2.6102	0.2379	4.1798	1.3113	5.7185	1.4320
10.0	0.0390	0.0364	0.0443	0.0610	0.1311	0.1737	0.4403	0.2566
AVERAGE	6.7793	0.0106	6.8339	0.0470	6.9866	0.0792	7.1986	0.1515

14) Partial Yttrium Coordination (O)

Oc Y – O (%)

n	**YAS-24 y=0.1**		**YAS-24 y=0.2**		**YAS-24 y=0.3**	
1.0	0.0000	0.0000	0.0000	0.0000	0.1729	0.2445
2.0	0.2075	0.2934	0.5201	0.5000	1.6199	1.0711
3.0	1.2385	0.4292	3.2008	0.5371	11.1770	1.0668
4.0	5.2545	0.4448	16.6476	2.0151	27.3289	2.9278
5.0	23.0999	0.3325	29.3256	2.0992	31.4479	3.5451
6.0	38.1790	1.5684	32.6736	0.4542	19.5530	4.3706
7.0	24.7499	1.6317	14.5264	1.2131	7.5533	1.1020
8.0	6.6808	0.4722	2.8512	1.4299	0.9762	0.5097
9.0	0.5845	0.0982	0.2548	0.3587	0.1710	0.2410
10.0	0.0055	0.0078	0.0000	0.0000	0.0000	0.0000
AVERAGE	6.0173	0.0401	5.4669	0.0040	4.8304	0.0500

Ohc Y – O (%)

n	**YAS-24 y=0.1**		**YAS-24 y=0.2**		**YAS-24 y=0.3**	
0.0	37.0113	1.1658	10.3768	1.9850	4.2180	1.2722
1.0	46.9372	2.1070	40.8266	1.2151	22.3029	0.0872
2.0	13.6418	0.3220	36.9259	2.0190	36.2158	5.7500
3.0	2.2022	0.3259	10.6077	0.6201	25.7142	4.3131
4.0	0.2075	0.2934	0.8490	0.0246	9.5516	1.8078
5.0	0.0000	0.0000	0.4141	0.5856	1.7862	1.2765
6.0	0.0000	0.0000	0.0000	0.0000	0.2113	0.2879
7.0	0.0000	0.0000	0.0000	0.0000	0.0000	0.0000
8.0	0.0000	0.0000	0.0000	0.0000	0.0000	0.0000
9.0	0.0000	0.0000	0.0000	0.0000	0.0000	0.0000
10.0	0.0000	0.0000	0.0000	0.0000	0.0000	0.0000
AVERAGE	0.8166	0.0069	1.5197	0.0751	2.2028	0.1324

15) Partial Yttrium Coordination (OH)

16) YAS24 Dry and Hydrated Clustering Ratios

Clustering R = N(obs)/N(hom)

Species	**YAS-24**		**YAS-24 y=0.1**		**YAS-24 y=0.2**		**YAS-24 y=0.3**	
OH – Si			**0.2791**	0.0162	**0.3476**	0.0014	**0.4397**	0.0208
OH – Al			**0.6994**	0.0222	**0.8237**	0.0015	**0.7379**	0.0011
OH – Y			**1.5968**	0.0081	**1.5701**	0.0122	**1.6030**	0.0535
Y – Y	1.1204	0.0184	**1.2041**	0.0210	**1.2300**	0.0388	**1.3012**	0.0029
Y – Si	1.3978	0.0038	**1.1506**	0.0136	**1.0422**	0.0628	**1.0284**	0.0025
Y – Al	1.0307	0.0093	**1.0414**	0.0081	**1.0116**	0.0609	**1.0005**	0.0052
Si – Si	1.0873	0.0200	**1.3810**	0.0008	**1.6058**	0.0075	**1.5386**	0.0164
Si – Al	1.1528	0.0030	**1.1589**	0.0048	**1.1128**	0.0067	**1.1858**	0.0069
Al – Al	1.6741	0.0623	**1.5378**	0.0040	**1.5568**	0.0526	**1.6390**	0.0029

17) A) Partial Yttrium Coordination due to Hydroxyls

B) Hydroxyl Coordination to Yttrium (Free OH)

C) Hydroxyls Coordinated to Yttrium attached to Si or Al

A) Ohc Y – O (%)						
n	**YAS-24 y=0.1**		**YAS-24 y=0.2**		**YAS-24 y=0.3**	
1.0	46.9372	2.1070	40.8266	1.2151	22.3029	0.0872
2.0	13.6418	0.3220	36.9259	2.0190	36.2158	5.7500
3.0	2.2022	0.3259	10.6077	0.6201	25.7142	4.3131
4.0	0.2075	0.2934	0.8490	0.0246	9.5516	1.8078
5.0	0.0000	0.0000	0.4141	0.5856	1.7862	1.2765
6.0	0.0000	0.0000	0.0000	0.0000	0.2113	0.2879
7.0	0.0000	0.0000	0.0000	0.0000	0.0000	0.0000
8.0	0.0000	0.0000	0.0000	0.0000	0.0000	0.0000
9.0	0.0000	0.0000	0.0000	0.0000	0.0000	0.0000
10.0	0.0000	0.0000	0.0000	0.0000	0.0000	0.0000
AVERAGE	**0.8166**	0.0069	**1.5197**	0.0751	**2.2028**	0.1324
	0.816572591		1.519679101		2.202824358	
B) FREE ONLY Ohc Y – O (%)						
n	**YAS-24 y=0.1**		**YAS-24 y=0.2**		**YAS-24 y=0.3**	
1.0	0.6257	0.2981	0.2354	0.2758	0.8603	1.1314
2.0	21.7333	4.3119	35.1651	6.0160	51.8454	5.7402
3.0	7.1007	2.7412	14.2863	0.7124	18.3635	0.3357
4.0	0.3776	0.4777	0.5723	0.2226	1.1497	1.2902
5.0	0.0000	0.0000	0.0000	0.0000	0.0000	0.0000
6.0	0.0000	0.0000	0.0000	0.0000	0.0000	0.0000
7.0	0.0000	0.0000	0.0000	0.0000	0.0000	0.0000
8.0	0.0000	0.0000	0.0000	0.0000	0.0000	0.0000
9.0	0.0000	0.0000	0.0000	0.0000	0.0000	0.0000
10.0	0.0000	0.0000	0.0000	0.0000	0.0000	0.0000
AVERAGE	**0.6690**	0.0201	**1.1571**	0.1478	**1.6424**	0.1878
C) Si/Al ONLY Ohc Y – O (%)						
n	**YAS-24 y=0.1**		**YAS-24 y=0.2**		**YAS-24 y=0.3**	
1.0	6.3231	2.2698	21.2633	5.6142	30.4880	3.5342
2.0	3.8653	0.2727	7.4775	0.8031	11.3876	2.1861
3.0	0.2329	0.3255	0.0119	0.0168	0.9264	0.7883
4.0	0.0000	0.0000	0.0000	0.0000	0.0000	0.0000
5.0	0.0000	0.0000	0.0000	0.0000	0.0000	0.0000
6.0	0.0000	0.0000	0.0000	0.0000	0.0000	0.0000
7.0	0.0000	0.0000	0.0000	0.0000	0.0000	0.0000
8.0	0.0000	0.0000	0.0000	0.0000	0.0000	0.0000
9.0	0.0000	0.0000	0.0000	0.0000	0.0000	0.0000
10.0	0.0000	0.0000	0.0000	0.0000	0.0000	0.0000
AVERAGE	**0.1475**	0.0270	**0.3625**	0.0727	**0.5604**	0.0554

1c) Supplementary Material – YAS30

Here, listed in tables are other relevant information regarding the simulations whereby YAS30 was hydrated.

1) Silicon Q^n Distribution

Si Qn (%)

n	**YAS30**		**YAS30+H y=0.1**		**YAS30+H y=0.2**		**YAS30+H y=0.3**	
0.0	4.0888	0.0441	0.6000	0.8485	1.2016	0.0023	0.4000	0.5657
1.0	24.9424	4.5119	13.2523	1.6194	9.5589	0.0000	6.7301	1.1087
2.0	40.5352	4.7552	29.8120	0.6091	29.8064	0.0000	28.4648	0.7863
3.0	24.8192	1.1178	36.3789	1.4169	41.7093	0.0000	45.4667	0.2414
4.0	5.6144	1.4052	18.3104	1.7008	17.7253	0.0000	18.9384	2.7021
5.0	0.0000	0.0000	1.2333	0.1014	0.0000	0.0000	0.0000	0.0000
6.0	0.0000	0.0000	0.3619	0.4748	0.0000	0.0000	0.0000	0.0000
7.0	0.0000	0.0000	0.0512	0.0724	0.0000	0.0000	0.0000	0.0000
8.0	0.0000	0.0000	0.0000	0.0000	0.0000	0.0000	0.0000	0.0000
9.0	0.0000	0.0000	0.0000	0.0000	0.0000	0.0000	0.0000	0.0000
10.0	0.0000	0.0000	0.0000	0.0000	0.0000	0.0000	0.0000	0.0000
NC	2.0293	0.0273	2.6395	0.0011	2.6520	0.0068	2.7581	0.0740

CROSS SiQn (%)

n	**YAS30**		**YAS30+H y=0.1**		**YAS30+H y=0.2**		**YAS30+H y=0.3**	
0.0	14.4208	1.6360	13.6099	1.1461	15.0771	2.6583	10.5480	1.5700
1.0	32.2528	2.1292	29.4088	1.1265	28.9792	3.1135	31.2320	3.1852
2.0	31.3936	3.5932	30.5523	2.1900	33.6763	10.5459	30.6320	4.7729
3.0	15.6560	0.4322	15.8856	1.4553	13.4344	2.0678	16.8360	1.0375
4.0	5.0288	0.5453	7.4429	2.4125	7.2659	2.5030	7.3755	0.2331
5.0	1.0312	0.4989	2.5005	0.1912	1.3453	0.4371	3.1621	1.1246
6.0	0.2112	0.2987	0.6000	0.8485	0.2176	0.2278	0.2144	0.3025
7.0	0.0056	0.0079	0.0000	0.0000	0.0043	0.0060	0.0000	0.0000
8.0	0.0000	0.0000	0.0000	0.0000	0.0000	0.0000	0.0000	0.0000
9.0	0.0000	0.0000	0.0000	0.0000	0.0000	0.0000	0.0000	0.0000
10.0	0.0000	0.0000	0.0000	0.0000	0.0000	0.0000	0.0000	0.0000
NC	1.6859	0.0419	1.8404	0.0402	1.7376	0.0099	1.8960	0.0473

2) Silicon Q^n Distribution – Si - O - Al

3) Silicon Q^n Distribution – Si - O - Si

LIKE SiQn (%)

n	**YAS30**		**YAS30+H y=0.1**		**YAS30+H y=0.2**		**YAS30+H y=0.3**	
0.0	60.4240	0.1652	28.6416	4.1740	23.9875	2.2722	24.2925	2.1108
1.0	31.3984	0.8463	44.1451	8.5185	44.6144	0.2715	43.9163	1.2498
2.0	7.9776	0.7286	22.3883	4.2894	26.5981	1.9780	25.7912	1.9923
3.0	0.2000	0.2828	4.1544	0.4107	4.4000	0.5657	5.6000	1.1314
4.0	0.0000	0.0000	0.6704	0.3553	0.4000	0.0000	0.4000	0.0000
5.0	0.0000	0.0000	0.0003	0.0004	0.0000	0.0000	0.0000	0.0000
6.0	0.0000	0.0000	0.0000	0.0000	0.0000	0.0000	0.0000	0.0000
7.0	0.0000	0.0000	0.0000	0.0000	0.0000	0.0000	0.0000	0.0000
8.0	0.0000	0.0000	0.0000	0.0000	0.0000	0.0000	0.0000	0.0000
9.0	0.0000	0.0000	0.0000	0.0000	0.0000	0.0000	0.0000	0.0000
10.0	0.0000	0.0000	0.0000	0.0000	0.0000	0.0000	0.0000	0.0000
NC	0.4795	0.0146	1.0407	0.0013	1.1261	0.0538	1.1390	0.0184

4) Aluminium Q^n Distribution

Al Qn (%)

n	YAS30		YAS30+H y=0.1		YAS30+H y=0.2		YAS30+H y=0.3	
0.0	0.0070	0.0099	0.0000	0.0000	0.0000	0.0000	0.0000	0.0000
1.0	1.0200	0.0481	1.8573	1.6160	0.5000	0.0000	2.1963	1.6919
2.0	8.2980	2.1043	7.9787	1.6612	7.6180	0.0000	9.0697	1.2158
3.0	22.4900	0.9475	28.6500	0.0160	27.1840	0.0000	22.8300	0.2300
4.0	39.0470	1.9332	35.7293	5.6371	43.3573	0.0000	37.8083	1.7569
5.0	25.9280	3.3093	22.8133	1.9827	19.0680	0.0000	24.1510	1.0658
6.0	3.1840	2.1383	2.9713	0.3932	2.2727	0.0000	3.6497	0.3295
7.0	0.0260	0.0141	0.0000	0.0000	0.0000	0.0000	0.2950	0.1843
8.0	0.0000	0.0000	0.0000	0.0000	0.0000	0.0000	0.0000	0.0000
9.0	0.0000	0.0000	0.0000	0.0000	0.0000	0.0000	0.0000	0.0000
10.0	0.0000	0.0000	0.0000	0.0000	0.0000	0.0000	0.0000	0.0000
NC	3.9020	0.0425	3.7858	0.0539	3.7969	0.0139	3.8478	0.0824

5) Aluminium Q^n Distribution – Al - O - Si

CROSS Al Qn (%)

n	YAS30		YAS30+H y=0.1		YAS30+H y=0.2		YAS30+H y=0.3	
0.0	7.1860	0.8089	6.2250	0.3125	7.5083	2.8817	4.4003	0.5662
1.0	21.2000	2.4862	21.7827	0.3158	22.7420	2.4673	20.7797	1.9719
2.0	29.5930	2.9911	30.5200	1.8064	34.9650	6.1730	29.2437	0.4078
3.0	27.2550	2.1114	24.1413	2.2939	20.8977	0.9829	30.5617	0.7189
4.0	12.6190	4.7164	12.6537	1.8851	9.3327	0.7854	10.0107	2.8709
5.0	2.1160	1.2841	4.1393	2.2411	3.0827	1.1879	4.2677	1.8323
6.0	0.0310	0.0071	0.2683	0.3785	1.2100	1.0343	0.4837	0.0165
7.0	0.0000	0.0000	0.2697	0.3814	0.2617	0.3701	0.2527	0.3564
8.0	0.0000	0.0000	0.0000	0.0000	0.0000	0.0000	0.0000	0.0000
9.0	0.0000	0.0000	0.0000	0.0000	0.0000	0.0000	0.0000	0.0000
10.0	0.0000	0.0000	0.0000	0.0000	0.0000	0.0000	0.0000	0.0000
NC	2.2339	0.0257	2.3006	0.0502	2.1720	0.0123	2.3700	0.0592

6) Aluminium Q^n Distribution – Al - O - Al

LIKE Al Qn (%)

n	YAS30		YAS30+H y=0.1		YAS30+H y=0.2		YAS30+H y=0.3	
0.0	8.8670	1.5684	10.3700	0.2630	9.1027	0.2564	11.4977	0.7010
1.0	22.8850	1.2488	25.1980	5.7379	25.5043	1.2836	23.8217	2.5640
2.0	33.5880	0.3734	31.9667	3.4884	33.7750	4.9285	31.0950	6.5417
3.0	23.0340	1.2134	21.6213	4.5575	20.2660	0.7429	21.4500	1.4585
4.0	9.4920	2.0110	8.5193	0.8532	9.4890	2.1623	9.7553	3.4318
5.0	1.9930	1.2912	2.0803	0.8518	1.6127	0.1292	2.1047	0.0547
6.0	0.1410	0.1994	0.2443	0.3399	0.2503	0.3540	0.2757	0.1570
7.0	0.0000	0.0000	0.0000	0.0000	0.0000	0.0000	0.0000	0.0000
8.0	0.0000	0.0000	0.0000	0.0000	0.0000	0.0000	0.0000	0.0000
9.0	0.0000	0.0000	0.0000	0.0000	0.0000	0.0000	0.0000	0.0000
10.0	0.0000	0.0000	0.0000	0.0000	0.0000	0.0000	0.0000	0.0000
NC	2.0794	0.0375	1.9994	0.0520	2.0137	0.0507	2.0156	0.0637

7) Total Silicon Coordination (OH+O)

TOTAL (Oc+OHc) Si - O (%)

n	YAS30		YAS30+H y=0.1		YAS30+H y=0.2		YAS30+H y=0.3	
1.0	0.0000	0.0000	0.0000	0.0000	0.0000	0.0000	0.0000	0.0000
2.0	0.0000	0.0000	0.0000	0.0000	0.0000	0.0000	0.0000	0.0000
3.0	0.4232	0.1640	0.0179	0.0087	0.7963	0.0053	0.6397	0.3390
4.0	99.5768	0.1640	99.9821	0.0087	99.2037	0.0053	99.3603	0.3390
5.0	0.0000	0.0000	0.0000	0.0000	0.0000	0.0000	0.0000	0.0000
6.0	0.0000	0.0000	0.0000	0.0000	0.0000	0.0000	0.0000	0.0000
7.0	0.0000	0.0000	0.0000	0.0000	0.0000	0.0000	0.0000	0.0000
8.0	0.0000	0.0000	0.0000	0.0000	0.0000	0.0000	0.0000	0.0000
9.0	0.0000	0.0000	0.0000	0.0000	0.0000	0.0000	0.0000	0.0000
10.0	0.0000	0.0000	0.0000	0.0000	0.0000	0.0000	0.0000	0.0000
AVERAGE	3.9958	0.0016	3.9998	0.0001	3.9920	0.0001	3.9936	0.0034

8) Partial Silicon Coordination (O)

Oc Si - O (%)

n	YAS30 y=0.1		YAS30 y=0.2		YAS30 y=0.3	
1.0	0.0000	0.0000	0.0000	0.0000	0.0000	0.0000
2.0	0.0000	0.0000	0.0000	0.0000	0.4000	0.5657
3.0	2.4179	1.1400	7.1960	2.8228	15.4059	1.9882
4.0	97.5821	1.1400	92.8040	2.8228	84.1941	2.5539
5.0	0.0000	0.0000	0.0000	0.0000	0.0000	0.0000
6.0	0.0000	0.0000	0.0000	0.0000	0.0000	0.0000
7.0	0.0000	0.0000	0.0000	0.0000	0.0000	0.0000
8.0	0.0000	0.0000	0.0000	0.0000	0.0000	0.0000
9.0	0.0000	0.0000	0.0000	0.0000	0.0000	0.0000
10.0	0.0000	0.0000	0.0000	0.0000	0.0000	0.0000
AVERAGE	3.9758	0.0114	3.9280	0.0282	3.8379	0.0312

9) Partial Silicon Coordination (OH)

Ohc Si - O (%)

n	YAS30 y=0.1		YAS30 y=0.2		YAS30 y=0.3	
0.0	97.6000	1.1314	93.6003	2.8280	84.8339	2.2148
1.0	2.4000	1.1314	6.3997	2.8280	14.7661	1.6492
2.0	0.0000	0.0000	0.0000	0.0000	0.4000	0.5657
3.0	0.0000	0.0000	0.0000	0.0000	0.0000	0.0000
4.0	0.0000	0.0000	0.0000	0.0000	0.0000	0.0000
5.0	0.0000	0.0000	0.0000	0.0000	0.0000	0.0000
6.0	0.0000	0.0000	0.0000	0.0000	0.0000	0.0000
7.0	0.0000	0.0000	0.0000	0.0000	0.0000	0.0000
8.0	0.0000	0.0000	0.0000	0.0000	0.0000	0.0000
9.0	0.0000	0.0000	0.0000	0.0000	0.0000	0.0000
10.0	0.0000	0.0000	0.0000	0.0000	0.0000	0.0000
AVERAGE	0.0240	0.0113	0.0640	0.0283	0.1557	0.0278

10) Total Aluminium Coordination (OH+O)

TOTAL (Oc+OHc) Al – O (%)

n	YAS30		YAS30+H y=0.1		YAS30+H y=0.2		YAS30+H y=0.3	
1.0	0.0000	0.0000	0.0000	0.0000	0.0000	0.0000	0.0000	0.0000
2.0	0.0000	0.0000	0.0000	0.0000	0.0000	0.0000	0.0000	0.0000
3.0	0.0000	0.0000	0.0000	0.0000	0.0000	0.0000	0.0000	0.0000
4.0	48.1940	3.0490	44.3353	0.8146	47.5760	3.9956	43.4153	1.3718
5.0	46.5000	5.4362	49.4430	0.0259	46.1620	5.9934	47.2763	1.5504
6.0	5.2800	2.3731	6.2213	0.7891	6.2603	1.9955	8.4990	0.3635
7.0	0.0260	0.0141	0.0003	0.0005	0.0017	0.0024	0.8093	0.5421
8.0	0.0000	0.0000	0.0000	0.0000	0.0000	0.0000	0.0000	0.0000
9.0	0.0000	0.0000	0.0000	0.0000	0.0000	0.0000	0.0000	0.0000
10.0	0.0000	0.0000	0.0000	0.0000	0.0000	0.0000	0.0000	0.0000
AVERAGE	4.5714	0.0065	4.6189	0.0160	4.5869	0.0200	4.6670	0.0065

11) Partial Aluminium Coordination (O)

Oc Al – O (%)

n	YAS30 y=0.1		YAS30 y=0.2		YAS30 y=0.3	
1.0	0.0000	0.0000	0.0000	0.0000	0.0000	0.0000
2.0	0.0000	0.0000	0.0000	0.0000	0.0000	0.0000
3.0	0.5867	0.5845	3.8923	0.8688	5.7877	0.3842
4.0	51.1640	0.5336	60.0147	2.3127	58.6307	3.5271
5.0	43.9040	0.5534	33.9777	2.0134	32.6070	4.9389
6.0	4.3453	0.5025	2.1147	1.1691	2.9747	1.0277
7.0	0.0000	0.0000	0.0000	0.0000	0.0000	0.0000
8.0	0.0000	0.0000	0.0000	0.0000	0.0000	0.0000
9.0	0.0000	0.0000	0.0000	0.0000	0.0000	0.0000
10.0	0.0000	0.0000	0.0000	0.0000	0.0000	0.0000
AVERAGE	4.5201	0.0013	4.3431	0.0522	4.3277	0.0327

12) Partial Aluminium Coordination (OH)

Ohc Al – O (%)

n	YAS30 y=0.1		YAS30 y=0.2		YAS30 y=0.3	
0.0	90.1220	1.4708	78.4575	5.6632	69.5573	2.4796
1.0	9.8773	1.4717	18.7127	4.1116	27.2200	2.0148
2.0	0.0007	0.0009	2.8298	1.5516	2.9543	0.7924
3.0	0.0000	0.0000	0.0000	0.0000	0.2683	0.3276
4.0	0.0000	0.0000	0.0000	0.0000	0.0000	0.0000
5.0	0.0000	0.0000	0.0000	0.0000	0.0000	0.0000
6.0	0.0000	0.0000	0.0000	0.0000	0.0000	0.0000
7.0	0.0000	0.0000	0.0000	0.0000	0.0000	0.0000
8.0	0.0000	0.0000	0.0000	0.0000	0.0000	0.0000
9.0	0.0000	0.0000	0.0000	0.0000	0.0000	0.0000
10.0	0.0000	0.0000	0.0000	0.0000	0.0000	0.0000
AVERAGE	0.0988	0.0147	0.2437	0.0721	0.3393	0.0262

13) Total Yttrium Coordination (OH+O)

TOTAL (Oc+OHc) Y – O (%)

n	YAS30		YAS30+H y=0.1		YAS30+H y=0.2		YAS30+H y=0.3	
1.0	0.0000	0.0000	0.0000	0.0000	0.0000	0.0000	0.0000	0.0000
2.0	0.0000	0.0000	0.0000	0.0000	0.0000	0.0000	0.0000	0.0000
3.0	0.0000	0.0000	0.0000	0.0000	0.0000	0.0000	0.0000	0.0000
4.0	0.0060	0.0085	0.1667	0.2357	0.0000	0.0000	0.1667	0.2357
5.0	2.3187	0.5412	2.5338	0.2206	0.6731	0.2285	1.2169	0.0471
6.0	23.3893	0.6883	27.9667	1.7191	18.1562	1.0864	13.6722	1.4994
7.0	44.3360	1.6235	42.6638	0.0820	42.6676	1.1521	42.5640	2.5022
8.0	24.3540	0.3215	21.2356	0.9522	31.3233	3.2763	30.7353	2.3423
9.0	5.2740	0.2951	4.9698	0.2332	7.0136	1.2172	10.9164	5.9190
10.0	0.2893	0.3300	0.4638	0.6307	0.1662	0.0490	0.7251	0.1461
AVERAGE	7.0750	0.0135	6.9903	0.0530	7.2635	0.0132	7.3811	0.1066

Oc Y – O (%)

n	YAS30 y=0.1		YAS30 y=0.2		YAS30 y=0.3	
1.0	0.0000	0.0000	0.0000	0.0000	0.1731	0.2448
2.0	0.0000	0.0000	0.0004	0.0006	1.2962	0.0437
3.0	0.4058	0.2351	1.6262	1.1433	8.5607	0.2146
4.0	3.6418	0.5431	8.9931	1.8589	17.2449	1.1232
5.0	22.4927	2.8633	28.6364	0.0308	29.4636	1.8894
6.0	34.4247	4.7502	35.8751	1.9975	27.6727	1.9551
7.0	26.5371	3.7558	20.3129	2.2125	10.9218	2.0170
8.0	10.0940	1.4020	3.6713	0.7791	4.0764	0.1873
9.0	2.4007	0.3089	0.8202	0.0537	0.5247	0.1945
10.0	0.0033	0.0022	0.0642	0.0663	0.0660	0.0933
AVERAGE	6.2295	0.0082	5.7887	0.0003	5.2523	0.0055

14) Partial Yttrium Coordination (O)

Ohc Y – O (%)

n	YAS30 y=0.1		YAS30 y=0.2		YAS30 y=0.3	
0.0	37.9144	2.8306	11.9349	0.8250	6.8753	1.1436
1.0	49.1642	2.7062	42.7160	0.9202	23.9876	2.1999
2.0	11.8429	1.4007	32.8973	0.3476	33.3918	6.2555
3.0	1.0784	1.5252	10.8411	0.1166	23.1538	2.2326
4.0	0.0000	0.0000	1.6107	0.3690	10.2704	1.1619
5.0	0.0000	0.0000	0.0000	0.0000	2.3169	1.7989
6.0	0.0000	0.0000	0.0000	0.0000	0.0042	0.0060
7.0	0.0000	0.0000	0.0000	0.0000	0.0000	0.0000
8.0	0.0000	0.0000	0.0000	0.0000	0.0000	0.0000
9.0	0.0000	0.0000	0.0000	0.0000	0.0000	0.0000
10.0	0.0000	0.0000	0.0000	0.0000	0.0000	0.0000
AVERAGE	0.7609	0.0448	1.4748	0.0135	2.1292	0.1006

15) Partial Ytrrium Coordination (OH)

16) YAS30 Dry and Hydrated Clustering Ratios

Clustering R = N(obs)/N(hom)								
Species	**YAS30**		**YAS30+H y=0.1**		**YAS30+H y=0.2**		**YAS30+H y=0.3**	
OH – Si			**0.368**	0.014	**0.180**	0.036	**0.303**	0.029
OH – Al			**0.973**	0.027	**0.798**	0.133	**0.704**	0.004
OH – Y			**1.469**	0.002	**1.576**	0.068	**1.589**	0.076
Y – Y	1.167	0.016	**1.217**	0.018	**1.240**	0.013	**3.289**	2.880
Y – Si	1.472	0.006	**1.179**	0.003	**1.184**	0.015	**1.128**	0.005
Y – Al	1.122	0.012	**1.110**	0.009	**1.078**	0.012	**1.040**	0.001
Si – Si	1.027	0.003	**1.522**	0.016	**1.546**	0.039	**1.824**	0.321
Si – Al	1.134	0.065	**0.889**	0.003	**0.973**	0.030	**1.005**	0.000
Al – Al	1.659	0.015	**1.342**	0.001	**1.378**	0.001	**2.034**	0.883

17) A) Partial Yttrium Coordination due to Hydroxyls

B) Hydroxyl Coordination to Yttrium (Free OH)

C) Hydroxyls Coordinated to Yttrium attached to Si or Al

Ohc Y – O (%)						
n	**YAS30 y=0.1**		**YAS30 y=0.2**		**YAS30 y=0.3**	
1.0	49.164	2.706	42.716	0.920	23.988	2.200
2.0	11.843	1.401	32.897	0.348	33.392	6.256
3.0	1.078	1.525	10.841	0.117	23.154	2.233
4.0	0.000	0.000	1.611	0.369	10.270	1.162
5.0	0.000	0.000	0.000	0.000	2.317	1.799
6.0	0.000	0.000	0.000	0.000	0.004	0.006
7.0	0.000	0.000	0.000	0.000	0.000	0.000
8.0	0.000	0.000	0.000	0.000	0.000	0.000
9.0	0.000	0.000	0.000	0.000	0.000	0.000
10.0	0.000	0.000	0.000	0.000	0.000	0.000
AVERAGE	**0.761**	0.045	**1.475**	0.014	**2.129**	0.101
	0.76085332		1.47476667		2.12923997	
FREE ONLY Ohc Y – O (%)						
n	**YAS30 y=0.1**		**YAS30 y=0.2**		**YAS30 y=0.3**	
1.0	0.000	0.000	0.169	0.235	0.474	0.199
2.0	11.953	0.694	23.789	2.355	35.479	0.313
3.0	12.842	1.833	22.431	0.475	31.452	2.910
4.0	0.748	0.112	0.816	0.267	1.027	0.195
5.0	0.000	0.000	0.014	0.019	0.098	0.139
6.0	0.000	0.000	0.000	0.000	0.000	0.000
7.0	0.000	0.000	0.000	0.000	0.000	0.000
8.0	0.000	0.000	0.000	0.000	0.000	0.000
9.0	0.000	0.000	0.000	0.000	0.000	0.000
10.0	0.000	0.000	0.000	0.000	0.000	0.000
AVERAGE	**0.654**	0.046	**1.184**	0.049	**1.704**	0.091
Si/Al ONLY Ohc Y – O (%)						
n	**YAS30 y=0.1**		**YAS30 y=0.2**		**YAS30 y=0.3**	
1.0	3.937	0.875	7.736	0.013	15.004	1.200
2.0	3.256	0.308	9.291	2.927	12.811	0.219
3.0	0.072	0.060	0.924	0.152	0.637	0.876
4.0	0.000	0.000	0.003	0.004	0.000	0.000
5.0	0.000	0.000	0.000	0.000	0.000	0.000
6.0	0.000	0.000	0.000	0.000	0.000	0.000
7.0	0.000	0.000	0.000	0.000	0.000	0.000
8.0	0.000	0.000	0.000	0.000	0.000	0.000
9.0	0.000	0.000	0.000	0.000	0.000	0.000
10.0	0.000	0.000	0.000	0.000	0.000	0.000
AVERAGE	**0.107**	0.001	**0.291**	0.063	**0.425**	0.010

2) YBG Yttrium Bioglass (With Phosphorus)

Here are the full set of clustering ratio values regarding the simulations in which YBG was hydrate. The bold numbers are the ratios and beside each ratio is the standard deviation.

1) Clustering Ratios for Hydrated YBG

Species	YBG_DRY		YBG_0.1		YBG_0.2		YBG_0.3	
OH – Si			**0.711**	0.120	**1.180**	0.025	**1.099**	0.010
OH – P			**1.766**	0.946	**1.668**	0.126	**1.569**	0.129
OH – Y			**2.011**	0.344	**1.893**	0.008	**1.899**	0.002
OH – Na			**1.186**	0.211	**0.744**	0.017	**1.165**	0.019
OH – Ca			**1.890**	0.105	**2.277**	0.028	**1.520**	0.027
Y – Y	**1.653**	0.098	**2.016**	0.092	**2.030**	0.007	**2.308**	0.032
Y – Si	**1.285**	0.012	**1.169**	0.022	**1.093**	0.007	**0.649**	0.569
Y – P	**2.000**	0.288	**1.049**	0.269	**2.196**	0.058	**0.615**	0.530
Y – Na	**1.053**	0.038	**1.224**	0.014	**1.052**	0.002	**0.652**	0.620
Y – Ca	**0.776**	0.033	**1.177**	0.010	**1.290**	0.030	**0.701**	0.695
Si – Si	**1.377**	0.000	**1.470**	0.022	**1.494**	0.003	**1.544**	0.033
Si – P	**0.274**	0.038	**1.110**	0.047	**0.968**	0.002	**0.597**	0.424
Si – Na	**1.234**	0.002	**1.082**	0.028	**1.092**	0.005	**0.670**	0.621
Si – Ca	**1.169**	0.008	**1.165**	0.029	**1.223**	0.031	**0.662**	0.604
P – P	**7.130**	0.007	**7.244**	0.004	**7.404**	0.001	**8.347**	1.139
P – Na	**1.312**	0.002	**1.067**	0.016	**1.148**	0.001	**0.629**	0.558
P – Ca	**1.334**	0.003	**0.741**	0.025	**0.454**	0.006	**0.420**	0.311
Na – Na	**1.244**	0.042	**1.729**	0.025	**1.798**	0.002	**1.595**	0.157
Na – Ca	**0.914**	0.028	**0.985**	0.012	**0.959**	0.000	**0.644**	0.516
Ca – Ca	**1.267**	0.065	**1.128**	0.023	**1.032**	0.011	**1.310**	0.199

3) YBG-P Yttrium Bioglass (Without Phosphorus)

Here are the full set of clustering ratio values regarding the simulations in which YBG-P was hydrated. The bold numbers are the ratios and beside each ratio is the standard deviation.

1) Clustering Ratios for Hydrated YBG-P

Species	YBG_DRY		YBG_0.1		YBG_0.2		YBG_0.3	
OH – Si			**0.857**	0.086	**1.099**	0.090	**1.179**	0.124
OH – Y			**1.851**	0.118	**1.750**	0.195	**1.976**	0.107
OH – Na			**1.240**	0.288	**0.725**	0.043	**1.196**	0.025
OH – Ca			**2.209**	0.556	**2.328**	0.046	**1.571**	0.045
Y – Y	**1.379**	0.486	**1.977**	0.038	**1.926**	0.140	**2.293**	0.010
Y – Si	**0.647**	0.914	**1.165**	0.017	**1.056**	0.045	**1.061**	0.012
Y – Na	**0.513**	0.725	**1.219**	0.005	**1.022**	0.045	**1.098**	0.011
Y – Ca	**0.399**	0.565	**1.201**	0.043	**1.351**	0.117	**1.205**	0.018
Si – Si	**0.879**	0.704	**1.506**	0.028	**1.519**	0.039	**1.427**	0.198
Si – Na	**0.617**	0.872	**1.113**	0.015	**1.122**	0.047	**1.005**	0.147
Si – Ca	**0.582**	0.822	**1.199**	0.077	**1.230**	0.042	**1.096**	0.010
Na – Na	**0.794**	0.595	**1.669**	0.060	**1.810**	0.014	**1.719**	0.018
Na – Ca	**0.467**	0.660	**0.844**	0.187	**0.975**	0.023	**1.007**	0.002
Ca – Ca	**0.791**	0.608	**1.109**	0.003	**1.007**	0.046	**1.173**	0.005